

UNCLASSIFIED

AD NUMBER

ADB022759

LIMITATION CHANGES

TO:

Approved for public release; distribution is unlimited.

FROM:

Distribution authorized to U.S. Gov't. agencies only; Test and Evaluation; SEP 1976. Other requests shall be referred to Air Force Materials Lab., Wright-Patterson AFB, OH 45433.

AUTHORITY

AFWAL ltr 26 Nov 1984

THIS PAGE IS UNCLASSIFIED

AD B022759

AUTHORITY:

AFWAL / 17, 26 Nov 84



ADB022759

AFML-TR-76-158

(1) 7

ESTABLISHMENT OF A CONTINUOUS WAVE CO₂ LASER WELDING PROCESS

SCIACKY BROS. INC.

SEPTEMBER 1976



TECHNICAL REPORT AFML-TR-76-158
FINAL REPORT FOR PERIOD JULY 1973 - JULY 1976

Distribution limited to U.S. Government agencies only; Test and Evaluation; statement applied ~~ASAP~~ Other requests for this document must be referred to AFML/LTM, Wright-Patterson AFB, Ohio 45433

AIR FORCE MATERIALS LABORATORY
AIR FORCE WRIGHT AERONAUTICAL LABORATORIES
Air Force Systems Command
Wright-Patterson Air Force Base, Ohio 45433

AD No.
DDC FILE COPY

NOTICES

When Government drawings, specifications, or other data are used for any purpose other than in connection with a definitely related Government procurement operation, the United States Government thereby incurs no responsibility nor any obligation whatsoever; and the fact that the Government may have formulated, furnished, or in any way supplied the said drawings, specifications, or other data, is not to be regarded by implication or otherwise as in any manner licensing the holder or any other person or corporation, or conveying any rights or permission to manufacture, use, or sell any patented invention that may in any way be related thereto.

Copies of this report should not be returned unless return is required by security considerations, contractual obligations, or notice on a specific document.

This final report was submitted by Sciaky Bros, Inc., Chicago, Illinois, under Contract F33615-73-C-5004, "Establishment of a Continuous Wave Laser Welding Process." Mr. Frederick R. Miller, AFML/LTM, was the laboratory monitor.

This technical report has been reviewed and is approved for publication.

Frederick R. Miller
FREDERICK R. MILLER
Project Monitor

FOR THE DIRECTOR

H A Johnson
H. A. JOHNSON
Chief, Metals Branch
Manufacturing Technology Division

SECURITY CLASSIFICATION OF THIS PAGE (When Data Entered)

REPORT DOCUMENTATION PAGE		READ INSTRUCTIONS BEFORE COMPLETING FORM
1. REPORT NUMBER 18 AFML TR-76-158	2. GOVT ACCESSION NO. 9	3. RECIPIENT'S CATALOG NUMBER
4. TITLE (and Subtitle) Final Report Establishment of a Continuous Wave Laser Welding Process,		5. TYPE OF REPORT & PERIOD COVERED Final report 1 July 1973-Oct 1976
7. AUTHOR(s) 10 Frederic D. Seaman		6. PERFORMING ORG. REPORT NUMBER N/A
9. PERFORMING ORGANIZATION NAME AND ADDRESS Sciaky Bros., Inc. 4915 W. 67th Street Chicago, Illinois 60638		8. CONTRACT OR GRANT NUMBER(s) 15 F 33615-73-C-5004
11. CONTROLLING OFFICE NAME AND ADDRESS Air Force Aeronautical Laboratories Air Force Systems Command AFML/LTM Ohio 45433		10. PROGRAM ELEMENT, PROJECT, TASK AREA & WORK UNIT NUMBERS Project 809-3
14. MONITORING AGENCY NAME & ADDRESS (if different from Controlling Office) N/A		12. REPORT DATE 11 Oct 1976
		13. NUMBER OF PAGES 332 12 338p.
		15. SECURITY CLASS. (of this report) Unclassified
		15a. DECLASSIFICATION/DOWNGRADING SCHEDULE
16. DISTRIBUTION STATEMENT (of this Report) Distribution limited to U.S. Government agencies only; test and evaluation results reported: October, 1976. Other requests for this document must be referred to the Air Force Materials Laboratory (AFML/LTM) Wright-Patterson AFB, Ohio 45433.		
17. DISTRIBUTION STATEMENT (of the abstract entered in Block 20, if different from Report) N/A		
18. SUPPLEMENTARY NOTES N/A		
19. KEY WORDS (Continue on reverse side if necessary and identify by block number) Shielding Gasses Underhead Tooling Laser Welding Procedures Laser Welding Titanium Gas Shields Laser Welding Nickel Base Alloys Reflectivity of Laser Welds Laser Welding Aluminum		
20. ABSTRACT (Continue on reverse side if necessary and identify by block number) In this program emphasis was placed on determining the maximum single pass thickness that could be welded using a 15 k W CO₂ laser. Additionally, laser welded test plates in representative aircraft materials were prepared, subjected to non-destructive examination and mechanically tested to failure.		

DDC
RECEIVED
NOV 9 1977
F

DD FORM 1 JAN 73 1473 EDITION OF 1 NOV 65 IS OBSOLETE

SECURITY CLASSIFICATION OF THIS PAGE (When Data Entered)

i

317600 ✓ *[Signature]*

20. (Cont)

Laser welds generally equalled base metal performance in fatigue and tensile tests. The fracture toughness of laser welds and high strength steel was shown to be very high, particularly when tests were conducted in the presence of synthetic sea water.

ACCESSION for	
NTIS	Section <input type="checkbox"/>
DDC	Section <input checked="" type="checkbox"/>
IC	Section <input type="checkbox"/>
BY	
DISTRIBUTION/AVAILABILITY CODES	
Dist	or SPECIAL
B	

SUMMARY

Multikilowatt CO₂ (CW) laser welding was shown to be a high-speed, low-distortion process that should be considered for the manufacture of aerospace structures whenever:

- There is need for high welding speeds
- Emphasis is placed on low distortion in large weldments
- Special access problems are encountered during welding
- Critical weld toughness or resistance to stress corrosion are required
- Automation of welding is considered .

In the course of the program certain limitations on the applicability of the laser process were observed. These include:

- Failure of aluminum alloys and thick (1/2 inch) nickel base alloys to respond to procedure development efforts.
- Requirement of full hood shielding for Titanium.

Studies of the equipment revealed stable and reproducible control systems. Final evaluation of welds revealed some focus instability in one optical train. This led to the conclusion that moving beam stability tests should be considered instead of single point sampling of weld cross sections when evaluating focus stability.

A review of nine procedure variables was carried out. Helium was observed to be the most effective shielding gas for transmission of beam energy to the work piece. Argon exhibited poor transmission as did still air. Very high speed welds required a mixture of helium with a small amount of argon to improve blanketing. Combination shields using helium in the beam area and argon on the solidifying weld were tested at speeds up to 240 ipm.

Optimum focus settings were found to be considerably below the work surface. These settings produce a "v" shaped weld that avoids cracking. Under proper focus settings high strength steel (280 ksi ULF) could be welded without preheat.

Thicker plates, 1/2 inch and higher, required a beam with relatively straighter sides than that used on 1/4 and 3/8 inch plate.

These straight sided beams were used to determine the maximum thickness that could be penetrated using 16 kW on the work surface (18 kW from the laser). These observed maximum thicknesses were:

- Low alloy steel and titanium: 0.6 inch
- Stainless steel and nickel base alloys
(Inco 718): 0.54 inches
- Aluminum (at 14 kW on work): 0.5 inch

Nondestructive tests indicated relative freedom from porosity. The following average distances between isolated pores were observed:

- Titanium (1/4 inch): 25½ inches
- Carbon Steel (1/4 inch): 25½ inches
- Nickel Base Alloy: Greater than 30 inches

Isolated problems with very limited titanium contamination while using a helium jet to suppress the beam impingement plasma lead to the conclusion that full hood shielding is preferred.

Mechanical tests, and post test examination of the all fracture surfaces, showed that there are no special laser related effects in laser welds. However, a characteristic defect can occur if the focal point periodically lifts upward. The weld cross section becomes pinched near the surface and blocks metal from the solidifying body of the weld. In the case of steel the result was randomly oriented freezing defect in welds made with a particular optical train.

Mechanical test performance of laser welds generally equaled that of the base metal reference in fatigue and tensile tests. Fracture toughness tests, performed on high strength steel and titanium indicated very good toughness. Precracked high strength steel specimens exposed to sea water performed exceptionally well with respect to the toughness tests. Titanium performance was typical for the material. Smooth bar specimens of high strength steel always failed in the base metal when exposed to stress near their yield and alternate salt water immersion providing welds were sound.

PREFACE

The report was prepared by Sciaky Bros., Inc., Chicago, Illinois, under USAF Contract F33615-73-C-5004, "Establishment of a Continuous Wave Laser Process". The work was administered under the technical direction of Mr. Frederick R. Miller (AMFL/LTM), Air Force Materials Laboratory, Manufacturing Technology Division, Metals Branch, Air Force Wright Aeronautical Laboratories.

This report covers work conducted from 1 July 1973 to 1 October 1976 and is submitted in fulfillment of the contract. The technical report was released by the author in August, 1976.

The program was directed by Mr. Frederic D. Seaman, Project Manager. Other Sciaky personnel contributing to this program were Mr. H. Harvey, Mr. W. Rudin, Mr. Stanley Ream and Mr. R. Reynolds. Assisting and associate contractors to the program were Avco Everett Research Laboratories, Inc., with Mr. R. Hella serving as Program Manager assisted by Messrs. R. Neal, and G. Gay; Douglas Aircraft Company, a division of McDonnell Douglas Corporation with Mr. M. Hayase assisted by Dr. T. Makey.

A special consideration is given to Mr. C. Harmsworth of AFML/MXB for his assistance in the testing of high strength steel welds.

This project has been accomplished as a part of the Air Force Manufacturing Methods Program, the primary objective of which is to develop on a timely basis manufacturing processes, techniques, and equipment for use in economical production of USAF materials and components.

Your comments are solicited regarding the potential utilization of the information contained herein as applied to your present and/or future production programs. Suggestions concerning additional manufacturing methods development required on this or other subjects will be appreciated.

CONTENTS

Section	Page
I INTRODUCTION	I-1
A. BACKGROUND	I-1
B. HIGH ENERGY DENSITY BEAMS IN INDUSTRY	I-1
C. LASER BEAMS AS WELDING TOOLS	I-2
D. PROGRAM OBJECTIVE	I-3
II EQUIPMENT	II-1
A. DESCRIPTION OF SYSTEM	II-1
B. OPTICS	II-3
C. TOOLING	II-4
D. CONTROLS	II-5
E. WORKPIECE ALIGNMENT LASER	II-5
F. SAFETY	II-7
G. SYSTEMS TESTS	II-8
1. Controllability	II-9
2. Regulation	II-11
3. Stability of Spot Location	II-12
4. Repeatability Under Welding Conditions.	II-17
III MATERIALS	III-1
IV PROCESS TECHNOLOGY	IV-1
A. PREWELD PREPARATION	IV-1
1. Cleaning Prior to Laser Welding	IV-1

CONTENTS (Cont.)

Section	Page
2. Surface Finish Effect and Reflectivity.	IV-5
3. Effect of Variations in Joint Fit Up.	IV-10
a. Mismatch	IV-11
b. Gap	IV-11
B. TOOLING	IV-11
1. Backstop Tooling	IV-13
2. Chill Spacing	IV-13
3. Effect of Underbead Gas Pressure	IV-18
C. SHIELDING GAS PERFORMANCE	IV-20
D. EVALUATION OF GAS SHIELDING METHODS	IV-31
1. The Off Axis Shield	IV-32
2. The Jet-Trailer Shield	IV-34
a. Reactive Metals	IV-37
b. Set-Up Tolerances	IV-37
c. Jet Gas Flow.	IV-40
3. Diffuser Hood	IV-40
a. Reactive Metals	IV-40
b. Aluminum	IV-40
4. Preplaced Gas Manifolds	IV-42

CONTENTS (Cont.)

Section	Page
5. Flood Shielding	IV-44
E. BEAM - WORKPIECE INTERACTION	IV-46
1. Speed-Focus	IV-49
2. Focus-Power	IV-51
3. Speed Joint Thickness Penetration	IV-53
4. Power-Speed	IV-55
a. Thickness F/Number	IV-55
b. F/Number and Focus Tolerance	IV-58
5. Beam Impingement Angle	IV-58
F. MAXIMUM PLATE THICKNESS	IV-60
G. REPAIR	IV-61
H. WIRE FEED	IV-66
a. Single Pass Welding	IV-68
b. Two Pass Welding.	IV-70
I. DISTORTION	IV-70
V LASER WELD EVALUATION	V-1
A. NONDESTRUCTIVE TESTING	V-1
1. Method	V-1
a. Radiographic Procedure	V-2
b. Fluorescent Penetrant	V-2

CONTENTS (Cont.)

Section	Page
c. Fluorescent Magnetic Particle Inspection	V-3
d. Ultrasonic Inspection	V-3
2. Overview of Quality	V-4
3. Disposition of Panels	V-9
B. LASER WELDS IN LOW ALLOY CARBON STEEL (300 M)	V-9
1. Base Metal Characteristics	V-9
2. Panel Welding	V-10
3. Welding Characteristics	V-11
4. Specimen Preparation	V-12
5. Mechanical Behavior	V-18
a. Tensile Tests	V-19
b. Axial Fatigue Tests	V-20
c. Fracture Testing	V-22
d. Notched Stress Corrosion	V-32
e. Stress Corrosion Cracking (Alternate Immersion)	V-38
f. Microhardness Examination	V-39
C. LASER WELDS IN TITANIUM ALLOY (6Al-4V)	V-47
1. Base Metal Characteristics	V-47
2. Panel Welding	V-47

CONTENTS (Cont.)

Section	Page
3. Welding Characteristics	V-49
4. Specimen Preparation	V-49
5. Mechanical Behavior	V-53
a. Tensile Tests	V-53
b. Axial Fatigue Tests	V-60
c. Fracture Testing	V-61
d. Notched Stress Corrosion	V-62
e. Microhardness Examination	V-68
D. NICKEL BASE ALLOY	V-69
1. Base Metal Characteristics	V-69
2. Panel Welding	V-77
3. Welding Characteristics	V-77
4. Specimen Preparation	V-80
5. Mechanical Behavior	V-81
a. Tensile Tests	V-81
b. Microhardness Examination	V-84
E. ALUMINUM ALLOY	V-84
1. Base Metal Characteristics	V-84
2. Panel Welding	V-86
3. Welding Characteristics	V-86
VI CONCLUSIONS	VI-1

CONTENTS (Cont.)

Section	Page
VII RECOMMENDATIONS	VII-1
APPENDIX A: Process Control & Safety	A-1
APPENDIX B: Results of Nondestructive Evaluation of "As Welded" Material	B-1
APPENDIX C: Correlation of Fracture Face Observation, Welding Procedure and Test Weld Cross Section	C-1
APPENDIX D: Correlation of Process Settings and Weld Cross Section	D-1
APPENDIX E: Test Specimen Design and Fabri- cation Drawings.	E-1

ILLUSTRATIONS

Figure	Title	Page
II-1	Basic Elements of a CO ₂ (CW) Laser System. . .	II-6
II-2	System Controllability Tests	II-10
II-3	Long Term Regulation of Run Power	II-13
II-4	Spot Stability Experiment	II-15
II-5	Repeatability Test Welds	II-19
IV-1	Relative Effectiveness of Cleaning Methods	IV-4
IV-2	Typical Surface Finish Tolerance Specimen.	IV-6
IV-3	Observed Penetration.	IV-8
IV-4	Fit-Up Test Plate	IV-9
IV-5	Effect of Joint Fit (Gaps) Up on Weld Cross Section	IV-12
IV-6	Underbead Tooling Experiment	IV-14
IV-7	Effect of Underbead Energy on Tooling	IV-15
IV-8	Experimental Chill Bar.	IV-15
IV-9	Relative Underbead Contour Effects From Chills	IV-16
IV-10	Effect of Underbead Pressure on Underbead Shape	IV-19
IV-11	Apparatus for Determining Effect of Shielding Gas	IV-23
IV-12	Effect of Shielding Gas on Penetration 60 ipm Stainless Steel	IV-25

ILLUSTRATIONS (Cont.)

Figure	Title	Page
IV-13	Effect of Shielding Gas on Penetration 60 ipm Low Alloy Carbon Steel	IV-26
IV-14	Effect of Shielding Gas on Penetration 60 ipm Other Program Material	IV-27
IV-15	Effect of Shielding Gas on Penetration 120 ipm All Program Materials	IV-28
IV-16	Effect of Shielding Gas on Penetration 240 ipm All Program Materials	IV-29
IV-17	Typical of Axis Shielding Nozzle	IV-33
IV-18	Typical Jet Trailer Shield	IV-36
IV-19	Metallographic Evidence of Contamination . .	IV-38
IV-20	Effect of Jet Trailer Shield Design on Shielding Capability.	IV-39
IV-21	Effect of Jet Flow Rates on Process Penetration	IV-39
IV-22	Water Cooled Diffuser Hood	IV-41
IV-23	Manifolds	IV-43
IV-24	Flood Shielding Test Apparatus	IV-47
IV-25	Weld Cross Section Related to Focus- Speed Characteristics	IV-50
IV-26	Suggested Area for Process Optimization . . .	IV-52
IV-27	Focus-Power Relationship for Program Materials	IV-52
IV-28	Speed-Thickness Relationship for Program Materials	IV-54

ILLUSTRATIONS (Cont.)

Figure	Title	Page
IV-29	Response of 3/8 Inch Thick Bench Mark Speeds to Power	IV-56
IV-30	Response of 1/2 Inch Thick Bench Mark Speeds to Power	IV-57
IV-31	Comparison of Process Survey Patterns for F21 and F7 Optical Systems . . .	IV-59
IV-32	Effect of Repair Procedures on Porosity . . .	IV-64
IV-33	Joint Configuration For Welds in Heavy Material	IV-64
IV-34	Effect of Filler Wire Addition on Penetration	IV-69
IV-35	Laser Weld in 3/4 Inch Plate	IV-71
V-1	Search Unit Calibration Procedure	V-5
V-2	Typical UT Indication	V-5
V-3	UT Pulse Echo C-Scan of 1/2 Inch Titanium Weld	V-6
V-4	Defect Verification from X-Ray and UT Indications	V-7
V-5	Relative Incidence of Porosity	V-8
V-6	Definition of Procedure Variables	V-14
V-7	Tooling Configuration for Panel Welding . . .	V-15
V-8	Typical Low Alloy Carbon Steel Weld Cross Sections	V-16
V-9	Crack in Pinched Cross Section (Steel) . . .	V-17

ILLUSTRATIONS (Cont.)

Figure	Title	Page
V-10	Tensile Results Low Alloy Carbon Steel. . . .	V-24
V-11	Axial Tension Fatigue Results Low Alloy Carbon Steel	V-25
V-11-a	Failure Initiation Site, Specimen W-5S	V-26
V-11-b	Failure Initiation Site, Specimen W-6S	V-27
V-11-c	Failure Initiation Site, Specimen W-11S.	V-27
V-11-d	Failure Initiation Site, Specimen W-12S	V-28
V-12	1/4 Inch Low Alloy Steel Fatigue Test Specimens	V-29
V-13-a	1/2 Inch Low Alloy Steel Fatigue Test Specimens	V-30
V-13-b	1/2 Inch Low Alloy Steel Fatigue Test Specimens (Continued).	V-31
V-14	Fracture Faces of Weld Toughness Tests Low Alloy Carbon Steel.	V-33
V-151	Low Alloy Carbon Steel Fracture Toughness Results	V-34
V-16	Low Alloy Carbon Steel Notched Stress Corrosion Specimens	V-36
V-17	Low Alloy Carbon Steel Notched Stress Corrosion Test Results	V-37
V-18	Anomalous Band Suggesting Ductile Failure in Low Alloy Steel Notched Stress Corrosion Tests	V-40

ILLUSTRATIONS (Cont.)

Figure	Title	Page
V-19	Low Alloy Steel Specimens Lifetimes Under Alternate Immersion Stress Corrosion (Bore)	V-41
V-20	Fracture Appearance and Initiation Site, Alternate Stress Corrosion Specimens Low Alloy Steel	V-42
V-21	Typical Intergranular Cracking at Failure Origins of Stress Corrosion Specimen (Low Alloy Steel)	V-43
V-22	Secondary Cracking in Low Alloy Steel Specimen SCS-2S	V-43
V-23	Comparative Fracture V in Tensile Specimen ALT-25 From Weld Defect	V-44
V-24	Hardness Survey Low Alloy Steel Weld (1/2 Inch - As Welded)	V-45
V-25	Hardness Survey Low Alloy Steel Weld (1/2 Inch - Heat Treated)	V-45
V-26	Hardness Survey Low Alloy Steel Weld (1/4 Inch - As Welded)	V-46
V-27	Hardness Survey Low Alloy Steel Weld (1/4 Inch - Heat Treated)	V-46
V-28	Centerline Porosity, 1/2 Inch Titanium Welds	V-50
V-29	Fractured Face of Specimen That Failed in Straightening	V-54
V-30	Electron Micrograph - Brittle Fracture in Specimen FTW-9T	V-55
V-31	Electron Micrograph - Ductile Fracture in Specimen FTW-9T.	V-55

ILLUSTRATIONS (Cont.)

Figure	Title	Page
V-32	Transverse Break in FWT-9T	V-55
V-33	Discoloration Beside Bead In Broken 1/4 Inch Titanium Weld	V-56
V-34	Discoloration Beside Bead In Specimen FWT-9T (1/2 Inch)	V-56
V-35	Electron Micrograph Top Edge 1/4 Fracture Specimen	V-57
V-36	Electron Micrograph Top Edge Specimen FWT-9T (1/2 Inch)	V-57
V-37	Tensile Results Titanium Alloy	V-57
V-38	Axial Tension Fatigue Results - Titanium Alloys	V-64
V-38-a	Failure Initiation Site Specimen W-4 (Pores)	V-65
V-38-b	Failure Initiation Site Specimen W-6 (Crack)	V-65
V-39	Fatigue Fracture Faces (1/4 Inch Titanium Alloy)	V-66
V-40	Fatigue Fracture Faces (1/2 Inch Titanium Alloy)	V-67
V-41	Fracture Faces of Weld Toughness Tests, Titanium Alloy	V-70
V-42	Titanium Alloy, Fracture Toughness Results	V-71
V-43	Titanium Notched Stress Corrosion Specimens	V-72

ILLUSTRATIONS (Cont.)

Figure	Title	Page
V-44	Stress Corrosion (Notched Test) Results in Titanium Alloy	V-73
V-45	Characteristic Stress Corrosion Failure Mode in Titanium Alloy	V-73
V-46	Hardness Survey Titanium Weld (1/4 Inch)	V-74
V-47	Hardness Survey Titanium Weld (1/4 Inch)	V-74
V-48	Hardness Survey Titanium Weld (1/2 Inch)	V-75
V-49	Hardness Survey Titanium Weld (1/2 Inch)	V-75
V-50	Tensile Results Nickel Base Alloy	V-83
V-51	Hardness Survey	V-85
V-52	Process Instability in Aluminum Welds	V-87
V-53	Selected High Speed Motion Picture Sequence of Aluminum Cavity Instability	V-88

LIST OF TABLES

Table	Title	Page
II-1	Spot Measurement Techniques	II-16
III-1	Program Materials	III-4
III-2	Program Materials	III-4
IV-1	Preweld Etching Solutions	IV-3
IV-2	Experimental Surface Condition.	IV-8
IV-3	Experimental Welding Procedure - Surface Finish Effect	IV-9
IV-4	Fit Up Test Welding Procedures	IV-14
IV-5	Experimental Chill Configurations	IV-17
IV-6	Experimental Welding Procedures - Tooling Tests	IV-17
IV-7	Experimental Welding Procedures - Shielding Gas Evaluation	IV-21
IV-8	Tolerance For Off Axis Shield Position Forward Flow.	IV-24
IV-9	Tolerance For Off Axis Shield Position Backward Flow	IV-35
IV-10	Experimental Welding Procedure - Manifold Shielding.	IV-45
IV-11	Observed Penetrating Capabilities	IV-62
IV-12	Experimental Welding Procedure For Maximum Penetration Capability.	IV-63
IV-13	Determination	IV-65
IV-14	Effect of Repair on Weld Strength	IV-67

LIST OF TABLES (Cont.)

Table	Title	Page
IV-15	Summary of Panel Distortion	IV-72
V-1	Low Alloy Steel Welding Procedures	V-13
V-2	Low Alloy Carbon Steel Tensile Results	V-23
V-3	Low Alloy Carbon Steel Axial Tension Fatigue & Fracture Surface Correlation Results	V-31
V-4	Low Alloy Carbon Steel Fracture Toughness Test Results	V-33
V-5	Low Alloy Carbon Steel Notched Stress Corrosion (K_{Isc}) Test Results	V-36
V-6	Compositions & Properties of Titanium Material Tested in Program	V-48
V-7	Titanium Alloy Welding Procedures	V-48
V-8	Titanium Alloy Tensile Results.	V-59
V-9	Results of Titanium Alloy Fatigue Tests	V-63
V-10	Titanium Fracture Toughness Test Results.	V-70
V-11	Titanium Alloy Notched Stress Corrosion Test Results	V-72
V-12	Composition of Nickel Base Materials Tested In Program	V-76
V-13	Mechanical Properties of Nickel Base Materials Tested In Program	V-76
V-14	Nickel Base Alloy Welding Procedures	V-78
V-15	Nickel Base Alloy Tensile Results	V-78
V-16	Welding Procedure For Instability Analysis	V-91

SECTION I

INTRODUCTION

A. BACKGROUND

Lasers produce energy in the form of coherent light. Coherent light, in contrast to thermal light, which is used for broad area illumination, can be brought to a very sharp focus. Thermal light when focused can burn wood. Focused coherent light can evaporate steel. Specific energy levels exceeding one million watts per square inch can be obtained, by focusing coherent light.

B. HIGH ENERGY DENSITY BEAMS IN INDUSTRY

The industrial significance of million-watt-per-square-inch beam technology can best be appreciated by reviewing the advantages that a similar beam, the electron beam, has brought to the industry in the past few years.

Recognized beam welding advantages:

- Deep narrow welds
- Weld strength approaching base metal strength
- Minimum, consistent predicatable distortion
- Simplified weld tooling
- Increased welding speeds
- Single pass penetration in very thick plate
- Unique welding capabilities
- More efficient part design

However, because the beam is made up of electrons, certain limitations on the welding of large aerospace structures are generally recognized. These are listed below.

Electron Beam Limitations:

- Electron gun must be in vacuum
- Workpiece completely or partially in vacuum

Large vacuum chambers are

- Expensive
- Inflexible
- Long lead procurement items

Beam-joint alignment influenced by magnetic
or electrostatic fields

The practical impact of these limitations has been sufficient to stimulate development of specialized local vacuum chambers and sliding seals - methods for reducing the constraint of the vacuum chamber.

C. LASER BEAMS AS WELDING TOOLS

The substitution of the laser beam for an electron beam lifts the vacuum constraints and can further improve on some of the electron beam advantages. These are listed below.

Potential Advantages From Substitution of a Laser Beam for
an Electron Beam

- No need for vacuum at workpiece
- No constraints from chamber dimensions
- Magnetic or vacuum tooling can be used
- Beam projected long distances

No magnetic deflection

No electrostatic deflection

There are also economic implications which result from the substitution of a laser for electron beam when large aerospace weldments are considered. Both processes require sizable and roughly equivalent, capital investment. It may be possible, under certain conditions, to realize a greater return for a given investment from a laser than from a large chamber electron beam installation.

For example, if size or shape of the component to be welded may change over a period, the laser should be considered. The electron beam chamber is closely linked to workpiece size and is the most expensive element of the electron beam system. An electron beam welding changeover may involve the cost and lead time requirement associated with pumps and chamber. A change in optics and workpiece tooling might be all that was required for a laser changeover.

Additionally the economics of E.B. are not improved by servicing three or four vacuum chambers of different dimensions and configurations from one energy source and control, because the latter equipment represents such a small portion of the total investment when compared to the cost of multiple chambers.

In the case of the laser, the energy source and its associated equipment is the most expensive element in the total welding system. The energy source can operate continuously, and the laser beam can be transported large distances without attenuation. Thus, once an initial investment is made, a single energy source can service a large number of welding fixtures, providing a substantially lower incremental investment and shortened lead time for each new application.

These same time sharing economics can be applied when it is advantageous to apply beam welding to several components on a single program. Additionally, the stations can also embrace heat treating and cutting since the laser is capable of both applications. Therefore:

Economic Advantages for the Laser

- Low incremental cost for each application
- Ability to service several applications on a time sharing basis
- Ability to do several metalworking operations
- Short lead time to minimize impact of inflation on program

D. PROGRAM OBJECTIVE

This program established a continuous wave (CW) Carbon-dioxide laser welding process.

The establishment of the process involved several steps carried out in sequence during two tandem phases.

PHASE I CO₂ Laser Evaluation
Equipment Performance Testing
Process Technology
Preweld Preparation
Tooling

Shield Gas Performance
Gas Shields
Beam-Workpiece Interactions
Maximum Penetration Trials

PHASE II Weld Testing
Procedure Development
Test Panel Welding
Non-Destructive Tests
Mechanical Tests
Analysis of Results (Correlation)

SECTION II

EQUIPMENT

An important requirement for equipment in any program that is directed toward development of welding procedures for the aerospace industry is commercial availability. The most powerful commercial laser available to this work was an AVCO HPL.* The nominal, warranted output of the cavity was 10 kW. However, power supplies were large enough to permit operation at power levels up to 15 kW (or higher).

A. DESCRIPTION OF THE SYSTEM

The AVCO HPL system has the following characteristics:

Basic Characteristics:

- Operates in the CW mode
- Emits light at 10.6 microns
- Uses CO₂, N₂, He and CO as a lasing medium
- Recirculates the lasing medium
- Performs with approximately 10% efficiency
 - . Near room temperature
 - . At .1 atmosphere
- Preionizes the gas (with a controllable electron discharge)
- Utilizes a high current moderate voltage electrical discharge to pump the gas
- Produces more than 10 kW beam power

Additionally the device has other features that are useful in manufacturing:

*Registered trade mark - Designed, developed, manufactured, and sold by the AVCO Everett Research Laboratory (A subsidiary of the AVCO Corp.)

Industrial Features:

Uses simple copper mirrors in external optics
Closes its control circuit on beam power
Permits rapid electronic shut-down or start-up
of beam
Can close out welds using up slope and down slope
Operates over a broad range of power settings
Can be preset to desired power level
Operates unattended using guard circuits

While the laser is the heart of the system there are
six other important sub-systems that are required (Fig. II-1).
A list of all sub-systems would include:

Basic Elements of a Laser System

1. Laser Chamber
2. Controls
 - Power Level
 - Sequence, Operating & Start-up
 - Tooling Motion
 - Safeguard Shutdown
3. Power Supplies
 - Discharge Sustainer Supply
 - Preionizer Supply
 - Other Special Power Requirements
4. Mechanical Services
 - Vacuum
 - Gas Makeup
 - Pneumatic Control Pressure
 - Cooling
 - Gas Stream after Discharge
 - Optical Elements
5. External Optics
 - Collimation
 - Transmission
 - Switching
 - Focusing
6. Tooling
 - Gas Shields
 - Work Piece Support
 - Work Piece Translation

Focal Point Placement
Within the Work
On the Weld Path

B. OPTICS

The optics of most metalworking laser systems, including the system used in this program (Fig. II-1), can be divided by function into two portions:

Functions of External Optics
Beam Transfer
Beam Focus (Working Optics)

Beam transfer optics may simply direct the beam to the working optics or they may perform several other functions:

Functions of a Beam Transfer System
Beam Power Sampling
Collimation
Switching (Time Sharing)
Splitting*
Dithering*
Transmission

Optical component transmission efficiencies are low for most materials in the infrared region. Potassium chloride and semiconductors such as gallium arsenide are exceptions. At the multikilowatt power level, energy densities impinging on optical components made of these materials are often high enough to create stability problems which affect integrity or optical stability. In order to avoid such problems, polished copper reflectors were chosen instead of transmission lenses as the basic optical element for the 10 kilowatt system used in this program.

The beam energy lost at each polished copper mirror is 1.3 - 1.5% of the impinging power. Thus, the off axis F/21 telescope in Fig. II-1 directs about 90% of the emitted beam onto the work surface using seven copper reflecting surfaces. This value has been verified by calorimetric tests.

* Not used in Program

The coaxial F/7 telescope has 95-96% of the beam delivered to its lower (small) mirror. However, calorimetric checks suggest that some of the beam bypasses the small mirror and is dissipated over a broad area on the work. As a result, only 70% (estimated) of the energy entering the F/7 telescope reaches the focal point. This is a characteristic of the specific telescope used in this program only. It is not a generic characteristic of coaxial telescopes.

The transmission discrepancy and low efficiency of the F/7 did not affect the program since sufficient power was available to produce working focal points with equivalent power in either system up to 12.5 Kw on the work. The F/21 could operate at 16.2 kw using the same power from the laser.

Note: In this program all comparative data involving the two telescopes and all referenced procedures are based on the power delivered to the focal point on the work unless specified as beam power or power at the aerodynamic window.

C. TOOLING

Workpiece movement was achieved and controlled through the use of calibrated D.C. motor drives attached to the feed screws of milling machine bases. The maximum stroke was 21-3/4 inches. Speeds up to 400 ipm could be obtained. Stroke length was varied by repositioning limit switches, by limiting run time, or by stopping the system manually.

Workpiece hold down was accomplished by mechanically clamping to a heavy carbon steel plate with a 1-inch-deep, 1-inch-wide underbead gas channel. A stiff bridge clamp with threaded force points was used on half inch plate welds to iron out waviness in the test coupons.

Several important elements of tooling were included in the experimental program and are discussed in Section IV. These are:

Experimental Tooling Evaluations

- Gas Shields (Existing Types)
- Underbead Chills
- Beam Stops

The shields were explored to optimize upperbead configuration. Underbead chills and beam stops were evaluated with respect to control of the prominent underbead extension that characterizes deep single pass welds. The beam stops were also evaluated with respect to the amount of beam energy that exists from the bottom of the cavity. Guidelines for the design and use of shields and chills will be found in Section IV - Process Technology.

D. CONTROLS

Each work station shown in Fig. II-1 is equipped with a set of controls that permits establishment of a welding procedure. These controls are:

Basic Work Station Controls

- Power
 - Run
 - Upslope
 - Downslope
- Process Speed
- Travel Delay
- Run Time (If Used)
- Shield Gas Delay (Station #1 Only)
- Stand by (Window Open)
- Sequence Start

Other set-up controls were placed on the main console. These include:

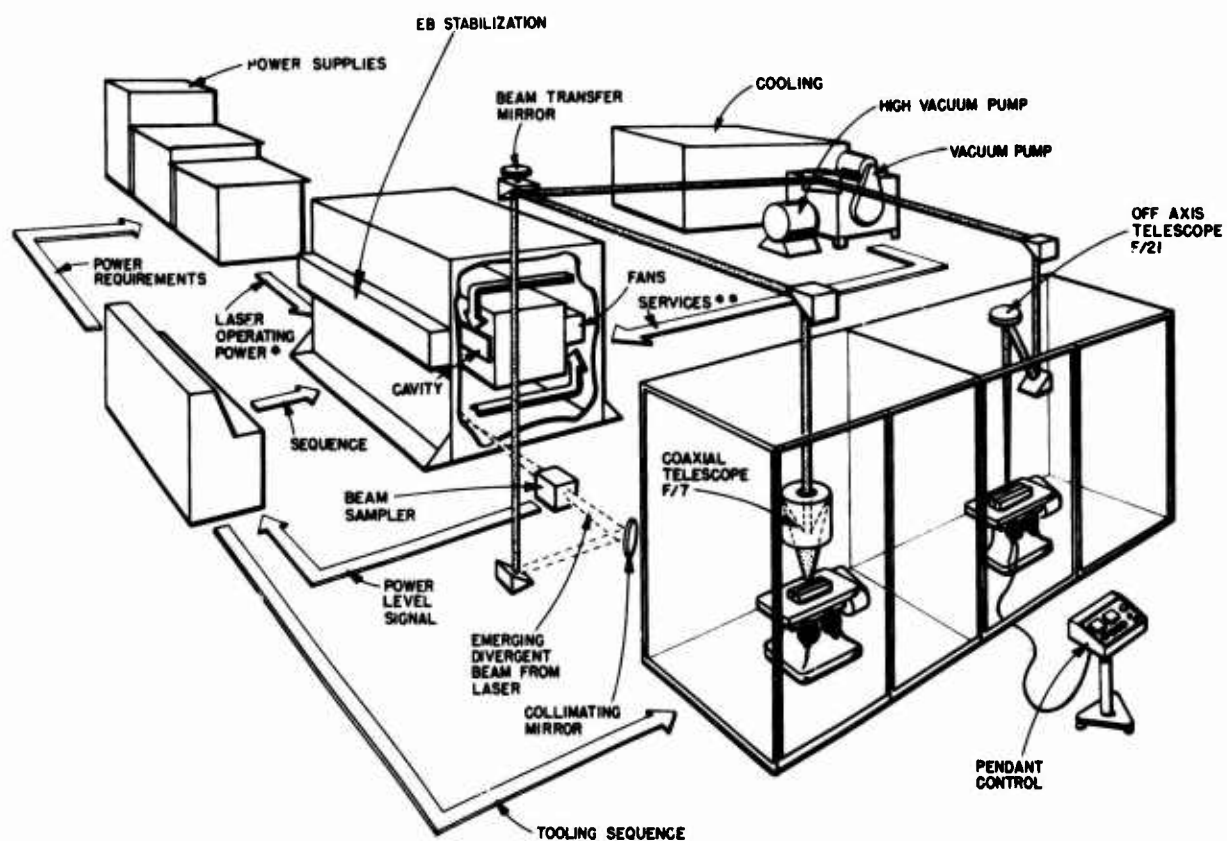
Set-up Controls

- Automatic Start-up Sequence (beginning of shift)
- Automatic Shut-down Sequence (end of shift)
- Sustainer
- Preionizer
- Make up Gas Controls

This set of controls was not involved in program test series.

E. WORK PIECE ALIGNMENT AUXILIARY He/Ne LASER

In deep penetration welding it is important that the relatively small spot be placed on the joint (and that the faying



* POWER FOR FANS, STABILIZATION AND DISCHARGE
 ** VACUUM (EB STABILIZATION AND CAVITY), MAKE UP GAS, AND COOLING (GAS AND MIRRORS)

Figure II-1. BASIC ELEMENTS OF A CO₂ (CW) LASER SYSTEM

surfaces of the joint be parallel to the beam axis for the entire section thickness). In the welding system used for this program, an auxiliary milliwatt (class 1) visible-red, beam is automatically injected into the external optical system whenever the main CO₂ beam is not being used.

The characteristics of this auxiliary system are:

Auxiliary Alignment Laser Sub-System

Power:	1.0 milliwatts
Injection:	Silvered mirror actuated when aerodynamic window opened or closed
Transmission to Work:	Coaxial with Main Beam $\pm 0.010"$
Focus At Work:	Coincident with CO ₂ Beam $\pm 0.030"$

The operator visually aligns the red spot with the top of the tightly closed butt weld. Periodically the spot position is checked by a very light tack weld made on a surface with the main beam. The red He/Ne spot is switched on to determine that its center visually coincides with the center of the tack weld.

Coincidence can be judged within about a half spot. Visual acuity plays a role in alignment. However, there is invariably a slight gap in the joint. The reflected light drops off noticeably as the major portion (approximately the center one third) of the small red spot coincides with this gap. This drop-off can be detected by anyone observing the operation. Thus, alignment really implies that the joint lies within the center one third of red He/Ne spot.

The alignment spot is approximately 0.015 ± 0.005 inch in diameter, thus the one third diameter target area represents about 0.005 inch and constitutes an envelope of uncertainty in spot-joint alignment. An F/7 CO₂ beam spot is approximately 0.040 inch in diameter. Thus, the 0.005 inch wide area of uncertainty represents about 1/8 of the working spot diameter exclusive of a possible 0.007 inch calibration error.

F. SAFETY

All work was accomplished within a light barrier type of

enclosure made of acrylic plastic. Eye level joints in the enclosure were inspected for radiation. Access was controlled by interlocks. Opening the enclosure to enter shuts off the preionization source, thus shutting down lasing action. The same action mechanically places a metal barrier in front of the beam exit in the side of the chamber. After personnel have left the enclosure and closed the doors these beam constraints can be removed. Removal requires two separate actions on the part of the operator at the console who must remove the barrier and activate the ionizer. Audible and visual warnings are activated when the first constraint (the metal barrier in the aerodynamic window) is removed.

With fixed hood type shielding and beam path enclosure to the shield, an enclosure might not be required. Very little radiation escapes from under a hood placed tightly against the work according to reflection tests run during the program. Appendix A discusses laser safety and maintenance in detail.

G. SYSTEMS TESTS

The application of a high power density energy source, such as the laser beam, to critical aerospace structural welding requires precise control and repeatability. The ability of the energy source to produce an output power equal to the preset power and to precisely control that output for the duration of the weld is as important in performing a welding development program as it is in welding.

Not only must the amount of power be controlled, but, since a sound weld joint is the objective of any welding process this power must be placed correctly on the workpiece to be joined. Assurance must be given that otherwise stable support structures do not move as the mirrors which they support deal with the thousands of Watts of power in the beam of multikilowatt (CW) lasers.

Additionally, if the He/Ne alignment laser is to be used as a reference it is important that its beam stay coincident with that of the 10.6 Micron beam during long, full-power runs.

The purpose of the experiments described under System Tests was to systematically and quantitatively evaluate the performance of the existing beam power control system and

also the stability of the external beam transmission and focusing optics (with their associated visible beam alignment laser) so that the effect of these control sub-systems could be related to the results obtained during the remainder of the program.

1. Controllability

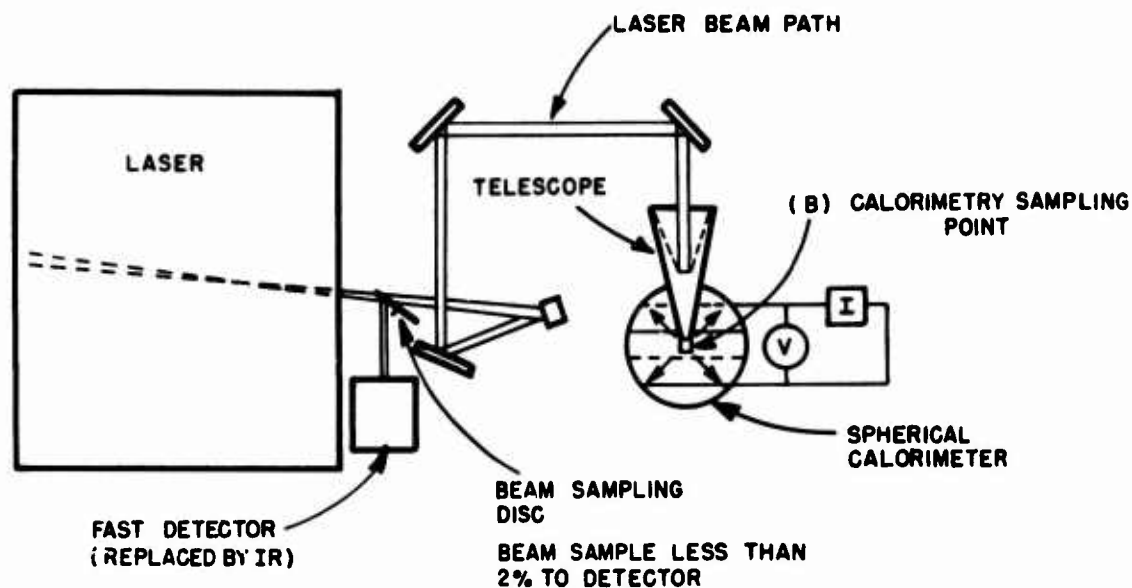
The objective of this task was to verify the correspondence between the setting of the power and the actual power output delivered from the aerodynamic window of the laser (Fig. II-2). These define controllability which in turn is made up of two characteristics:

Repeatability of measuring instrument
Linearity of response

In these tests a reference IR detector replaced the fast response pyro electric detector normally used. The laser power was monitored by instrumentation which received a sample of the beam power many times per second from a set of rotating reflectors at the aerodynamic window. The instrument is a continuous power meter, commercially available from Coherent Radiation Laboratories, for CO₂ laser power measurements. The CRL meter gives a continuous, on-line readout of laser power. A second part of this task was to compare the response of the CRL meter to power changes against a calorimeter which absorbs a large part of the energy of the beam and responds by changing temperature in direct proportion to laser power. By using the time-temperature response of such a calorimeter it is possible to verify that CRL meter response is proportional to power.

The experimental procedure was as follows:

1. Determine Percentage of Beam Sampled for IR Detector.
2. Observe IR Detector Output at Five Power Levels.
3. Repeat Step 2 seven times in a 48 hr. period.
4. Convert Detector Output to Beam Power Using Data from 1.
5. Determine Calorimeter Output at Highest of the 5 power levels.



EXPERIMENTAL SET UP

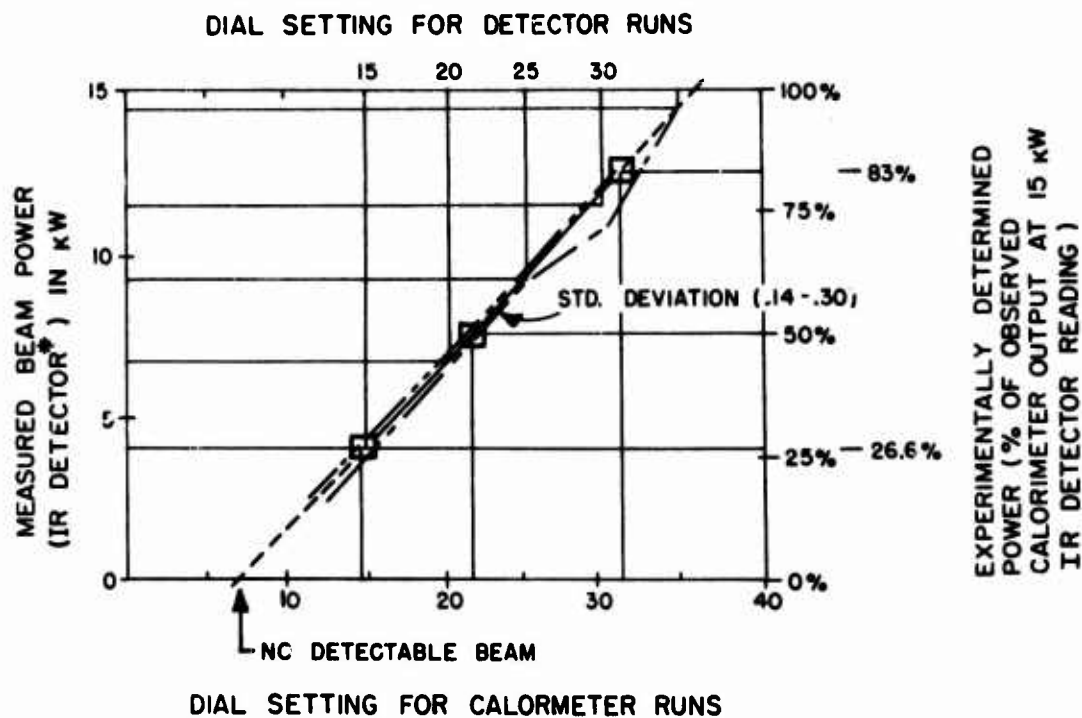


Figure II-2. SYSTEM CONTROLLABILITY TESTS

6. Observe proportional relationship at other 4 power levels.

The observed results suggest that the beam energy called for by the control dial settings was delivered by the laser to the instrumentation in seven tests at eight power levels during the two day test with accuracies of $\pm .5\%$ over a range of powers from 4.1 kW to 14.5 kW. A slightly reduced repeatability was observed at 11.5 kW. Using the time-temperature response of a calorimeter as a reference it was determined that the power values reported by the CRL meter reliably respond to changes in beam power resulting from proportional changes in control settings.

The absolute value of the power delivered from the aerodynamic window was established by IR instrumentation techniques that represented the industry standard - a CRL power meter. Power levels up to 14.5 kW were thus measured.

2. Regulation

The laser used in this program is capable of continuous operation at maximum power for sustained periods of time. Maximum power operation is only acceptable for aerospace manufacturing if it:

Can Be Sustained for Long Periods of Time
Represents Preset Value
Can Be Regulated Thruout Length of Run

This task demonstrated the program laser's ability to meet these requirements.

For these tests, the laser was operated on automatic control by first setting the power dial at the desired power and then pushing the laser "On" button. The controls were not touched by the operator for the duration of the run. Fig. II-3 illustrates the arrangement of the laser for these tests. The fast response pyro-electric detector monitored the laser power and supplied a signal to the closed loop control system which maintained the constant preset output power value. The signal from the detector is proportional to the power directed into it. If the power into the detector changes from the preset value, the closed loop system

automatically makes the appropriate corrections to increase or decrease the laser power to keep the signal coming into the detector at the desired value.

To assure detection of small changes in power the gain of the recorder was set maximum. As a result there is considerable noise in the trace produced by the recorder as shown in Fig. II-3.

The laser power was monitored by observing and recording the output of the fast detector for three 25 minute runs in the 14-15 Kw range. Fig. II-3 illustrates a typical run. RMS displacement of the power curve was investigated by selecting six points (such as points A-E in Run 1382, Fig. II-3) that appeared to represent maximum and minimum power levels and determining the location of a point midway between the extremes of high frequency noise pattern.

An analysis of six sample power levels for each beam power trace suggests that up to 15 Kw the RMS variation over the 25 minute run was less than 115 watts out of 15,000 watts (0.7% of the nominal power). At 15.5 Kw the RMS variation increased to 298.6 watts over the entire run.

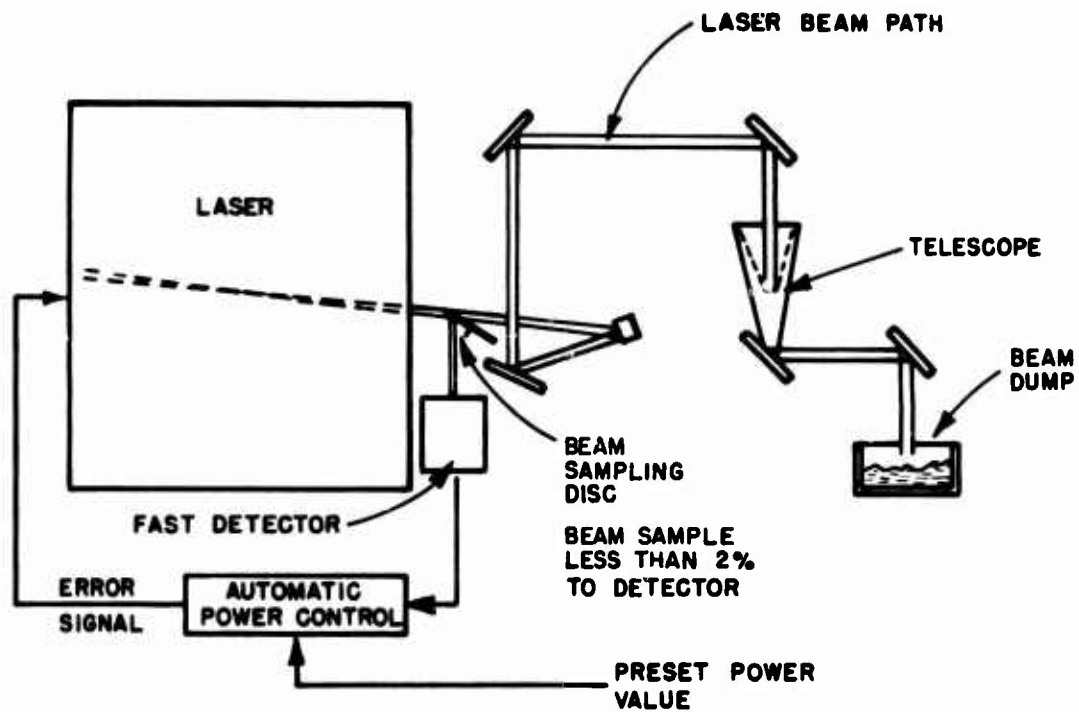
3. Stability of Spot Location

This task verified the reproducibility of the six water cooled copper mirrors that form the optical path between the aerodynamic window and the beam impingement point on the work-piece. A secondary objective established the coincidence of the visible beam from the Helium-Neon alignment laser relative to the impingement point of the invisible 10.6 micron beam from the CO₂ laser. The Helium-Neon laser used the same mirrors as the main laser beam, plus an additional set of mirrors and lenses to introduce its beam into the main beam optical path.

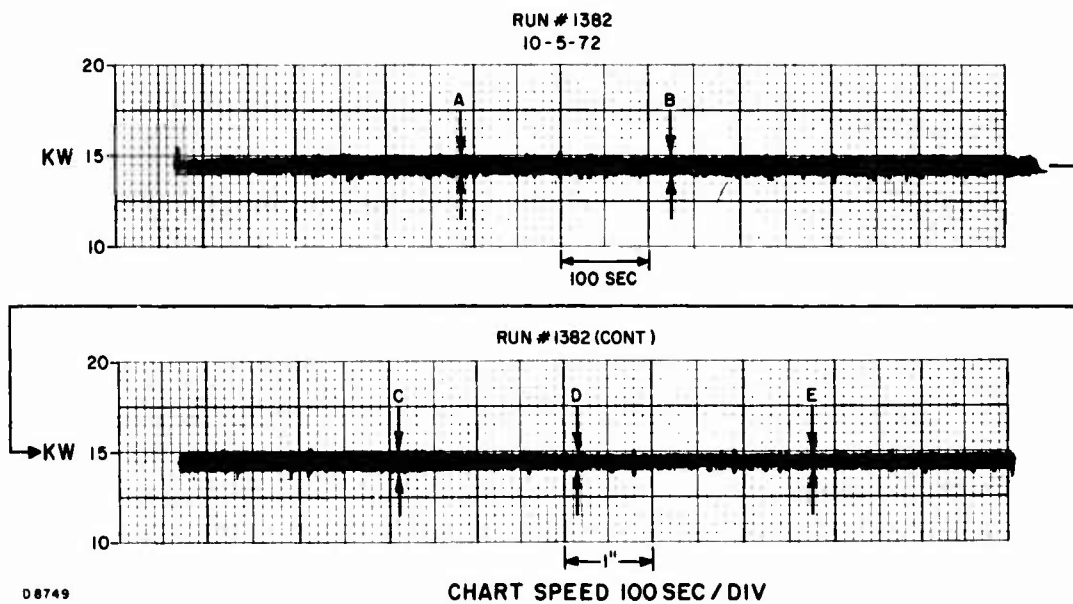
For these tests several series of experiments separated by a run at high levels of power were carried out as follows:

Step 1 Prerun Tests

1.1 Place unmarked graphite target under beam



EXPERIMENTAL SET UP



TYPICAL POWER TRACE (14.5 KW)

Figure II-3. LONG TERM REGULATION OF RUN POWER

- 1.2 Measure location of alignment spot ($\pm 0.001"$)
- 1.3 Fire CO₂ laser.
- 1.4 Observe ($\pm 0.01"$ at 5x) coincidence of CO₂ mark on graphite alignment laser spot.
- 1.5 Repeat 1.1, 1.2, 1.3, 1.4 six times

Step 2 Run CO₂ Laser 30 minutes at 15 kW

- 2.1 Leave workpiece in place
- 2.2 Deflect beam into dump

Step 3 Post Run Tests

- 3.1 Place unmarked graphite sample in target
- 3.2 Measure location of alignment spot
- 3.3 Fire CO₂ laser
- 3.4 Repeat 3.1, 3.2, and 3.3 six times

Step 4 Measure all CO₂ Target Marks ($\pm 0.001"$)

Step 5 Compare Data from Step 1 with Data from Step 3

Step 6 Analyze significance of Step 5 comparison

Fig. II-4 illustrates the experimental set up. In carrying out the above steps three measurement techniques were required. These are described in Table II-1.

Note: Fixed blade of micrometer located against machined surface of target for reference. Same surface used with cross hairs.

These techniques are illustrated in Fig. II-4.

The observed arithmetic averages of the CO₂ beam spot marks from Step 1 and Step 3 suggested that the location of one diameter shifted 0.0055 inches (less than $\frac{1}{4}$ of a F/7 focal spot diameter). The other diameter did not shift (Fig. II-5). This shift in recorded position of the beam spot was analyzed statistically and was determined not to be significant. Additionally, an almost identical shift in the position of the same diameter was reproduced simply by re-measuring the same target six times - suggesting that the shift results from block placement for measurement.

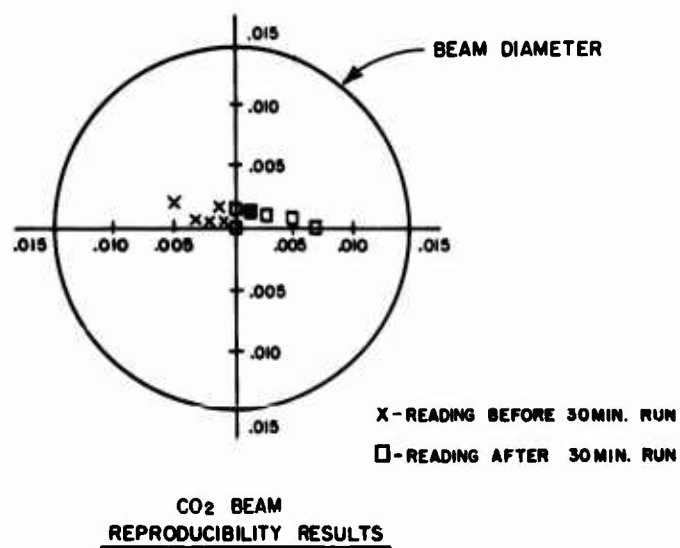
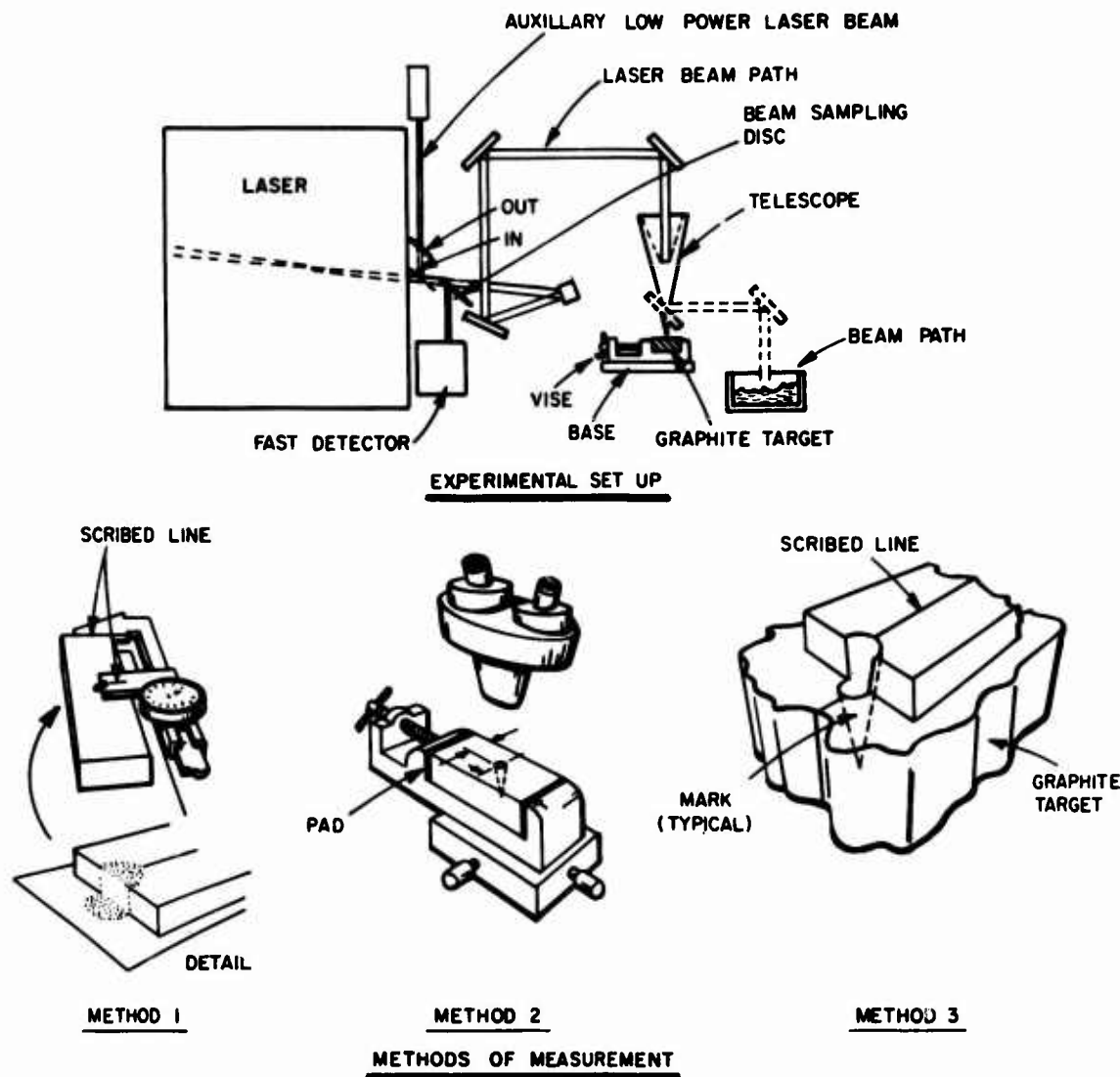


Figure II-4. SPOT STABILITY EXPERIMENT

Method	Variable	Measuring Tool	Remarks
1	Alignment spot location on graphite target (Step 1.2 & 3.2)	Vernier Caliper with special reference line on moving blade.	Line placed coincident with spot dia. using 5X eye loop. Vernier read to nearest 0.001" Two observations 90° apart.
2	CO ₂ laser spot location in graphite target (Step 1.3 & 3.3)	Micrometer stage on 25X microscope with cross hair reticle in eye piece.	Cross hair placed coincident with diameter of hole in target using 25X microscope. Micrometer read to nearest 0.001". Two observations 90° apart.
3	Coincidence of alignment spot with mark in target	Scribed reflector at target surface covering 1/2 of mark in target.	Estimated using 5X eye loop (0.01"). Two observations 90° apart.

Table II-1. SPOT MEASUREMENT TECHNIQUES

The findings are summarized in the following paragraphs:

The position of the auxiliary low power laser in the visible range was checked at 5x against a scribed mark on a precision vernier caliper and there was no observed shift from run-to-run or between groups of runs separated by a 30 minute full power run.

The reproducibility and control of the mirror focusing system for the 10.6 micron welding beam was verified by accurately measuring the position of target marks produced prior to and after the 30 minute full power run. The indicated movement is less than 25% of the beam diameter and has no statistical significance. The apparent movement appears to come from experimental error in placement of the block for measurement.

4. Repeatability Under Welding Conditions

In these tests all the elements of the laser system associated with making welds were tested by producing butt welds with a time interval of at least 48 hours between each weld. This demonstrated an ability to reproduce a desired weld after an extended period of time during which the laser was used for other tasks.

Eight plates of Type 321 stainless steel, 0.250" thick, 6" wide, and 12" long were prepared by machining and cleaning with acetone. The eight plates provided material for four butt weld samples using the following procedure:

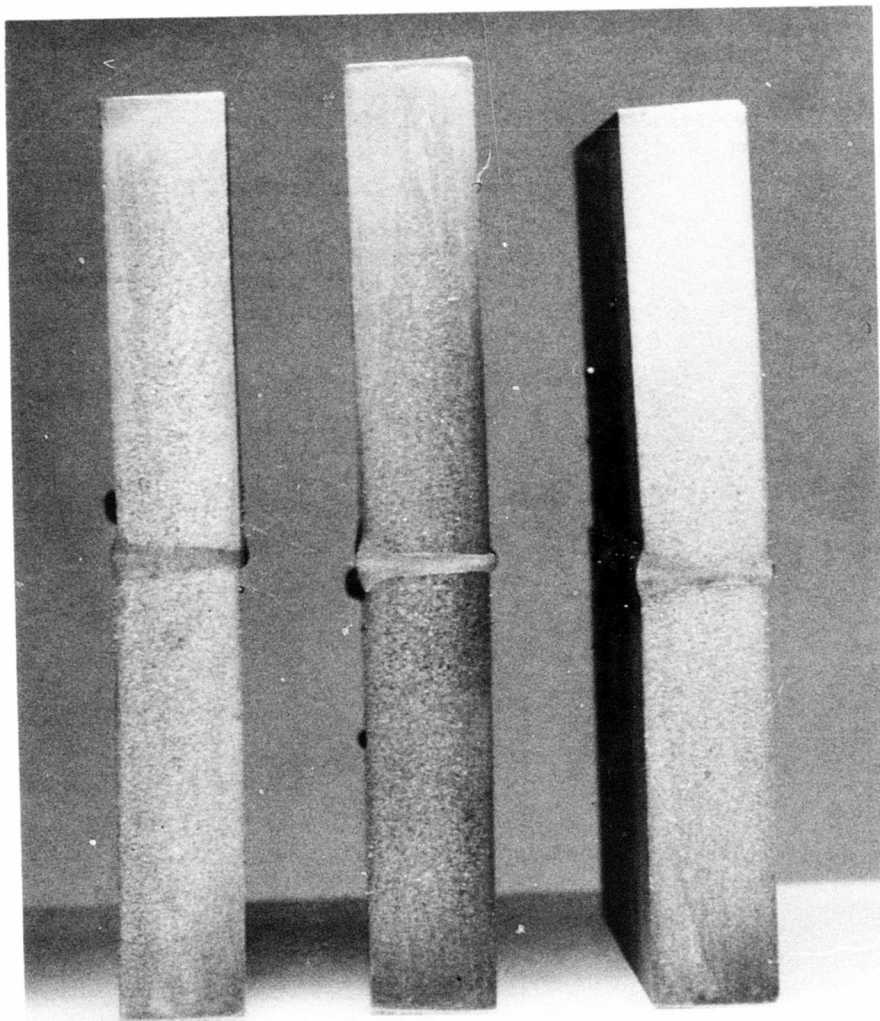
Laser Power:	15 kW (aerodynamic at window) *
Speed:	100 IPM
Focus:	1/16" below plate surface
Beam Angle:	90° to plate surface
Beam Spot Size (F/NO):	F/7
Type and Place of Shielding Gas:	Top: Helium in off axis gas lens 45° 200 CFH Bottom: Argon 6 CFH in 1"x1" back up channel

* 10.5kW on work

On each of four days, spaced at least two days apart, each sample was welded by setting the procedure variables directly onto the controls without adjustment and initiating the automatic welding cycle. The laser was used for other tasks during the time interval between the welds. The procedure selected to produce the weld was based on prior welding experience. It is not intended to represent an optimum combination of welding variables as Task 6 was aimed at exploring the interaction of power, speed, focus, beam angle and selecting the best combination.

The off axis shield was used to provide a non-turbulent flow of Helium Gas over the beam interaction point. Without the inert gas, a standing ionization or plasma cloud would form above the weld, absorbing a large portion of the laser power and thus preventing the desired weld penetration. This type of shielding over the weld samples was sufficient for this task. The welded samples were sectioned and etched to allow a visual observation of the weld zone.

The weld profiles, Fig. II-5 indicate the same depth-to-width ratio of the molten zone. The small changes in the cross section profiles were typical of variations seen along the length of any given welded seam. The top bead may be influenced by the gas shielding but does not change significantly. All the welds had complete penetration along the entire length of the seams.



MATERIAL - AISI TYPE 321
THICKNESS - 1/4"
POWER - 15 kW BEAM POWER
SPEED - 100 IPM
SHIELDING GAS - HELIUM (TOP)
ARGON (BOTTOM)

Figure II-5. REPEATABILITY TEST WELDS

III - PROGRAM MATERIALS

Aerospace structures are produced from a large number of materials. The materials selected for this program represent a broad cross section of useful engineering and manufacturing characteristics.

Program Materials

Type

- Titanium Alloy (Ti6Al-4V)
- Nickel Base Alloy (718)
- Low Alloy High Strength Steel (300M)
- Aluminum Alloy (2219-T87)
- Austenitic Stainless Steel *(AISI321)

* Phase one only

Each alloy was investigated at several nominal thicknesses:

Program Materials

Nominal Thickness

0.25 inch
0.37 inch
0.50 inch
0.75 inch

The base metals selected for this program represent a range of materials, compositions and strengths to show the diverse capabilities of laser welding. All are used currently throughout the aerospace industry and will be used in the foreseeable future in both welded and nonwelded applications. Each has attractive design properties such as toughness, strength, stress corrosion resistance and elevated temperature stability. All are considered weldable by one or more processes. Table III-1 sets forth alloy designation. Nominal strength and procurement specification. Table III-2 lists program thicknesses.

A. ALUMINUM ALLOY

Aluminum Alloy 2219-T87 represents an extensive background in both welded and nonwelded applications, particularly where strength is required at moderate elevated temperatures, compared to the new or slightly higher strength 7XXX series alloys such as 7039, 7007 and 7106. It has also demonstrated good resistance to stress corrosion cracking with various weld, post-weld heat treatments compared to 2XXX series alloys such as 2014, 2021 and less weldable 2024. Recently, 2219-T851 was selected for major air frame structures because of its good fracture toughness and elevated temperature stability. It has also been selected as base line alloy for liquid engine tankage.

B. STAINLESS STEEL

Stainless Steel 321 is considered a good representative of the 18-8 type stainless series with Ti added as a carbide stabilizer to avoid heat affected zone intergranular cracking from welding or elevated temperature service. It finds wide usage in aerospace applications requiring formability, weldability, moderate strength at elevated temperatures and corrosion resistance. Alloy 21Cr-6Ni-9Mn was also considered a candidate as the next step to a higher strength stainless and is being initially used as hydraulic tubing in several large commercial jet aircraft. However, it is considered that 321 will be more representative of the stainless family at this time. Stainless was welded in Phase 1 only of this program.

C. TITANIUM ALLOY

Titanium Alloy 6Al-4V is the most universally accepted alloy for the majority of titanium applications in the aerospace industry. It is available in all product forms and applications range from small fasteners heat treated to 160 UTS to large plate and die forgings in the annealed condition. Structural applications utilize the annealed condition to take advantage of good strength and high toughness so this condition is selected for this program. Ti-6Al-2Sn and Ti-8Al-1Mo-1V were also considered but lower toughness and poorer weldability of the former and fewer existing applications of the latter, generally in sheet gauges, were their main drawbacks. The more recently developed Beta alloys were also considered and have potential for future application after final development. The alpha beta 6Al-4V is more representative of current and future applications.

D. NICKEL BASE ALLOY

Nickel Base Alloy 718 achieves the highest strength of the nickel base alloys and is considered more weldable than other popular nickel base alloys such as Waspalloy or Rene 41. Its main advantage is stability at elevated temperatures up to 1000°F so it is applied mainly in engine areas such as hangers, ducting fasteners and fittings. It is also used in turbine manifolds and gas generators. It is used in both "as welded" and "Weld plus STA", the former welds can be located in low load areas.

E. LOW ALLOY HIGH STRENGTH STEEL

Low Alloy High Strength Steel 300M quenched and tempered, is used extensively as heavy section high strength landing gear components and is the highest strength commercially available steel acceptable to design engineers for critical applications. Although not universally used in components, it has been flash welded. Repair fusion welds have been satisfactorily accomplished. It is a good candidate for fabricating large components by welding but undoubtedly will require quench and tempering after welding. That post weld heat treatment was used in this program. The Maraging steels and HP 9Ni-4Co series alloys were also considered at lower strength levels for ease of fabrication, forming and their higher toughness level, but their composition does not fall within the scope of the program's low alloy high strength steel definition.

System Classification	Alloy Designation	Product	F _{TU} Capability (DS1)	Procurement Specification
Aluminum Alloy	2219-T87	Plate	62	MIL-A-8920A
Stainless Steel	321 ANN	Plate	75	MIL-S-6721
Titanium Alloy	6AL-4V ANN	Plate	130	MIL-T-9049
Nickel Base Alloy	Inconel 718	Plate	180	AMS 5596 (1)
Low Alloy, High Strength Steel	300M, Q&T	Bar	275	DMS 1935 (2)

- (1) Procured in solution treated condition and aged after welding.
(2) Processed in normalized condition for welding prior to Q&T.

Table III-1. PROGRAM MATERIALS

System Classification	Specimen Thickness			
	.25	.37	.50	.75
Aluminum Alloy	.25	.37	.50	.75
Stainless Steel	.25	.37	.50	.75
Titanium Alloy	.25	.37	.50	.75
Nickel Base Alloy	.25	.37	.50	.75
Low Alloy, High Strength Steel	.25	.37	.50	.75

Table III-2. PROGRAM MATERIALS

SECTION IV

PROCESS TECHNOLOGY

A number of the tasks throughout the program had as their objective the development of laser welding process technology in support of the preparation of plates for NDE and mechanical testing. These include:

- Phase I - Task 1: Reflectivity
- Phase I - Task 2: Evaluation of Shield Gases
- Phase I - Task 3: Tooling
 - 3.1: Tooling for Gas Shielding
 - 3.2: Underhead Tooling
- Phase I - Task 4: Effect of Surface Finish
- Phase I - Task 6: Effect of Process Variables
- PhaseII - Task 1: Procedure Development, Cleaning & Preparation
- PhaseII - Task 1: Procedure Development, Joint Fitup (gaps & mismatch)

This information has been brought together in Section IV because these tasks constitute the nucleus of a manufacturing technology. This technology could be of assistance in evaluating equipment, tooling concepts and production approaches to the implementation of heavy plate laser welding in the aerospace industry.

A. PREWELD PREPARATION

Preweld preparation requirements were identified during procedure development in Phase II - Task 1. Their welds were the first program welds to be subjected to radiography to check internal soundness. Internal soundness is an important criterion in selection of a preweld cleaning process.

1. Cleaning Prior to Laser Welding

Wire brushing plus acetone cleaning was found to be an effective method of cleaning titanium, nickel base alloy and carbon steel. Aluminum cleaning was not reviewed. Only total oxide removal was evaluated for aluminum.

In this program the plate edges to be fusion welded were prepared by blanchard grinding. Blanchard grinding places a premium on deburring and cleaning. Grinding produced heavy, rolled burrs at the edge of the plate where the wheel exited.

This edge was found to be a potential source of entrapment for grinding fluid and wheel debris. And, had to be completely removed by deburring. The ground face was suspected of holding some imbedded grit particles.

Aluminum edges were prepared by dry milling.

In all, four commonly employed preweld preparation processes were evaluated:

- Method I : Deburr, Acetone clean with wire brush.
- Method II : Same as Method I plus detergent wash (Alconox - Tri Sodium Phosphate) rinse.
- Method III: Same as Method II plus chemical etch/rinse (see Table IV-1 for etchants).
- Method IV : (Aluminum Only) Mechanically remove oxide film by scraping surface with a sharp edged tool. No other treatment was evaluated on aluminum.

In developing the procedures for the manufacture of test plates, several set-up welds were made using each of the above methods under similar speed, power, focus and shield gas settings. These welds were radiographed and rated according to the amount of observed porosity. Fig. IV-1 summarizes the ratings for each method of preparation.

Careful deburring, followed by wire brushing and acetone sluicing exhibited the lowest porosity index for each material on which this simple cleaning method was applied. (Carbon steel, Titanium, and the Nickel base alloy).

Where facilities are equipped to carry out detergent cleaning or chemical etching under close process control, these methods might also be adopted. Their results were not markedly different from the wire brush/acetone methods. Optimization of chemical cleaning procedures, however, was not within the scope of this study nor was it consistent with available facilities.

Aluminum cleaning methods have been extensively reviewed in other programs (Ref. IV-1). The method chosen represents a procedure that has been used to avoid porosity in GTA & GMA welding of critical components. Total removal of the oxide film eliminates the major base metal related source of hydro-

PROGRAM MATERIAL	COMPOSITION (500 ml BATCH)
Low Alloy Carbon Steel (300M)	Fe Cl ₃ 30 gms H Cl 100 ml H ₂ O (Tap) 400 ml Temp. 100° F Time 10 - 15 minutes
Titanium Alloy (6Al - 4 V)	HNO ₃ 225 ml HF 20 ml H ₂ O (Tap) 445 ml Temp. 100° F Time 10 - 15 minutes
Nickel Base Alloy (Inconel 718)	HNO ₃ 100 ml HF 10 ml H ₂ O (Tap) 390 ml Iron (Fe) 5 gms Temp. 100° F Time 10 - 15 minutes
Aluminum Base Alloy (2219 - T87)	Not etched

Table IV-1. PREWELD ETCHING SOLUTIONS

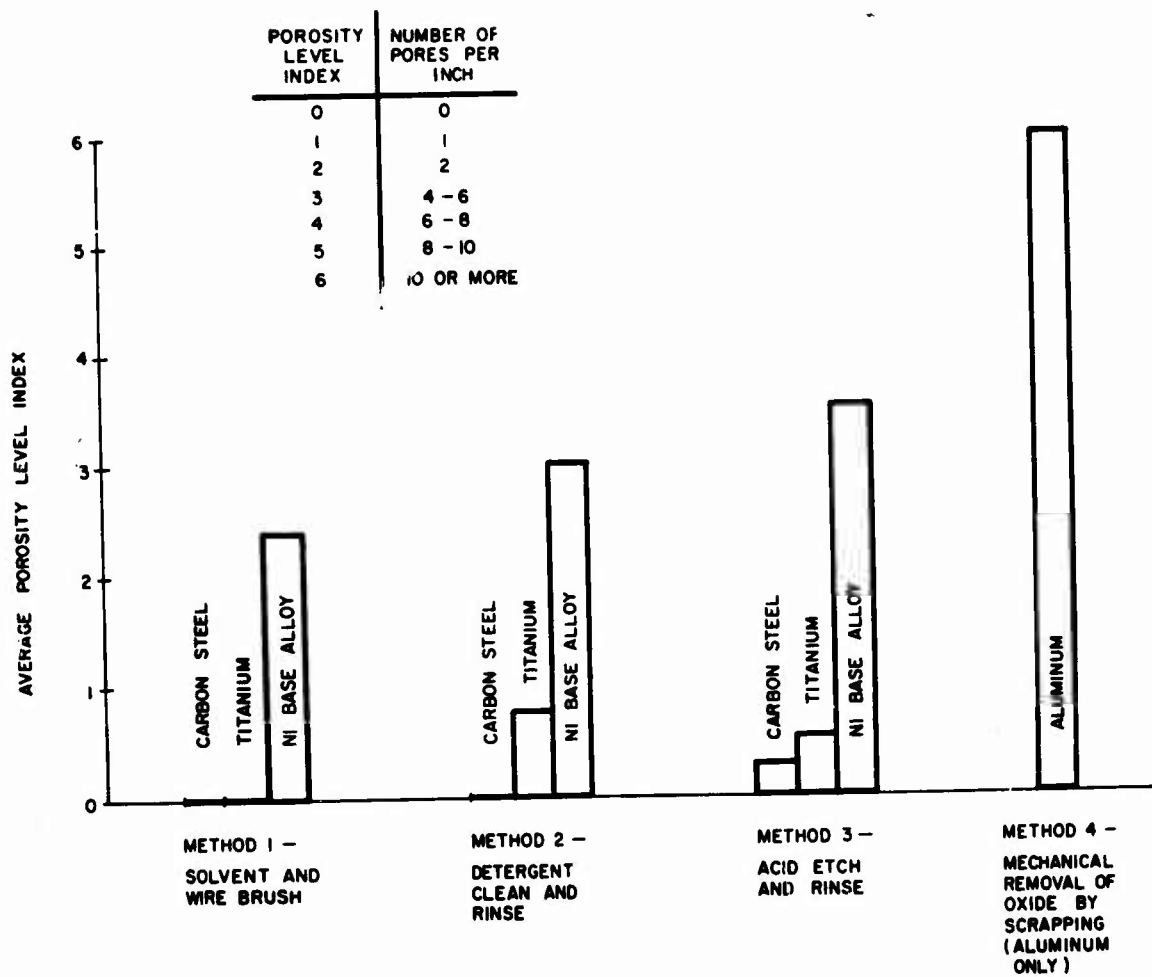


Figure IV-1. RELATIVE EFFECTIVENESS OF CLEANING METHODS

gen. Hydrogen is a major source of porosity in aluminum. As noted in Fig. IV-1, even this fully developed method of cleaning failed to produce an acceptable laser weld in aluminum. The basic need was therefore assumed to be for further aluminum welding process development - not better cleaning.

2. Surface Finish Effect and Reflectivity.

Task 2 - Phase I measured reflection during welding to determine if phenomena, which are characteristically associated with deep penetration welding (particularly the cavity), actually do cause much of the beam to be absorbed. The beam of a CO₂ laser (10.6 micron wavelength) exhibits high reflectivity from metal surfaces when the power level is sufficiently low so that the surface is not disturbed or oxidized. However, in order to effect a narrow deep weld, several phenomena are involved which may change the reflectivity situation. These are:

- Melting
- Vaporization
- Cavity Formation

Additionally, some oxidation of the weld pool may be assumed under conditions of marginal shielding.

All of the above factors influence reflectivity of the impinging beam.

In Task 4 - Phase I tests were conducted to determine if work piece surface finish might also be a factor - one which would have to be taken into consideration with respect to penetration control in production.

The results of Task 4 suggest that the program materials can present greatly varied surface finishes to the laser beam without influencing the ability of the beam to penetrate the material.

The average penetration depths observed in the presence of the various surface finishes are shown in Fig. IV - 2. No significant effect was observed. The maximum difference in penetration for all surface conditions is only 3.5%. Averaging all materials together reduces the maximum observed difference to 1.39%. It would be difficult to separate effects such as these from run power variations or measurement inaccuracies. If workpiece conditions did influence the welding beam, the effect might be expected to be more

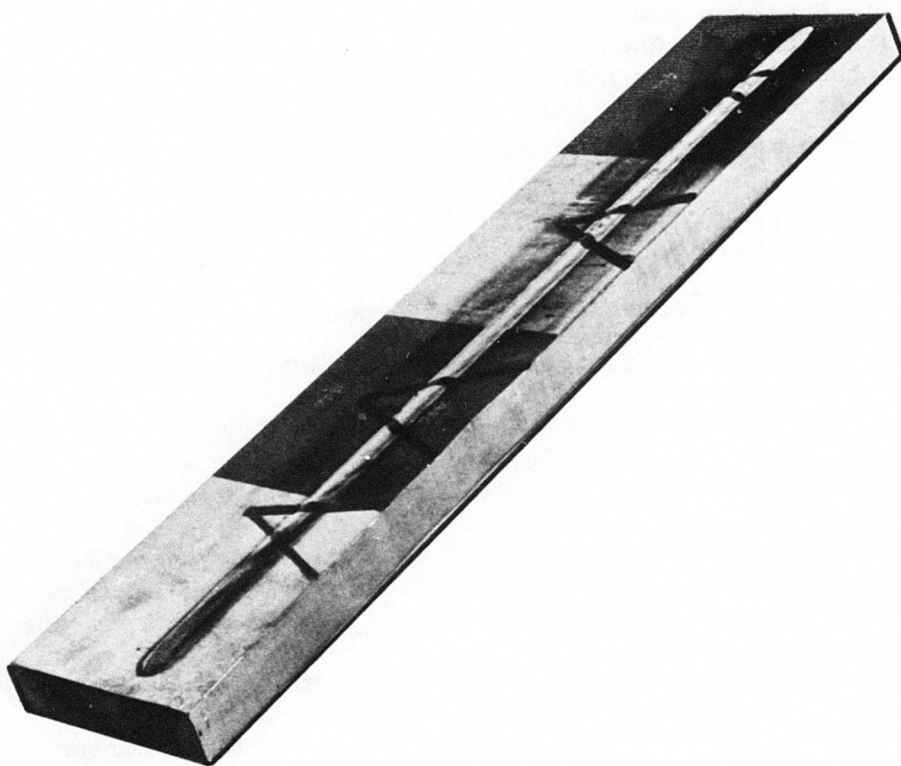


Figure IV-2. TYPICAL SURFACE FINISH TOLERANCE SPECIMEN

apparent in the aluminum samples. In these samples one area had been scraped and polished. This area could have had, at most, only a light natural oxide. At the opposite end of the same sample the aluminum was covered with a heavy mill oxide. According to Fig. IV - 2 the penetration at both areas was identical.

Tables IV - 2 and IV - 3 describe the conditions under which a half inch thick plate of each program material was prepared with four zones representing different surface conditions and welded (bead-on-plate, partial penetration) with a 15kw beam (10.5kw on work). A welded sample is shown in Fig. IV - 3. The depth of penetration was measured metallographically at two points within each zone. Experimental finishes ranged from bright polished surfaces through rough machined surface conditions to the as-received finish. (Table IV - 2).

A second set of reflectivity tests measured the beam impingement region reflection at 7% of the incoming energy when welding stainless steel, carbon steel, titanium, and nickel base alloy. Aluminum reflected about 14% of the beam.

The experiment was conducted by placing a calibrated thermopile at declination angles of 20° , 40° , and 75° with respect to the laser beam. The thermopile was optically filtered (long pass) to prevent visible and near infrared light from entering. The power of the laser and thermopile readings were recorded simultaneously. The data from the off axis reading was plotted and extrapolated to 0° to permit an estimate of the irradiance where it reaches its maximum, coincident with the beam path location. Readings at various declination angles were checked at a second azimuthal position 90° from the initial position to assure that reflectance was equal in all directions. When this assumption had been verified total irradiance was calculated by integrating thermopile readings over a hemisphere with the surface of the work piece as its base and the weld at its center. Corrections were then made for filter and optical train transmission. The correct reflected power value was then divided by the recorded laser power.

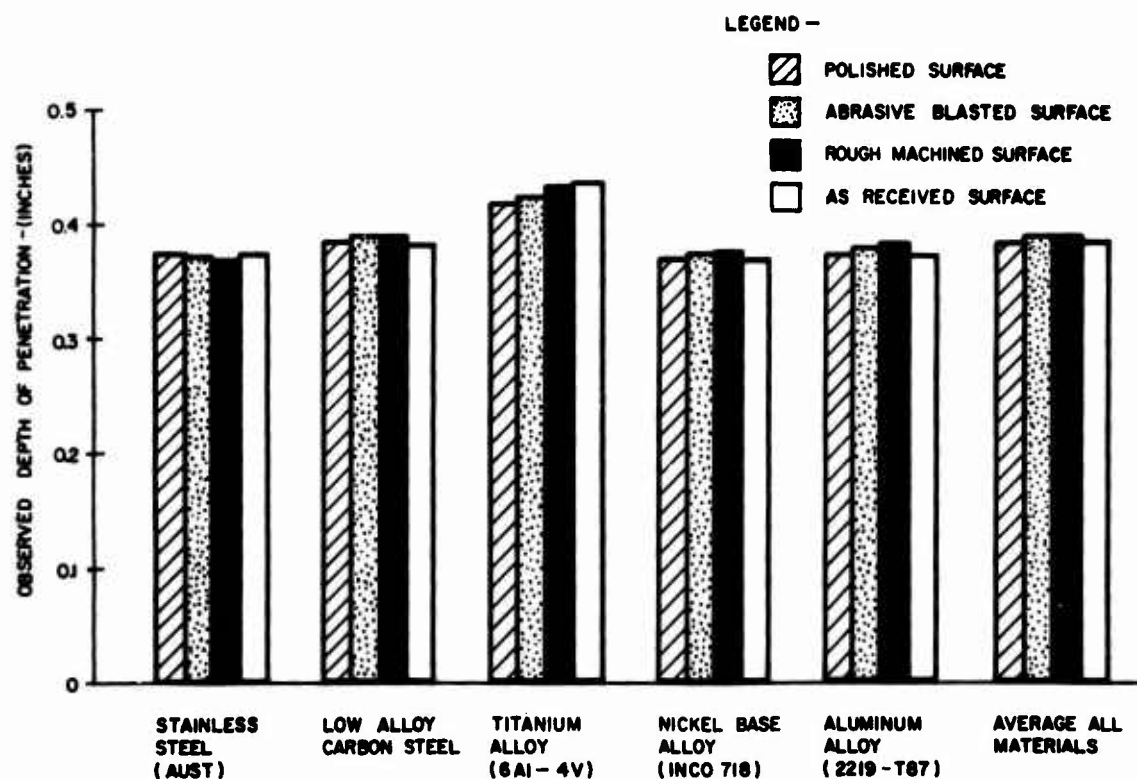


Figure IV-3. OBSERVED PENETRATION

CONDITION	DESCRIPTION
Mechanically Polished	Produced by placing end of test bar on metallurgical silicon carbide abrasive polishing belt with 280 wet paper, resulting in a bright metallic finish.
Abrasive Blasted	Blasted at 90 psig with dry 250 grit non-recycled silicon oxide grit resulting in a uniform matte gray finish.
Rough Machined	Generated with a single point tool mounted in a shaper so that distinct grooves (30/inch) were scribed approximately 0.015 inches into the surface.
Received	Aluminum was left with the original gray heat treating oxide from the mill on its surface. All other materials were scale free and pickled to a light matte gray as they came from the mill.

Table IV-2. EXPERIMENTAL SURFACE CONDITION

<u>VARIABLE</u>	<u>SETTING</u>
Power (kW)	15 (10.5 on Work)
Speed (inches per minute)	20
Telescope-Work Distance	28-1/16
F/Number	7
Surface Condition	Variable
Shielding	
Upper Surface Gas	90/10 HeA (126 CFH)
Lower Surface Gas	none
Tooling	10" Hood

Table IV-3. EXPERIMENTAL WELDING PROCEDURE-
SURFACE FINISH EFFECT

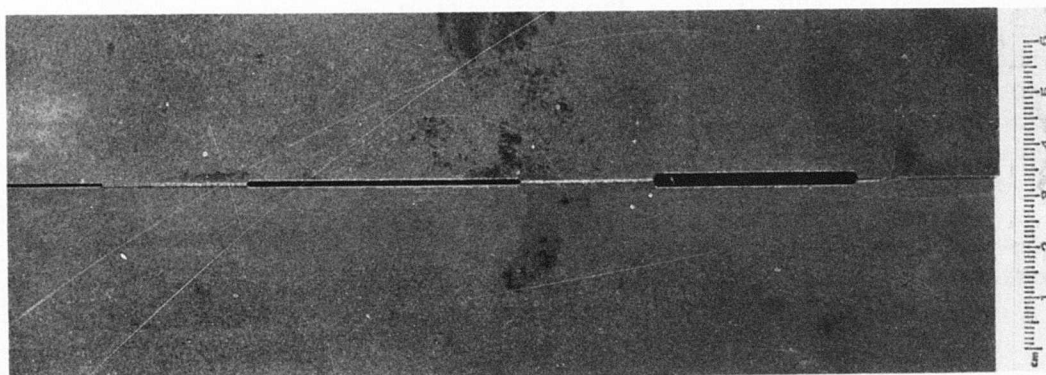


Figure IV-4. FIT-UP TEST PLATE

The percent reflection of as-received surfaces was as follows:

Stainless Steel	7%
Titanium	7%
Low Alloy Carbon Steel	7%
Nickel Base Alloy	7%
Aluminum	14%

The true values for reflection may be slightly less than those listed above. Unavoidable spillover of low intensity beam energy onto the test plate occurs each time welding is carried out. This light fell well outside of the weld zone but within the viewing area of the detector. With its low specific energy this spillover light would reflect rather efficiently from any metal surface which it struck. This extraneous source of 10.6 micron light was minimized by painting the cool area of the plate black using colloidal graphite.

3. Effect of Variations in Joint Fit-Up

Because the beam can penetrate substantial plate thicknesses in a single pass, the accepted joint geometry for laser welding is that of the butt weld. However, variations in the preweld fit-up of butt joints occasionally occur. The plates may not be aligned across the joint (mismatch). This is particularly common in circumferential joints between cylindrical sections.

The faces of the joint may not touch all points along the length of the joint. This is called gap. In arc welding, gap may affect heat flow patterns ahead of the slow moving process. In the case of high energy beams, this effect is probably not important. However, the gap does permit the beam to pass between the plates and usurps the role of the cavity. This creates a special problem for beam welding processes which depend on the cavity.

In this program, the effects of variations in preweld fit-up were studied as a part of Task 1, Phase II and the following observations were made:

a. Mismatch. Mismatch conditions of as much as 1/16 inch were encountered in 1/2 inch thick titanium butt welds with no effect on the exterior appearance of the weld. The mechanical testing of joints with mismatch was beyond the scope of this program.

b. Gap. A specimen was designed (Figure IV-4) with segments of the butt joint face ground back to create a series of increasing gaps. Each gap was approximately 1 inch long. In these studies, standard welding procedures were subjected to inconsistent joint fit-up conditions in the form of these manufactured gaps in 1/4 inch plates of program materials. Gaps up to 0.14T were investigated.

Small	0.02T (0.005")
Medium	0.04T (0.010")
Large	0.08T (0.020")
Very Large	0.14T (0.035")

Gaps between abutting faces of a joint cause the crown to sink and, if the gap is severe, the underbead pulls up. Weld cross section is reduced. Ultimately, the beam drops through the joint without interacting with the faces of the joint at all.

Figure IV-5 illustrates the effect of variable fit-up in the form of gaps on weld cross section. Even the smallest (0.02 T) gap influences joint cross section, but gaps of about 0.04 T can be tolerated before the cross section drops below full (100%) plate thickness.

At the 0.08 T gap, both crown and underbead were recessed so that only a thin joint was formed at mid-thickness.

B. TOOLING

Welding processes such as electron beam and laser penetrate the work by forming a vapor cavity in the joint at the point of beam impingement. When full penetration is achieved, this cavity extends through the plate. Experience in the design of tooling in vacuum electron beam welding has suggested that

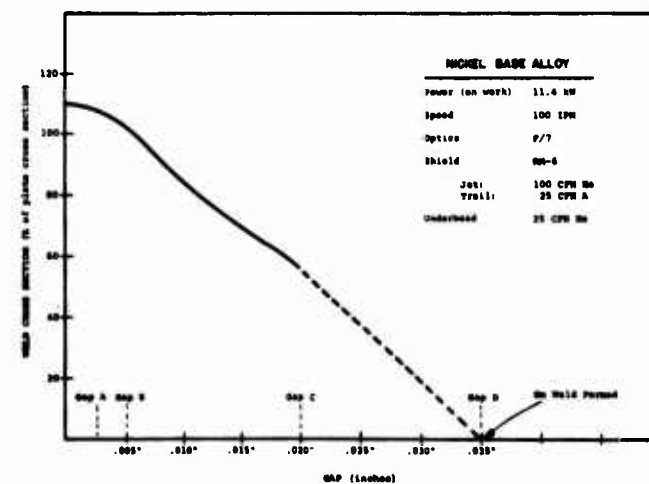
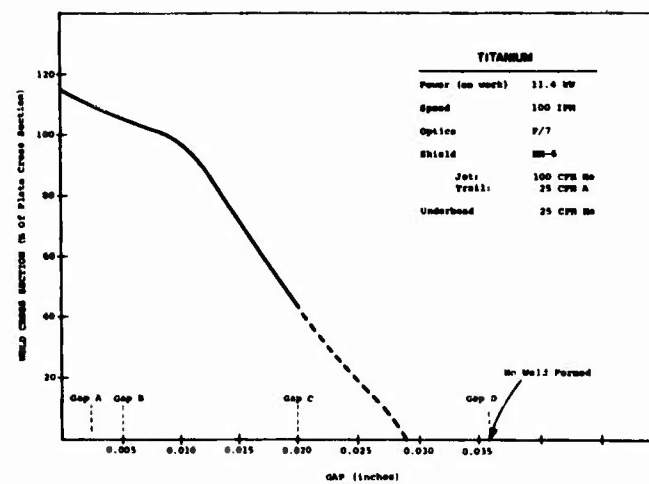
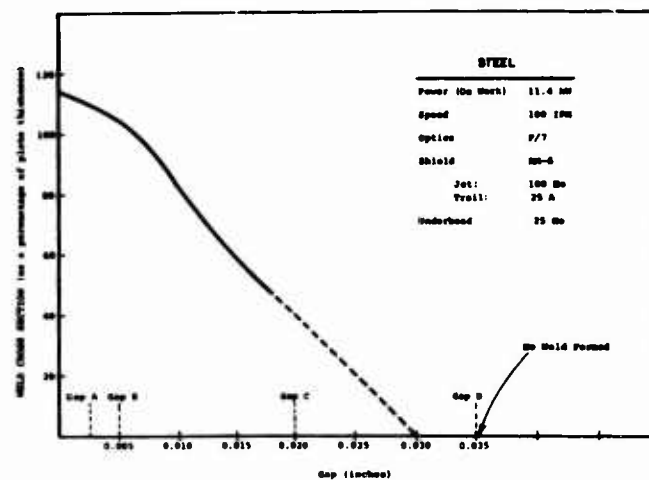


Figure IV-5. EFFECT OF JOINT FIT (GAPS) UP ON WELD CROSS SECTION

a portion of the beam energy (and some molten metal) exits from the bottom of the cavity. This energy/metal stream interacts with either the underbead tooling, or if the tooling does not provide a backstop, with any work piece surfaces that may be located within several inches of the weld underbead.

In these tests (Task 3.2 Phase I) tooling considerations for laser welds were considered.

1. Backstop Tooling

The need for underbead backstop material did not appear to be as important for laser welds as it is for electron beam. Surfaces 1 1/4 inches below the weld were not damaged by the laser beam. The electron beam would have affected such surfaces. Surfaces 1/4, 1/8 and 1/16 below the surface did receive molten metal. Surfaces 1/8 and 1/16 inches below the work also received beam energy, Figure IV-6.

Beam stops of copper, graphite and stainless steel were all placed 1/16, 1/8 and 1/4 inches below the workpiece to determine if there was an optimum placement - material combination that would affect underbead width, drop thru or contour. No overall trend was noted.

Thus the back stop portion of tooling appeared to represent a means for protecting other workpiece surfaces but exercised no effect on the underbead size or contour of the underbead.

2. Chill Spacing

Underbead chill proved to be more effective than backstop placement in controlling underbead size and contour. Figure IV-7 shows the stepped test chill bar, Table IV-5 lists the spacing levels, and Figure IV-8 shows the tooling used to establish uniform contact with the chill.

Increasing chill results in a sharper underbead extension according to Figure IV-9. Spacing chills less than one joint thickness apart does not appear to be desirable if a flat smooth underbead is desired.

Weld Parameters	Low Alloy Carbon Steel	Titanium Alloy	Nickel Base Alloy
Base Metal Specification	300 M (MIL S 8844 C12 Cond. E2)	6Al-4V (MIL-T-9046)	Inconel 718 (AMS 5596)
Heat Treat Cond. (as welded)	Normalized and Annealed	Annealed	Solution Treated
Thickness	0.25"	0.25"	0.25"
Travel Speed	100 ipm	Same	Same
Focus	f/i at 21-11/32"	Same	Same
Surface Preparation	Deburr, wirebrush and rinse with acetone	Same	Same
Shielding Gas Jet Trailer Set Back Lift Off Filler Wire Tooling Conf. Gap Mismatch	100 CFH He 25 CFH Argon 7/16" 0.040 (nom.) Not used F24 W/RM#6 Experimental Var. 005 Max. Unless Noted	Same Same Same Same Not Used Same Same Same	Same Same Same Same Not Used Same Same Same

Table IV-4. FIT UP TEST WELDING PROCEDURES

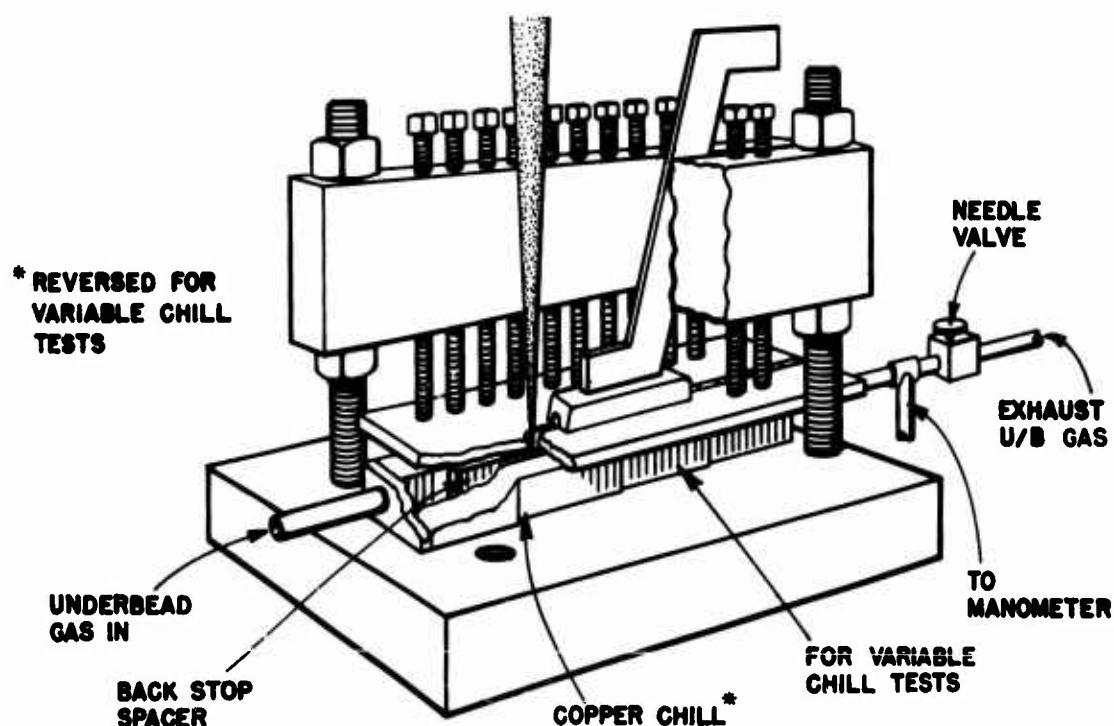


Figure IV-6. UNDERBEAD TOOLING EXPERIMENT

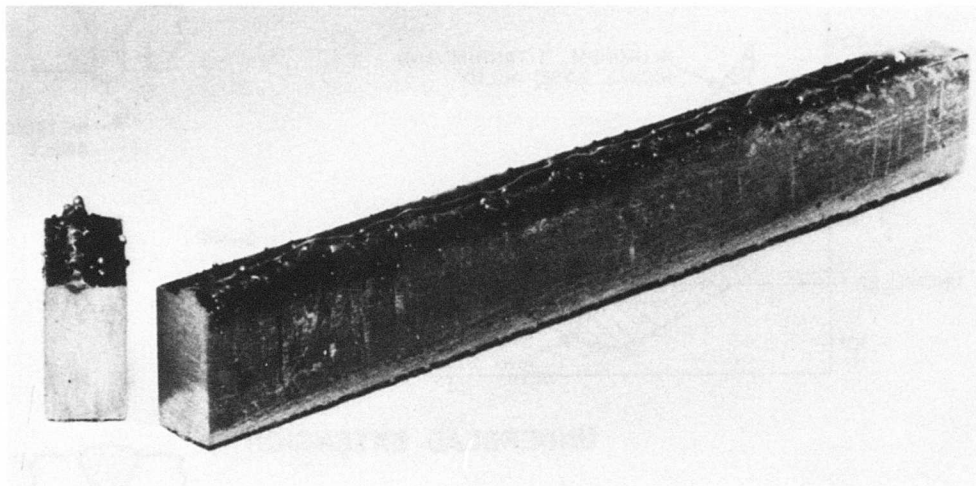


Figure IV-7. EFFECT OF UNDERBEAD ENERGY ON TOOLING

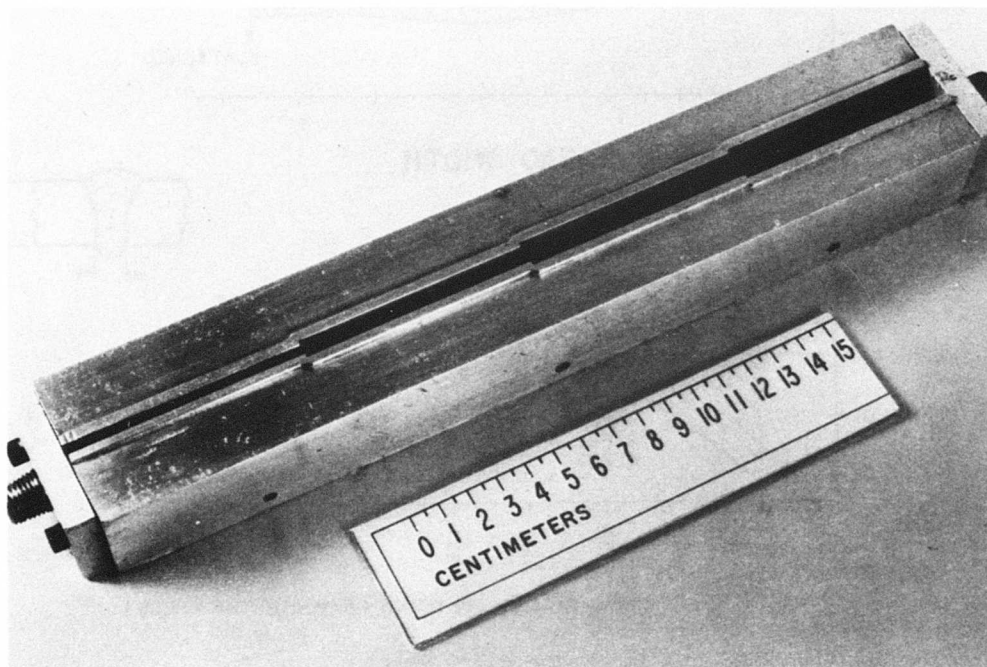


Figure IV-8. EXPERIMENTAL CHILL BAR

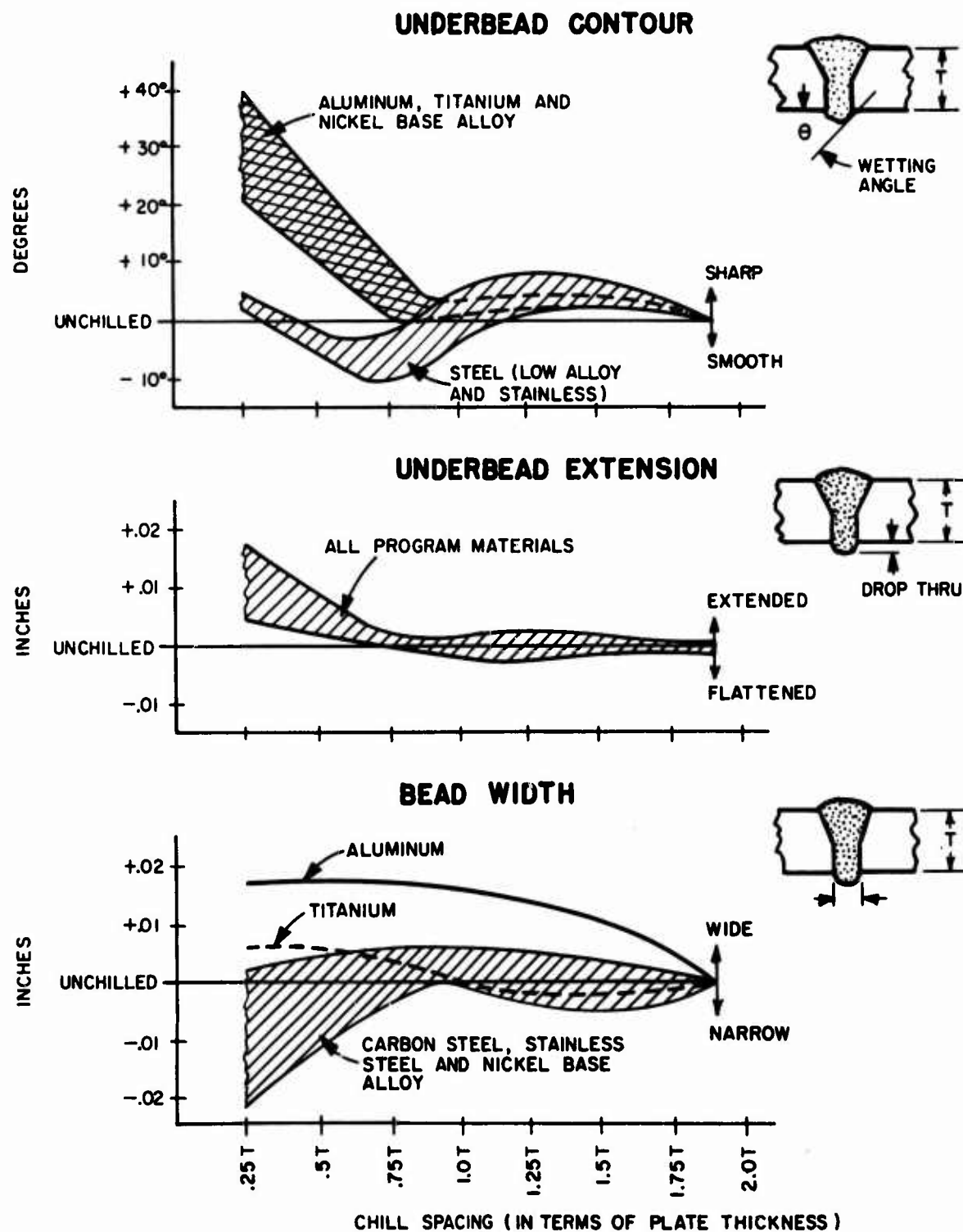


Figure IV-9. RELATIVE UNDERBEAD CONTOUR EFFECTS FROM CHILLS

VARIABLE	SETTING				
	Stainless Steel (AISI 321)	Low Alloy Carbon Steel (AISI 4130)	Titanium Alloy (6Al-4V)	Nickel Base Alloy (Inconel 718)	Aluminum Alloy (2219-T87)
Power ⁽¹⁾ (KW)	15	15	15	15	14
Speed (ipm)	90	85	100	85	130
Telescope-Work Distance	(2)	(2)	(2)	(2)	(2)
F/Number	7	7	7	7	7
Surface Condition	(3)	(3)	(3)	(3)	(3)
Shielding					
Upper Surface (Type)	(4)	(4)	(4)	(4)	(5)
(Gas/Flow-CFH)	He/50	He/50	H3/50	He/50	He/200
(Trail Gas/Flow/CFH)	A 25	A 25	A 25	A 25	N/A
Lower Surface (He/A in CFH)	4-2	4-2	4-2	4-2	4-2
Tooling (spacing of variable width copper chill bars - see Table IV-6)	A	A	A	A	A
Type Off Joint	BOP	BOP	BOP	BOP	BUTT

(1) Measured at beam exit from laser cavity.
 (2) All experiments run at a 28 inch distance from the telescope and also a distance of 28-1/16 inches.
 (3) All plates cleaned in accordance with Table III-2.
 (4) A composite hood with jet located in the forward lip of the trailer was used in all tests.
 (5) Diffuser manifolds placed one inch apart face-face along weld and sealed to plates with tape.

Table IV-5. EXPERIMENTAL WELDING PROCEDURES - TOOLING TESTS

CONFIGURATION	CHILL SPACING AT					
	ZONE A Inches	% (2)	ZONE B Inches	%	ZONE C Inches	%
I	0.062	25 (27)	0.186	75	0.311	125
II	0.100	40	0.224	90 (99)	0.349	140 (155)

(1) Thickness as a percentage of the 0.25 nominal plate thickness (percentage values in parentheses refer to the thickness-chill space relationship for the 0.227 inch thick Inconel 718 material).
 (2) Chill Bars made from copper, specimen rests on 1/8 x 1/8 inch lip machined into upper surface of bar. Narrow lip assures high unit pressure at plate-copper interface and assures good contact between specimen and chill bar.

Table IV-6. EXPERIMENTAL CHILL CONFIGURATIONS

Data for Figure IV-9 is presented in terms of relative change because discussion of absolute changes would have involved absolute bead widths. At this point in the program (Task 3.2 Phase I) no procedure development had been carried out and absolute data may have represented over or under welding in addition to chill effects.

3. Effect of Underbead Gas Pressure

The presence of identifiable droplets of ejected metal on the surface of backstop implies that pressure plays a role in the formation of the underbead. The possibility that slight underbead pressure might counteract the drop through of metal, was evaluated in this part of Task 3, Phase I.

These tests showed that underbead pressure has a definite effect on the somewhat protruding underbead of deep, narrow welds such as the laser (or electron beam) produces. Because the laser operates in air, this pressure could be adjusted to reduce underbead protrusion.

The effect of underbead pressure on laser welds is to push the protruding bead up toward, or even into, the test plate (Figure IV-10). The effect of pressure seems related to metal density. That is, the amount that the underbead is pushed up by a given pressure is roughly proportional to the density of the metal.

According to Figure IV-10, an underbead pressure of 18 mm of water would cause an aluminum bead to become flush with the test plate surface. A pressure of 22 mm would do the same for titanium. Figure IV-10 shows that the process is critical for these materials. Therefore, establishing and maintaining pressure within a fraction of a millimeter would be necessary to keep the process in control.

Nickel base alloys, carbon steel, and stainless steel respond less to a pressure change so that approximately 40 mm is required to produce a flush underbead. But, even 30 mm results in a lesser underbead projection than occurs at ambient pressure. For these heavier materials, significant control of underbead by pressure occurs over a range of pressures and appears to be practical.

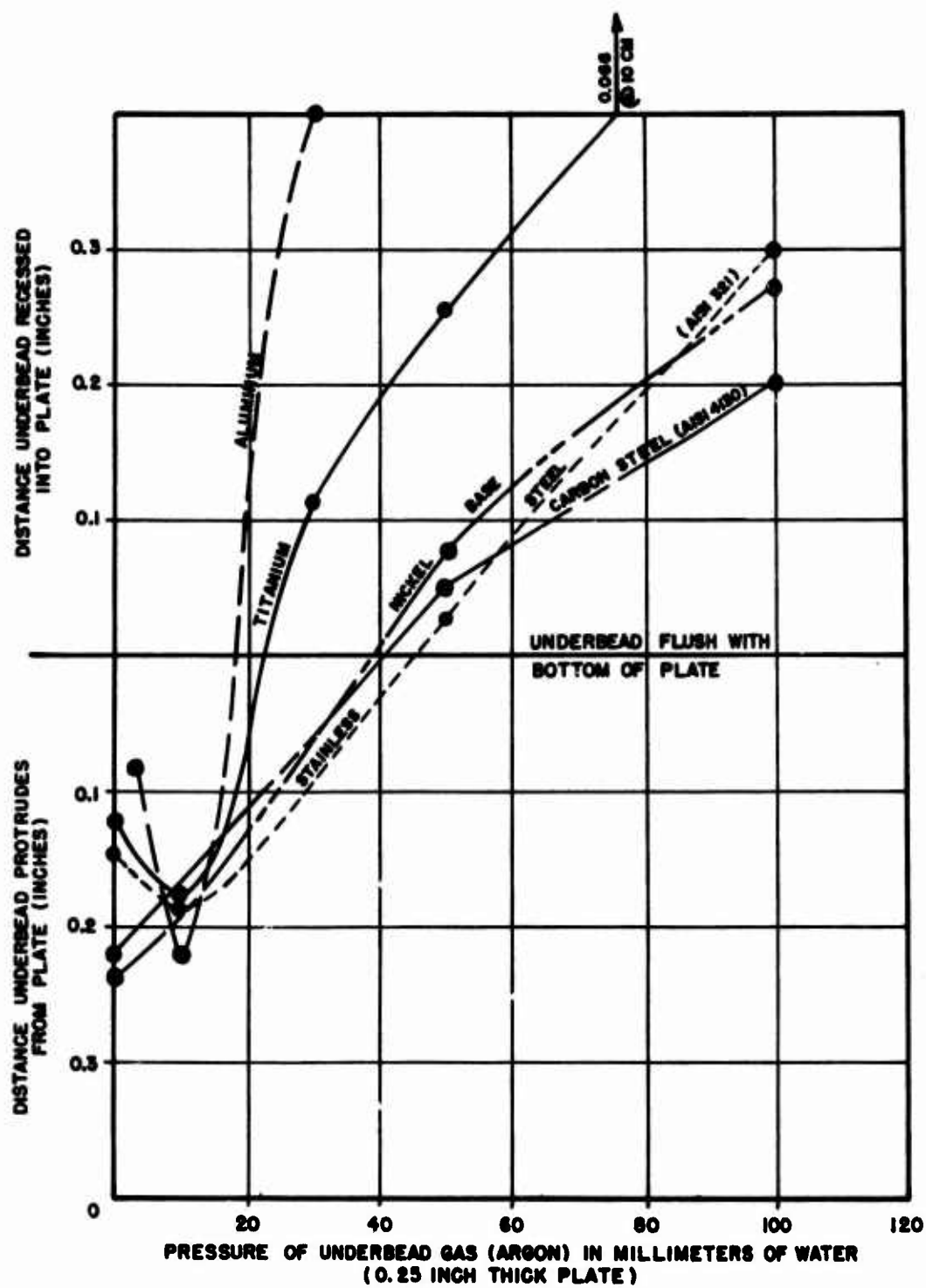


Figure IV-10. EFFECT OF UNDERBEAD PRESSURE ON UNDERBEAD SHAPE

As a corollary to the above ideas, it should be noted that failure to assure proper venting of underbead gas in tooling designs may cause inadvertent pressure changes with a loss of control over underbead contour. This would be particularly true of aluminum. The basic tooling arrangement shown in Figure IV-8 was used.

Measurements were taken at a point approximately 2 inches from the beginning of the weld. At this point the plate was fully penetrated and gas temperature (and pressure) had not begun to rise. Pressure readings are accurate ± 2 mm of water. The welds were produced in the test plate according to the procedure shown in Table IV - 8. The test material was 0.25 inches thick.

C. SHIELDING GAS PERFORMANCE

Unlike electron beams, the laser beam does not need a vacuum to produce a narrow deep weld in metals. The metals, however, need some form of shielding if the resulting welds are to be free of porosity.

The objective of Task 2, Phase I was to determine the suitability of several gases, and gas mixtures, to shield metals that were being welded by lasers. A suitable shielding gas for laser welding is one which:

- ... does not interact with the laser beam and thus reduce the amount of power available for penetrating the joint
- ... has good blanketing characteristics at the high speeds which characterize laser welding procedures
- ... is metallurgically compatible with the base material

In this task the effect on penetration of a candidate shielding gas was given first priority. Additionally, gases were qualitatively evaluated in terms of blanketing capability. Concepts of metallurgical compatibility were adapted from conventional welding practice. For example, although hydrogen mixtures were tested on austenitic stainless steel and carbon steels to confirm their effect on penetration, no endorsement of such practice without further metallurgical evaluation is implied.

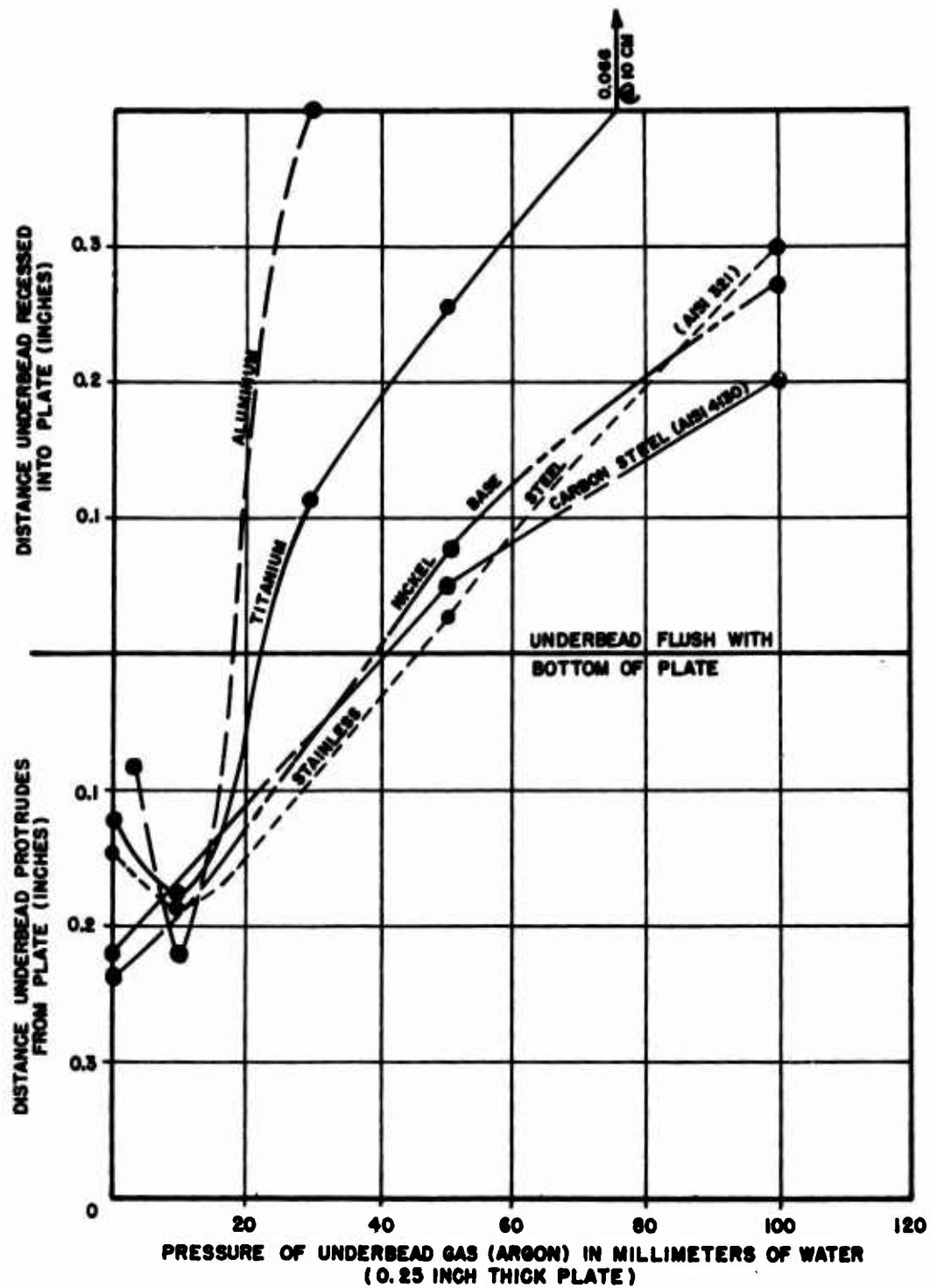


Figure IV-10. EFFECT OF UNDERBEAD PRESSURE ON UNDERBEAD SHAPE

As a corollary to the above ideas, it should be noted that failure to assure proper venting of underbead gas in tooling designs may cause inadvertent pressure changes with a loss of control over underbead contour. This would be particularly true of aluminum. The basic tooling arrangement shown in Figure IV-8 was used.

Measurements were taken at a point approximately 2 inches from the beginning of the weld. At this point the plate was fully penetrated and gas temperature (and pressure) had not begun to rise. Pressure readings are accurate ± 2 mm of water. The welds were produced in the test plate according to the procedure shown in Table IV - 8. The test material was 0.25 inches thick.

C. SHIELDING GAS PERFORMANCE

Unlike electron beams, the laser beam does not need a vacuum to produce a narrow deep weld in metals. The metals, however, need some form of shielding if the resulting welds are to be free of porosity.

The objective of Task 2, Phase I was to determine the suitability of several gases, and gas mixtures, to shield metals that were being welded by lasers. A suitable shielding gas for laser welding is one which:

- ... does not interact with the laser beam and thus reduce the amount of power available for penetrating the joint
- ... has good blanketing characteristics at the high speeds which characterize laser welding procedures
- ... is metallurgically compatible with the base material

In this task the effect on penetration of a candidate shielding gas was given first priority. Additionally, gases were qualitatively evaluated in terms of blanketing capability. Concepts of metallurgical compatibility were adapted from conventional welding practice. For example, although hydrogen mixtures were tested on austenitic stainless steel and carbon steels to confirm their effect on penetration, no endorsement of such practice without further metallurgical evaluation is implied.

VARIABLE	SETTING
Power	15 KW (except as noted in data)
Speed	Low Speed (easy shielding): 60 IPM Intermediate Speed: 120 IPM Very Fast (diffucult shielding): 240 IPM
Telescope-Work Distance	28-1/16 inch \pm 1/32 inch
F/Number	7
Surface Condition	Per Table III-2 each alloy
Shielding	
Upper Surface	140 CFH total flow \pm 7 CFH (experimental gases listed in Table V-1)
Lower Surface	None (partial penetration welds)
Tooling	10 Inch Hood (see Figure V-2) No Underbead Tooling
Note: All experimental inert gases and CO ₂ are welding grade, H ₂ and O ₂ are 99.999 purity.	

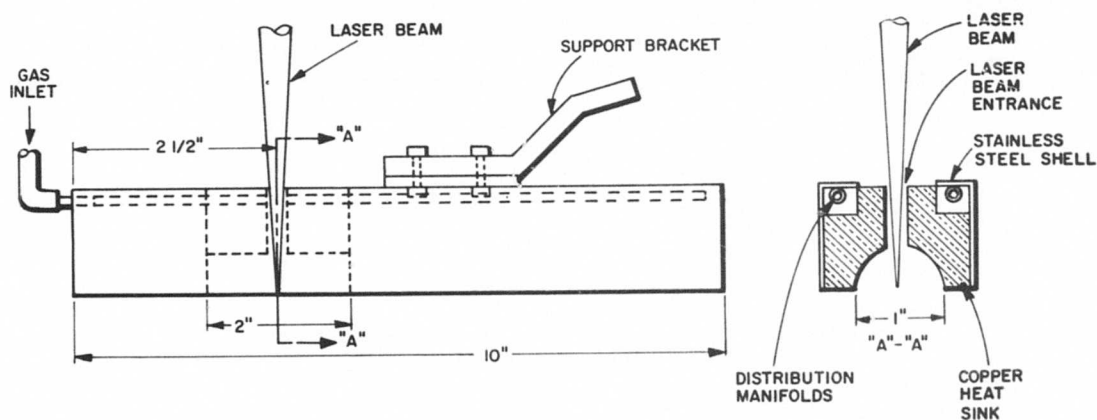
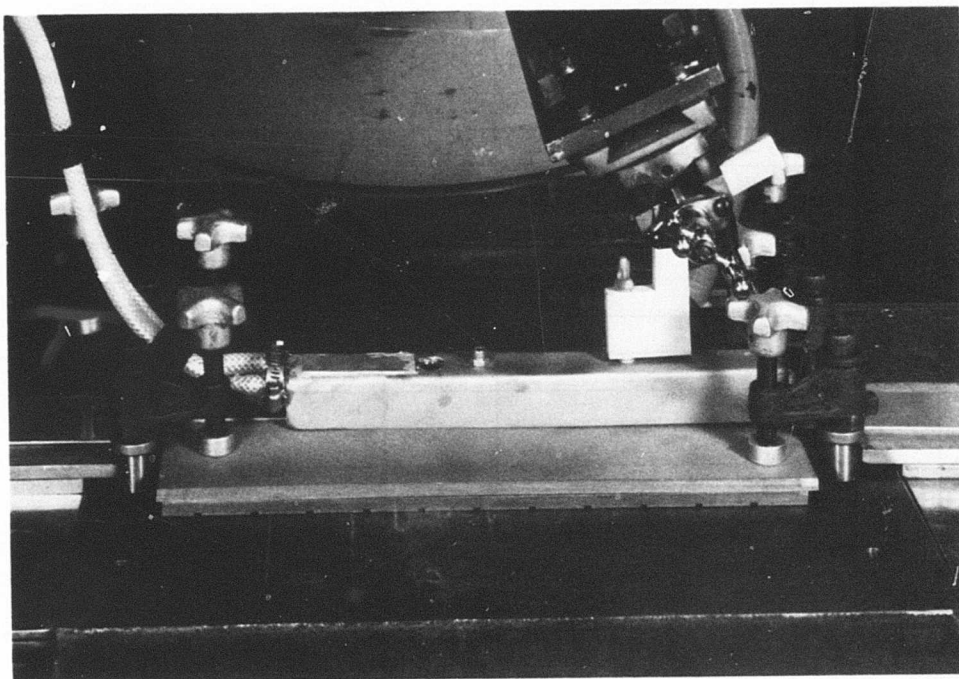
Table IV-7. EXPERIMENTAL WELDING PROCEDURE -
SHIELDING GAS EVALUATION

The full coverage hood and welding fixture are shown in Figure IV-11. The welding procedure is listed in Table IV-7.

It was observed that some shielding gasses actually enhance penetration when the results are compared to air. Helium results in an almost 100% improvement over air. Hydrogen and mixtures of helium with other gasses provide various blanketing qualities and also increase the penetrating action of the beam as opposed to its action in air. Some of the improvements that were observed when welding on austenitic stainless steel are:

Gas Mixture	Penetration (Air = 1)	Blanketing	Metallurgical Effect
100% Helium	1.78	Fair	None
90% Helium, 10% Argon	1.92	Good	None
70% Helium, 10% Argon	1.69	Very Good	None
99% Helium, 1% Hydrogen	1.98	Poor	Possible
50% Hydrogen, 50% Argon	1.14	Good	Very Possible
100% CO ₂	1.28	Surface Oxidized	None

Figures IV - 12, 13, 14, 15 and 16 show the effects of these and other gasses on all program materials and at higher speeds. From these figures, certain general observations can be made. Helium permitted the best penetration. Argon seemed to react with the beam (perhaps by formation and maintenance of a plasma) and inhibited penetration. Helium did not provide perfect blanketing of the weld in high speed shielding situations. When shielding was less than perfect, the intrusion of air had a severe effect on penetration. Additions of 10% argon improved blanketing. The exclusion of air by argon resulted in a greater penetration improvement than the offsetting plasma forming tendency of the argon. Mixtures of 30% argon with helium usually resulted in some loss of penetration. At 50% argon concentration (in helium) shield damage was frequent unless welding speed kept the welding cycle very short. Thus, the limiting amount of argon seemed to fall between 30 and 50 per cent with little to be gained from concentrations over about 10%.



DESIGN OF SHIELD USED TO ESTABLISH ATMOSPHERE ABOVE TEST WELD

Figure IV-11. APPARATUS FOR DETERMINING
EFFECT OF SHIELDING GAS

Weld Number	Gas Stream Length	Variance Angular Relationship		Gas Flow CFH	Radiographic Results
		Weld to Stream	Stream to Surface		
140	.56"	coaxial	52°	30	porous full length incomplete penetration
142	.56"	coaxial	52°	60 ²	clear
143	.56"	1/4" to one side	52°	60	clear
147	1.27"	coaxial	52°	60	clear
144	.79"	coaxial	52°	60	clear
145	.95"	coaxial	52°	60	clear
146	1.11"	coaxial	52°	60	clear
153	2.22"	coaxial	52°	60	clear
152	2.06"	coaxial	52°	60	clear
151	1.90"	coaxial	52°	60	clear
154	2.38"	coaxial	52°	60	clear
150	1.74"	coaxial	52°	60	clear
149	1.58"	coaxial	52°	60	clear
148	1.42"	coaxial	52°	60	clear
156	.56"	5° stream directed at pool	52°	60	clear
155	.56"	5° stream directed at pool	70°	60	clear
1. Procedure Material - low alloy carbon steel 1/4" thick; power - 15 kw; speed - 100 ipm; telescope-work distance - 28-1/16 - 1/32; F/Number - 7; surface condition - as received, shielding - upper surface: off axis nozzle 100% helium (flow as noted), lower surface - none; tooling - multichannel fixture.					

Table IV-8. TOLERANCE FOR ALL AXIS SHIELD
POSITION FORWARD FLOW

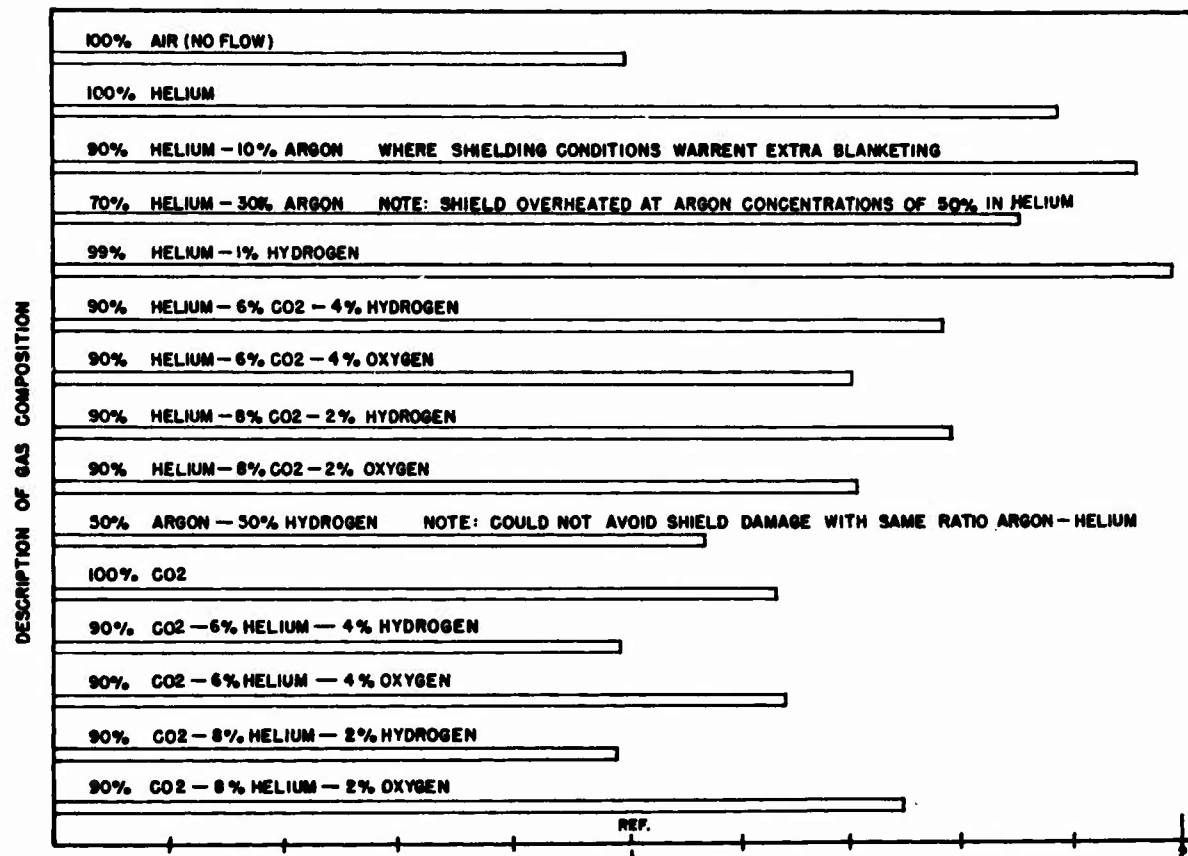


Figure IV-12. EFFECT OF SHIELDING GAS ON
PENETRATION 60 IPM STAINLESS STEEL

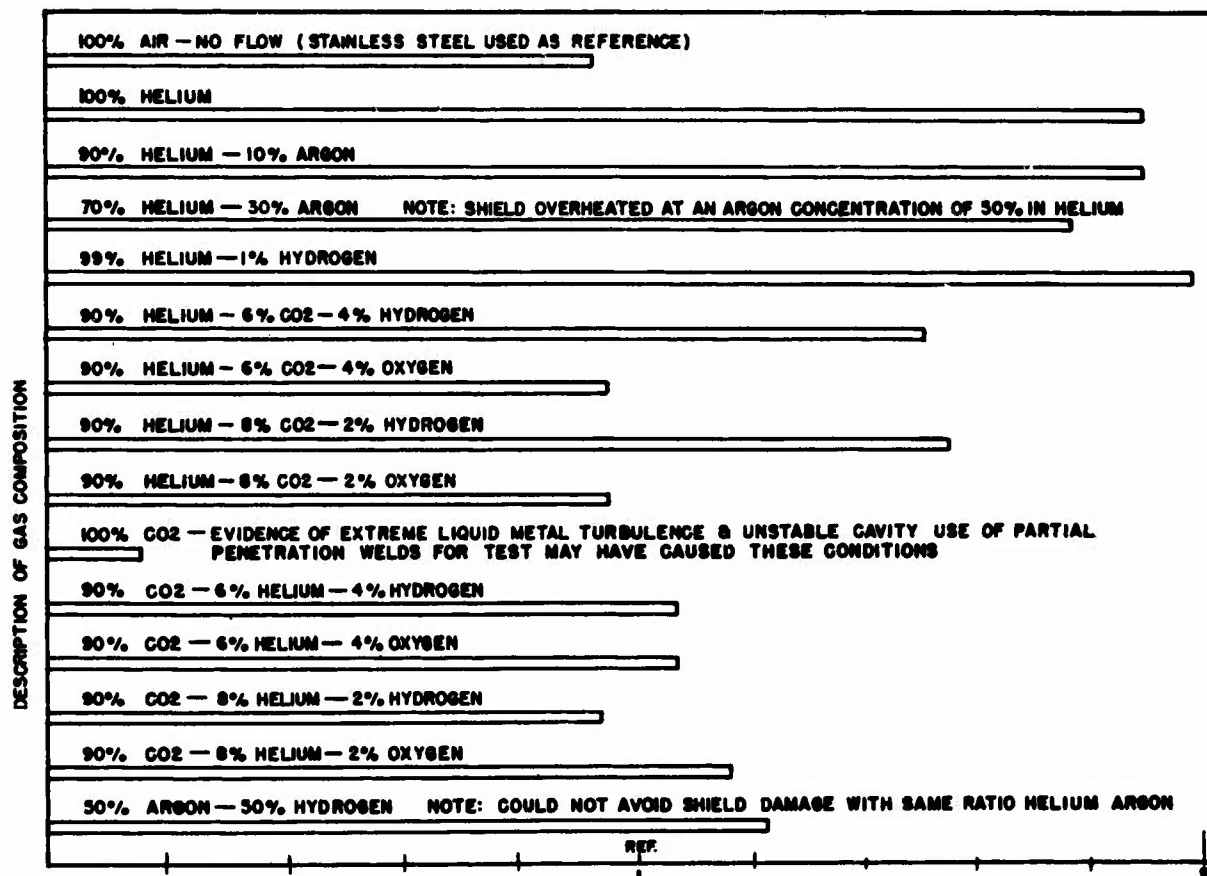


Figure IV-13. EFFECT OF SHIELDING GAS ON PENETRATION
60 IPM LOW ALLOY CARBON STEEL

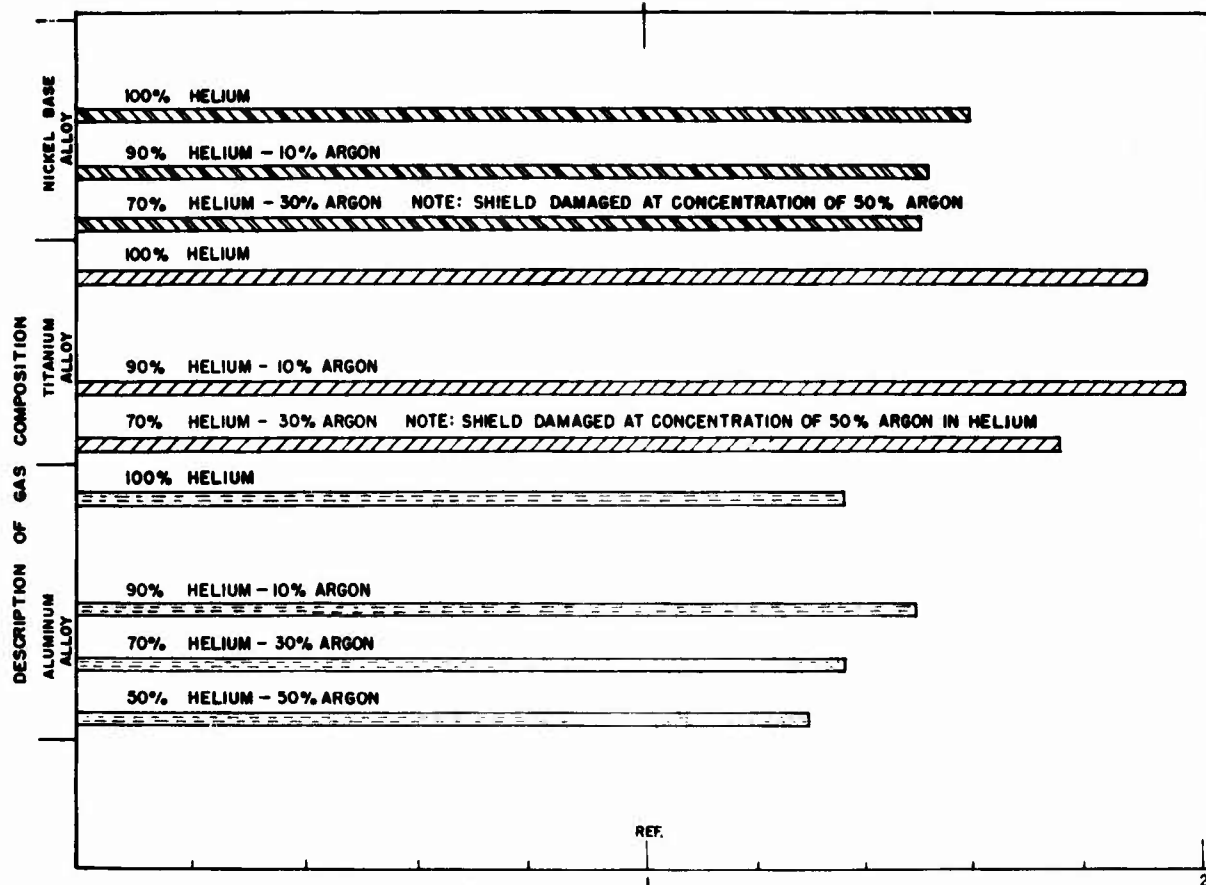


Figure IV-14. EFFECT OF SHIELDING GAS ON PENETRATION
60 IPM OTHER PROGRAM MATERIAL

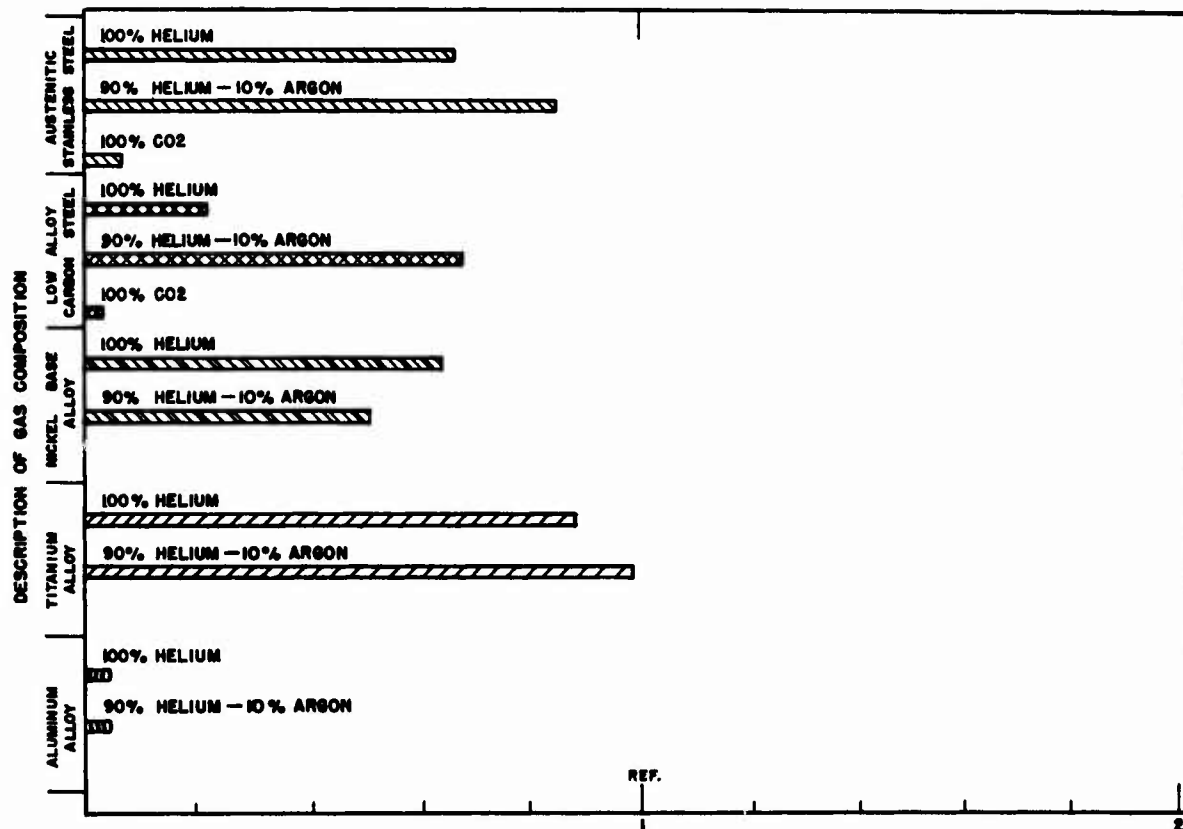


Figure IV-15. EFFECT OF SHIELDING GAS ON PENETRATION
120 IPM ALL PROGRAM MATERIALS

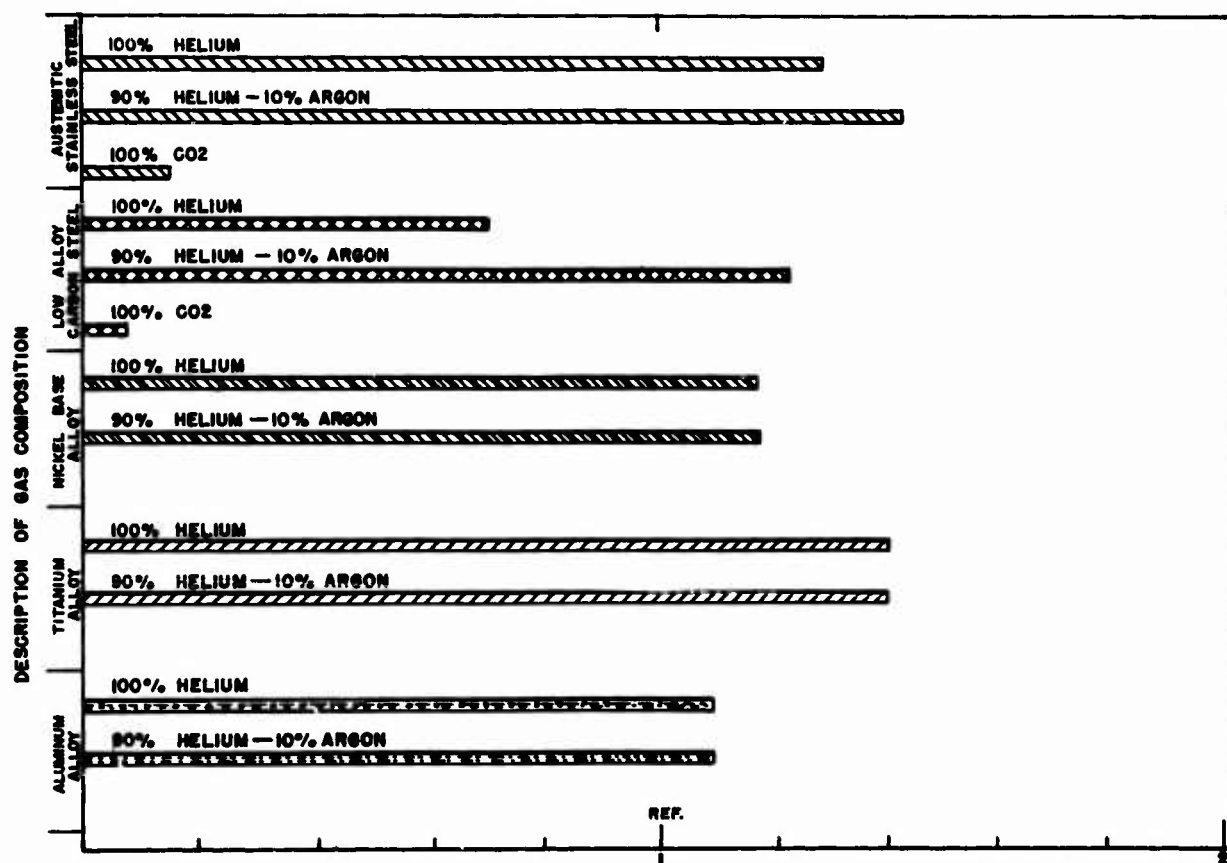


Figure IV-16. EFFECT OF SHIELDING GAS ON PENETRATION
240 IPM ALL PROGRAM MATERIALS

CO₂ marginally improved penetration on austenitic steel when compared to welds made in air. Penetration in low alloy carbon steel was less than that of the referenced weld. The type of weld may have affected results. The improvement was not nearly as great or consistent as that conferred by helium or helium 10% argon mixtures.

Hydrogen provides slight benefits with respect to penetration when added to helium. Experiments with small amounts of H₂ and O₂ suggested that the role of hydrogen can change. If it is in an inert atmosphere, it benefits penetration. If air, or another source of oxygen, such as CO₂ is present the hydrogen forms water vapor which interferes with the penetrating ability of the beam. Hydrogen improved the appearance of CO₂ welds on steel. However, there was evidence of hydrogen rejection during freezing. The metallurgical effects of hydrogen should be studied before it is used.

Small quantities (2%) of oxygen can be used with CO₂ or helium without a severe effect on penetration.

The flow rate used throughout the experiment was 140 CFH. The rate was established to conform to experimental requirements for positive shielding. It does not represent an optimum or necessarily an economically feasible flow rate. Tests showed that the experimental helium flow rate could be halved at 60 ipm without causing a great loss in penetration. CO₂ must have slightly greater blanketing power than helium because no effect was observed at 60 ipm when the experimental gas flow rate was halved.

The higher speed (120 ipm) processes appeared to be more sensitive to reduction in flow with respect to helium. Thus the process speed must always be considered with discussing flow rates. This would be particularly true when light gasses were involved.

In considering shielding gasses, the introduction of air must always be considered. In these tests the shield skirt was placed within 1/32 inch above the plate surface. A small amount of air can, potentially, enter under the skirt. Absolute sealing is impractical since there is also a beam entrance in the top of the hood that must be open to

the atmosphere. The small amount of air that could enter under the skirt provided a good visual indicator of the blanketing characteristics of the inert gasses. The amount of air increases with speed and decreases with blanketing capacity of the gas.

The thermal stability of the shielding device must also be considered in terms of air leakage and its effect on penetration. When the shield is heated, it bows. The ends raise and air can enter at the front edge of the hood as the plate is moved under it.

In evaluating the data from this task, the following experimental procedures should be considered. The distance that the fixed experimental welding procedure penetrated into the 1/2 inch thick specimen was measured by cutting and etching each weld at two points. Penetration of the weld into the plate was interpreted as a function of the experimental gas atmosphere above the plate surface.

The blanketing characteristics of experimental gasses were evaluated by observing the color of the upper beads of the experimental welds.

D. EVALUATION OF GAS SHIELDING METHODS

In order to capitalize on the ability of the laser to operate in the shop, inert gas delivery shields must be considered. Such shields were evaluated in Task 3.1 of Phase I.

Inert gas shields for multikilowatt lasers must have two characteristics:

- ... Ability to provide the required level of shielding over the entire process area - and ability to do so at very high welding speeds.
- ... A free path for the beam from the telescope to the work surfaces. Solid window materials were not available at the power levels employed in this program.

The experimental arrangement was the same as that used to study the effect of shielding gasses except that several experimental shield configurations were substituted for the full hood shield configuration used during shield gas tests. These configurations were:

- Off Axis
- Jet Trailer
- Diffuser Hood
- Static (Fixed to Work)
- Manifolds Integral with Hold Down Bars
- Flood Shield

1. The Off Axis Shield

This shield configuration (Fig. IV-17) is the simplest and most flexible of the four methods evaluated. It is particularly useful in complex structures, for example, box-like weldments or weldments where the relatively bulky and directional full hood type of shield cannot be manipulated. This flexibility is gained by completely decoupling the shield from the workpiece - in contrast to trailers or hoods which must be operated close to the work surface. In this program, the off axis concept was tested on 0.30% C low alloy steel. Marginal shielding is readily detected radiographically in steels with such carbon levels. Nickel base alloy and stainless steel are not as sensitive to shielding as high carbon steel, and Titanium cannot be adequately shielded by the localized flow which is characteristic of the off axis nozzle. Thus, testing was confined to carbon steel.

In these tests the off axis shield with its coherent stream from its gas lens, provided sufficient shielding to permit radiographically clear welds to be made in a C.25 inch low alloy carbon steel (AISI 4130) under a number of commonly encountered manufacturing conditions.

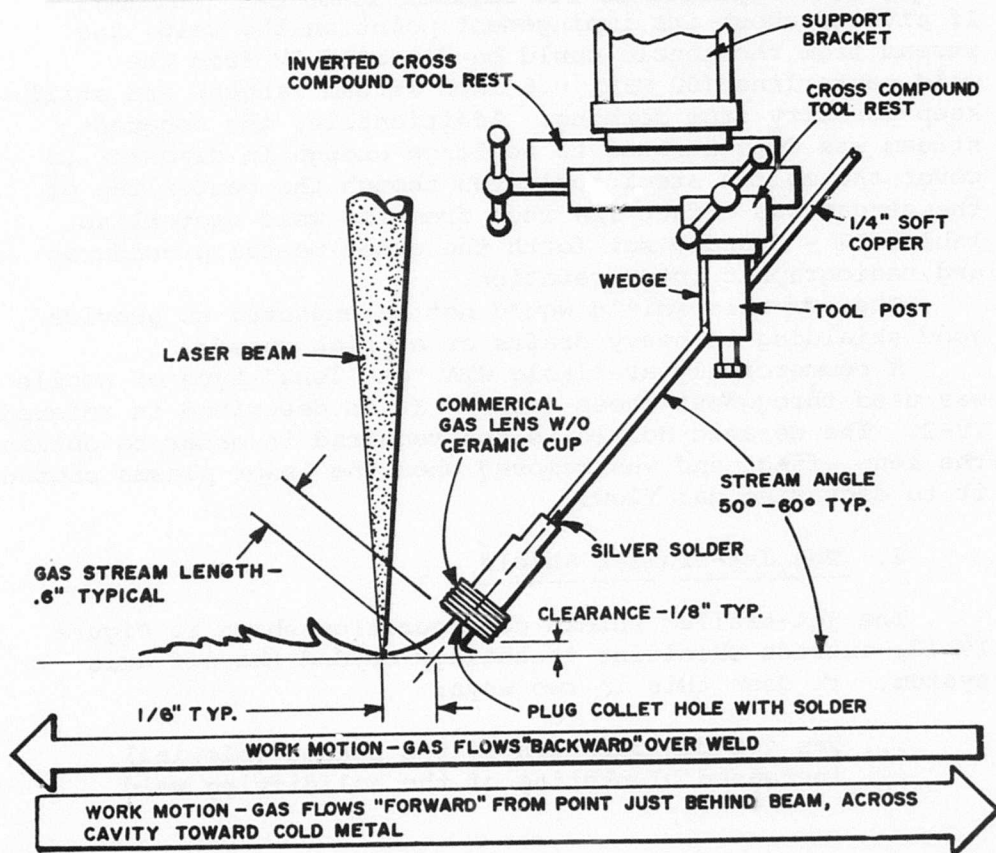
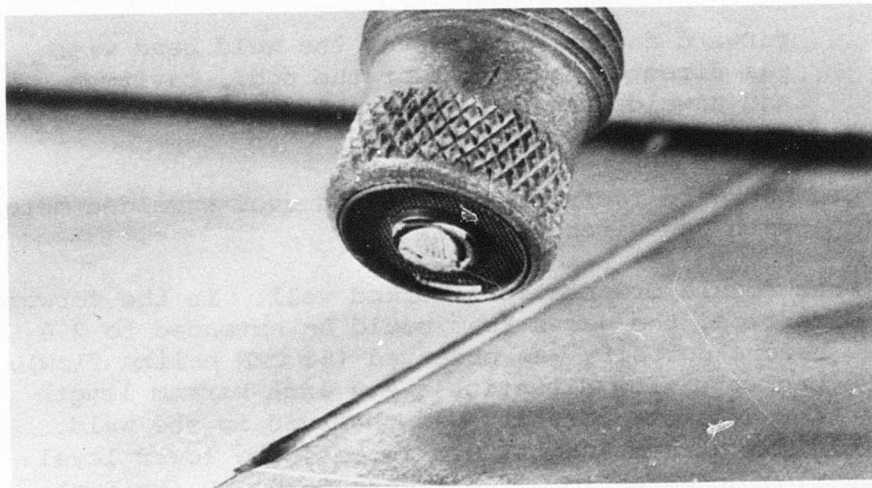


Figure IV-17. TYPICAL O/F AXIS SHIELDING NOZZLE

For example, bead-on-plate welds through 1/4 inch thick carbon steel were produced with two nozzle orientations:

- ... forward facing nozzle over the weld bead with gas directed forward over the pool, cavity, and unwelded metal. This orientation is required to weld into a corner.
- ... backward facing nozzle placed over unwelded metal with gas directed backward.

Both nozzle orientations worked well. In the forward flow direction, the gas stream could be extended to 2.6 inches before porosity was observed (60 CFH helium flow). In the backward flow direction a 1.7 inch stream length was achieved before porosity was observed in the weld. At a minimum stream length, 0.6 inches, the lower level of gas flow appeared to lie between 50-60 CFH (helium). If pivoted about its impingement point on the weld, the stream from the nozzle could be directed 5° from the weld centerline (60 CFH, 0.6 inch stream length) and still keep porosity from forming. Additionally, the coherent stream was demonstrated to be large enough in diameter to cover the molten steel pool even though the centerline of the stream was offset 1/4 inch from the weld centerline. Tables IV - 8 and 9 set forth the experimental procedures and radiographic interpretation.

The off axis shield would not be expected to provide good shielding in heavy drafts or at high speeds.

A commercially available GTA "gas lens" type of nozzle was used throughout these tests. It is described in reference IV-2. The ceramic nozzle is not required in order to obtain the lens effect and was removed when the laser plasma caused it to degrading gas flow.

2. The Jet-Trailer Shield

The jet-trailer shield configuration shown is Figure IV-18, extends shielding technology beyond the off axis system. It does this in two ways:

- ... gas jet manipulation of the plasma (blowing)
- ... increased blanketing of the solidifying weld

Weld Number	Gas Stream Length	Variance Angular Relationship		Gas Flow CFH	Radiographic Results
		Weld to Stream	Stream to Surface		
198	.562"	coaxial	38°	30	porous full length (incomplete penetration)
199	.562"	coaxial	38°	60	clear
200	.702"	coaxial	38°	60	clear
201	.877"	coaxial	38°	60	clear
202	1.096"	coaxial	38°	60	clear
203	1.370"	coaxial	38°	60	clear
204	1.712"	coaxial	38°	60	clear but 5° incomplete penetration
205	2.130"	coaxial	38°	60	clear but 25% incomplete penetration
206	.562"	nozzle on seam 5° to left	38°	60	porous full length
207	.562"	1/4" to one stream	38°	60	clear
208	.562"	5° strain (directed at pool)	52°	60	clear (flatter U/B)
209A	.562"	coaxial	52°	40	first 30% porous
209B	.562"	coaxial	52°	50	one pore (typical U/B)
¹ Procedure Material - low alloy carbon steel 1/4" thick, power - 15 KW, speed - 100 ipm; telescope-work distance - $28-1/16 \pm 1/32$; F/Number - 7, surface condition - as received, shielding - upper surface: off axis nozzle, 100% helium flow as noted, lower surface: None, tooling - multichannel fixture.					

Table IV-9. TOLERANCE FOR ALL AXIS SHIELD
POSITION BACKWARD FLOW

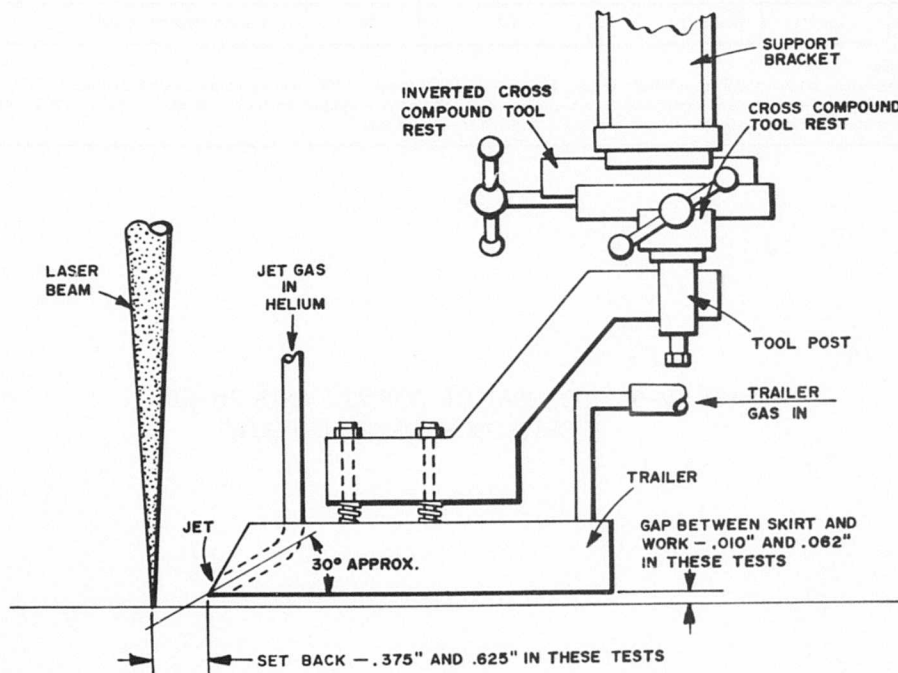
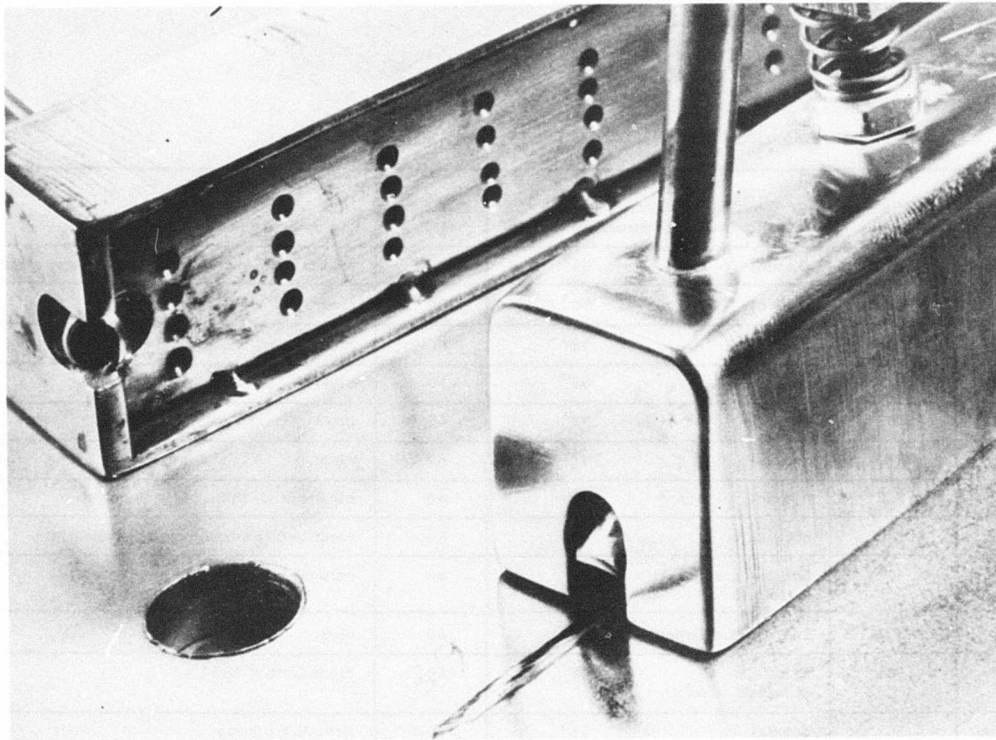


Figure IV-18. TYPICAL JET-TRAILER SHIELD

a. Reactive Metals

One application for the jet-trailer shield is high speed welding procedures. This is an important consideration since multikilowatt laser welds are often carried out at speeds above 100 ipm.

The jet-trailer does not provide full shielding for reactive materials however. Titanium welds produced with the jet-trailer exhibited very small zones of contamination on either edge of the fused zone (Figure IV-19). In the early stages of the program, it was felt that jet-trailer shields would provide reliable coverage for titanium. Rigorous examination of welds in Phase II indicated that the jet-trailer was not reliable or consistent under all circumstances. Careful adjustment of jet flows, coupled with metallographic examination might eliminate this effect.

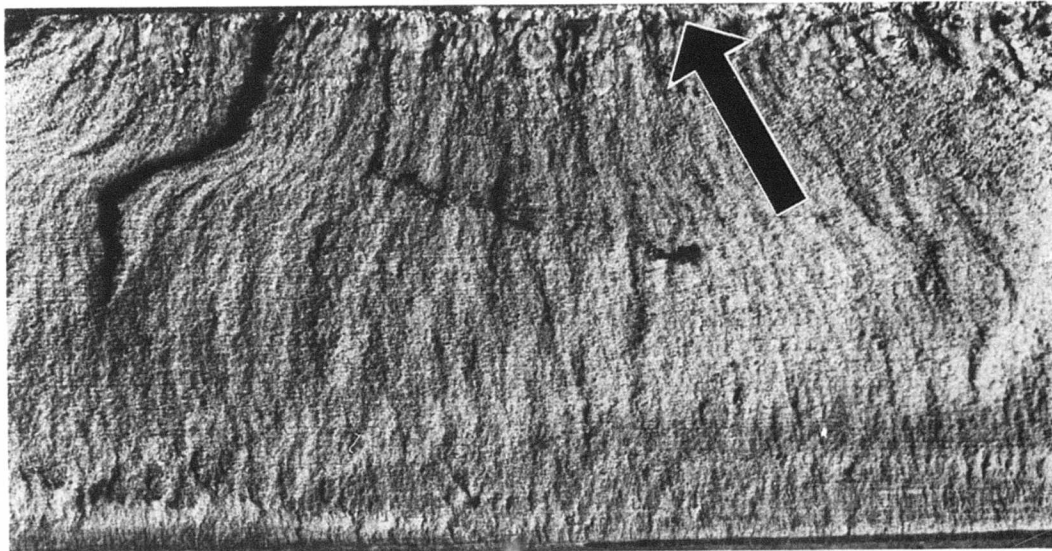
b. Set-Up Tolerances

The effect of the hood setback (distance from the beam) and lift off above the plate surface were evaluated. These are important tooling considerations. Setting the hood too close to the beam might require a complex cooled structure to withstand the plasma radiation. Running the trailer skirt too close to the plate might cause unnecessary stubbing of the shield and a resulting defect.

Figure IV-20 confirms that shielding is best if the trailer does run reasonably close (0.375") to the beam and is set close (0.010 inches) from the plate. Under these conditions trailer gas flow can be reduced by a factor of four. In fact, only when the trailer is close to the beam can significant skirt lift off be used. Significant skirt lift off is also limited to very high speeds where the dwell time of the molten metal between the cavity and the hood is short, and to maximum trailer gas flow. When a large set back (0.625") was employed, only the minimum lift off setting was effective; and then only when maximum gas flow was used.

Over the life of an extended application, the cost of hoods designed for operation near the plasma and close to the work might be justified. Justification would be based on the 75% reduction in trailer gas that appears possible.

Note: Arrow indicates brittle region at top edge.



Neg. No. LQ-746

Mag. 6.1X

Figure IV-19. METALLOGRAPHIC EVIDENCE OF CONTAMINATION

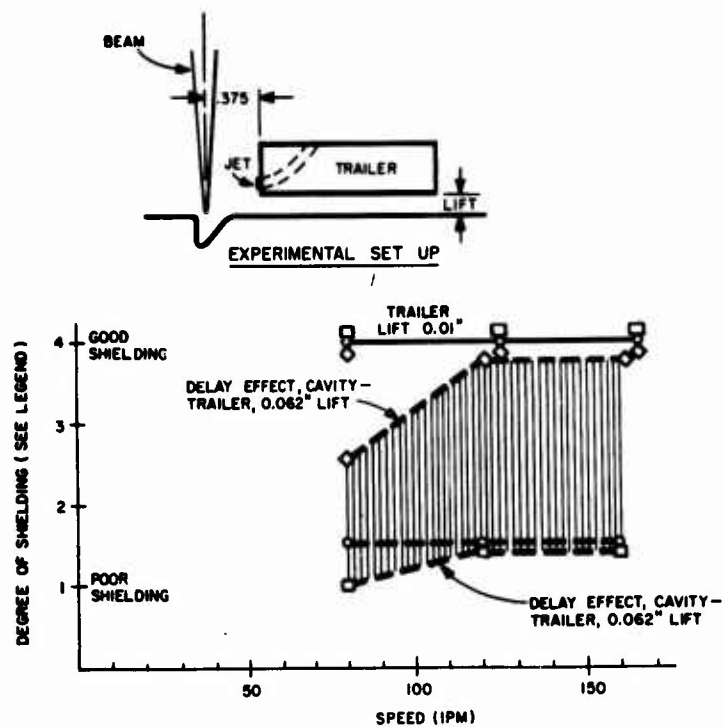


Figure IV-20. EFFECT OF JET TRAILER SHIELD DESIGN ON SHIELDING CAPABILITY

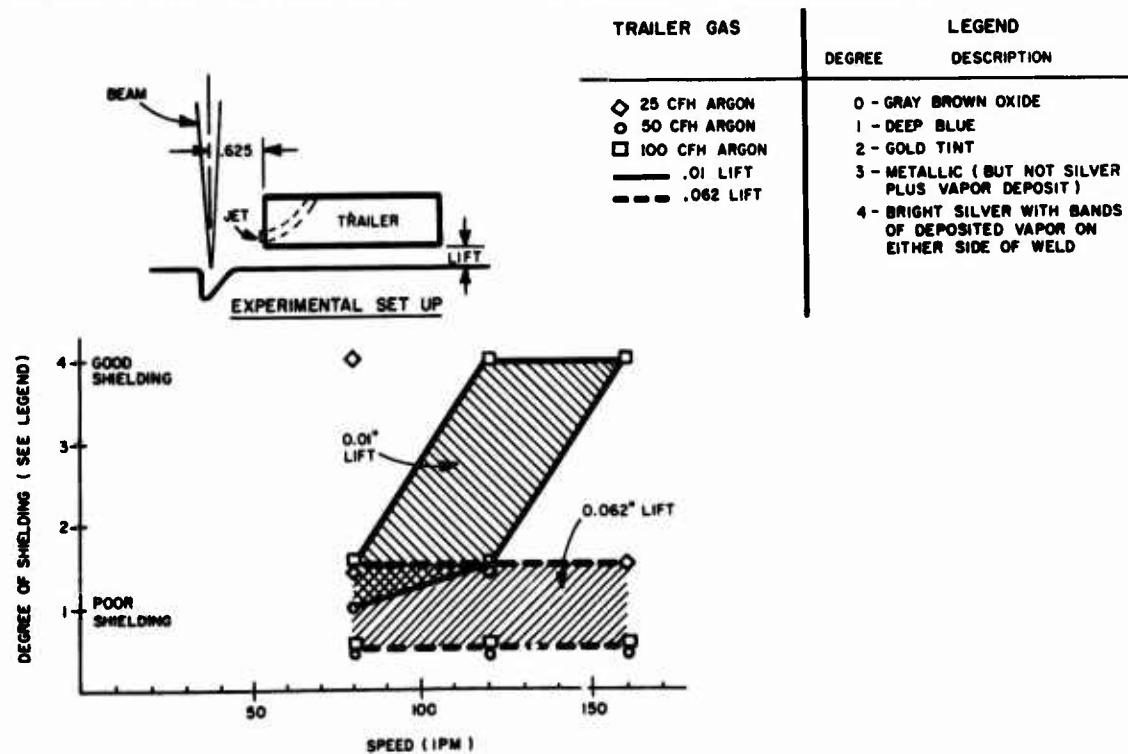


Figure IV-21. EFFECT OF JET FLOW RATES ON PROCESS PENETRATION

c. Jet Gas Flow

The jet gas flow rate was considered and its effect on the process (in terms of penetration) is shown in Figure IV-21.

Apparently this particular jet trailer shield achieved the maximum jet effect at 50 CFH helium. Jet configuration may vary from shield to shield such that the values in Figure IV-21 could not be transferred, but the trend should be similar.

3. Diffuser Hoods

Hoods of the type shown in Figure IV-22 were introduced into the program to:

- ... provide high speed, full coverage shielding
- ... eliminate the inconsistent shield of the jet on titanium
- ... eliminate metal turbulence from off-axis and jet stream when welding aluminum

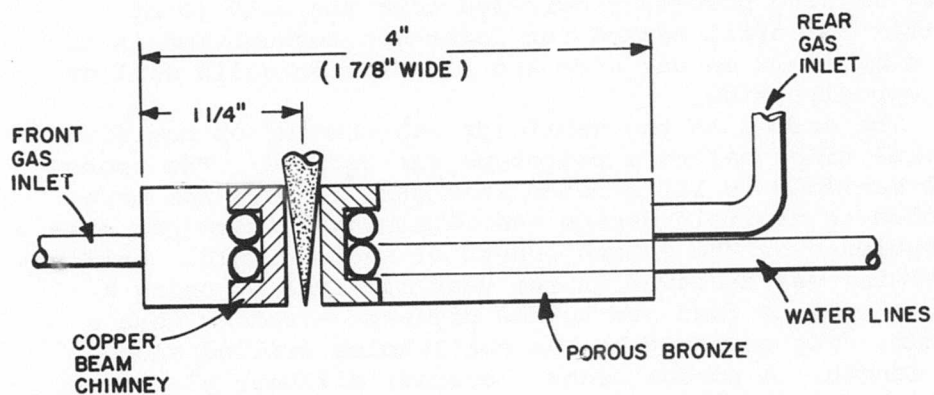
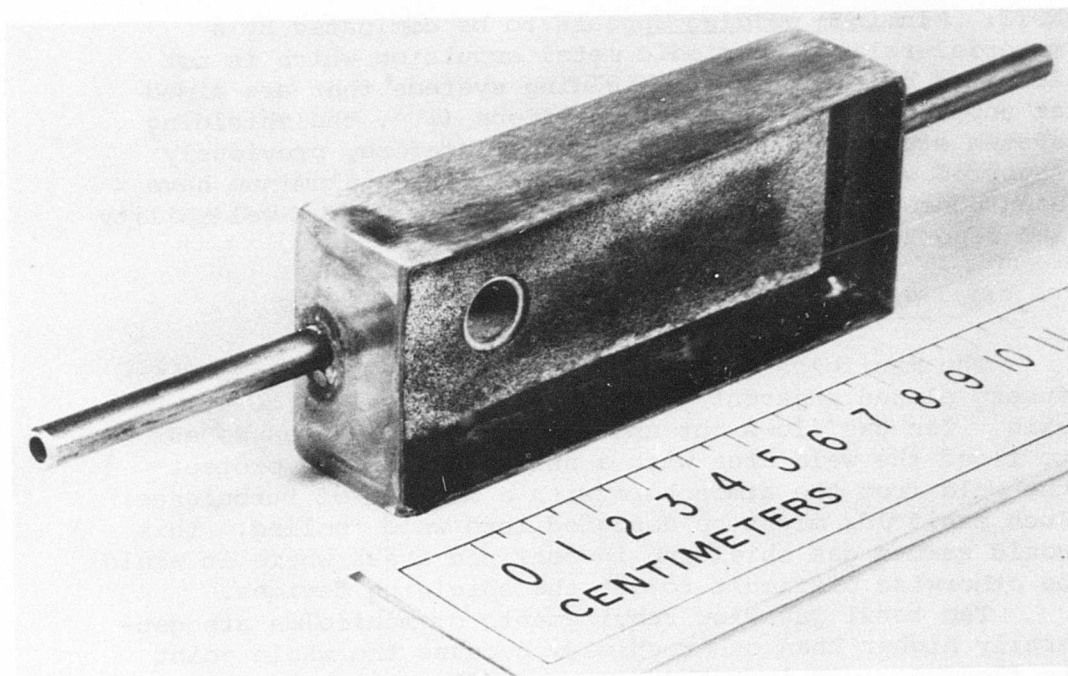
This type of hood was not evaluated as systematically as those previously described because it was not part of Phase I, Task 3.2. Instead, it was used to assist in Weld Procedure Development Phase II, Task 1.

a. Reactive Metals.

The diffuser hood successfully overcame the weld line contamination that had been observed when the jet trailer was used to produce initial 1/4 inch thick titanium fatigue test panels. Even at weld speeds of 100, ipm full shielding was observed with the diffuser hood.

b. Aluminum.

The use of the diffuser hood on aluminum produced smooth welds with acceptable levels of scattered, metallurgical (hydrogen related) porosity at gas flows of 50 CFH of helium plus 10 CFH argon, based on studies described in Ref. IV-3.



SCHEMATIC ARRANGEMENT OF DIFFUSER

Figure IV-22. WATER COOLED DIFFUSER HOOD

NOTE: Aluminum welding appears to be dominated by a material-related, periodic metal expulsion which is not affected by the kind of shielding systems that are aimed at suppressing gas - metal reactions (i.e. the shielding system studied in this program). Therefore, previously reported observations of shield effects on aluminum have been consolidated under the subject of aluminum weldability and reported in this context.

4. Preplaced Gas Manifolds

The manifolds described in Figure IV-23 are gas diffusers placed adjacent to the weld and parallel to its axis. The gas flows out and across the weld area so as to flood the weld area with a shielding gas and protect the weld from the atmosphere with a minimum of turbulence. Such manifolds might be designed into weld tooling. This would assure gas shielding in confined areas where it would be otherwise difficult to get the shielding devices.

The total gas flow requirements of manifolds are generally higher than other shields because the whole joint is flooded - not just the molten puddle. To save gas on very long welds, the manifolds might be segmented so that the gas flow could be directed to specific segments as the laser welding process progressed down the weld joint. Another potential method for lower gas consumption is to use a manifold on one side and a buffer or solid wall on the opposite side.

The design of the manifolds was changed or modified several times before a prototype was defined. The prototype manifold is illustrated in Figure IV-23. The main problem in manifold design was obtaining uniform gas distribution over the entire length of the manifold. Uniform shielding was achieved in the test manifold by using a copper tube to feed gas to the diffuser - rather than a plenum. The copper tube has small holes drilled along its length. A porous bronze (coarse) diffuser plate was placed over the tube to insure an even flow of gas. In some manifolds, steel wool and a copper screen were used in place of the porous bronze.

The manifolds had to be held securely against the weld plate. The manifolds, therefore, also acted as tooling clamps to hold the test plate in place. The distance

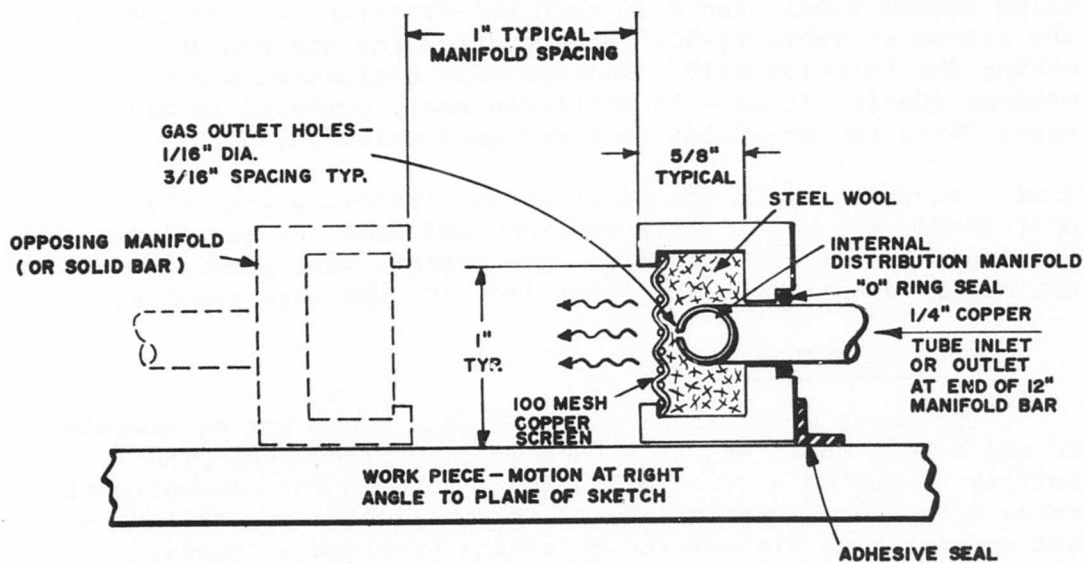
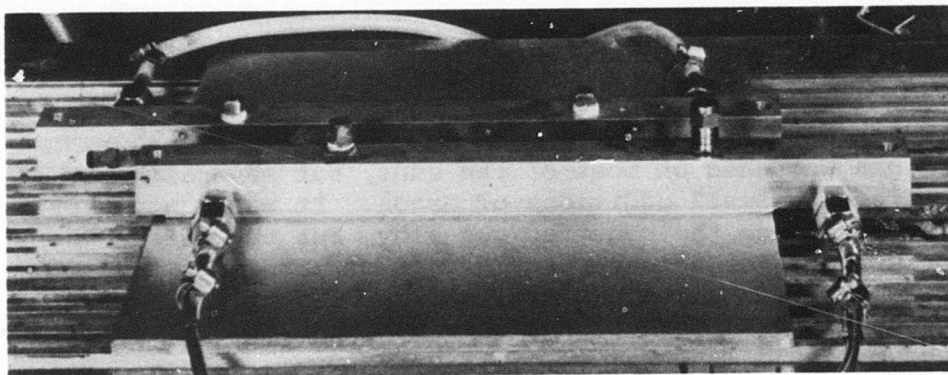


Figure IV-23. MANIFOLDS

between the manifolds was varied from 1/4 inch to 1 inch to determine practical limits on spacing. Special precautions were taken to make sure that air could not seep under the manifold from the back face. A piece of tape or caulking was placed on the outside of the manifold configuration, between the manifold and the test plate, to prevent this chimney effect. A high temperature elastomer seal could be built into the manifold.

Bead-on-plate welds in 1/4 inch thick stainless steel suggested that manifold spacings greater than 1 inch produced contamination. Runs made with one manifold removed and a flat solid plate substituted reduced gas consumption 40%. Helium gas was used on most of the runs, but several runs were made with small additions of argon. It was hoped that this would reduce the required gas flow, but the effect was not observed. For this particular set of manifolds, any flow below 150 CFH of helium per manifold had a noticeable effect on the shielding. The optimum flow appeared to be 220 CFH per foot of manifold length.

Demonstration butt welds on several types of materials were made using optimum flows and manifold locations. Welds were produced in 0.25 inch 304 stainless steel, 0.25 inch low alloy carbon steel, and 0.25 inch 6Al-4V titanium. Procedures are listed in Table IV-10. Backup shielding gas was used in making the titanium weld. Radiographic evaluation showed a useable quality level with scattered small porosity in all areas where the manifolds provided good shielding.

NOTE: In these tests the manifold was traveling with the part during the weld. This movement affected the gas flow near the ends of the manifold. The effects were generally not observed until travel speeds over 150 ipm were reached.

5. Flood Shielding

The laser beam can be directed into areas not accessible to any other fusion or resistance welding processes. The ability to design a structure without concern for conventional rules of welder accessibility lifts some design constraints - but creates some significant shielding problems if hoods, nozzles or manifolds must be used.

VARIABLE	SETTING			
Material	Aluminum	Carbon Steel	Stainless Steel	Titanium
Power Beam (KW)	19	19	17	19
Power Work (KW)	13.3	13.3	11.9	13.3
Thickness	1/4"	1/4"	1/4"	1/4"
Speed	175 ipm	100 ipm	100 ipm	120 ipm
Telescope-Work Distance	28-1/16"	28-1/16"	28-1/16"	28-1/16"
F/Number	7	7	7	7
Surface Condition	handscraped	sandblasted	as machined	filed
Shielding				
Upper Surface	220 CFH He /manifold	220 CFH He /manifold	220 CFH He/manifold	220 CFH He /manifold
Lower Surface	none	none	none	20 CFH He
Tooling	#102 with strap clamps	#102 with strap clamps	#102 with strap clamps	#102 with strap clamps with underbead shield tube

Table IV-10. EXPERIMENTAL WELDING PROCEDURE -
MANIFOLD SHIELDING

THIS REPORT HAS BEEN DELIMITED
AND CLEARED FOR PUBLIC RELEASE
UNDER DOD DIRECTIVE 5200.20 AND
NO RESTRICTIONS ARE IMPOSED UPON
ITS USE AND DISCLOSURE.

DISTRIBUTION STATEMENT A

APPROVED FOR PUBLIC RELEASE,
DISTRIBUTION UNLIMITED.

An initial assumption was made that - if the enclosure was above the beam (overhead), helium could be used to displace air and provide adequate shielding. On the other hand, if the weld had to be made downhand, helium could not be expected to flood the joint; and an experiment would have to be carried out using an argon blanket. Unlike helium, argon has a severe attenuating effect on the beam.

These experiments attempted a general solution to the attenuation problem by limiting the thickness of the argon blanket above the joint.

The adjustable level flood-box shown in Figure IV-24 was built and slowly filled from the bottom until the argon gas reached the height of the adjustable plastic weir gates on either end. Two levels were explored - 3/16 inch above the Titanium test plate and 1 inch above the plate. Only the 1 inch deep blanket produced test (spot) welds with a silver color. A 6 KW (beam) procedure was then run (by moving the gas filled box under the beam) using the 1 inch blanket. This weld was compared with welds made by the same procedure using a full shield (Fig. IV-11). The hood shielded welds exhibited a 600% increase in penetration and a silver bead. The color of the argon blanketed weld suggested that the gas blanket was disturbed when the specimen moved under the beam. The penetration indicated that thicker argon blankets would all but eliminate welding process penetration and tests were terminated. There was no way, on available equipment, to produce a weld bead without moving the work.

The silver spot welds suggest that it is possible to do some downhand welding using flood shielding if the 1 inch gas blanket is not disturbed. Seventy-five per cent reduction in penetration would be expected.

E. BEAM - WORKPIECE INTERACTION

In this portion of the program a practical method for establishing an optional CO₂ (CW) laser welding procedure was evaluated using each of the program materials, and working over a range of thicknesses from 1/4 inch to 1/2 inch.

It is necessary to introduce the topic of weld procedure establishment by considering the five procedure variables that must be adjusted to produce an optimum laser weld. The three equipment-related variables associated with high energy

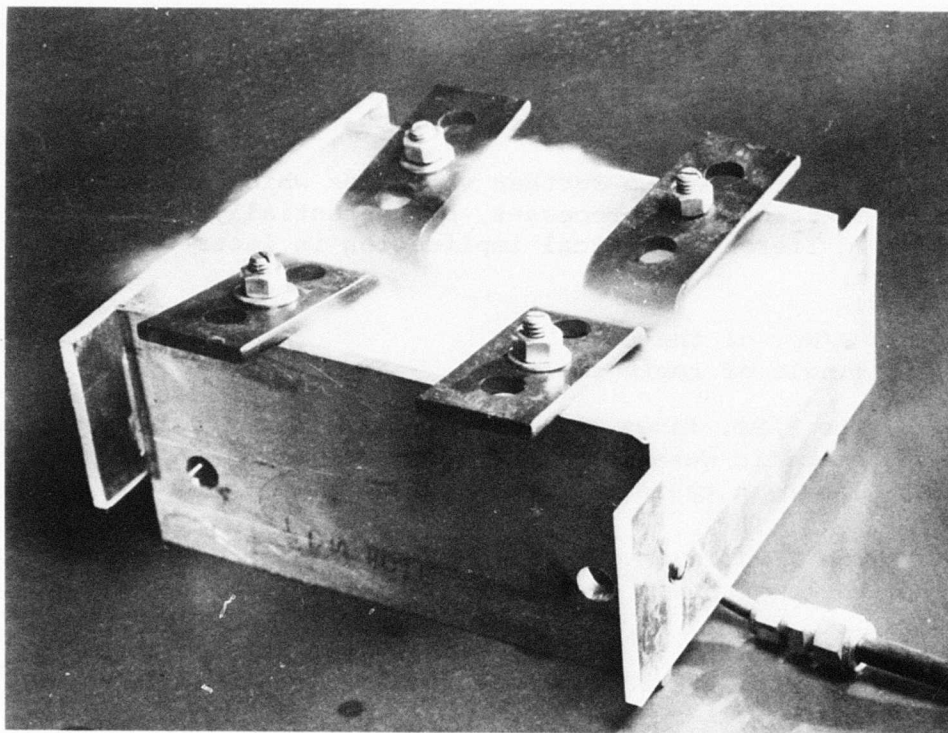


Figure IV-24. FLOOD SHIELDING TEST APPARATUS

beams (such as laser and electron beams) are known from electron beam technology to include:

Process Speed

Focal Point Placement (with respect to the work-
piece surface)

Beam Power at the Focal Point

The laser has two further variables which are encountered in electron beam processes, but potentially have a somewhat different practical implication in laser welding. These are:

F/No. of the Beam

Angle of Impingement

The F/No. fixes the focal spot size and depth of focus for any specific wave length of laser energy (10.6 microns for the CO₂ laser in these studies). The effect is as follows:

Large F/No.'s (e.g. F/21) have large diameter spots with lower power densities and large focal depths.

Small F/No.'s (e.g. F/7) have sharp, intense focal spots with little depth of focus.

NOTE: Spot size changes in direct proportion to the change in F/No. (doubling the F/No. doubles spot size). Depth of focus changes as the square of the F/No. (doubling the F/No. increases the depth of focus approximately four times).

The impingement angle effect was also felt to be potentially important. It suggested a means for directing the beam to miss the vapor plume above the work surface thereby avoiding whatever effect the vapor might have on the beam.

In a production welding procedure, other variables would have to be controlled. These might include wire feed rates (if appreciated) and surface preparation, shielding gas flow and rates. The latter two variables were previously considered in this report. This portion of the study deals with primary variables which might be defined as the minimum equipment adjustments necessary to control beam workpiece interaction.

1. Speed and Focus

These two variables can be logically interrelated in the process and thus serve as a good starting point for arriving at an optimum procedure for obtaining, in this case, a full penetrating weld. Assuming a given power level such as 10 KW on the work surface, it is reasonable to conclude that as speed (1) is increased and focal point placement varied in, and out of the plate some speed will be reached at which only one critical focal point setting will result in full joint penetration. This setting is the most efficient focal point placement and thus can serve as a unique data point.

The observations from such an experiment are shown in Figure IV-25. The maximum speed and most efficient focal point setting occur where the boundaries of the central, full joint penetration area intersect. This is a unique set of conditions for the procedure under study. As such it might be called the process "benchmark" and it can be used as a reference in establishing characteristics of the full penetration process. It is used in this program as a point of comparison with other processes where one or more variables have been modified.

As speed is decreased below the benchmark condition some conduction melting starts to take place in the process, and a number of focal point placements result in a full penetration process. The weld cross sections in Figure IV-25 suggests favoring those placements that keep the work surface slightly closer to the telescope than it was at the most efficient focus. That is, those settings that drive the focal point deeper into the work than the benchmark. A review of the cross sections in Figure IV-25 suggest that focal point placement has the following implications:

... pulling the focal point out produces a pinched cross section.

- (1) Speed could be held constant and power reduced, but speed is a totally independent variable with respect to optics - while power may influence beam quality and thus is not truly independent as suggested in the section on Focus and Power.

1/4" STAINLESS STEEL WELD CROSS SECTIONS RELATED TO BENCH
MARK SURVEY

LASER BEAM POWER - 10.2 KW
TELESCOPE F/NO. - F/7

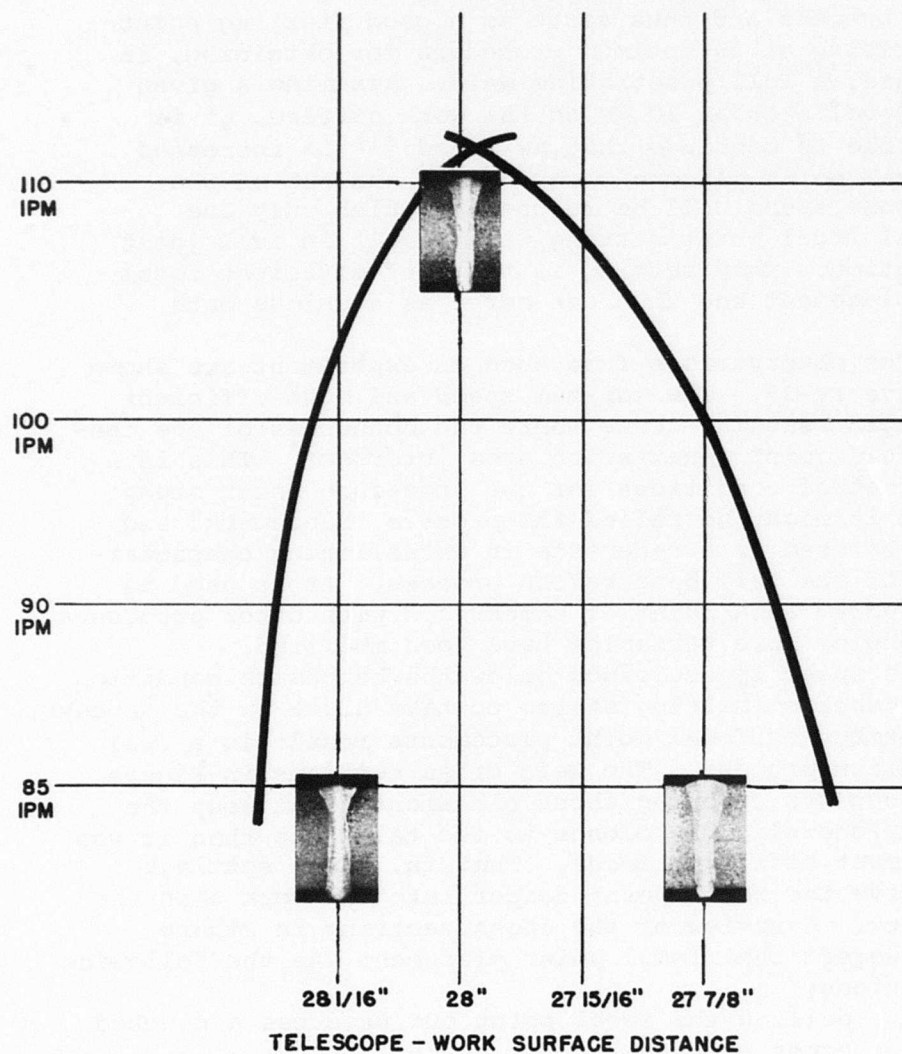


Figure IV-25. WELD CROSS SECTION RELATED TO
FOCUS-SPEED CHARACTERISTICS

- ... pinching the upper portion of the weld can cause solidification cracking
- ... pushing the focal point into the work produces a wedge shaped cross section
- ... wedge shaped cross sections tend to freeze from the bottom without cracking

These isolated low alloy steel cracks from a marginal focal point setting point up the practical desirability of determining process boundaries (Fig. IV-25), and working well within them to offset the effect of external process influences. Changes in power, the introduction of air or argon to the weld area and other factors that influence penetration, can shift these boundaries. Processes should not operate near their limits.

The increasing amount of conduction heating that occurs as speed is reduced 15 ipm from the critical benchmark region can be observed in terms of the increased heat affected zone (Figure IV-25). Nevertheless, a deep narrow low distortion weld is still produced. Additionally, this speed reduction has the advantage of providing some tolerance for focus - about 3/16 inch at 95 ipm in Figure IV-25.

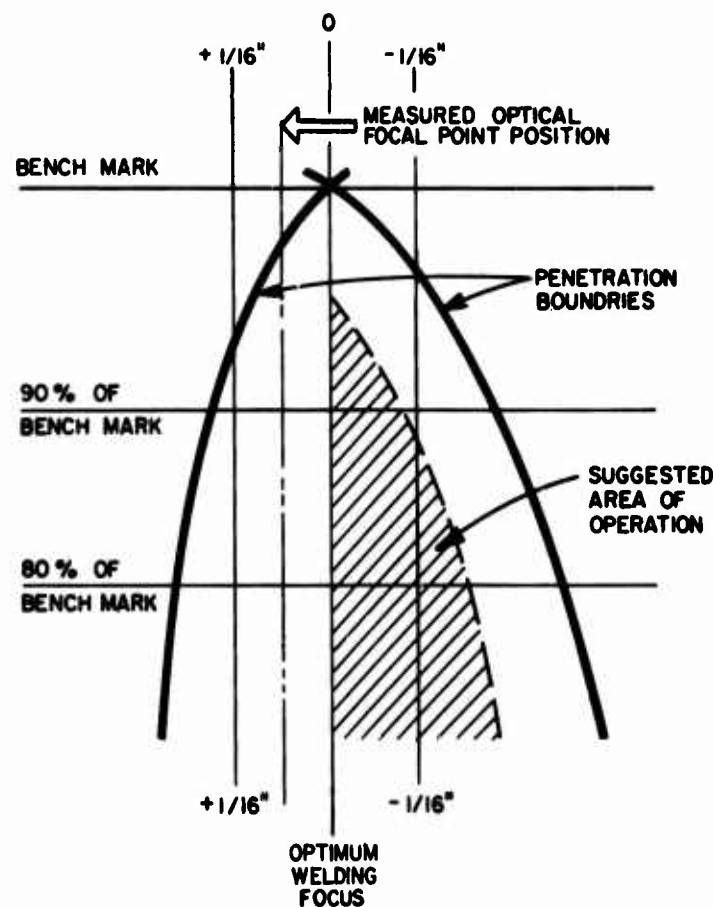
A final advantage that can be gained from working below the benchmark. The tolerance for porosity is increased at these lower process speeds as is the case in arc welding.

When speeds drop too far, conduction heating dominates and the process takes on the characteristics of an arc weld. This may or may not be detrimental since this laser may have been applied for reasons other than its ability to make a fast, deep narrow weld.

Figure IV-26 illustrates a typical optimum process region. Further refinement may be required within this region to realize special crown and root configurations. Such refinements detract from process tolerance but are often necessary to meet weld quality standards.

2. Focus - Power

These procedure variables appear to bear a relationship to one another according to Figure IV-27. As power was increased from 10 KW beam to 18 KW (beam), the observed benchmark focus position changed. Increased power resulted in an increase in the telescope-work distance that is measured in terms of benchmark. If it is assumed that the actual optical focal point did not change with respect to the telescope as power increased, Figure IV-27



DISTANCE, SURFACE TO TELESCOPE

Figure IV-26. SUGGESTED AREA FOR PROCESS OPTIMIZATION

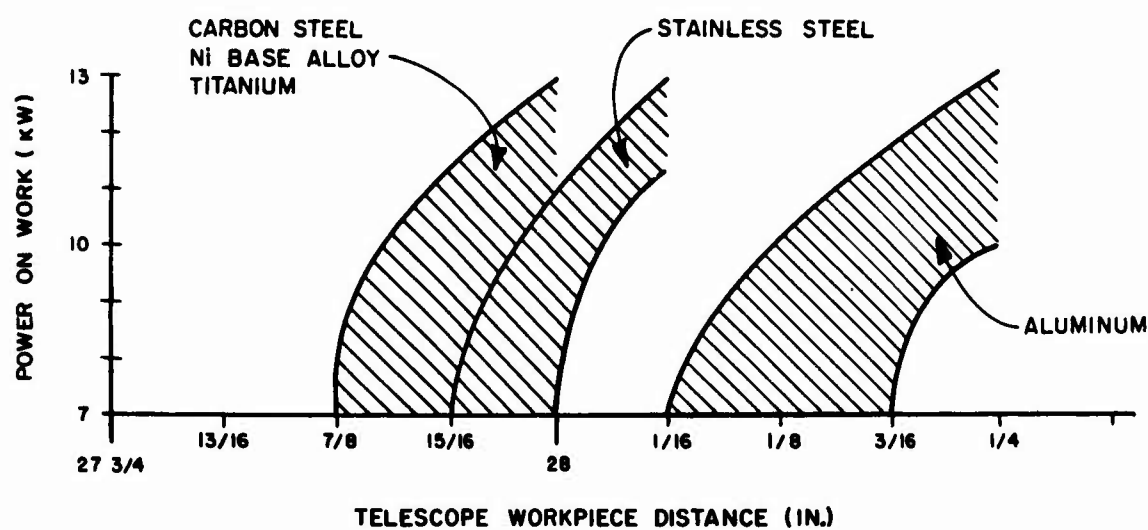


Figure IV-27. FOCUS-POWER RELATIONSHIP FOR PROGRAM MATERIALS

implies that the best placement of the focal point within the work is shallow at higher powers. Therefore, the possibility that focal point settings must be reviewed if power levels are changed in the process should be kept in mind.

3. Speed Penetration

The speed joint thickness relationship was observed to be relatively constant between 3/8 and 1/4 inch thicknesses (Figure IV-28). Greater thickness required that both power on the work and the optical system delivering it be changed, which interrupted data curves at the 3/8 inch thickness level.

A knowledge of the effect of thickness on variables, such as speed, has practical advantages in establishing a process. For example, thickness varies with the machining practice used to prepare the joint. Under such circumstances, Figure IV-28 can be used to determine the effect of a + 0.015 inch variance in thickness in terms of the effect on the benchmark speed of the process. Within the range of thicknesses shown in Figure IV-28, a downward speed adjustment of 15 ipm would be needed to accommodate such a variance. A cost analysis of many potential laser applications might reveal that a sacrifice of 15 ipm in process speed would more than pay for itself in the reduced machining costs associated with a + 0.015 inch machine tolerance.

A more obvious application of Figure IV-28 is in estimating the effect on the process of a change in nominal joint thickness for a given material. From Figure IV-28 it appears that increasing the workpiece thickness of a titanium weldment from 1/4 inch to 3/8 inch would shift the benchmark speed for this process downward from 138 to 54 inches.

In the following section of the report, it will be shown that the above situations can also be dealt with in terms of process power adjustments.

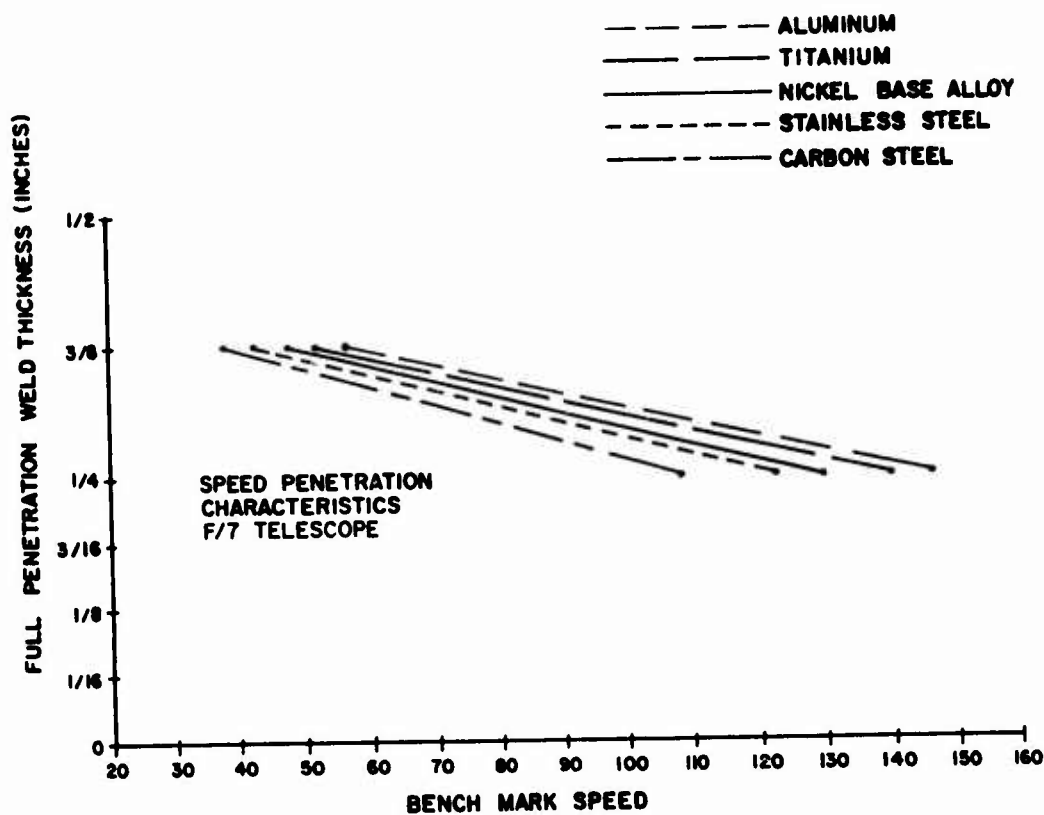


Figure IV-28. SPEED-THICKNESS RELATIONSHIP FOR PROGRAM MATERIALS

4. Power - Speed

The power-speed relationships for all program materials are shown in Figure IV-29 (3/8 inch) and Figure IV-30 (1/2 inch). The speed referred to is, as in the preceding section on Speed-Penetration, the maximum speed at which full penetration was observed at the most effective focal point setting (e.g. the benchmark speed).

From Fig. IV-29 it appears that the coefficient of change in speed with change in power varies from material to material in 3/8 inch thick welds:

- ... Carbon Steel 5.4 ipm/KW
- ... Stainless Steel 7.6 ipm/KW
- ... Nickel Base Alloy 7.1 ipm/KW
- ... Aluminum 7.6 ipm/KW
- ... Titanium 9.2 ipm/KW

Therefore an estimate can be made (from 1/4 inch to 3/8 inch) of offsetting adjustments that might be required for the workpiece changes such as those discussed in the previous section:

To Accommodate:	Adjust Speed:	or	Adjust Power
+0.015 inch thickness variance	151 ipm		2.7 KW (on work)
1/8 inch change in nominal thickness, Ni Base Alloy	84 ipm		11.1 KW (on work)

The latter value suggests that some other factor is going to have to be changed if sections thicker than 3/8 inch are to be welded with lasers of any reasonable power.

a. Thickness - F/Number

The factor that put the laser welding process into contention for plate more than 3/8 inches thick was the availability of higher F number optics. Figure IV-30 suggest that:

Straighter sided beams with large focal depths (F/21) worked better on thicker plates than did more tapered beams with small focal depths (F/7) in spite of their lower specific energy.

The above statement regarding spot size undoubtedly must be limited to specific energies above 6×10^6 w/in², which is an often cited threshold value for E.B. and laser cavity formation.

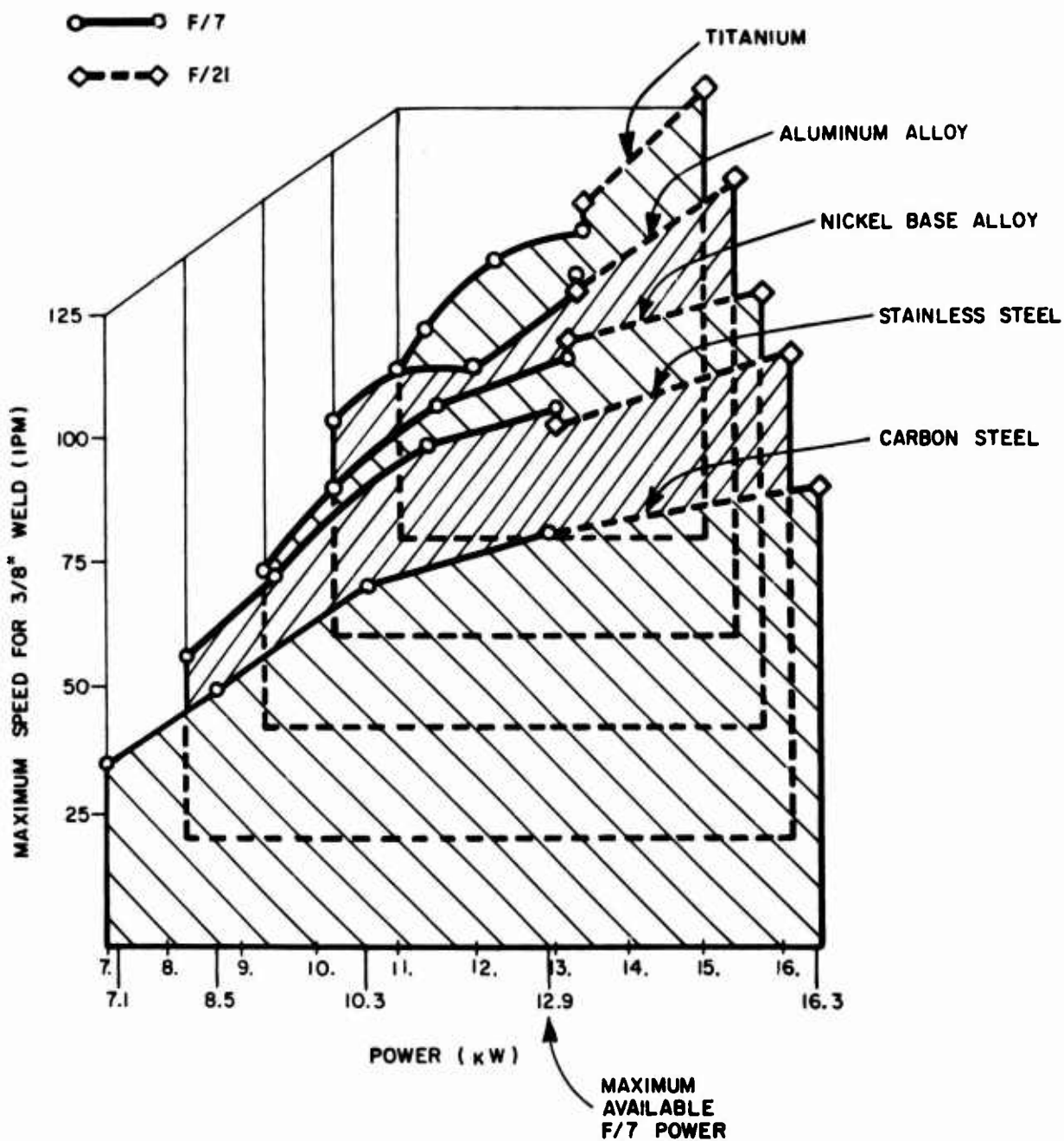


Figure IV-29. RESPONSE OF 3/8 INCH THICK BENCH MARK SPEEDS TO POWER

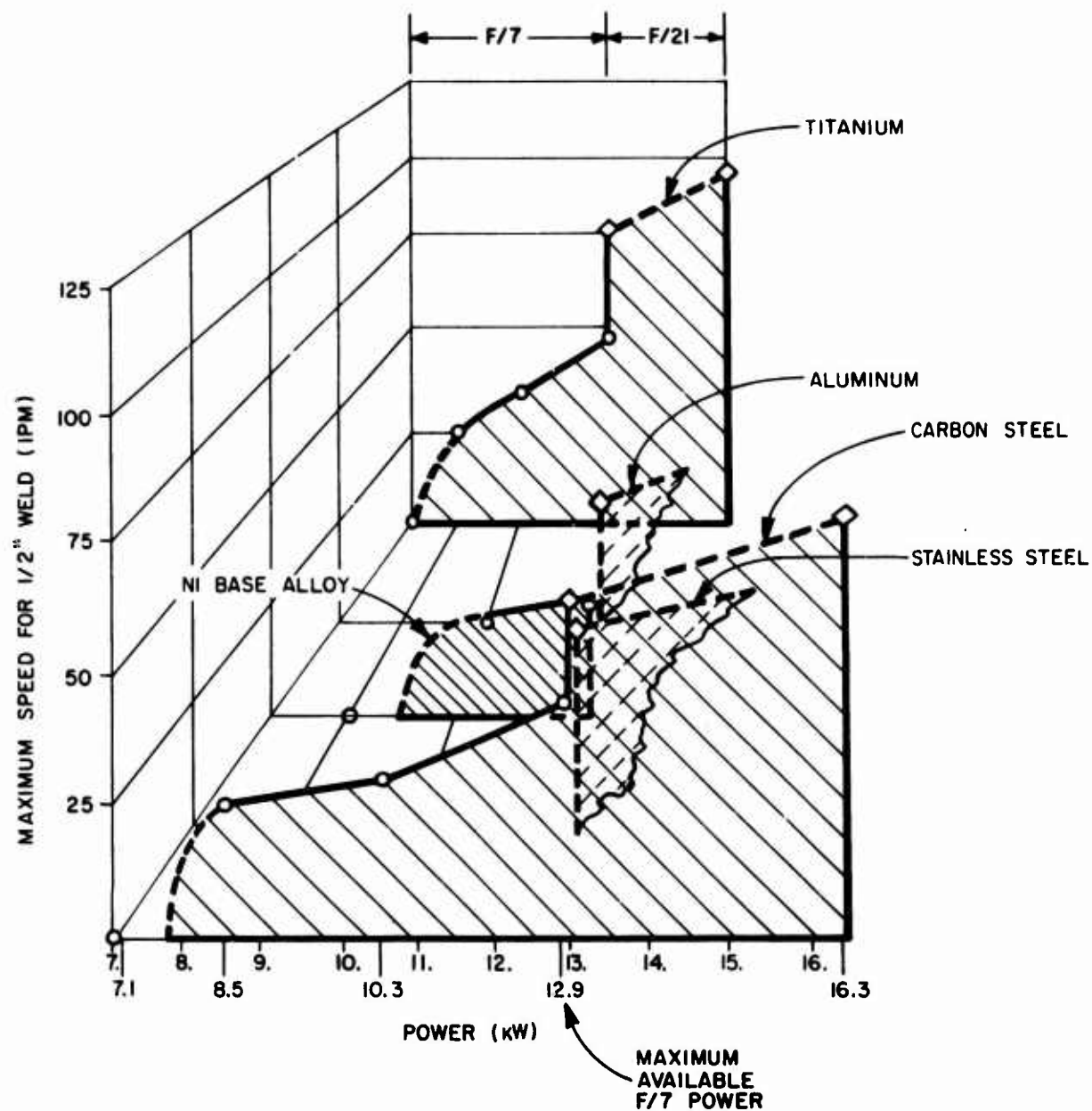


Figure IV-30. RESPONSE OF 1/2 INCH THICK BENCH MARK SPEEDS TO POWER

b. F/Number and Focus Tolerance.

F/Number and focus tolerance would seem to be related because the focal depth varies, approximately, as the square of the F/Number spot placement within the work should not be so critical for optics with high F/Numbers as it is with the more sharply focused, low F/Number optics.

A comparison (Figure IV-31) of the full penetration boundaries of processes operated at the same power on 3/8 inch titanium shows that at 90% of the benchmark speed:

F-7	3/16 inch tolerance
F-21	1/2 inch tolerance

Recalling that within this range some focal point placements produce better cross-section geometries than others, it is probably more useful to state that:

Focal Point placement for an F/21 telescope can be varied about twice as far, at 90% of benchmark, than can an F/7 telescope and it will still maintain a given weld geometry.

5. Beam Impingement Angle

When the laser beam strikes the work, a vertical plume of vapor is observed. In this experiment, the beam was tilted 5° to determine if moving its axis so that it was not coincident with the plume of vapor might reduce energy loss to the vapor and increase process speed for a given power.

Initial tests were run on 1/2 inch thick stainless steel to determine if any improvement could be made in the conduction dominated welds observed in earlier, marginally powered benchmark tests. No effect was observed in weld appearance. Penetration was achieved only at the original, low speed and at the same focus. Tests were made with the beam tilted and pointed into unfused metal and also backward into the molten pool. The anticipated increase in process speed, with an attendant improvement in weld width and uniformity, was not observed.

The tilted beam was also applied to aluminum. Tilted electron beams can reduce the size of the underbead. Large and irregular underbeads are characteristic of laser welds in heavy aluminum plate. However, no effect on the underbead was observed when the tilted beam was applied. Nor was any improvement in penetration observed when previously determined speed-focus data points were reexamined with the 5° beam tilt.

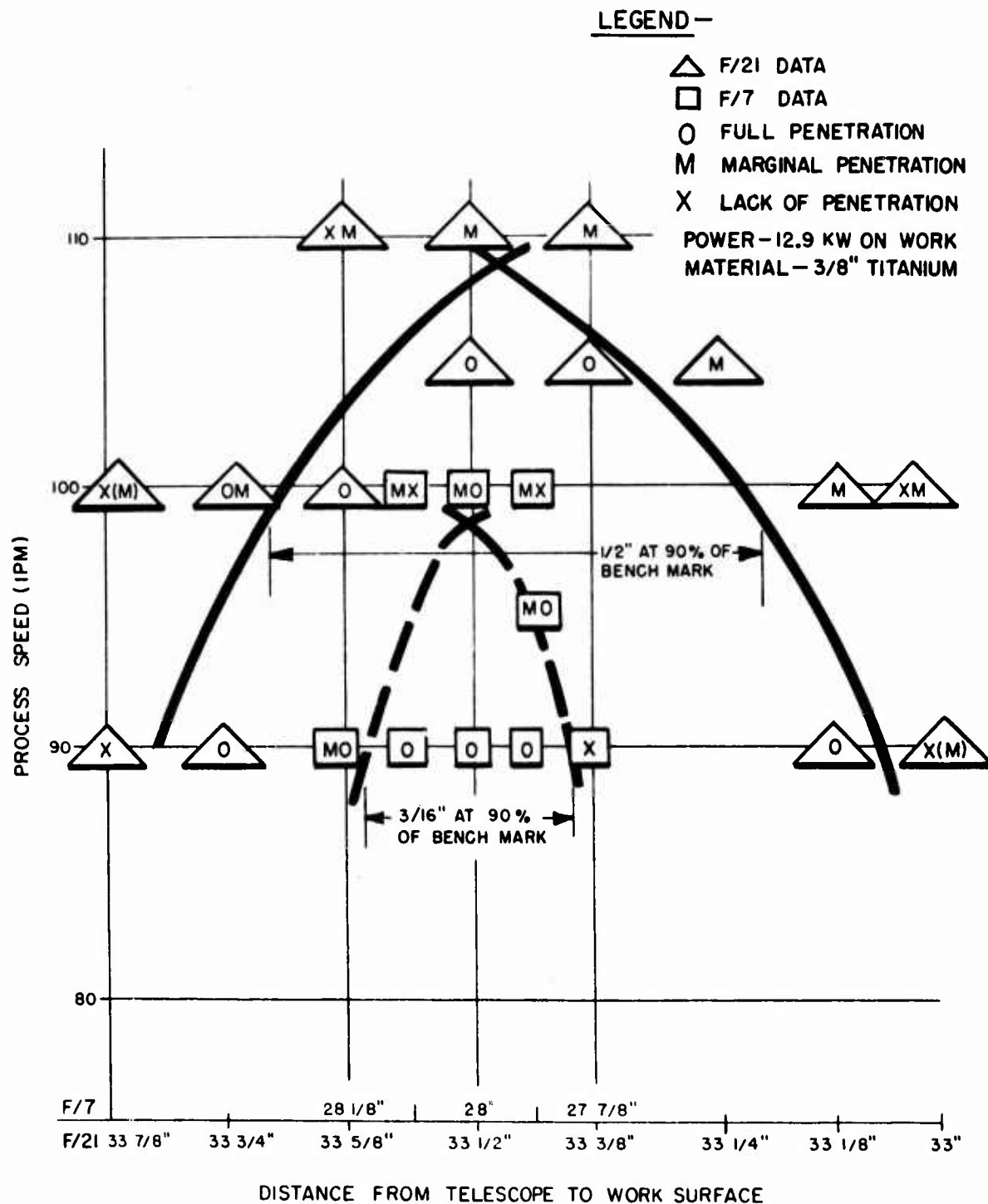


Figure IV-31. COMPARISON OF PROCESS SURVEY PATTERNS
FOR F21 AND F7 OPTICAL SYSTEMS

The tests run on stainless steel, duplicated an earlier trial. Both procedures used 13 KW on work, 25 ipm and 28-1/16 inch focal distance with jet-trailer hood (100 CFH helium in jet, 25 CFH argon in trailer). Tests in aluminum also duplicated earlier test points in that they were run at reduced power of 8.5 KW on work (to avoid hood damage), 50 ipm and focal distances of 28-3/16" and 28-1/8 inch, 40 CFH helium, 10 CFH argon used in the hood. Eighty CFH helium with no argon was also tested.

In these tests the beam was set at the maximum possible angle to increase the likelihood of an effect. An angle of 5° is the maximum angle permitted by the experimental facility. Structures added to the system limit rotation to approximately 5°. Additionally, a tilt of 5° requires that the specimen be placed at the extreme end of the work table. The jet-trailer shielding device was used on all materials except aluminum. In the case of aluminum, the diffuser hood was also tilted 5° to permit the F/7 beam to pass through its chimney. A wedge shaped skirt was added to prevent air from entering under the raised end as the weld progressed. After tilting the telescope, adjustments were made in the downhand mirror that feeds the telescope to make sure that all of the energy was directed into it. The beam settings were measured + .002 inches along the tilted axis to the point of beam impingement in the work. The chill bars were the same as those used in the reference experiments.

F. DETERMINATION OF MAXIMUM PLATE THICKNESS FOR FULL PENETRATION WELDING AT 15 KW (BEAM POWER)

If a process speed is selected that is slow enough for heavy welding, but which still permits the weld to operate through efficient cavity formation, then the following joint thicknesses represent the current maximum penetrating capability of the HPL industrial laser at 15KW (13.9 KW on the work) when an F/21 optical system is used:

Carbon Steel	0.6 + .005 inches
Titanium	0.6 + .005 inches
Nickel Base Alloy	0.57 + .005 inches
Stainless Steel (AISI 321)	0.544+ .005 inches

Aluminum was tested at slightly lower power (13 KW on the work) to conserve the diffuser hood. The maximum thickness penetrated was:

Aluminum	0.5 \pm .005 inches
----------	-----------------------

The minimum process speed referred to above is estimated to have been 40 ipm. In this series of tests the speed was first reported as 50 ipm. However, this should have been the benchmark for the thicknesses tested. The welding speed would be expected to fall 10 - 20 per cent below 50 ipm. Further, similar welds in subsequent tasks could be made only in the 30 - 40 ipm range -- not at 50 ipm. Finally, evidence from all previous welds suggests that the lowest speed for good cavity formation in the plate thickness was 30 ipm. The data in Tables IV-11 and IV-12 have been corrected to reflect 40 ipm as the minimum process speed, below which it is not desirable to operate.

G. REPAIR

Successful repair welds were made using a simple refusion technique (Fig IV-32).

Repair procedures were investigated in conjunction with the development of the initial welding procedures in 3/8 inch carbon steel, nickel base alloy, and titanium. Marginal trial welds were selected.

The first approach to repair was to run back over the weld without any intermediate cleaning operation. However, when these repaired welds were radiographed, severe porosity was observed in welds which has been relatively pore free.

These initial reweld procedures (Table IV-13) represented a slightly higher heat input to minimize the chance of porosity entrapment.

The rewelded surfaces were metallic colored and shiny. This suggested that the fault with the initial reweld repair lay in the presence of a contaminant on the surface - not in inert gas coverage.

Accordingly, the surfaces of the porous welds from the initial reweld process were carefully ground to remove the powdery smut and any small amounts of oxide which characterize an as-welded surface under laser shielding conditions. The smut is probably deposited metal vapor from the cavity. It is protected from

Material	Thickness ⁽¹⁾ of Butt Joint (inches)	Trial Speed (ipm)	Results Penetration				Remarks
			None	Partial	Good	Heavy	
Titanium (6Al-4V)	0.600±0.005	70	X				Demonstration (2)
		60		X			
		50		X			
		45			X		
		40				X	
Carbon Steel (300M)	0.600±0.005	60	X				Demonstration (2)(3)
		45		X			
		42-1/2		X			
		40			X		
		40 (33-3/8 focus)		X			
		40 (33-5/8 focus)		X			
		30				X	
Stainless Steel (AISI 321)	0.544 (Actual)	50		X			Demonstration (2) Irregular Drop Through (3)
		40			X		
		30				X	
Nickel Base Alloy (Inconel 718)	0.570 (Actual)	60	X				Irregular Drop Through (3)
		50		X			
		40			X		Unstable Plasma Severe Undercut
		40 (33-3/8 focus)		X			
(1) Selected so that penetration would be achieved at process speeds not less than 30 ipm.							
(2) Two 11" demonstration welds run at this speed to verify laser stability at this power.							
(3) Irregular drop through corrected by increasing flow of helium underbead gas until flow could be detected.							

Table IV-11. OBSERVED PENETRATING CAPABILITIES

	All Program Materials Except Aluminum	Aluminum
Laser Power (KW)	15	14.4
Power on Work (KW)	13.5	13
Speed (ipm)	Variable (40 Nominal)	Variable (40 Nominal)
Telescope-Work Distance (inches)	33-1/2 (except where noted)	33-5/8
F/Number	21	21
Surface Condition	Acetone Brushed Detergent Cleaned, Alcohol Dried	Acetone Wiped, Hand Scraped
Shielding		
Upper Surface Shield	Jet-Trailer	Diffuser
Gas	Jet: 100 CFH Helium Trailer 22-1/2 CFH Argon	Mixture: 100 CFH Helium and 30 CFH Argon
Lower Surface Shield		
Gas	Helium at Detectable Flow Along Underside of Weld	Helium at Detectable Flow Away Underside of Weld
Tooling		
Chill Bars	Copper with 1/8 inch Ribs	Copper with 1/8 inch Ribs
Spacing	1/4 inch	1/4 inch

Table IV-12. EXPERIMENTAL WELDING PROCEDURE FOR
MAXIMUM PENETRATION CAPABILITY DETERMINATION

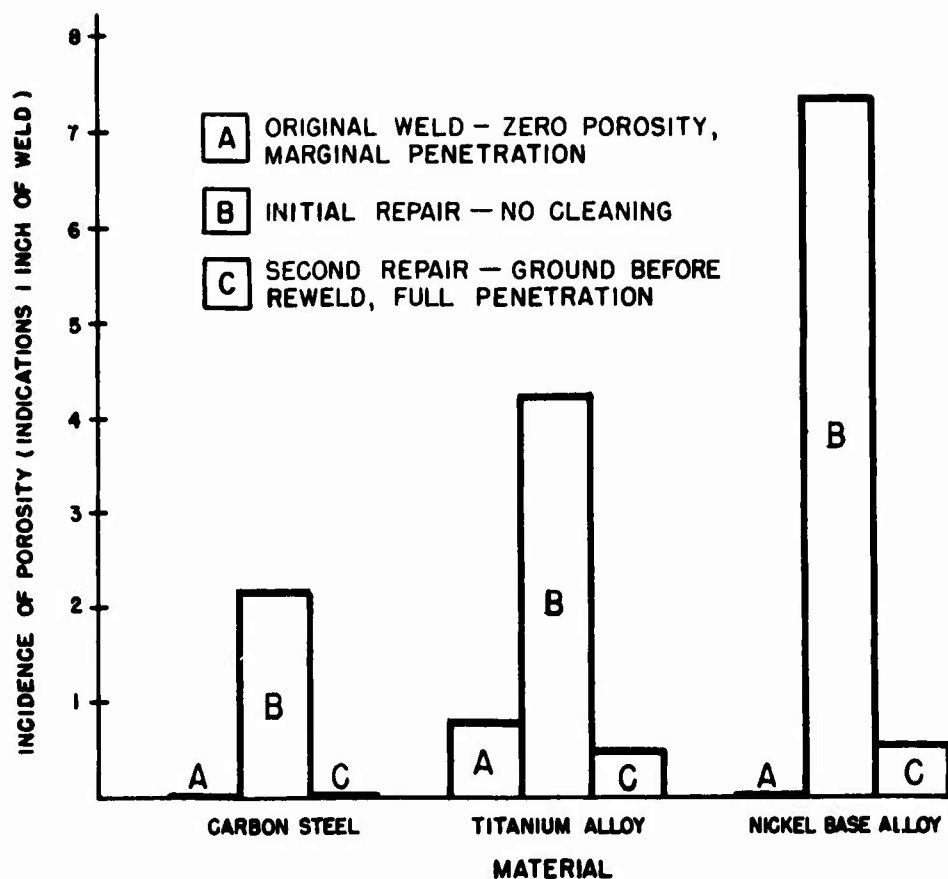


Figure IV-32. EFFECT OF REPAIR PROCEDURES ON POROSITY

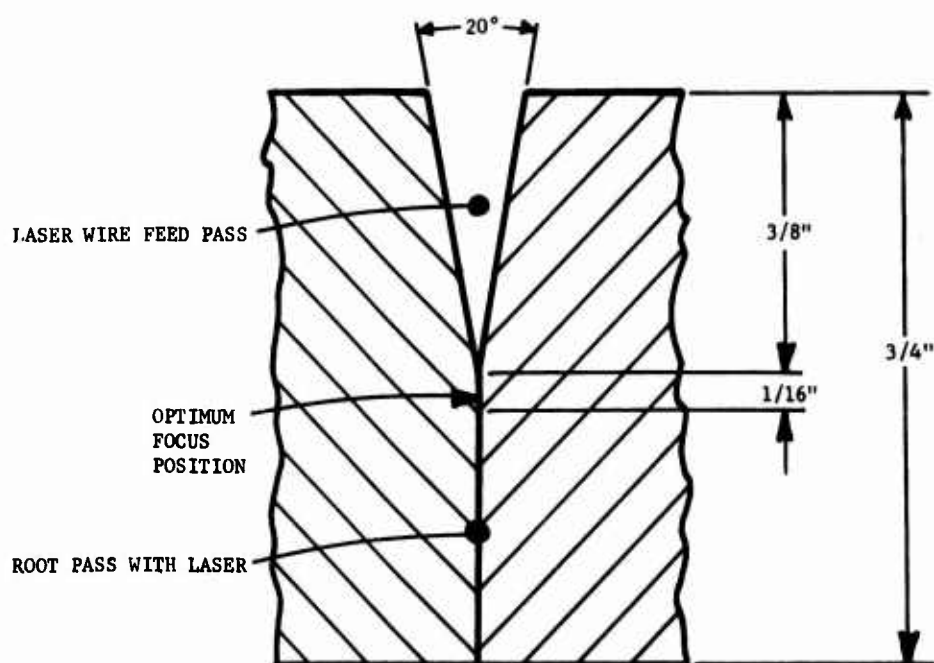


Figure IV-33. JOINT CONFIGURATION FOR WELDS IN HEAVY MATERIAL

	TITANIUM			NICKEL BASE			CARBON STEEL		
PROCEDURE VARIABLE	ORIGINAL	1st REPAIR	2nd REPAIR ⁽²⁾	ORIGINAL	1st REPAIR	2nd REPAIR	ORIGINAL	1st REPAIR	2nd REPAIR
Weld Identification	#254F	#288B	42B	#252A	#288C	36B	#256C	#288A	36
Power (KW)	16	16	16	16	16	15	15.7	15	16
Beam on Work	11.2	11.2	11.2	11.2	11.2	10.5	11.0	10.5	11.2
Speed (ipm)	70.0	63.0	63	75.0	67.5	67.5	65.0	58.0	58.0
Optics (F/No.)	F/7	F/7	F/7	F/7	F/7	F/7	F/7	F/7	F/7
Focus (Inches) ¹	28-1/16	27-31/32	28-1/16	28-1/16	27-31/32	28-1/16	28-1/16	27-31/32	28-1/16
Preparation	Wire brush Rinse with Acetone	None Weld Back Over the Original	Wire brush Rinse with Acetone	Wire brush Rinse with Acetone	None, Weld Back Over the Original	Wire brush Rinse with Acetone	Wire brush Rinse with Acetone	None, Weld Back Over the Original	Wire brush Rinse with Acetone
TOOLING									
Base	#F-24	#T-24	#F-24	#F-24	#F-24	#F-24	#F-24	#F-24	#F-24
Gas Shield (Jet Trail)	#SR-7	#SR-7	Hood	#SR-7	#SR-7	Hood	#SR-7	#SR-7	Hood
SHIELDING GAS									
Jet (CFH/Type)	100/He	100/He	50/He+12/A	100/He	100/He		100/He	100/He	100/He
Trailer (CFH/Type)	25/A	25/A	None	25/A	25/A		25/A	25/A	only
Underbead (CFH/Type)	20/He	20/He	20/He	20/He	20/He		20/He	20/He	20/He
NOTES:									
(1) F/7 Telescope was changed to F/10 and then reassembled as F/7 with a resulting 3/32 shift in optimum focus.									
(2) Carried out over a portion of 254F that had not been rewelded by 288B in order to show that this improved procedure would have worked on original welds.									

Table IV-13. PROGRESSIVE REPAIR PROCEDURES

oxidation by the hoods and trailer shields used in this program, and is usually evidence of good shielding. Smut does not appear in poor or marginal shielding situations.

The welds with ground surfaces were then subjected to a second repair trial (Table IV-13) and were found to be virtually free of porosity in spite of the heavy porosity present before this second reweld was applied.

Fig. II-4 illustrates the relative severity of porosity observed in the original weld and two successive rewelding steps.

It should be noted that the initial titanium weld was, in itself, a refused "repair" weld since the original pass was aborted and the procedure rerun. Presumably, the aborted pass also had smut and oxide on its surface. But porosity was not severe when the rerun was examined (condition "A", Figure IV-32). The difference may be the time between initial welding and initial refusion repair. When this time is as long as it was in the repair trials, the powdery smut can undoubtedly absorb moisture and contaminants from the air. Under ideal circumstances, an immediate reweld can be attempted with smut in place as was the case after the aborted pass on the initial titanium weld.

However, careful wire brushing and wiping to remove smut prior to any repair is a more practical recommendation for repair than setting a time limit between weld and repair. How long the smut could remain and still not influence a refusion repair weld depends too much on the amount of moisture in the atmosphere. Cleaning before a refusion repair appears to be the more reliable procedure if refusion is to be successfully used for repair.

The data in Table IV-14 suggest that repair had no effect on the strength of welds in program materials. The shrink cracking observed in the repaired steel welds was also observed in original welded joints. It is related to a short section of weld with a pinched cross section. Pinched cross sections are believed to be equipment related.

H. WIRE FEED

During procedure development tests (Phase II, Task I), wire feed techniques were considered. Testing was conducted on heavy section (3/4 inch) titanium carbon steel and nickel base alloy.

MATERIAL	TEST CONDITION			
	As Welded		Repaired	
Titanium (1)				
Ult (KS1)	138.2 (2)	-	139.7	139.5 (2)
Yld (KS1)	134.6 (2)	-	135.8	134.4 (2)
Elong (% in 1")	19.0	-	16.0	17.0
Ni Base Alloy				
Ult (KS1)	190.6, 199.3		187.1	199.3
Yld (KS1)	173.4, 169.0		169.1	167.3
Elong (% in 1")	5.0, 11.0		7.0	11.0
Low Alloy Steel (4)(5)				
Ult (KS1)	256.4, 256.4		252.9	252.9
Yld (KS1)	223.5, 225.4		225.4	224.3
Elong (% in 1")	9.0, 10.0		10.0	10.0
<p>(1) Stress relief only</p> <p>(2) Base metal failure</p> <p>(3) Aged after welding</p> <p>(4) Quenched and tempered after welding 1600° F 0.1 quench and temper</p> <p>(5) Post test examination revealed shrink cracking associated with variable cross section freezing</p>				

Table IV-14. EFFECT OF REPAIR ON WELD STRENGTH

a. Single Pass Welding (0.75 inch Material)

In the first series of tests, an appropriate joint configuration was established (Figure (IV-33)). The root thickness was established at 3/8 inch. This is the maximum thickness on which the available F/7 optics could be used effectively. A thicker root might be considered if an F/21 had been used. Acceptable welds thru 0.6 inch have been made with its straighter sided beam.

A simple "V" configuration was selected for ease of machining. Originally, the included angle was 10° . This divergence of the joint faces should have been greater than the convergence of the beam as it entered. However, some wall interaction was observed at all experimental focal point placements and the joint was opened, successfully, to 20° .

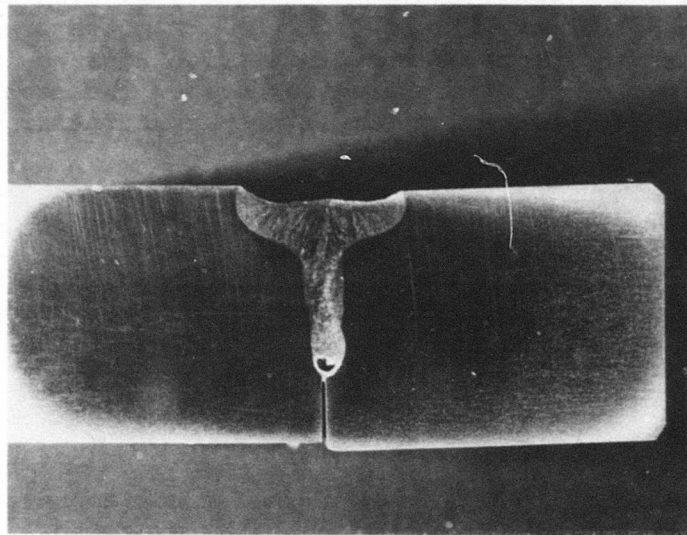
Focal point placement ranged from 1/16 inch above the top of the root to 1/16 inch below it. The deepest penetration was observed with the focal point placed at the top of the root. A movement of 1/16 inch in either direction reduced penetration about 50%.

A full penetration process was established using the joint configuration and focal point placement operating at 20 ipm using 15 KW (beam power - 10.5 KW on work). It was felt that the overwelding condition would be offset by the introduction of wire feed at the rate of 10 inches of 1/16 inch diameter wire for each inch of weld.

The wire was easily melted at the 200 ipm feed rate. However, this auxiliary molten filler metal gets in the path of the beam. The cavity fills. Efficiency is reduced as evidenced by increased plasma above the work, a distinct widening of the weld and a loss of all penetration between the root faces (Figure IV-34).

Initial wire feed was into the forward edge of the process. It was then felt that the previously mentioned molten metal effects might be avoided if the metal was fed into the pool at the trailing-edge, as far as possible from the beam interaction point. Tests with the wire melt-off point located 1/4 inch behind the beam, produced the same effect as that observed with the beam in front of the beam.

Two kilowatts were added to the procedure. This should have been more than enough to melt the few ounces of wire involved. No change was observed.



MATERIAL - NICKEL BASE ALLOY (0.75" THICK)

MAG. 2X

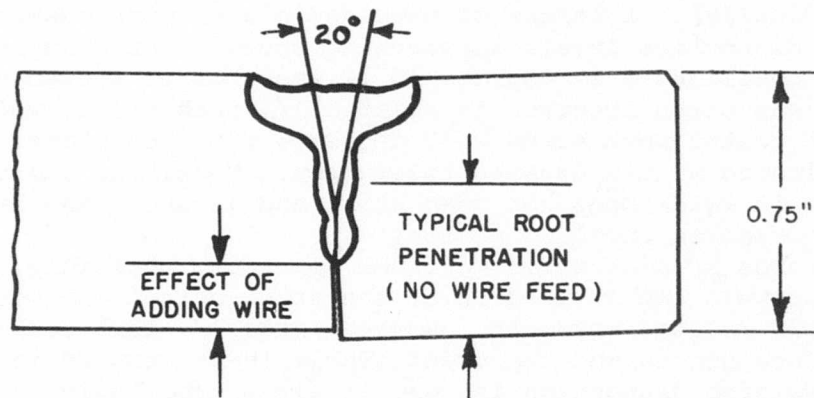


Figure IV-34. EFFECT OF FILLER WIRE ADDITION ON PENETRATION

Because added power failed to correct, or even influence, the loss of penetration, it was concluded that the presence of molten metal is the cause of the penetration loss - - not the quenching effect of melting the extra metal. The result in any case is a loss of the characteristic deep penetrating capability of the laser welding process.

b. Two Pass Welding (0.75 inch Material)

In the second set of tests a separate root pass procedure was established at 40 ipm and 15 KW (beam power). Figure IV-35 shows a cross section of such a weld. Filling of the "V" shaped portion of the weld was easily accomplished.

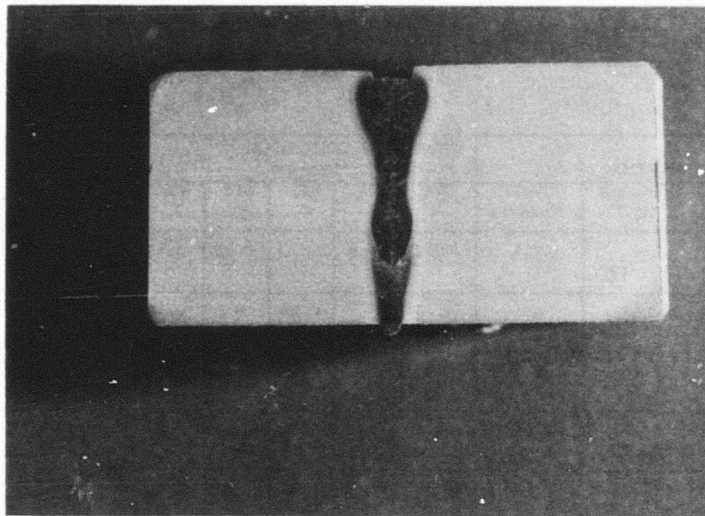
I. DISTORTION:

A review of all panels showed that minor amounts of transverse and longitudinal distortion could be expected. One panel of each of the Task 2 welding procedures was selected for detailed study. Table IV-15 lists the measured angles (transverse and longitudinal).

In general, these angles are very low (typically 0.2 - 0.4 degrees transverse, and either 0.3 or else less than 0.1 longitudinally). A number of unwelded plates were observed to have distortion levels approaching these. For example, distortion equalling 0.12 degrees (0.02 inch bow in a span of 18 inches) was often observed in sheared 1/4 inch stock, while 1/2 unwelded plates were bowed 0.37 degrees; yet such plates would be considered within useable tolerances. Thus, the distortion observed in welds does not seem high, and is about the same as that observed in unwelded plates.

Trends in distortion were not apparent. Possibly, the slight preweld camber in much of the stock offset the very small weld-related movement. However, the 1/4 inch carbon steel was surface ground and the trend (Table IV-15) toward increasing transverse distortion is very likely a true indication of metal movement when laser welding this particular material. No significant restraint was used.

It should be noted that an angular change of 0.25 degrees represents only about 0.005 inches of plate movement per foot of distance away from (or along) the weld.



Material - Low Alloy Steel

Mag 2X

Preparation: 20° included "V", Root face 3/8"

Pass #1 - Root Pass Procedure: 15kW, 40 ipm, 27-31/32 inches
(just at bottom of "V")

Pass #2 - Filler Wire Procedure: Same as above with 60 ipm of
1/8 inch filler wire added

Figure IV-35. LASER WELD IN 3/4 INCH PLATE

PLATE IDENTIFICATION				TRANSVERSE DISTORTION (angular degrees)					Longitudinal Distortion (degrees)	Power (Work KW)	Procedure Speed (ipm)
Material	Ident.	Thickness (in.)	Weld Numbers	STA A	STA B	STA C	STA D	STA E			
Titanium	D	1/4 24" x 18"	91A	0.13	0.48	-	0.35	0.20	0.32	7.0	100
Steel	C	1/4 24" x 12"	95D	0.45	-	0.28	-	0.14	0.01	7.7	100
Ni Base	E	1/4" 24" x 12"	94D	0.48	0.39	0.38	0.19	0.10	0.07	7.0	100
Titanium	H	1/2 24" x 24"	244A&B	0.31	0.27	-	0.31	0.32	0.04	13.1	30
Steel	I	1/2 24" x 12"	203A&B	0.17	0.72	0.57	0.38	0.11	0.29	13.5	30

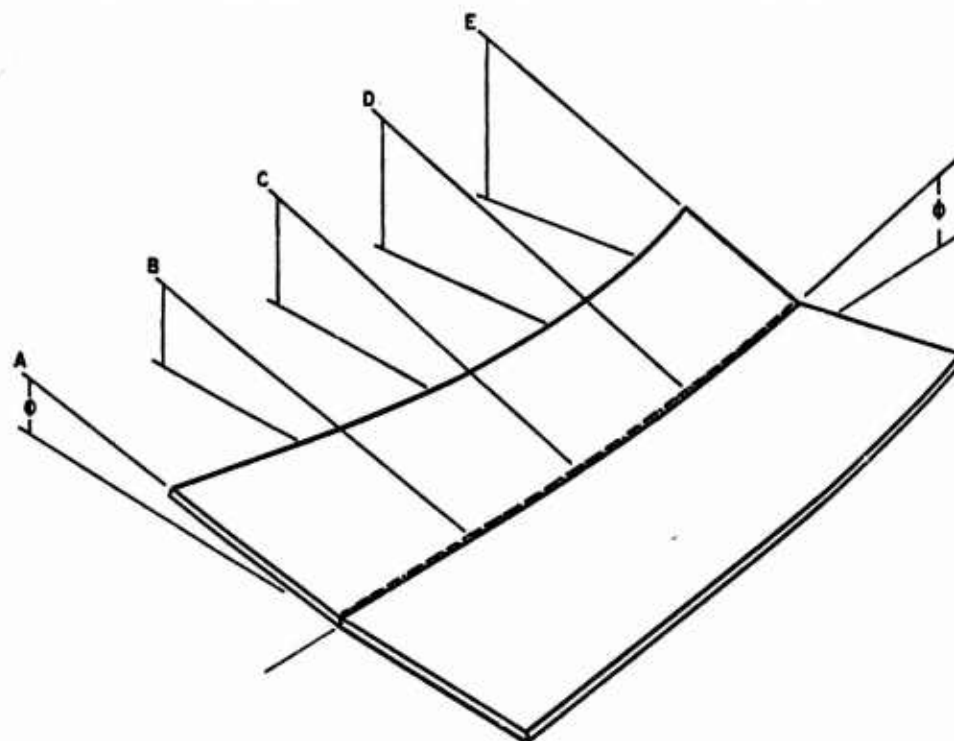


Table IV-15. SUMMARY OF PANEL DISTORTION

SECTION V

LASER WELD EVALUATION

This section describes the behavior of laser welds in non-destructive testing and in destructive mechanical tests.

The non-destructive tests are covered in a separate sub-section in order to set forth the NDT procedures applied. NDT indications are tabulated in Appendix B to provide an overview of the quality of the laser welds obtained in this study.

Mechanical test results are discussed separately for each program material (Carbon Steel, Titanium Base Alloy, etc.). Related information such as the chemical and metallurgical characteristics of the base material is included along with observations relating to specific welding behavior of each material. A typical series of mechanical tests subjected a material to the following:

- Tensile Tests (three thicknesses)
- Axial Tension Fatigue Tests (two thicknesses)
- Fracture Toughness (maximum thickness)
- Alternate Immersion Stress Corrosion Tests
(smooth specimen)
- Notched Stress Corrosion Tests
- Tensile Tests of Repaired Welds

A. NON-DESTRUCTIVE TESTING OF LASER WELDS

Non-destructive testing in the last phase of the program provided the first check on internal weld quality. Most of the information in Section IV had to be based on external appearance and macro sections only. A number of non-destructive test methods were evaluated on set up welds that were known to contain various types of defects.

The best procedure for each method was then applied to welded test panels. Non-destructive testing was accomplished by the Process Engineering Department, Douglas Aircraft Corp., Long Beach California.

1. Method

The following test methods were applied:

Radiography
Penetrant
Magnetic Particle (penetrant)
Ultrasonic

The approach to inspection on these laser welds was the same as that applied to actual parts in aircraft production. It is in contrast to the materials engineering approach of achieving final specimen thickness and then applying maximum sensitivity examinations to assure that response to the mechanical test is entirely a function of material properties.

The use of the simulated production inspection to select test specimens from sites that appear to be defect-free was coupled with a careful post-test evaluation of fracture surfaces. A correlation of the inspection records with fracture surfaces provides a more practical picture of the reliability of laser welds under manufacturing conditions than does the application of maximum sensitivity inspection procedures to provide an unrealistic degree of assurance that the weld metal is defect-free prior to test. The latter is useful in obtaining material properties, but the objective of the program is to assess laser welding as an aerospace manufacturing process.

a. Radiographic Procedure

Radiography was performed on all welded panels and appeared to provide the most comprehensive survey of defects. A 300 KVp Picker X-ray Machine was used by Douglas Aircraft Corporation for their investigation of 1/2 inch titanium and some of the 1/4 inch carbon steel. Structrix D-4 film supplied by the Gevaert Company was used in this radiographic survey. Radiography of the remainder of the material was accomplished by a certified NDE laboratory using a GEOX 250 machine and Kodak type M film to show a 2-2T penetrameter artifact.

b. Fluorescent Penetrant

This technique was used to inspect for surface defects in all materials that were to be mechanically tested (titanium, nickel and carbon steel). The penetrant materials were:

Cleaner:	Dubl-check	DR61, Turco (Trace Sulfur)
Penetrant:	ZL-60	Magnaflux Corp. (0.5% Sulfur)
Developer:	D-100	Sherwin Company

c. Fluorescent Magnetic Particle Inspection

Surface and subsurface defects can be detected by this method as long as the material is magnetic. This test was, therefore, applied only to welds in steel. The materials used were as follows:

Magnetic Oxide:	Magnaglow, Type 14AM Magnaflux Corporation
Field Source:	Parker probe, portable electromagnet

d. Ultrasonic Inspection

The contact pulse-echo, shear wave method specified in ASTM E-164, was applied. No artificial reference reflector standards were prepared because of the variations in specimen thickness and the diversity of materials. Instead, an aerospace calibration procedure was applied as follows:

Step 1: Search unit position adjusted so that beam reflects from edge of plate.

Step 2: Search unit position adjusted to obtain first top corner reflection (Fig. V-1 Top).

Step 3: Instrument gain adjusted until the signal from the first to corner reflection is just saturated (Fig. V-1 bottom). The second bottom corner reflection is about 80% saturated.

With this calibration procedure, it was found necessary to select a search unit geometry that placed the first bottom reflection at the root of the weld before the front edge of the search unit could touch the top bead. Specifically, a 1/4 square inch, 2.5 mHz, 45° crystal was used. In initial tests with this search unit, reflections from the side of the characteristically heavy underbead reinforcement were observed to obscure root area defects. The underbead had to be removed. When the underside of the weld had been ground flush, the fine linear pores observed in the X-rays were detected on the CRT of the ultrasonic equipment. Search angles of 45° and 60°, as well as frequencies of 2.5 and 5 mHz, worked equally well as long as the search unit was

sized to avoid the top bead and still place its first bottom reflection at the weld root (1/4 square inch with the transducer 1/2 inch from the leading edge of the search unit in the case of 1/2 inch welds). The unobstructed use of the first bottom reflection and removal of root reinforcement appeared to be necessary if this technique (Fig. V-2) was to detect root porosity.

Pulse-echo techniques were used to analyze the distribution of fine linear porosity in Titanium. After initial inspection by X-ray, the weld was cut from the panel. The sides parallel to the direction of welding were ground. The pulse was directed into one ground side and reflected from another. Flat bottom holes were used for calibration. The indications recorded during a C-scan were then confirmed by sectioning. Fig. V-3 is the C-scan trace. Fig V-4 is a sketch of the radiographic and metallographic correlation. The indications along the length of the scan are echos from root and crown contours. The patches identified as A1, A2, B1, and B2 are the porosity.

2. Overview of Quality

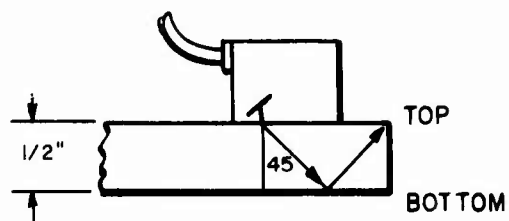
Sixty four welds were tabulated in this overview including the 59 welds required for the program. An overview of the yield in terms of useable weld can be obtained by applying a criteria that accepts isolated porosity but rejects any internal linear defect. Such a rudimentary criteria would have resulted in the rejection of only fifteen plates as follows:

Titanium (1/4 inch) - Nine plates produced/no rejections
Low Alloy Steel (1/2 inch) - Fifteen plates produced / no rejections

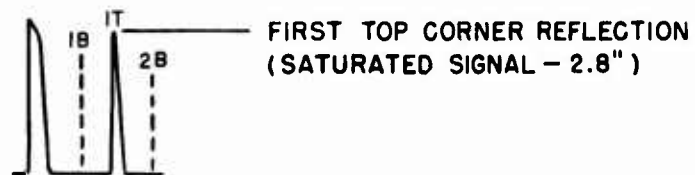
Inconel (1/4 inch) - Nine plates produced/one rejection
Low Alloy Steel (1/4 inch) - Thirteen plates produced/ two rejections

Titanium (1/2 inch process development) - Five plates/ two rejections

Titanium (1/2 inch) - Twelve plates - produced and rejected for a microporosity condition not previously observed in program.

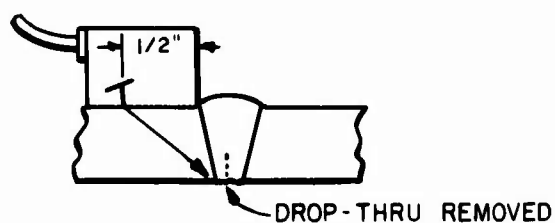


CALIBRATION POSITION OF SEARCH UNIT

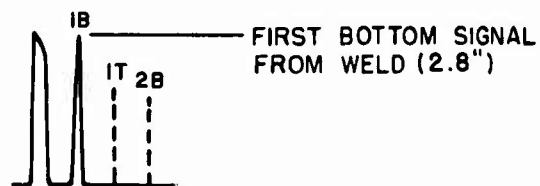


CRT PRESENTATION OF REFLECTION FROM TOP CORNER OF PLATE DURING CALIBRATION.

Figure V-1. SEARCH UNIT CALIBRATION PROCEDURE



SEARCH UNIT POSITION



CRT DISPLAY

Figure V-2. TYPICAL UT INDICATION

SPECIMEN-(TI-FF) 1/2" THICK

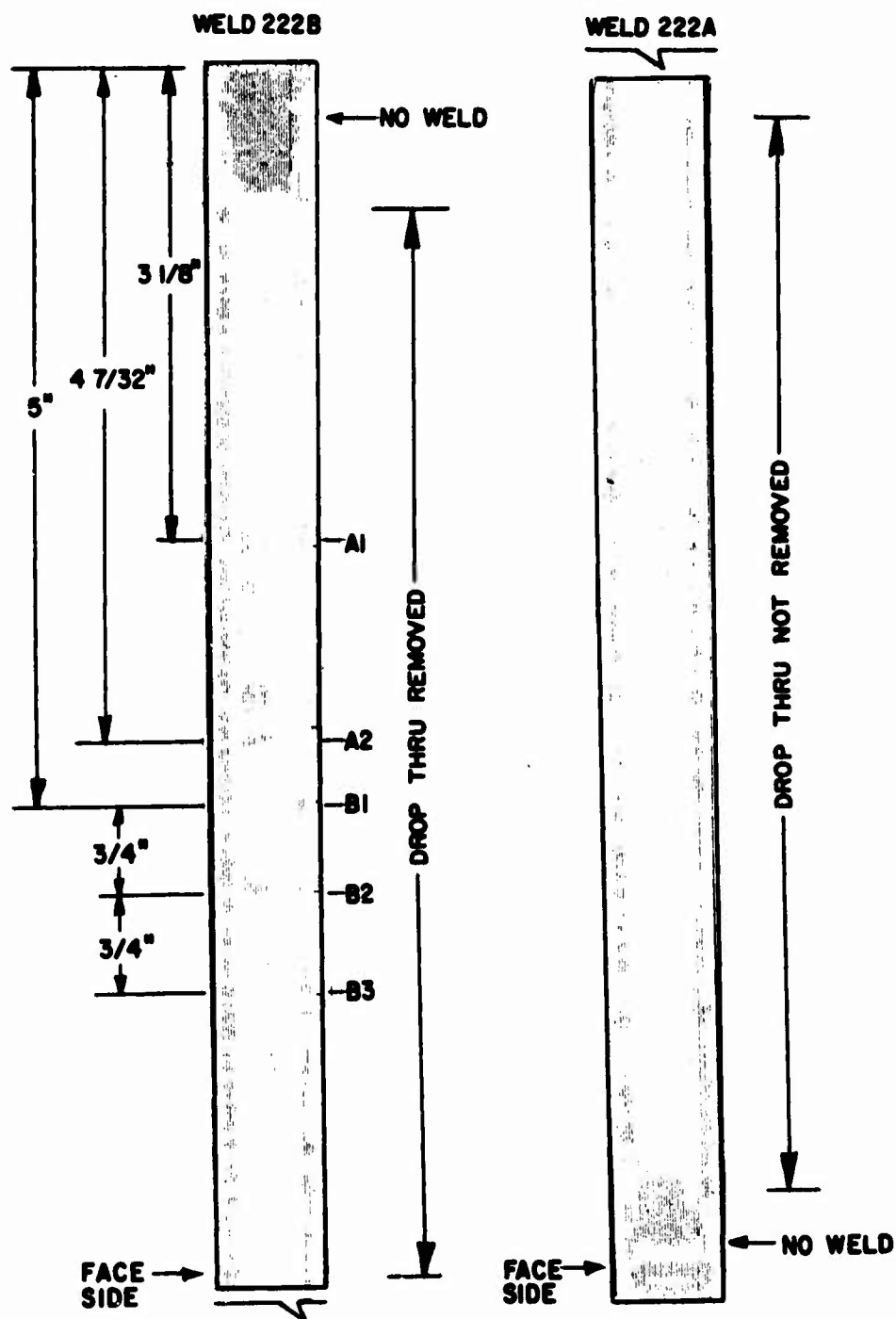
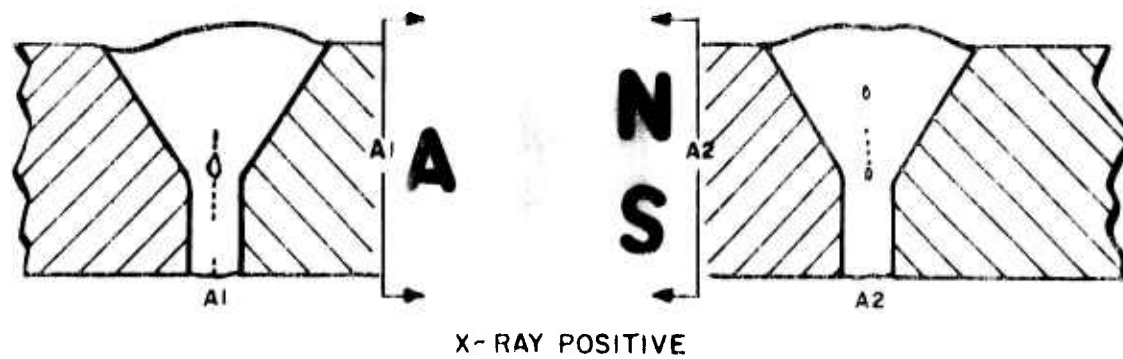
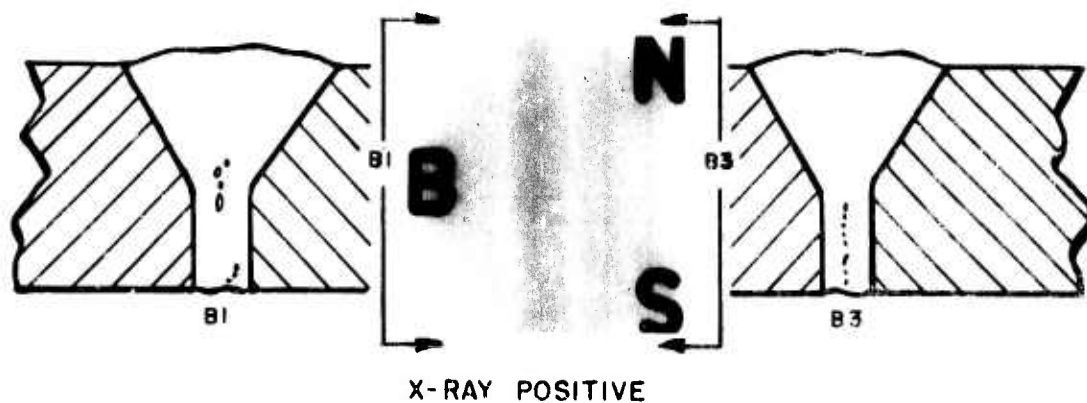


Figure V-3. UT PULSE ECHO C-SCAN OF
1/2 INCH TITANIUM WELD

SPECIMEN (TI-FF) WELD 222B



X-RAY POSITIVE



X-RAY POSITIVE

Figure V-4. DEFECT VERIFICATION FROM
X-RAY AND UT INDICATIONS

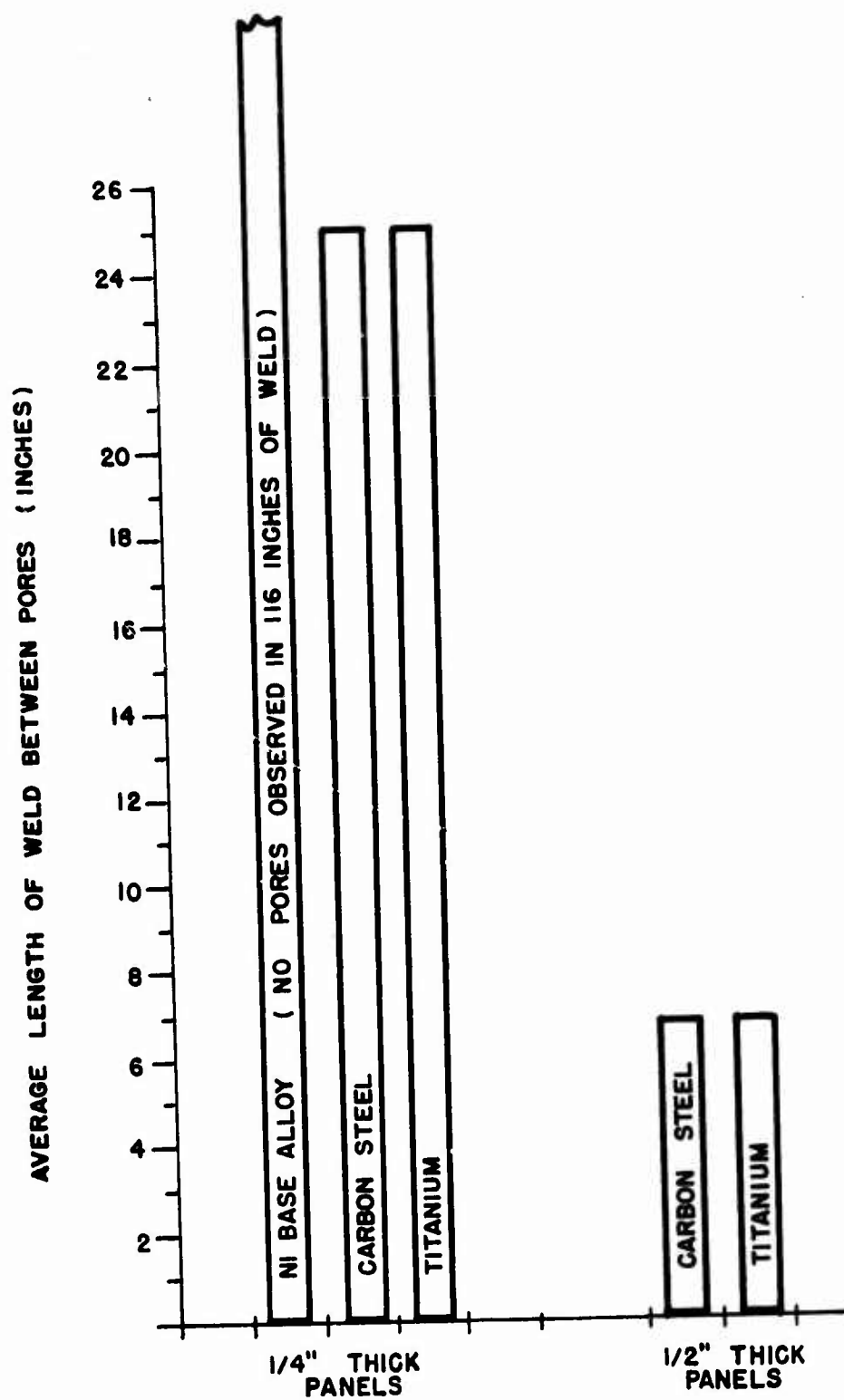


Figure V-5. RELATIVE INCIDENCE OF POROSITY

Fig. V-5 sets forth the incidence of all detectable porosity in test panels. As thickness increased, the incidence of porosity also increased. Nickel base alloys resulted in the most pore-free welds. The quality of carbon steel and titanium welds was high enough, however, to suggest that they would easily meet aerospace standards (at least in the 1/4 inch thickness).

3. Disposition of Panels

The above non-destructive evaluations were used as the basis for selecting test specimen coupons from weld sections that appeared to be defect-free. The location of indications detected using standard aerospace NDE practice is shown in Appendix B.

After the selected specimen sections of the welds had been machined into test specimens and subjected to mechanical test, the surfaces of the broken fatigue test specimens were inspected at 25X (or by scanning electron microscope). A correlation was carried out between the results of these first NDE findings and the number (and type) of defect that was revealed by inspection of the fracture face. This correlation is summarized for each alloy in appendix C, and the implications are discussed in terms of each program material in the following sections.

B. LASER WELDS IN LOW ALLOY CARBON STEEL (300M)

As noted in Section III, this material was selected for its inherent strength, weldability and unusual fracture toughness.

1. Base Metal Characteristics

The program material came from a single heat of 300M alloy. The composition of this alloy is that of a silicon (1.6% Si) modified 4340 low carbon steel with minor increases in carbon and molybdenum. Vanadium is also added.

The actual compositions used in this program were:

C	Mn	Si	Ni	Cr	Mo	V	Fe	Billet
Nominal(%)								Ident.
0.40	0.75	1.60	1.85	0.85	0.40	0.08	Bal.	-----

Furnished* to Program								Billet
C	Mn	Si	Ni	Cr	Mo	V	Fe	Ident.
0.041	0.70	1.60	1.77	0.77	0.43	0.08	Bal.	1T
0.042	0.69	1.61	1.75	0.77	0.42	0.08	Bal.	1B
0.042	0.70	1.62	1.76	0.78	0.43	0.08	Bal.	7T
0.041	0.69	1.60	1.75	0.78	0.42	0.08	Bal.	7B

*Latrobe Steel - Latrobe, PA Heat C24402 (Ingots 1 and 7)

The material was in flat bar form with as-rolled(rounded) edges. All bars were six inches wide. For welds made parallel to the rolling direction (transverse test welds), the rounded edge was ground back far enough to produce a square surface preparation.

Bar stock rolled less than 3/8 inches thick is not available. Therefore, 1/4 inch thick test pieces were produced by Blanchard grinding 1/16" from each face of 3/8 inch flat rolled bar.

The material was produced to the following specification:
MIL-S-8844C, Class 3, Cond E-2
LPS DECARB Specification Tolerances
Grain size was reported to be ASTM Six and One Half to Seven and One Half

The bar was produced by vacuum arc melting, hot rolling, and then heat treated at the mill by normalizing and annealing.

Ultimate Tensile Strength: 286 - 294 Ksi
Yield Strength: 240 - 246 Ksi (0.2% Offset)
Elongation: 9.0 - 11.2 (% in 4D)
Reduction of Area: 32.2 - 44.9 (%)

Some variance of strength was observed at the several test locations throughout the billets (1 top and 1 bottom; 7 top and 7 bottom), producing the above spread of properties.

2. Panel Welding

The welding set-up tests used to establish the procedures employed to weld the low alloy carbon steel panels and photographs of the resulting development welds are shown in Appendix D.

Table V-1 summarizes the low alloy steel test panel welding procedures which included wirebrush and acetone rinse as a

pre-weld cleaning procedure. Fig. V-6 sets forth the details of shield set-up. Fig. V-7 shows the tooling that was used to hold the panels for welding. The quality of the resulting test panels was high (see Fig. V-5) and is described for each welded test panel in Appendix B. Appendix B also reports the following experimental information in detail:

Panel Identification Size Orientation and Shape
Identification Orientation and Location of Each
Weld in Panel
Procedure Details for each Weld in the Panel
Location of all Non-Destructive Indications
In Each Weld
Location of Test Specimen Coupons in each Weld
Relationship between NDT Indications and Test
Specimen Location

3. Welding Characteristics

Behavior during welding that sets 300M apart from other program materials was noted throughout the program and is summarized here.

The low alloy carbon steel (300M) used in these tests was the most weldable of all program materials. Procedures were readily established in all program test plate thicknesses (1/4, 3/8 and 1/2 inches). In spite of its high hardenability, it could be laser welded without preheat in sections up to 0.5 inches. No post-solidification cracking was observed. The metal utilizes laser energy more efficiently than any other program material and exhibited, with titanium, the greatest penetrability observed in the program -- 0.6 inches. As noted in the NDT overview section, welds of very high quality were easily obtained.

The distortion of the 1/2 inch welds documented in Section IV - Table IV-15 was slightly greater than Titanium probably because the steel undergoes a transformation on cooling. Welds in thinner program thicknesses (where less volume of steel is involved) exhibited distortion levels almost identical to titanium and the nickel base alloy.

The cross sections of the low alloy steel welds have very high (5:1 or 6:1) depth to width ratios. They compare to the nickel base alloy in this respect. Titanium typically exhibited 4:1 ratios. However, the carbon steel

cross sections in thinner plates indicated an improper focus condition, which produced pinched cross sections (Fig. V-8). As noted in Section IV, this condition suggests that the focal point was too close to the plate surface. Occasionally, a slight change in focus occurred (Weld 118 Section A compared to 118 Section B). The 1/4 inch plates from which weld 118 was made had been ground - removing warpage as a cause. Apparently, the F/7 optical system contained an instability.

The pinching of the cross section leads to cracking shown in Fig. V-9 (Weld 118 Section A). In all, twelve instances of cracking were observed. All were very short suggesting that focal condition causing the pinched section occurred over only a short length of weld.

The ability of the laser to weld the 300M grade of low alloy carbon steel, without preheat, is of considerable practical significance. No preheat was used in any thickness and no evidence of quench cracking was observed.

4. Specimen Preparation

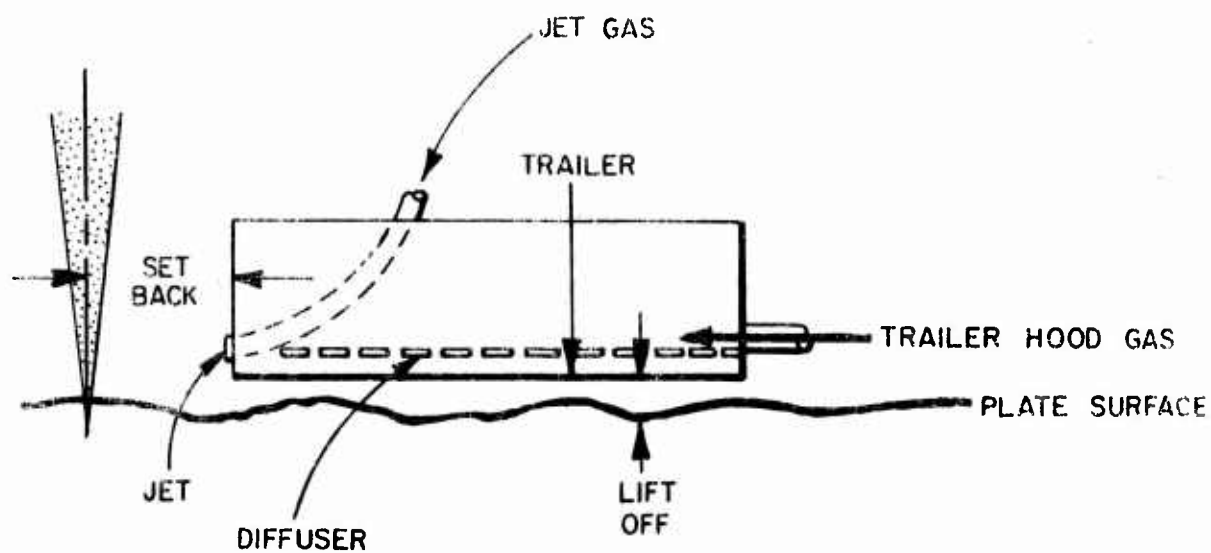
Once low alloy carbon steel panel weldments were completed at the AVCO Everett Research Laboratories, Everett, Massachusetts, they were identified and shipped to the Long Beach, California plant of the Douglas Aircraft Corporation for weld evaluation. At that site, the following steps were implemented in processing the material from this welded panel form to finished test specimens:

- A. Receive test panels
- B. Non-Destructive evaluation, welded plates only
- C. Specimen location and layout in areas with no NDT indications
- D. Remove coupons from plates (Band Saw)
- E. Reduce weld hardness for machining (normalize and temper to Rc 32)
- F. Check and straighten
- G. Machine to finish dimensions
- H. Copper plate against decarburization
- I. Austenitize (1600°F) oil quench, strip copper and temper to 275-305 KSI ULT, descale by abrasive blast

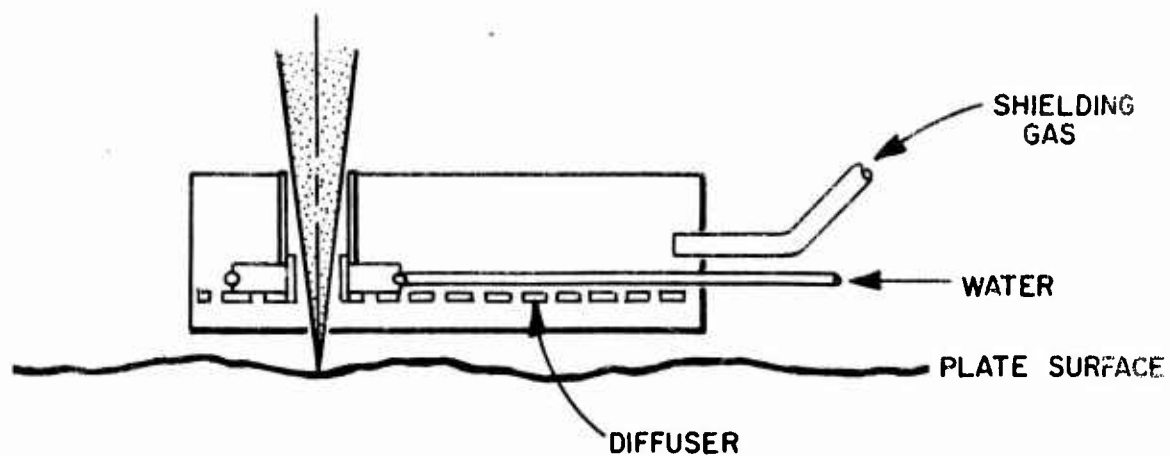
NOTE: Some straightening was done in the heat treatment cycle resulting in the breakage of one specimen and cracking of several others.

Welding Parameters	PANEL THICKNESS		
	1/4 inch	3/8 inch	1/2 inch
Power, Beam (KW) Power on Work (KW)	11.0 7.7	16.0 11.2	15.0 13.5
Process Speed (ipm)	100	65	30
Optics (F/No.)	7	Same	21
Focal Distance (in)	28-1/16	Same	32.5
Surface Preparation	Deburr, Wire Brush Rinse w/Acetone	Same	Same
Shielding Gas (Type/CFH)			
Jet	Helium / 100	Same	Same
Trailer Hood	Argon / 25	Same	Same
Underbead	Helium / 10*	Same	Same
Shield Position			
Set Back (in)	7/16	Same	3/8
Lift Off (in)	0.03	0.04**	0.03
Gap	002*	Same	Same
Mismatch	005*	Same	Same
Tooling	Figure V-7	Same	Same
Filler Wire	Not Used	Same	Same
<p>* Unless noted for a specific panel in Appendix B.</p> <p>** In some panels, surface height varied 0.062 in. such that hood lift-off approached 0.1 inches. This is excessive at the nominal 25 CFH flow rate but appeared to be acceptable if the flow rate was raised to 50-60 CFH.</p>			

Table V-1. LOW ALLOY STEEL WELDING PROCEDURES



JET TRAILER SHIELD



FULL HOOD SHIELD

Figure V-6. DEFINITION OF PROCEDURE VARIABLES

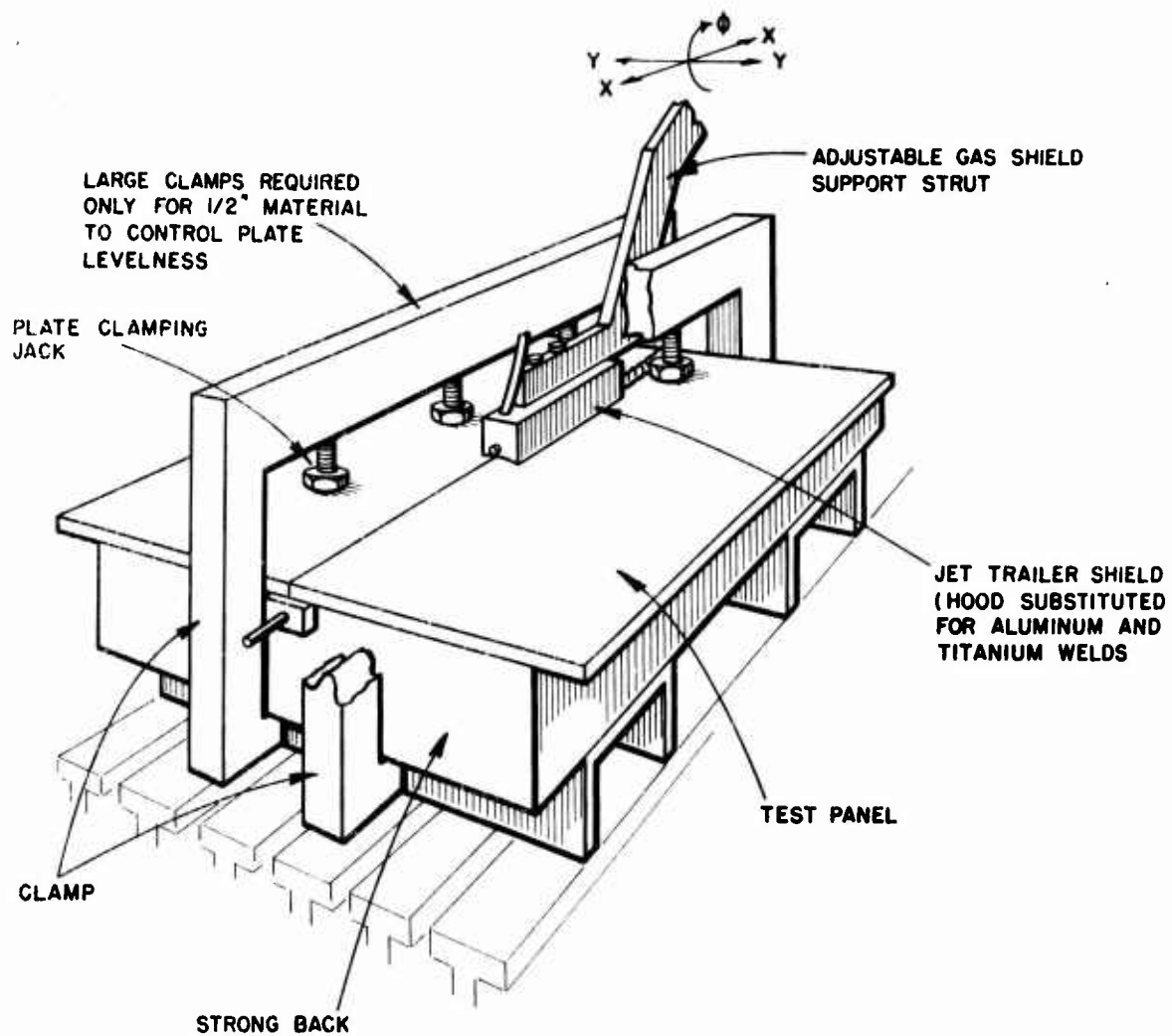
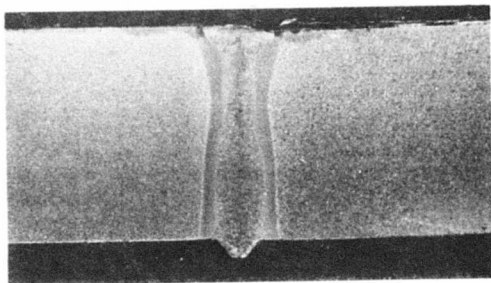
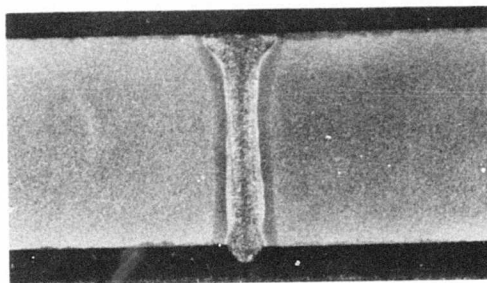


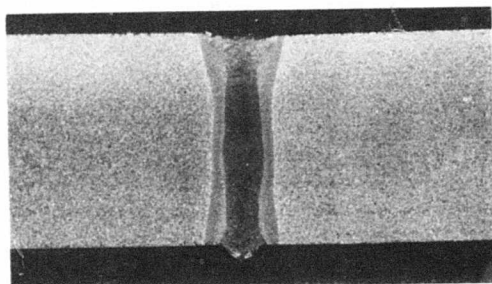
Figure V-7. TOOLING CONFIGURATION FOR PANEL WELDING



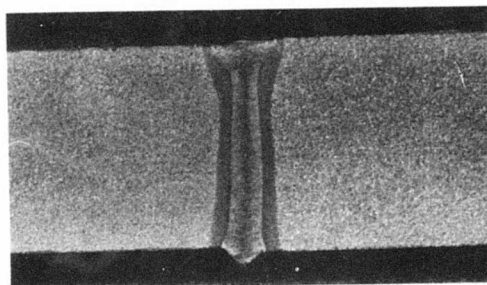
Negative No. LR-215 Mag. 4.9X
(a) Weld No. 118A



Negative No. LR-216 Mag. 4.7X
(b) Weld No. 118B

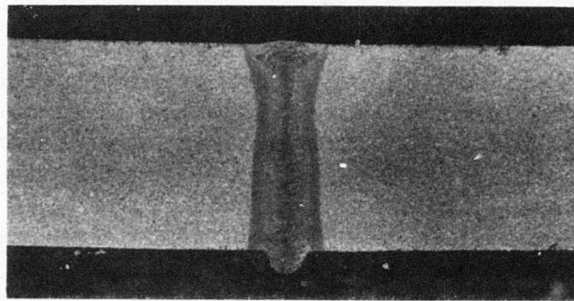


Negative No. LR-217 Mag. 4.7
(c) Weld No. 118C



Negative No. LR-218 Mag. 4.8
(d) Weld No. 118D

Figure V-8. TYPICAL LOW ALLOY CARBON STEEL
WELD CROSS SECTIONS



Negative LR-220
Weld No. 118F

Mag. 4.7X

Figure V-9. CRACK IN PINCHED CROSS SECTION (STEEL)

- J. Inspect (magnetic particle)
- K. Clean up cracks (controlled surface grinding)
- L. Re-inspect for cracking or burning.

All of the 300M alloy steel test specimens were evaluated by magnetic particle testing to confirm freedom from cracks after heat treatment. This evaluation is a normal precaution with this alloy. Three (1/4 inch thick) fatigue specimens (No's FTW-1S, FTW-5S, FTB-3S) were found to have numerous surface indications at the test section. These indications are sufficient to require removal prior to any testing. Specimen FTW-3S broke during straightening.

The three 1/4 inch thick steel fatigue test specimens were magnetic particle tested after surface grinding to remove magnetic particle indications and were found to be free of surface defects. It was necessary to remove 0.005 inches from specimen #FTW-5S and 0.015 inches from specimen #'s FTW-1S and FTB-3S.

Two 1/2 inch steel (300M) base metal fatigue specimens were magnetic particle inspected and found to be free of surface defects after grinding to improve surface finish in an attempt to reduce test point scatter.

All of the notched (fracture toughness and KISCC stress corrosion) test specimens exhibited magnetic particle indications at the root of the notch. However, only one was found to be cracked so as to make the specimen (#FBM-4S) useless for test purposes. The remaining specimens appeared to be suitable for testing without additional work.

All fatigue specimens were dimensionally checked after all work was completed. All were within tolerance, which assures that bending stresses cannot exceed + 4 KSI.

5. Mechanical Behavior

As a final task in the program, low alloy carbon steel weld specimens were subjected to the following tests:

- Tensile (including tests of repaired welds)
- Axial Fatigue Tests
- Fracture Toughness K_{Ic}
- Notched Stress Corrosion K_{ISCC}
- Smooth Bar Stress Corrosion Alternate Sea Water Immersion
- Microhardness

Each of these tests are described in the following sections in terms of:

- ... Test Procedure
- ... Test Objective
- ... Results

a. Tensile Tests

Tensile specimens containing welds (with the reinforcement left on) never exhibited less than 98.8% of the strength of the base metal.

Procedure. The transverse tensile weld specimens were designed to place the maximum length of laser welded joint under test. This amount was limited by available testing machine capacity and the length of specimens that could be removed from the weld test panel. The width of the gauge section of the longitudinal samples was also selected within the above constraints to provide the maximum amount of wrought metal on either side of the fused metal plus heat affected zone of the weld. This practice makes for easier delineation of the relative ductility of the three elements of a weld (cast metal, heated metal, or supporting base metal).

The selected gauge sections for longitudinal and transverse specimens were:

- 1/4 inch thick x 0.75 inch
- 3/8 inch thick x 0.75 inch
- 1/2 inch thick x 1.00 inch

Specimen designs are listed in Appendix E.

The testing equipment employed on the 1/2 inch thickness was a 400,000 pound Tinius Olson equipped with extensometers. A similar machine with a 120,000 capacity was used on 3/8 inch material. The 1/4 inch tests were run on a 60,000 Baldwin tensile testing machine.

Base metal test specimen designs followed similar principles. Tests were made parallel to the rolling direction and transverse to the rolling direction.

The objective of these tests was to determine the weld joint efficiency of heat treated welds in transverse tension with crown and root intact (except for the crown and root of the 3/8 inch welds). Additionally, longitudinal test welds were broken,

and examined after testing to determine whether the weld, the heat-affected zone, or the base metal was the least ductile portion of the joint.

The resulting tensile yield strength and elongation values show that the welds performed much like the base metal. Table V-2 and Fig. V-10 weld strengths ranged from 293 - 273 KSI ULT. Joint efficiencies exceeded 98.8% in all cases. Occasionally, the reinforcement caused joint strength to exceed base metal strength. Failure in all transverse steel welds was in the weld -- usually associated with the slight depression observable on either side of the crown.

Much of the plastic strain was absorbed by the relatively narrow welds. Therefore, elongation measured over two inches appeared to be low. When a one inch length was used, it increased the volumetric influence of the strain-absorbing characteristics of the weld. The elongation values based on a one inch gauge length approached those of the base metal specimens (i.e. 9-11% for base metal vs. 8-9% for welds).

An analysis of the longitudinal welded specimens after breaking (Table V-2) showed that the weld had taken nearly as much strain as the heat affected zone or the base metal. Weld failure and the adjacent fracture faces showed a ductile mode.

Macroscopic examination of the fracture faces revealed a shrinkage crack of the type shown in Fig. V-9 in Specimen ATT-9, ALT-1, ALT-2 and ALT-3. The crack would not be expected to influence the longitudinal ALT specimen as it is parallel to the direction of stress. It had little effect on the transverse (ATT) specimen.

b. Axial Fatigue Tests

Welded fatigue tests appeared to perform about as well as base metal in these tests. Scatter tended to obscure results.

Procedure. The transverse axial fatigue specimens were designed to place the maximum amount of laser weld under test. This amount was limited by available testing machine capacity and the length of specimens that could be removed from the weld test panel. The selected gauge sections were:

1/4 inch thick x 0.75 inch wide
1/2 inch thick x 1.00 inch wide

Specimen designs are listed in Appendix E.

The testing equipment employed was a 200 KIP capacity electro-hydraulic fatigue machine using MTS self aligning hydraulic grips. Testing was conducted at a minimum/maximum stress ratio = 0.1 and at a frequency of 3 hertz. Upon completion of initial tests, there was evidence that some bending was being introduced and the loading of all subsequent specimens was monitored by strain gauges placed on the specimens.

The objectives of this limited testing program were to:

- 1) Compare base metal and laser weld performance
- 2) Reveal defects that were not detected by prior non-destructive examination and consider the implications in terms of process control

The determination of a definitive endurance limit for either base metal or welds was not attempted. Some reference data is shown for comparison.

The results are shown in Fig. V-11. Considerable scatter can be observed in both base metal and welded specimens. There is far too much scatter to establish any definitive design criteria. If the results are averaged, however, it appears that the welds met the objective of this initial test, i.e., they have about the same range of strengths as the base metal shown in the shaded zone. Their tendency to range beyond the boundaries of base metal performance may be indicative of:

- 1) More welded samples than base metal
- 2) More complex structure in the weld than in the base metal
- 3) Occasional defects not detected by conventional NDT were influencing performance

The scatter does not seem to be the result of laser welding since it was also observed in the base metal.

Table V-3 lists the test data for each specimen in the program, and correlates these with the post-test observations of the fracture face. Note that some data was not used.

Fig. V-12 and 13 illustrate some of the observed fracture face conditions described in Table V-3 under Post Test Examination.

Some implications regarding the effect of the various defects on performance can be drawn from the correlation data (Table V-3). Principally, the implication of freeze

cracking should be considered because it is related characteristically to the laser process through improper (shallow) focus settings.

The presence of freeze cracking (such as that shown in Fig. V-9) definitely dropped the fatigue performance of welds below that of the base metal. Such cracking is difficult to detect by x-ray and was not picked up by shear wave techniques. The dendrite freezing pattern in a pinched weld is similar to that found in a cylindrical mold, so that there is not necessarily a pronounced centerline - and with it, a predictable crack surface orientation.

Overall, eight shrinkage cracks were found in post-test examination. They were in:

- One Alternate Immersion Stress Corrosion Specimen
- Two Fatigue Test Specimens
- Four Tensile Tests (one 1/4 inch and three 3/8 inch tensile specimens)
- One Macro Section

All but one specimen were steel. The other specimen was nickel base alloy.

Porosity did not have as pronounced an effect on fatigue performance as did shrinkage cracks. The location of the pore is important. For example, Table V-3 shows that the origin of failure in two welds (W-8 and W-9) was a small pore. Yet W-9 considerably exceeded base metal results, and W-11 performed very well. Thus, the tendency of a pore to act as a fatigue initiation point does not necessarily mean that overall specimen performance will suffer. In fact two other welds (W-2 and W-10) that performed marginally (Table V-3) with respect to the base metal standard showed no evidence of any defect at the failure origin upon close post-test examination. However, when a pore was observed at the origin and also at the surface, the performance of the weld was very poor (specimen W-7, Fig. V-13).

c. Fracture Testing

Low alloy carbon steel laser welds performed exceptionally well in tests designed to measure their toughness after heat treatment. They exceeded base metal results and exhibited great toughness with respect to published data (Fig. V-15).

Specimen			Elongation (%)			Ultimate Strength (psi)	
Thk.	Description	Ident.	(1")	Weld***	(1")	Tensile'	Yield
1/4"	Transverse Base Metal	TTB-1S			8.5	288.308	246.268
		TTB-2S			7.6	288.403	245.983
	Longitudinal Base Metal	LTB-1S			9.0	288.347	244.680
		LTB-2S			8.8	290.483	245.142
	Transverse Welded	ATT-1S	8.5		3.1	289.515	245.609
		ATT-2S	6.4		1.6	286.467	241.442
		ATT-3S	6.7		1.6	289.017	242.511
	Longitudinal Welded	ALT-1S	7.2	3.0	4.1	294.133	244.450
ALT-2S		6.4	2.4	3.8	285.496	236.641	
ALT-3S		9.4	3.4	5.0	297.875	250.524	
3/8"	Transverse Welded	ATT-4S	9.0		5.0	256.400	223.500**
		ATT-5S	10.0		5.0	256.400	225.400**
1/2"	Transverse Base Metal	TTB-5S			11.8	276.435	*
		TTB-6S			12.2	272.595	229.349
	Longitudinal Base Metal	LTB-5S			10.6	275.682	229.251
		LTB-6S			14.2	276.690	233.105
	Transverse Welded	ATT-7S	13.3		7.2	273.121	230.250
		ATT-8S	7.8		3.3	275.514	235.157
		ATT-9S	8.7		4.0	276.756	239.985
	Longitudinal Welded	ALT-7S		6.0	7.6	273.586	233.690
ALT-8S			9.9	11.1	276.830	231.695	
ALT-9S			11.6	12.7	275.667	231.833	

* Extensometer Malfunction

** Shrink Tear

*** Measurement of weld metal ductility when supported by the base metal and forced to yield at the same rate as the base metal. This determination of ductility is not affected by base metal weld strength differences. See sketch.

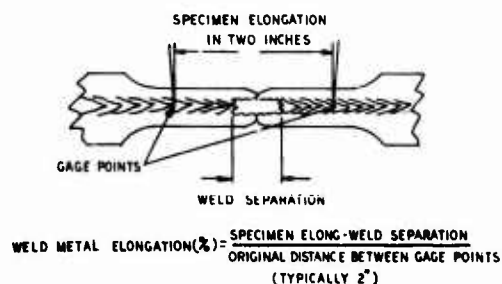


Table V-2. LOW ALLOY CARBON STEEL TENSILE RESULTS

/ Ultimate Tensile Strength
 ■ Yield Strength
 ■ Elongation (2" Gage Length)
 □ Elongation (1" Gage Length)

AUSTENITIZED AND TEMPERED TO 275-305 KSI
 ULTIMATE TENSILE STRENGTH
 REINFORCEMENT LEFT ON (EXCEPT 3/8" DATA)

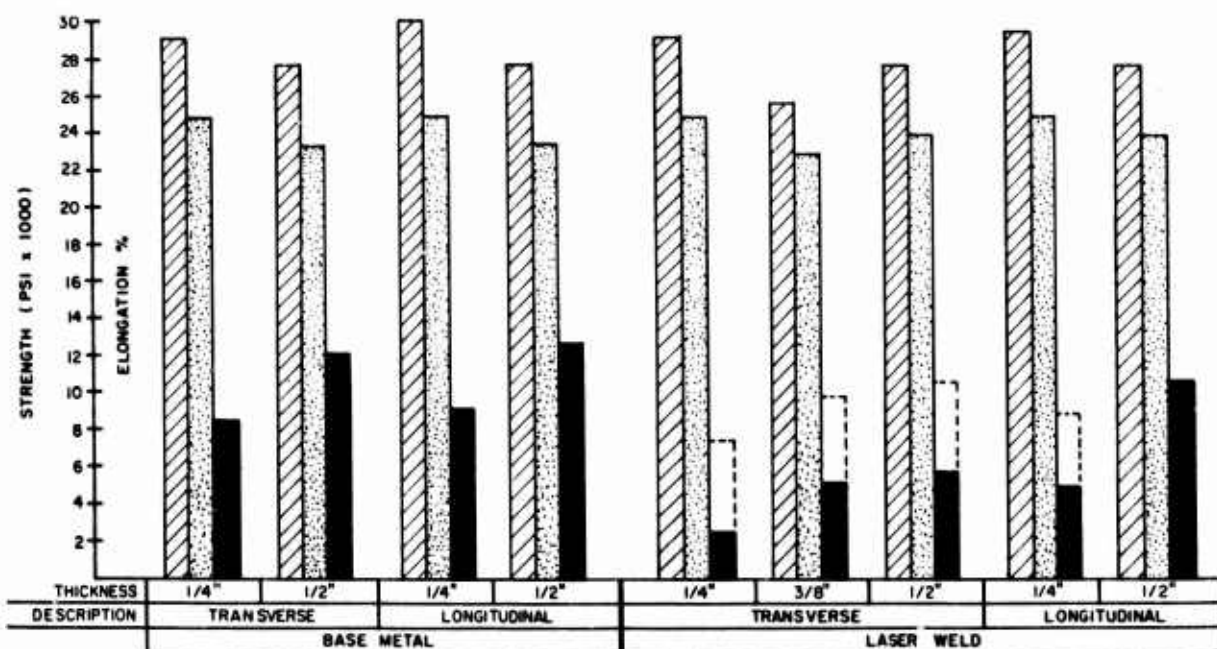


Figure V-10. COMPARATIVE TENSILE PROPERTIES (STEEL)

MATERIAL — 300M ALLOY STEEL

STRESS RATIO — +0.1

TEST TEMPERATURE — AMBIENT (R.T.)

● WELD SPECIMEN 1/4" THICK

○ BASE METAL 1/4" THICK

▲ WELD SPECIMEN 1/2" THICK

△ BASE METAL 1/2" THICK

C CRACKED*

S SURFACE PORE*

*SEE APPENDIX C FOR FRACTURE
FACE CHARACTERISTICS.

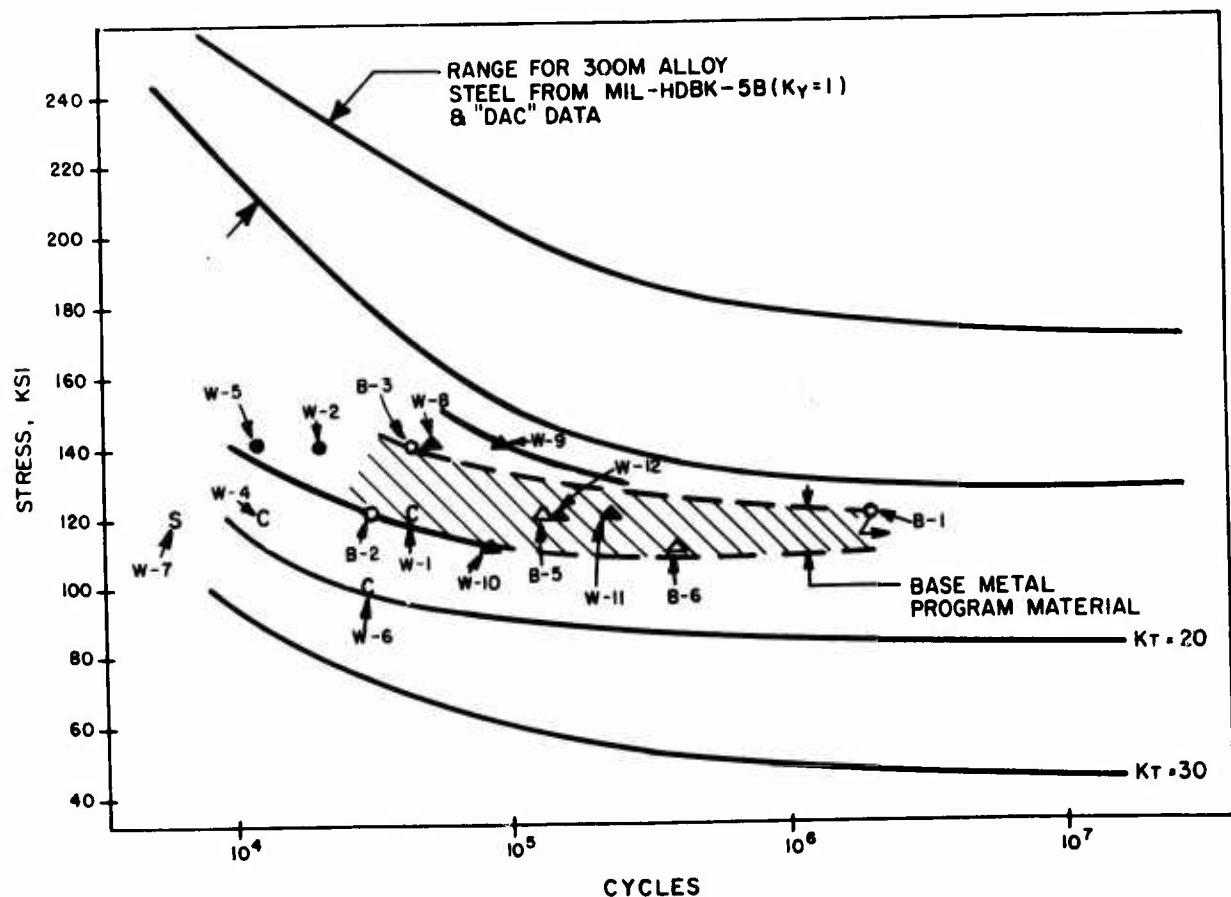
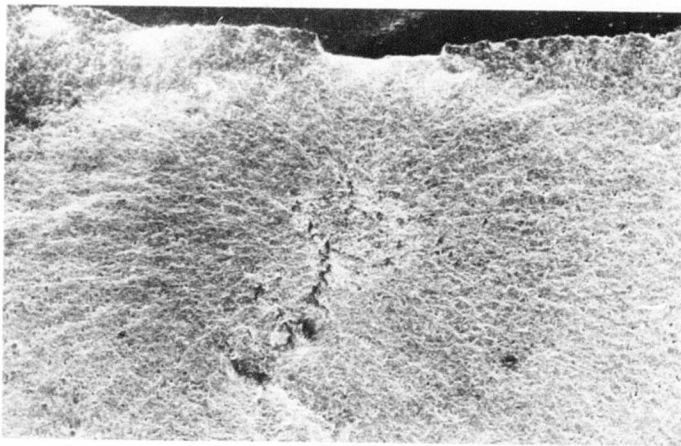
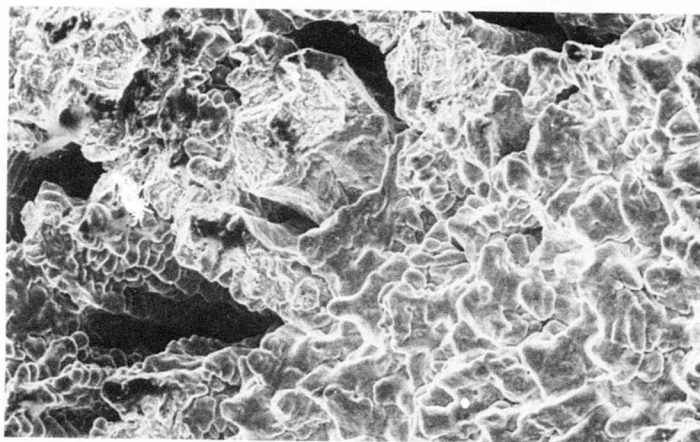


Figure V-11. AXIAL TENSION FATIGUE RESULTS (STEEL)



Negative No. SR-900

Mag. 29X

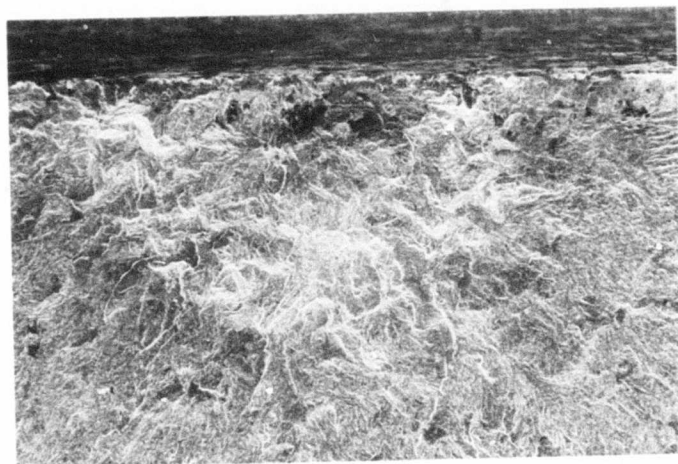


Negative No. SR-902

Mag. 585X

Top: Macro Photo of Area
 Bottom: Enlargement of Failure Site

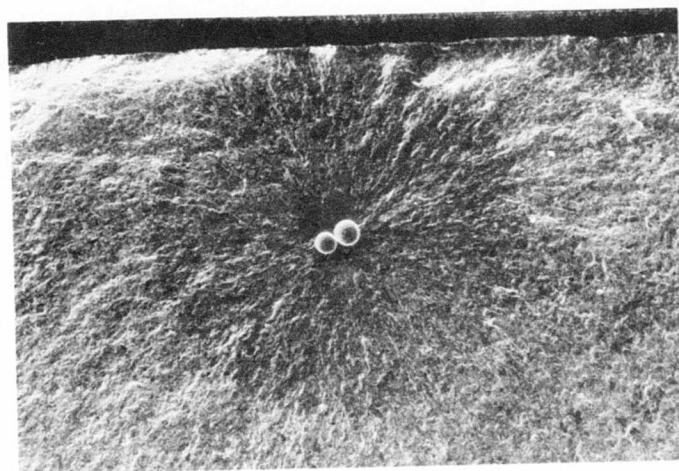
Figure V-11-a. FAILURE INITIATION SITE, SPECIMEN W-5S



Negative No. SR-909

Mag. 197X

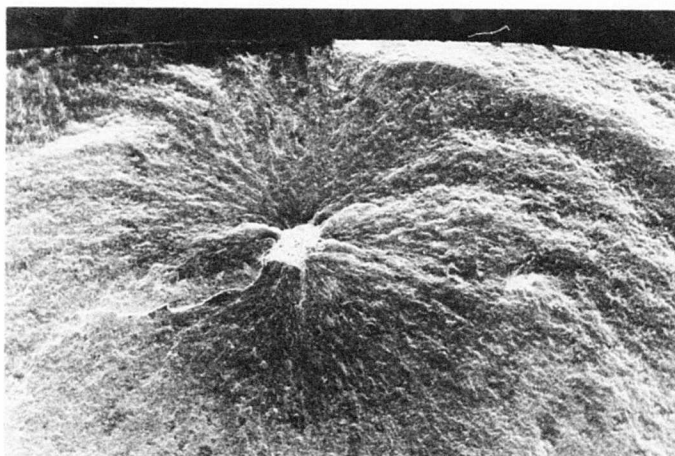
Figure V-11-b. FAILURE INITIATION SITE, SPECIMEN W-6S



Negative No. SR-912

Mag. 35X

Figure V-11-c. FAILURE INITIATION SITE, SPECIMEN W-11S



Negative No. SR-915

Mag. 20X

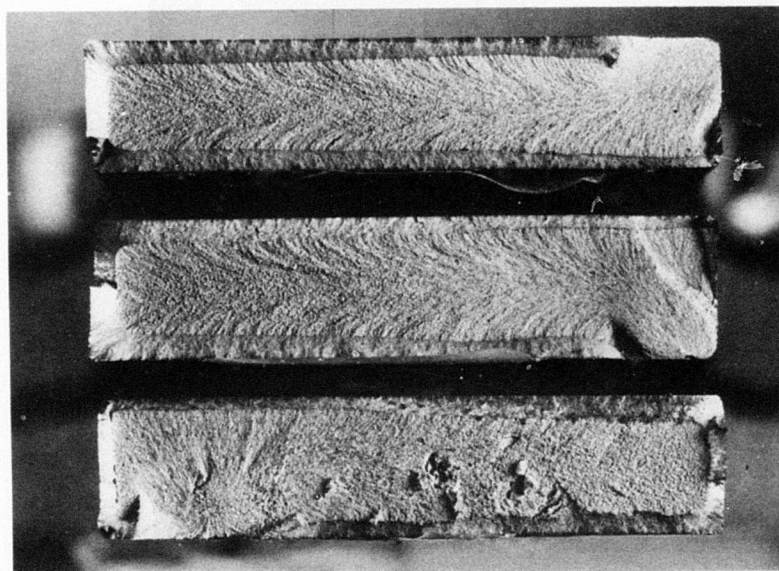


Negative No. SR-917

Mag. 814X

Top: Macro Photo of Area
Bottom: Enlargement of Failure Site

Figure V-11-d. FAILURE INITIATION SITE, SPECIMEN W-12S

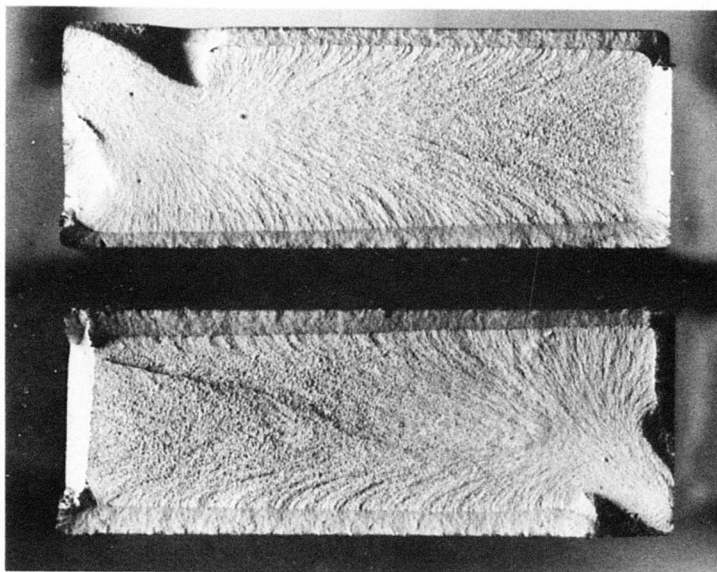


Negative No. 495

Mag. 3.8X

Top: W-1
Middle: W-2
Bottom: W-3

Figure V-12. FATIGUE TEST SPECIMENS (1/4 INCH STEEL)

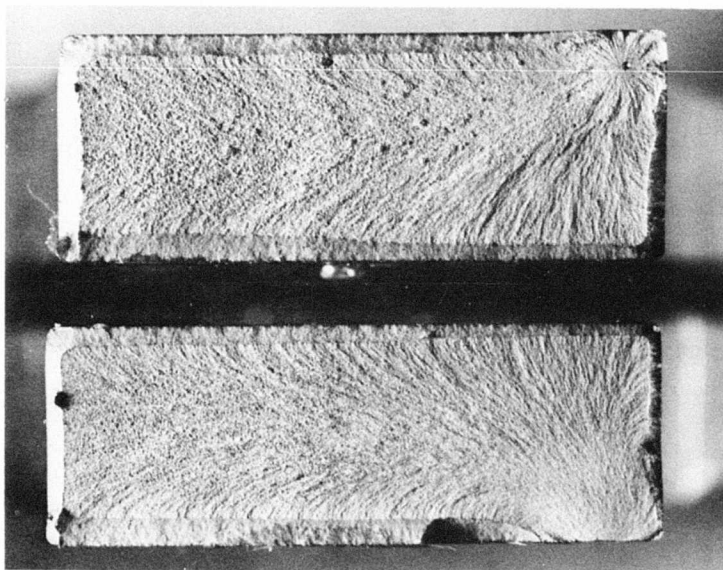


Specimen W-7

Specimen W-8

Negative LR-496

Mag. 2.9X



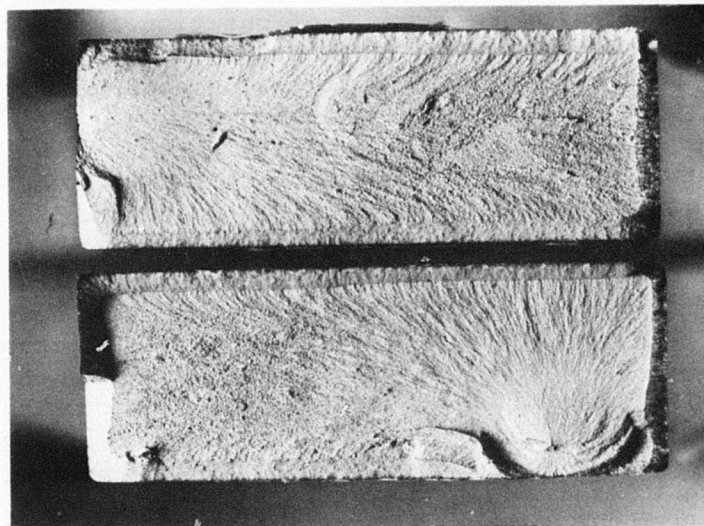
Specimen W-9

Specimen W-10

Negative L9-497

Mag. 2.9X

Figure V-13-a. FATIGUE TEST SPECIMENS (1/2 INCH STEEL)



Specimen W-4

Specimen W-12

Negative LR-498

Max. 2.9X

Figure V-13-b. FATIGUE TEST SPECIMENS (1/2 INCH STEEL)
(CONTINUED)

Specimen		Ident.	Stress KSI	Cycles to Failure	Post Test Examination									
					Type of Defect at Origin				Initiation Point					
Thk.	Condition				None	Pores	Crack	Other	Surface	Subsurf.	Corner	Weld	Base Metal	
1/4"	Base Metal	B- 3	140	4.4x10 ⁴	X				X				X	
		B- 2	120	3.2x10 ⁴	X						X		X	
		B- 1	120	2x10 ⁶	X				No Failure					
	Welded	W- 5	140	1.2x10 ⁴	X			X (1)	X	X		X	X	
		W- 2	140	2.0x10 ⁴										
		W- 4	120	1.8x10 ⁴										
		W- 1	120	4.3x10 ⁴										
		W- 6	110	3.0x10 ⁴										
	1/2"	Base Metal	B- 4	140	2.5x10 ⁴	X			X (1)	X				X
			B- 5	120	1.35x10 ⁵									
			B- 6	110	3.7x10 ⁵									
Welded		W- 8	140	5.2x10 ⁴	X	X		X (1)	X	X	X	X	X	
		W- 9	140	9.4x10 ⁴										
		W-12	120	1.4x10 ⁵										
		W-11	120	2.2x10 ⁵										
		W- 7	120	5x10 ³										
		W-10	110	8.5x10 ⁴										

(1) Residual crack from specimen manufacturing operations.

Table V-3. LOW ALLOY CARBON STEEL AXIAL
TENSION FATIGUE RESULTS

Procedure. Tests were conducted and evaluated in accordance with ASTM E 399-74. The specimen configuration is described in VC 008251 in Appendix E. ASTM E 399-74 requires that the precrack front be essentially flat upon post-test examinations (e.g. that crack front measurements $L_{2,3,4}$ in the sketch on Table V-4 not vary more than 5%). It was possible to meet this, and other, criteria for plane strain fracture in all but one low alloy carbon steel specimen.

Table V-4 shows how the stress intensity factor at the tip of each crack (K_Q) was determined from the crack front dimensions. Fig. V-14 shows the profile of the fracture faces of the specimens. Examination of the profile, or of the crack front dimension values in Table V-4, indicates plane strain conditions of failure. Therefore, K_Q is equal to the threshold stress intensity factor (K_{Ic}) which delineates material toughness. For information, the K_{max} fatigue loads are also shown in Table V-4.

The equipment used for pre-cracking was a Krause Lever Arm Fatigue Testing Machine. Crack growth was monitored by a 16X optical scope. The pre-crack specimen was then placed in a Riehle 30,000 pound machine equipped with an MTS compliance gauge.

The notch and crack were centered in the fused portion of the weld cross section on the welded samples.

The objective of these tests was to compare the toughness of base metal with the toughness of a laser weld.

The results of the fracture toughness calculations, the K_{Ic} values, are plotted with respect to the base metal performance, and also with respect to available handbook data, in Figure V-15. The fracture toughness of the weld is greater than the toughness of the base metal and the test results are also quite attractive when compared to the reference data.

d. Notched Stress Corrosion Test (K_{Isc})

The threshold stress intensity for stress corrosion to occur (K_{Isc}) in low alloy carbon steel welds appeared to be 42% of the K_{Ic} . This is considered exceptionally good performance for a high strength steel subjected to both stress and corrosion in the presence of a notch. An anomalous mode of failure, dimpled rupture, was observed ahead of the characteristic intergranular fracture.

Type	Ident. No.	Thickness Inches B 1, 2, 3	Depth* Inches W 1, 2	CRACK FRONT DIMENSIONS, INCHES*						** K Max.	Ult. Load Lbs.	*** K Q	K IC
				L 1	L 2	L 3	L 4	L 6	L 2,3,4				
Base Metal	FBM-4S	.4683	1.0065	HEAT TREATMENT CRACK									
	FBM-5S	.4681	1.0070	.5488	.5644	.5656	.5532	.5592	.5611	27.4	2150	58.9	58.9
	FBM-6S	.4687	1.0068	.5448	.5460	.5452	.5540	.5524	.5484	26.2	2180	57.1	57.1
Welded	FAW-4S	.4681	1.0065	.5486	.5610	.5654	.5660	.5546	.5643	27.7	2750	76.3	76.3
	FAW-5S	.4683	1.0068	.5572	.5840	.5816	.5812	.5516	.5823	29.6	2895	85.6	****
	FAW-6S	.4687	1.0068	.5506	.5582	.5594	.5598	.5554	.5591	27.2	2850	77.5	77.5

NOTE: Testing and calculations performed in accordance with ASTM specification E399-74.

* See sketch of specimen dimension.

** Calculation: $K_{max} = \frac{(\text{Fatigue Load}) W [f(a/w)]}{B(W-L)^{3/2}}$

*** Calculation: $K_Q = \frac{(\text{Ultimate Load}) W [f(a/w)]}{B(W-L)^{3/2}}$

**** Pre-crack front not in compliance with ASTM requirements for valid test. (Variation of crack front measurements more than 5% of L 2, 3, 4).

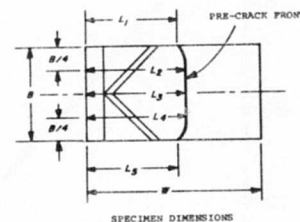
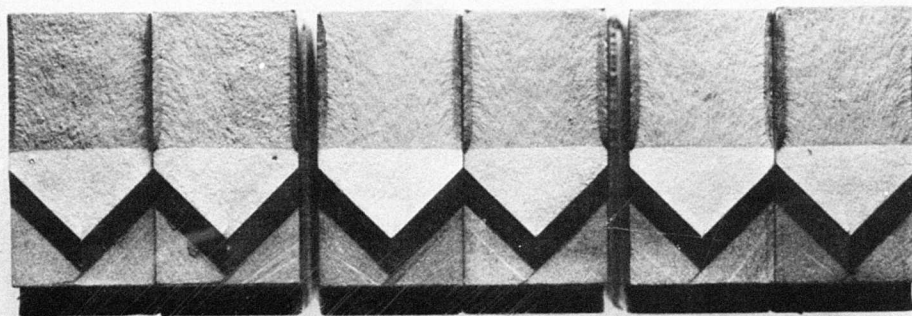


Table V-4. LOW ALLOY CARBON STEEL FRACTURE TOUGHNESS TEST RESULTS



Negative No. LR-584

Mag. 2X

- (a) Left: Specimen FAW-4S
- (b) Middle: Specimen FAW-5S
- (c) Right: Specimen FAW-6S

Figure V-14. WELD TOUGHNESS SPECIMENS (STEEL)

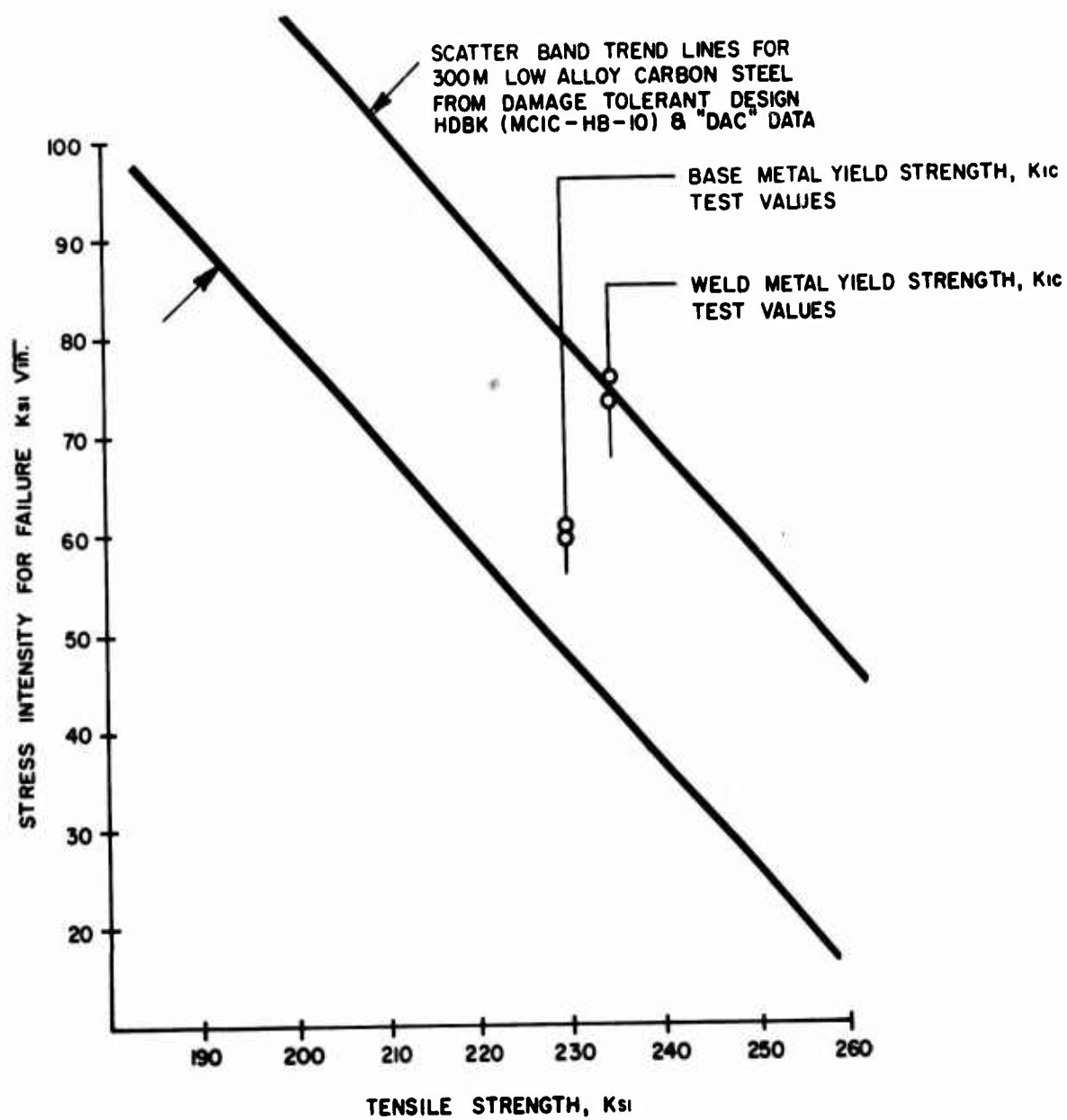


Figure V-15. FRACTURE TOUGHNESS RESULTS (STEEL)

Procedure. There is no established test method for notched stress corrosion testing. Therefore, test specimens were pre-cracked and evaluated essentially in accordance with ASTM E 399-74 which generally describes fracture toughness testing. The specimen configuration is VC 008951 described in Appendix E, and is identical to that used for fracture toughness determination.

Table V-5 indicates the method of determining the stress intensity K_I for each specimen. Fig. V-16 shows the failed specimens and crack profile. Fig. V-17 relates stress intensity to time of failure. Therefore, Fig. V-17 indicates the threshold value of stress intensity below which, in spite of the presence of a corrodent such as saltwater, a defect such as a crack would not be expected to progress. The value $K_{I\max}$ has been calculated and is shown in Table V-5 for information.

The equipment used for both pre-cracking and final fracture was a Krause Lever Arm Fatigue Tester. Crack growth was monitored by an auto-collimator at 16X. Final breakage was accomplished by manually applying pre-load through a load cell. The load cell output was monitored by cathode ray tube and adjustments made as needed. The corrosive media was substitute sea-water (ASTM 1141-52; pH 7.8 - 8.2; specific gravity 1.02 - 1.03). The solution is fed to the crack through a gauze wick.

The objectives of this test were to compare the toughness of laser welds to the toughness of the base metal under corrosive conditions.

The test results in Fig. V-17 suggest that the stress intensity threshold, termed $K_{I\text{SCC}}$, is 34 KSI in for low alloy carbon steel welds.

Electron microscopic examination of the notched stress corrosion specimen fracture face was performed to confirm the effectiveness of the tests technique. This examination revealed that the fractures were typical of stress corrosion in that they were produced by intergranular cracking. However, there is an unusual band representing a dimple rupture mode at the leading edge of the pre-crack front (Fig. V-16). The band is less than 0.003 inches wide and represents ductile failure. Fig. V-18 is a magnified view of this anomaly with conventional intergranular failure at the top of each photo. The

Ident. SCK	Thickness Inches B _{1, 2, 3}	Depth Inches W _{1, 2, 3}	CRACK FRONT DIMENSIONS, INCHES						K Max.	Load (lbs.)	K Q	Lifetime Minutes
			L 1	L 2	L 3	L 4	L 5	L _{2, 3, 4}				
4	0.469	1.006	0.569	0.577	0.582	0.586	0.579	0.582	29.6	2000	59.1	20
5a	0.469	1.006	0.571	0.583	0.577	0.572	0.568	0.577	29.0	1750	50.8	42.5
5b	Same	Same	Same	Same	Same	Same	Same	Same	Same	1000	29.00	2820 No fail
6	0.469	1.006	0.573	0.581	0.581	0.589	0.580	0.584	29.7	1500	44.5	580

NOTES: $K_{max.} = \frac{\text{Fatigue Load} \times W}{B(W-L)^{3/2}} [f(a/w)]$

$K_Q = \frac{\text{Load} \times W}{B(W-L)^{3/2}} [f(a/w)]$

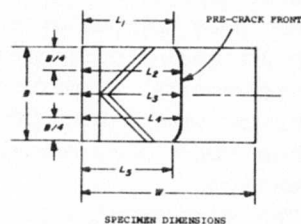
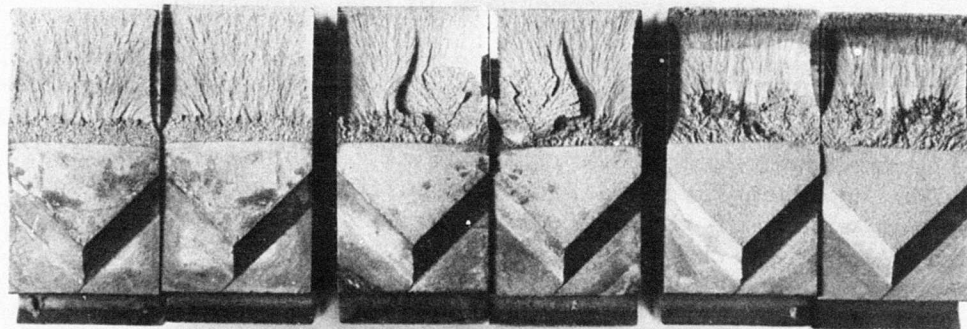


Table V-5. LOW ALLOY CARBON STEEL NOTCHED
STRESS CORROSION (K_{Isc}) TEST RESULTS



Negative No. 436

Left: SCK-4

Center: SCK-5

Mag. 2X
Right: SCK-6

Figure V-16. NOTCHED STRESS CORROSION SPECIMENS (STEEL)

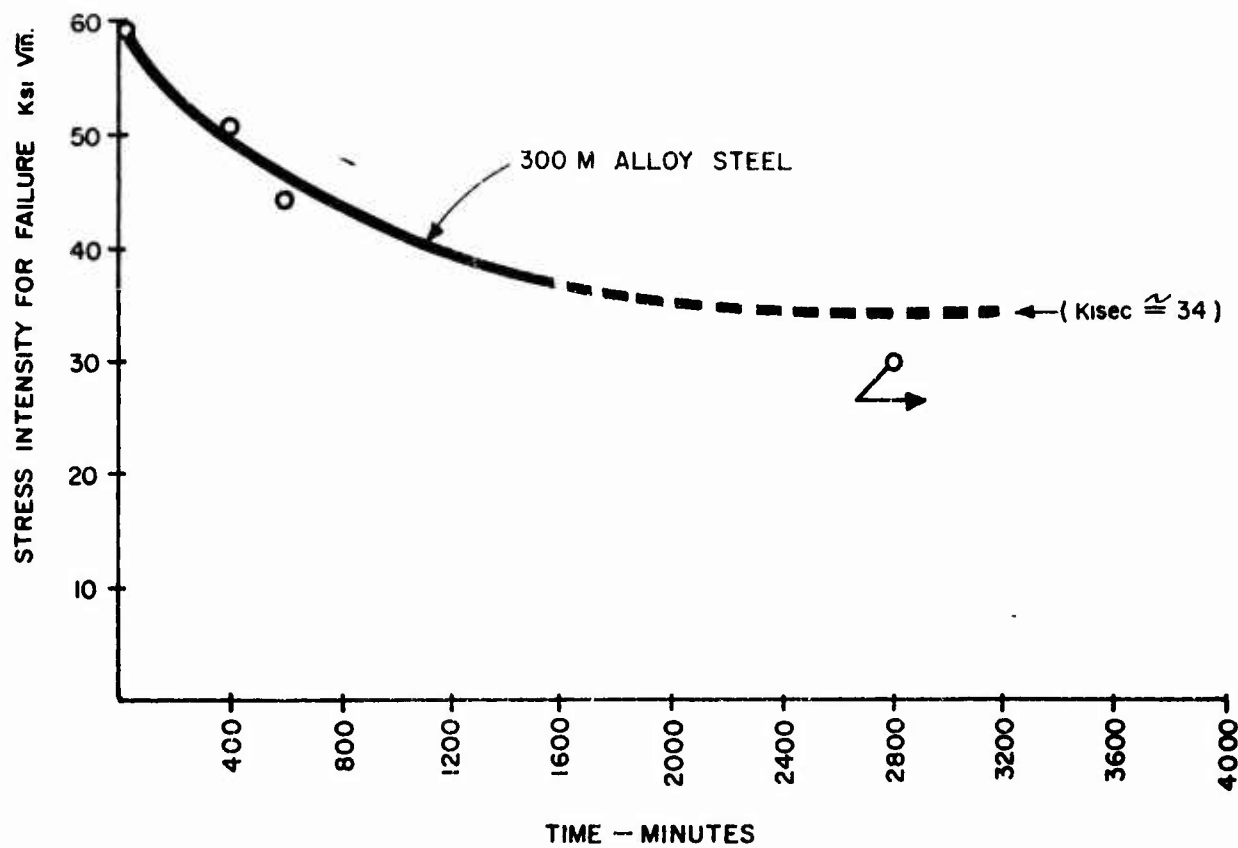


Figure V-17. NOTCHED STRESS CORROSION RESULTS (STEEL)

0.003 inch band of dimpled failure mode extends a short distance above the dark band in Fig. V-18.

No explanation is available for the band.

e. Stress Corrosion Cracking Characteristics
(Smooth Bar Specimen - Alternate Sea Water Immersion).

A sound weld, austenitized, quenched, and tempered after welding will fail in the base metal rather than in the weld if all three elements are exposed to stress corrosion conditions.

Procedure. Alternate immersion testing was performed in a "Dunker." Preloaded specimens are immersed in synthetic sea water (ASTM 665-60B-with Ph 7.8 - 8.2) for 10 minutes followed by a 50 minute exposure to air at room temperature.

Preloading to 75% FTY is accomplished in coil spring fixtures carefully coated to prevent galvanic inter-action with the specimen.

The specimens were of a flat, smooth bar design (ZC00 8251). All specimen drawings will be found in Appendix E.

The Tests Objective emphasized the relative location of the stress corrosion failure with respect to the three elements of any weldment.

- 1) Base metal unaffected by welding
- 2) Heat Affected Zone
- 3) Fused Weld Metal

Test Results. Fig. V-19 is a graphical representation of the lifetime exhibited by the specimens.

Metallographic sections of the stress corrosion test specimens revealed that the failures occurred in the base metal in the two specimens SCS-1S, SCS-3S, which exhibited the longest lifetime. Specimen SCS-2S failed in the weld metal. Fig. V-20 shows macrographs of the resulting fracture appearance in SCS-2S. The arrows indicate the initiation site of the failure.

Scanning electron microscopic examination of the fractures resulting from stress corrosion testing (smooth) of the 300M steel confirmed that the three specimen failures initiated by intergranular cracking typical of stress corrosion. Fig. V-21 illustrates the characteristic intergranular features observed at the failure origin of these specimens. However, Specimen SCS-2S which failed through the weld metal, exhibited some discontin-

uities which were too large to be secondary cracking. The features of these discontinuities (Fig. V-22) are similar to flaws observed in tensile Specimen ALT-2S (Fig. V-23). Therefore, the early failure of Specimen SCS-2S seems to have been caused by a welding related defect. Further, when laser welds are defect free they are less susceptible to corrosion than the base metal. This statement applies to specimens that were hardened and tempered after welding and is supported by the performance of Specimens SCS-1S and 3S. Both specimens failed in the base metal away from the weld.

f. Microhardness Examination

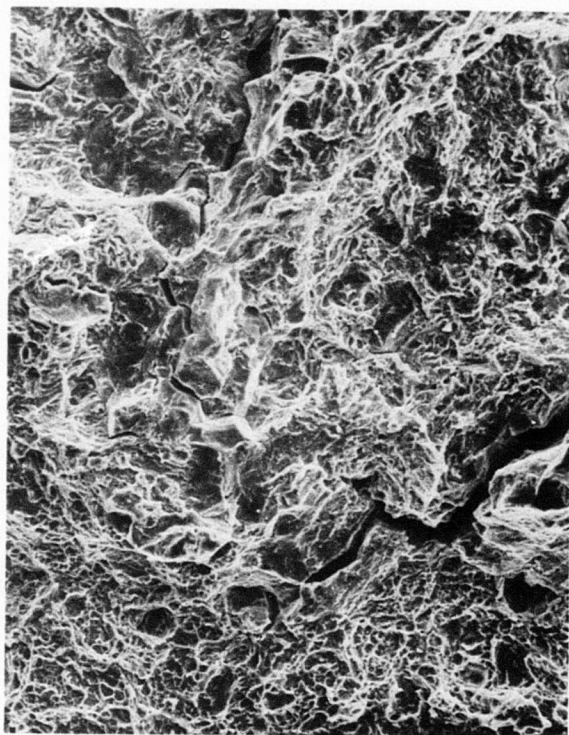
Although as-welded hardness reached $R_C 60$, and no preheat was used, there was no evidence of quench cracking. After a post-weld heat treatment (austenitize and temper), weld metal and HAZ responded within 2-5 R of base metal.

Procedure. A Knoop Microhardness tester was used. Hardness impressions were uniformly spaced 0.014 inches apart.

Test Objective sought to verify as-welded hardness in view of the observation that no quench cracking had been observed. This is a highly hardenable steel and no preheat had been used. Additionally, the response of the weld to heat treatment was observed in tests of relative weld - HAZ - base metal hardness.

Test results. Micro hardness surveys of the weld metal and heat affected zones of selected representative sections of laser welds were made. These are shown in Figures V-24, V-25, V-26 and V-27. Welds before and after heat treatment are included. The results of these measurements are considered consistent with expectations for welds made using a high power density beam.

Although the "as welded" fusion and heat affected zone of the low alloy steel was found to be extremely hard, no evidence of "auto cracking" (quench cracks) was detected in spite of welding without the preheating or post-heating usually associated with deep hardening steels of this type. This is consistent with the results of electron beam welding of deep hardening steels.



Intergranular Mode

Dimple Rupture

Normal

Negative No. SR-815

Mag. 560X

Figure V-18. DUCTILE FAILURE, NOTCHED
STRESS CORROSION TESTS (STEEL)

MATERIAL — 300M ALLOY STEEL

TEST CONDITIONS —

STRESS @ MINIMUM CROSS SECTION — 182,000 psi (75 % YIELD STRENGTH)

TEST TEMPERATURE — AMBIENT (R.T)

CORROSIVE MEDIUM — SUBSTITUTE SEA WATER (ASTM -1141-52)

PH 7.8-8.2

SPECIFIC GRAVITY 1.02-1.03

IMMERSION — 10 MINUTES PER HOUR

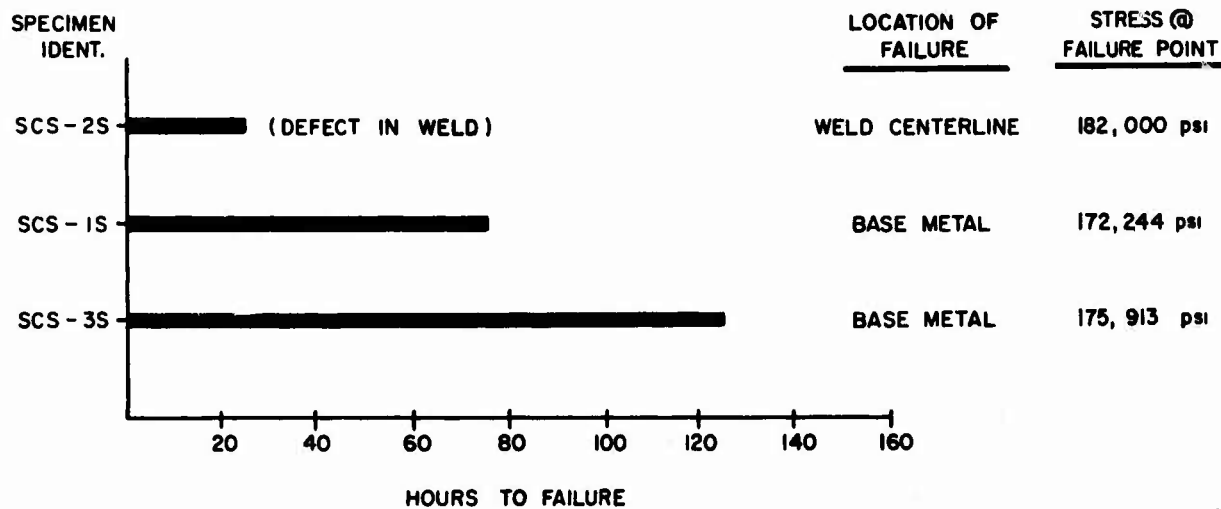
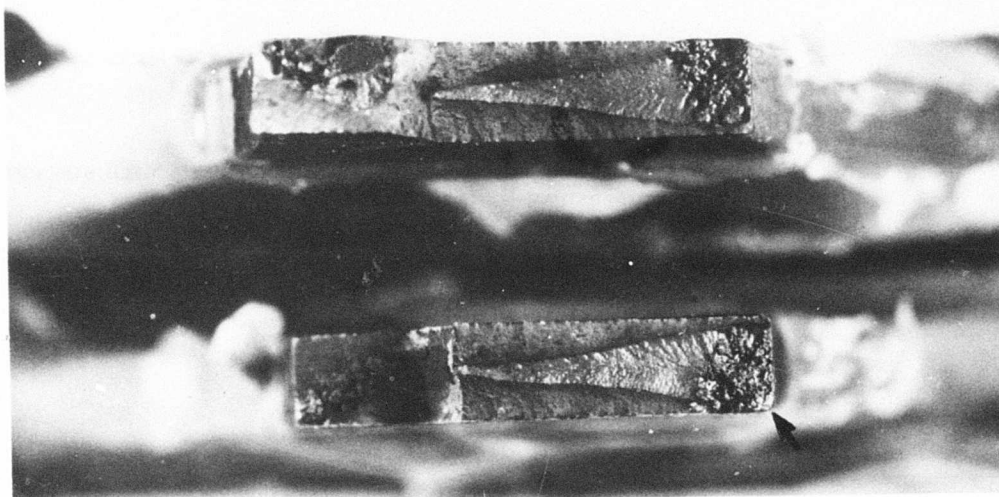


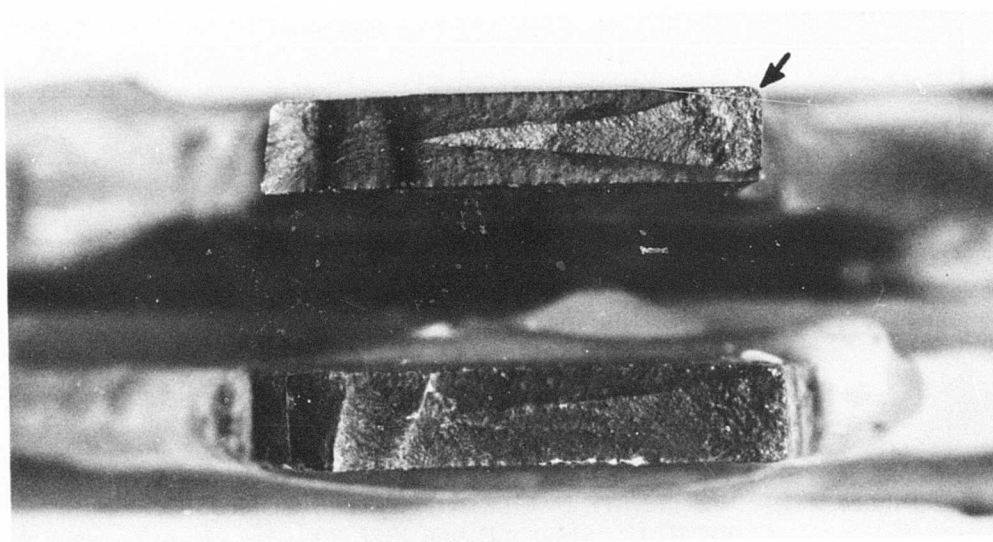
Figure V-19. ALTERNATE IMMERSION STRESS CORROSION RESULTS, SMOOTH BAR (STEEL)



Negative No. IQ-1087

Mag. 7.2X

Stress Corrosion Spec. #SCS-1S

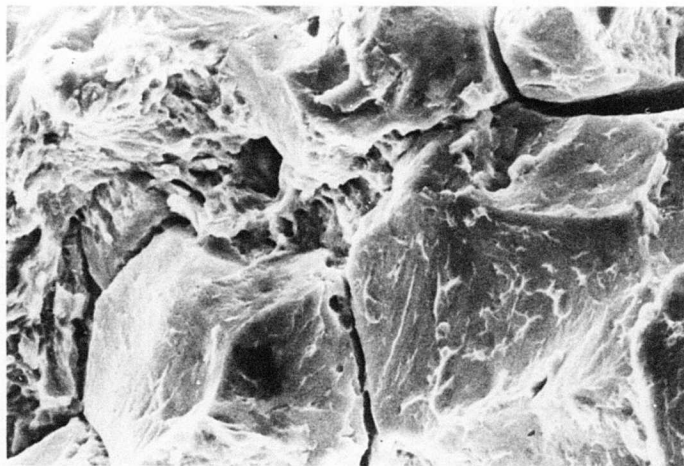


Negative No. IQ-1088

Mag. 7.2

Stress Corrosion Spec. #SCS-3S

Figure V-20. ALTERNATE STRESS CORROSION SPECIMENS,
SMOOTH BAR (STEEL)

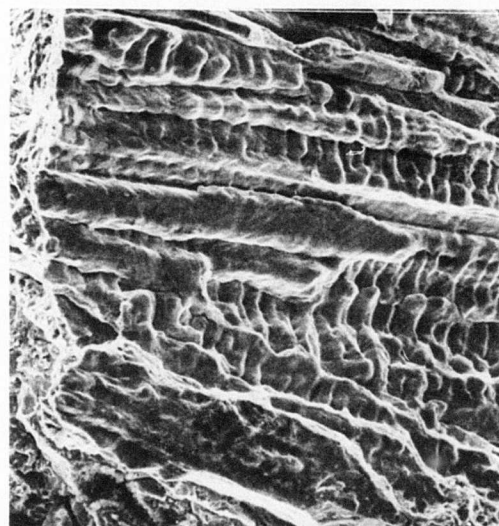


Negative No. SQ-1363

Mag. 2000X

Specimen #SCS-2S Failure Origin

Figure V-21. FAILURE ORIGINS OF STRESS CORROSION
SPECIMEN (STEELS, INTERGRANULAR CRACKING)



Negative No. SQ-1365

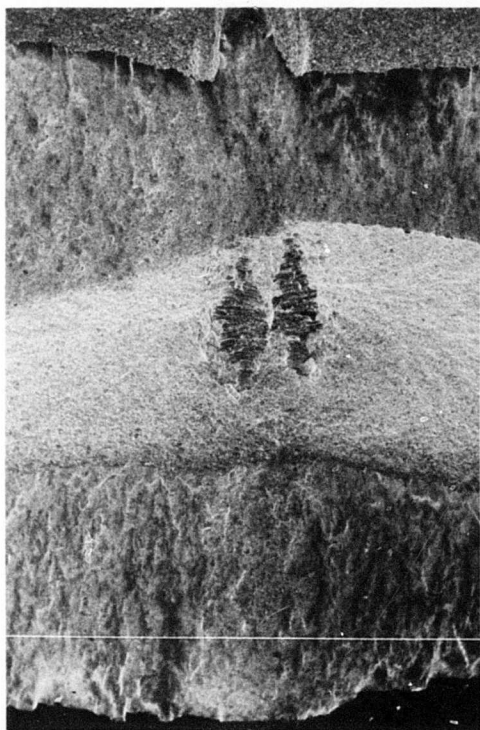
Mag. 614X

Negative No. SQ-1366

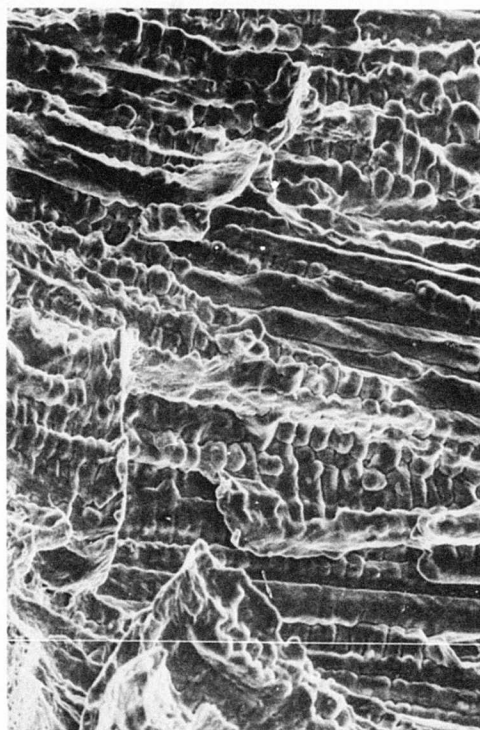
Mag. 614X

Specimen No. SCS-2S - Weld Related Cracking at Failure Site

Figure V-22. SECONDARY CRACKING, SPECIMEN SCS-2S (STEEL)



Negative No. SR-918 Mag. 12.7X



Negative No. SR-921 Mag. 508X

Figure V-23. WELD FLAW IN TENSILE SPECIMEN ALT-25 (STEEL)

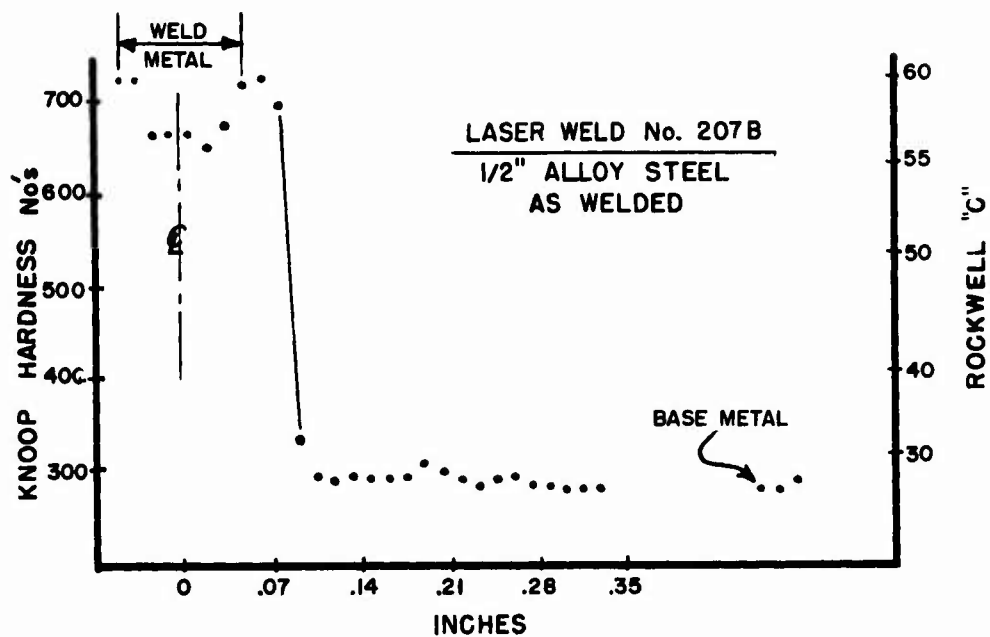


Figure V-24. HARDNESS SURVEY (1/2 INCH STEEL - AS WELDED)

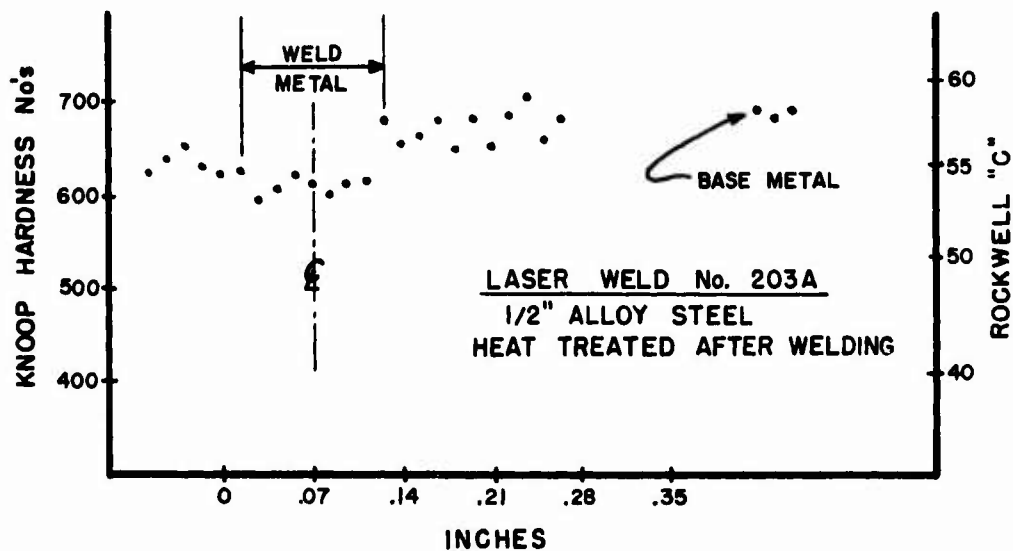


Figure V-25. HARDNESS SURVEY (1/2 INCH STEEL - HEAT TREATED)

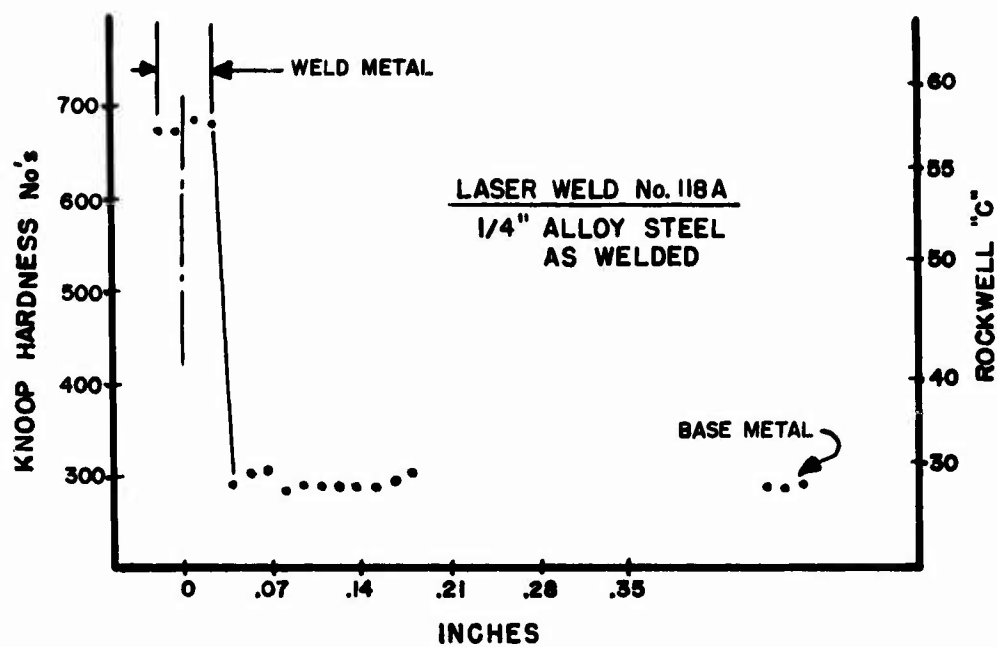


Figure V-26. HARDNESS SURVEY (1/4 INCH STEEL - AS WELDED)

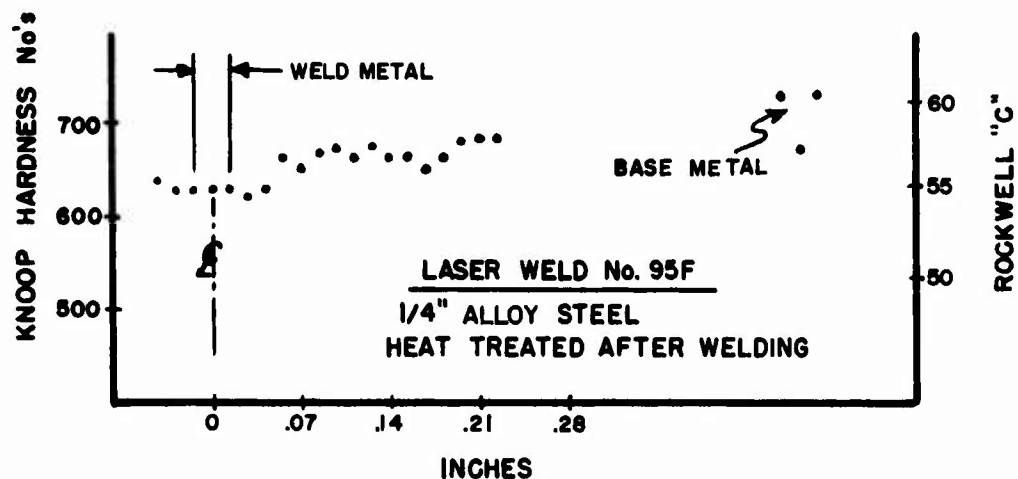


Figure V-27. HARDNESS SURVEY (1/4 INCH STEEL - HEAT TREATED)

C. LASER WELDS IN TITANIUM ALLOY (Ti 6 Al, 4V)

As noted in Section III, this material was selected for its good strength, high toughness in the annealed condition, and broad acceptance throughout the aerospace industry.

1. Base Metal Characteristics

The material came from five separate heats. The compositions are listed in Table V-6. The nominal composition of this Alpha-Beta alloy is as follows:

C	N	Fe	Al	V	O	H
.08 (max)	.05 (max)	.3 (max)	5.5/6.5	3.5/4.5	.2 (max)	.015 (max)

The material was procured to the following specification:
MIL-T-9049

The ingot was produced by vacuum arc melting, hot rolling and then mill annealing. Detailed mechanical properties are listed in Table V-6.

Some variance of strength was observed at different locations throughout the 1/4 inch plate. The strength of the 1/4 inch plate was 6-11% lower than the other thicknesses but is within specification limits.

2. Panel Welding

The welding set up tests used to establish the procedures employed to weld the titanium alloy panels and photographs of the resulting development welds are shown in Appendix E.

Table V-7 summarizes the titanium alloy test panel welding procedures which included wirebrush and acetone rinse as a pre-weld cleaning procedure. Fig. V-6 sets forth the details of shield set-up. Fig. V-7 shows the tooling that was used to hold the panels for welding.

The quality of the resulting welded test panels was high (see Fig. V-5) and is described for each panel in Appendix B. Appendix B reports the following experimental detail:

Panel Identification Size Orientation & Shape.
Identification Orientation & Location of Each
Weld in the Panel.
Procedure Details for each Weld in the Panel.
Location of all Non-Destructive Indications in
Each Weld.

Thickness Inches	Ingot Number	ANALYSIS							PROPERTIES			Application in Program	
		Ingot (%)							Plate 1	Ult. KSI	.2% Yld. KSI		Elong (%)
		C	N	Fe	Al	V	O	PPM H					
0.25	704312	.03	.015	.16	6.4	4.1	.172	81	See Below Note 2 and 3			All Mech. Tests	
0.375	295561	.02	.01	.2	6.1	4.0	.126	66	L-138.1 T-147.9	L-130.2 T-141.3	14.0 14.0	All Mech. Tests	
0.500	900705	.02	.011	.2	6.5	4.1	.153	62	L-149.5 T-155.2	L-139.1 T-146.5	15.0 17.0	0.5 in Fatigue Tests	
0.500	800770	.01	.013	.17	6.4	4.0	.174	48	L-155.8 T-156.6	L-144.9 T-144.6	14.0 14.0	All Other 0.5 in Tests	
0.750	800887	.02	.012	.2	6.5	4.1	.168	61	L-146.4 T-155.6	L-135.9 T-145.6	12.0 14.0	Not Used in Mech. Tests	
1. All plate except 0.25 inch production annealed 1450°F, 15 min, air cooled and checked for surface contamination.													
2. 0.25 inch plate properties reported as: Ult $\frac{L-153.2/153.7}{T-154.0/157.6}$; Yield $\frac{L-145.4/145.9}{T-147.2/151.5}$; Elong $\frac{L-11.0/12.0}{T-10.0/11.0}$													
3. 0.25 inch plate production annealed (1450°F) for 1 hour instead of 15 min.													

Table V-6. COMPOSITIONS & PROPERTIES OF TITANIUM MATERIAL TESTED IN PROGRAM

Welding Parameters	PANEL THICKNESS		
	1/4 inch	3/8 inch	1/2 inch
Power, Beam On Work (kW)	10.0 7.0	16.0 11.2	14.9 13.2
Process Speed (ipm) OPTICS (F/No) Focal Distance (in.)	100 7 28-1/8	70 Same Same	30 21 32.5
Surface Preparation	Deburr, Wirebrush Rinse w/Acetone	Same	Same
Shielding Gas (Type/CFH) Jet Trailer Hood Underbead	Helium / 100 Argon / 25 Helium / 10*	Same Same Same	Same Same Same
Shield Position Set Back (in.) Lift Off (in.)	7/16 0.04	Same 0.04 **	3/8 0.04
Gap	002*	Same	Same
Mismatch	005*	Same	Same
Tooling	Figure V-7	Same	Same
Filler Wire	Not Used	Same	Same

* Unless noted for a specific panel in Appendix D.

** In some panels, surface height varied 0.062 inches such that hood lift-off approached 0.1 inches. This is excessive at the nominal 25 CFH flow rate, but appeared to be acceptable if flow rate was raised to 50 - 60 CFH.

Table V-7. TITANIUM ALLOY WELDING PROCEDURES

Location of Test Specimen Coupons in Each Weld.
Relationship between NDT Indications and Test Specimen Location.

3. Welding Characteristics

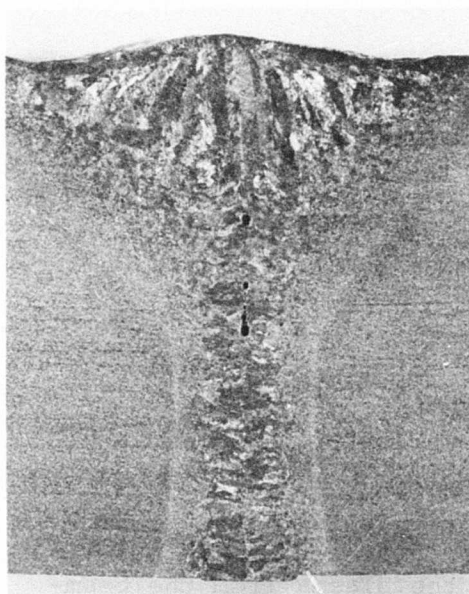
Behavior during welding that sets the titanium alloy apart from other program materials was noted throughout the program and is summarized here.

The titanium alloy used in these tests was the second most weldable of all program materials. Procedures were readily established in all program test plate thicknesses (1/4, 3/8 and 1/2 inches). The metal utilizes laser energy as efficiently as any other material in the program. It exhibited, with low alloy steel, the greatest penetrability observed in the program - 0.6 inches. Characteristically, titanium alloy welds have a distinct wine glass shape with a broad top and underbead.

As noted in the NDT overview section, welds of high quality were easily obtained. However, shielding must be carefully controlled. For example, variances in the performance of a jet, used to control the plasma from the beam-plate interaction, apparently caused a centerline porosity condition at several locations in the final 1/2 inch test plates (Fig. V-28). Similar jet-trailer shields were used successfully on over 100 inches of weld prior to this incident. Additionally, the variable jet performance caused the upper rim of the cavity to be exposed to air. This resulted in a shallow line of contaminated material just below the edge of the upper bead. As noted in Section IV, full hood shielding is recommended for most titanium welding. The final quarter inch fatigue tests were run in this manner.

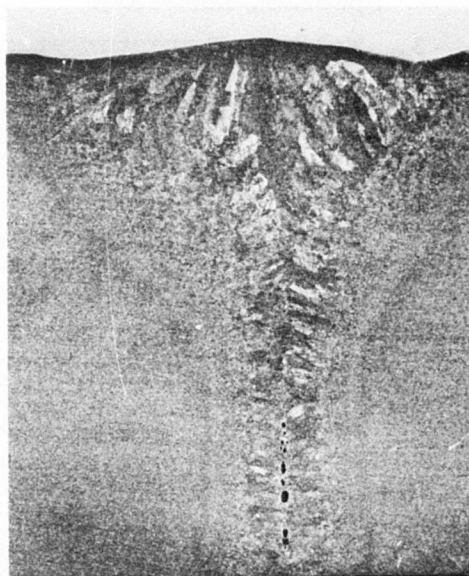
4. Specimen Preparation

Once titanium alloy panel weldments were completed at the AVCO Everett Research Laboratories, Everett, Massachusetts, they were identified and shipped to the Long Beach, California plant of the Douglas Aircraft Corporation for weld evaluation. At that site, the following steps were implemented in processing the material from this welded panel form to finished test specimens:



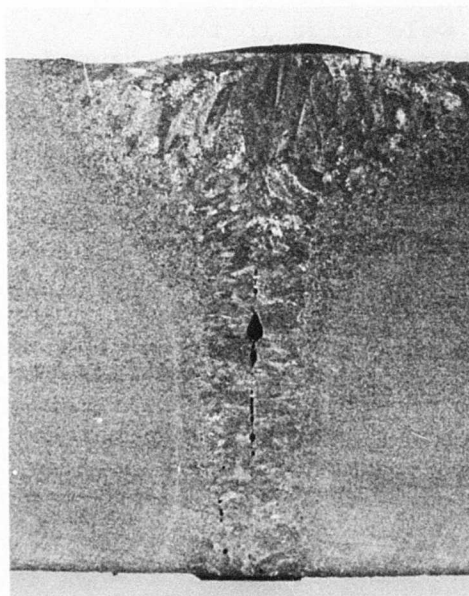
Negative No. IQ-477

Mag. 7X



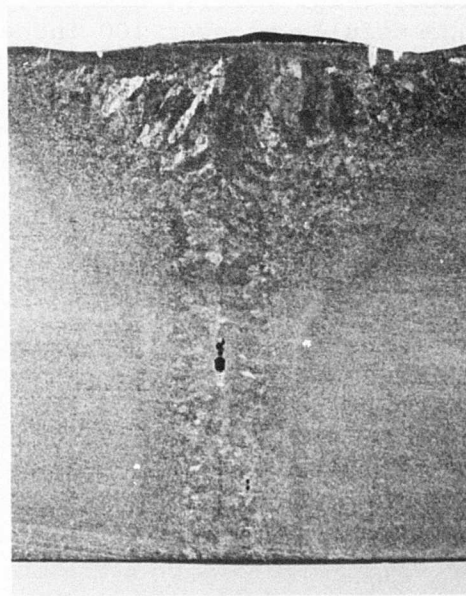
Negative IQ-479

Mag. 7X



Negative No. IA-476

Mag. 7X



Negative IQ-478

Mag. 7X

Figure V-28. CENTERLINE POROSITY, FROM IMPROPER SHIELD (TITANIUM)

- A. Receive test panels
- B. Non-destructive evaluation, welded plates only
- C. Specimen location and layout in areas with no NDT indications
- C. Remove coupons from plates (band saw)
- E. Stress relieve for 60 minutes at 1050°F, AC.
- F. Check and straighten
- G. Machine to finish dimensions (3/8 inch specimens had both beads removed)

Note: Some straightening was done after the heat treatment cycle resulting in the breakage of one 1/2 inch specimen.

- H. Inspect

During the process of specimen fabrication, one 1/2 inch thick titanium test coupon failed during the check and straightening operation. Fractographic examination of this specimen has revealed that the failure initiated in the weld at the fusion line. The point of origin was found to be in a small zone of embrittled weld metal. The remainder of the weld was found to have failed in a ductile manner. Fig. V-29 is a macrograph showing the face of the fracture.

Figures V-30 and V-31 are electron micrographs showing the detail of characteristics of fracture in the various zones. It is apparent that a small portion of the weld and adjacent base metal, at the fusion line, was embrittled by some type of contamination.

Close examination of the titanium weld faces revealed that the edges close to the weld (top face only) were badly discolored in a fashion usually associated with contaminated inert gas shielding. Except for this characteristic, the welds would be considered in compliance with most requirements for coloration after welding.

A length of 1/2 inch thick titanium weld was broken across the weld to permit a cross-sectional view of the affected area. Fig. V-32 is a macrograph of the fracture face of this specimen. The embrittled zones can be seen at the edges of the weld.

A 1/4 inch thick titanium weld was also broken in the same fashion to determine whether the width of the weld was a factor involved in the embrittlement. Fig. V-33 is a macrograph of the face of the 1/4 inch thick titanium weld near the fracture. The discoloration of the edges of the

edges of the weld bead can be seen. Fig. V-34 is a macrograph of the 1/2 inch thick titanium weld. In addition to the discoloration at the fusion line, cracking can be seen in the embrittled zone.

Figures V-35 and V-36 are electron micrographs showing the top edge of the fracture faces of both 1/4 inch and 1/2 inch thick specimens at the embrittled zone. In the case of the 1/4 inch thick specimen, the brittle cleavage type failure can be seen surrounded by the more desirable dimple rupture type of failure mode. The arrow indicates the embrittled zone.

Based on these observations, it was concluded that the jet flow of inert gas did not provide a suitable inert gas shield for titanium weld puddles. Because of the relatively high speed of welding, effectiveness of the trailer shield, and the small amounts of contaminants, the effects have not been apparent in the body of the weld. However, at the edges of the weld, a relatively small quantity of metal is melted, exposed to the contaminants, and solidified before shielding is provided by the trailer shield. It is believed that the relatively slow solidification of the large bulk of the weld metal in the effective trailer shield atmosphere is sufficient to permit dispersion of the contaminants.

This investigation has indicated that this embrittlement zone extends to 0.020 inch in depth for the 1/2 inch thick specimens and less than 0.002 inch for the 1/4 inch thick welds. In order to avoid the possible effects of this embrittlement, a minimum of 0.020 inches was removed by machining from the affected surfaces of all 1/2 inch titanium test specimens. It was believed that the small amount detected in the 1/4 inch thick specimen should be eliminated by the normal processing and no special rework was applied to these specimens.

Representative titanium welds of both thicknesses were chemically analyzed to determine the level of oxygen and nitrogen content. An analysis was carried out to determine whether the contamination significantly affected the composition of the weld bead. No significant indication was discovered. Results obtained are as follows:

1/2" Weld #243B	0.189% Oxygen, 0.14% Nitrogen
1/2 " Base Metal	0.187% Oxygen, 0.11% Nitrogen

1/4" Weld #90C	0.182% Oxygen, 0.14% Nitrogen
1/4" Base Metal	0.172% Oxygen, 0.14% Nitrogen

It was concluded that the contamination was limited in quantity but was concentrated in the embrittled zones.

Microscopic examination of a representative section of the 1/4 inch thick titanium fatigue specimen revealed no evidence of alpha case or machining tears in either the "as received" or machined surfaces. Microhardness was also used in an effort to detect the hardening expected with atmospheric contamination detected at the fusion line of the titanium welds. No evidence of hardness increase in this zone was detected (see microhardness test results).

Visual examination of the titanium material, welded using revised shielding techniques to eliminate the apparent atmospheric contamination observed on previous specimen material, showed significant improvement.

5. Mechanical Behavior

As a final task in the program, titanium alloy weld specimens were subjected to the following tests:

- Tensile (including tests of repaired welds)
- Axial Fatigue Tests
- Fracture Toughness K_{Ic}
- Notched Stress Corrosion K_{Isc}
- Smooth Bar Stress Corrosion Alternate Sea Water Immersion
- Microhardness

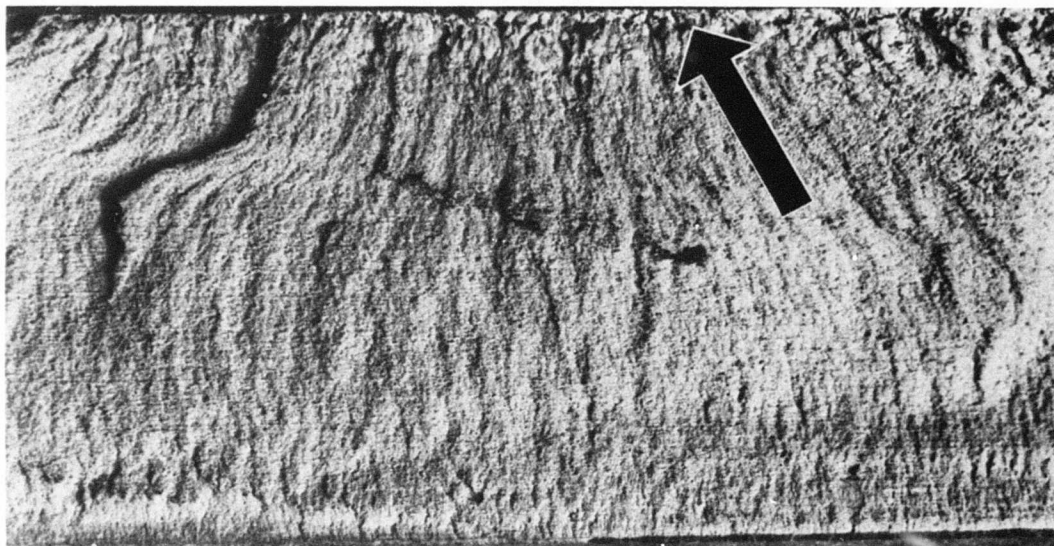
Each of these tests are described in the following sections in terms of:

- Test Procedure
- Test Objective
- Results

a. Tensile Tests

Tensile specimens containing welds (with the reinforcement left on) never exhibited less than 98.7% of the strength of the base metal.

Note: Arrow indicates brittle region at top edge.

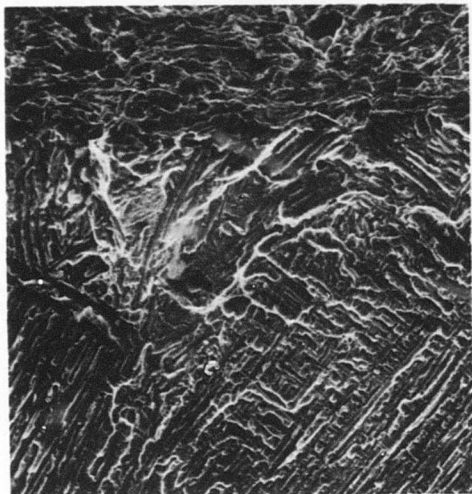


Neg. No. LQ-746

Mag. 6.1X

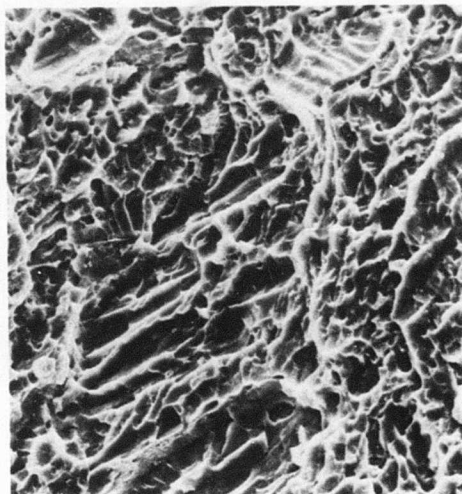
Specimen #FTW-9T

Figure V-29. FRACTURED FACE OF SPECIMEN THAT
FAILED IN STRAIGHTENING (TITANIUM)



Negative No. SQ-634 Mag. 497X

Figure V-30. BRITTLE FRACTURE,
SPECIMEN FTW-9T (TITANIUM)



Negative No. SQ-637 Mag. 1269X

Figure V-31. DUCTILE FRACTURE,
SPECIMEN FTW-9T (TITANIUM)



Negative No. LQ-747

Mag. 5.9X

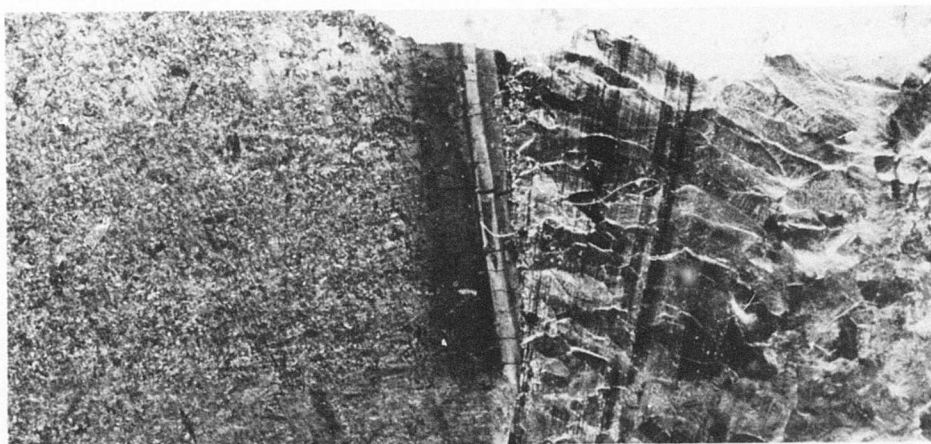
Figure V-32. TRANSVERSE BREAK IN FWT-9T (TITANIUM)



Negative No. IA-749

Mag. 8.9X

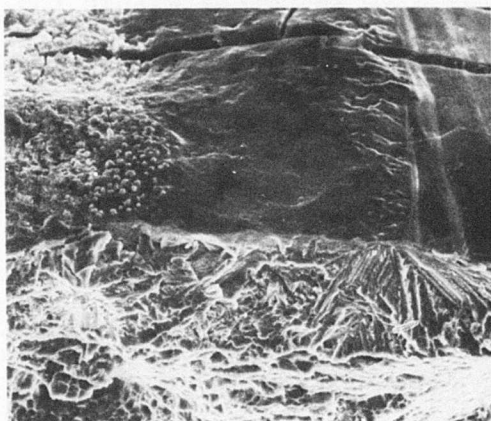
Figure V-33. DISCOLORATION BESIDE BEAD IN BROKEN
1/4 INCH TITANIUM WELD



Negative No. IQ-748

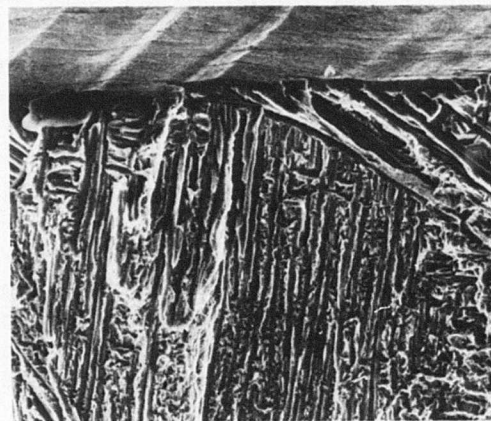
Mag. 10.5X

Figure V-34. DISCOLORATION BESIDE BEAD IN
SPECIMEN FWT-9T (1/2 INCH)



Negative No. SQ-739

Mag. 616X



Negative No. SQ-689

Mag. 561X

Figure V-35. ELECTRON MICROGRAPH,
TOP EDGE
1/4 FRACTURE SPECIMEN

Figure V-36. ELECTRON MICROGRAPH,
TOP EDGE
SPECIMEN FWT-9T

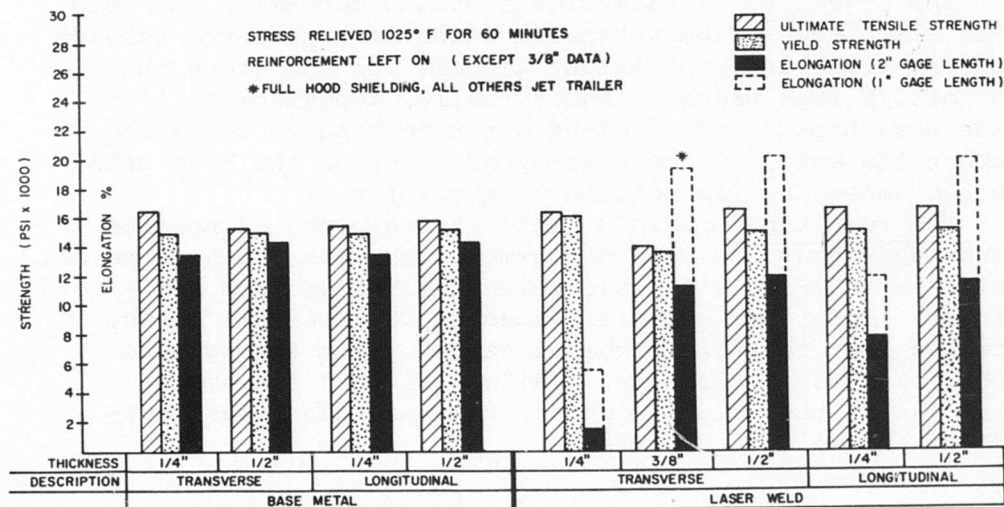


Figure V-37. TENSILE RESULTS (TITANIUM)

Procedure. The transverse tensile weld specimens were designed to place the maximum length of laser welded joint under test. This amount was limited by available testing machine capacity and the length of specimens that could be removed from the weld test panel. The width of the gauge section of the longitudinal samples was also selected, within the above constraints, to provide the maximum amount of wrought metal on either side of the fused metal plus heat affected zone of the weld. This practice makes for easier delineation of the relative ductility of the three elements of a weld (cast metal, heated metal, or supporting base metal.)

The selected gauge sections for longitudinal and transverse specimens were:

1/4 inch thick x 0.75 inch

3/8 inch thick x 0.75 inch

1/2 inch thick x 1.00 inch

Specimen designs are listed in Appendix E.

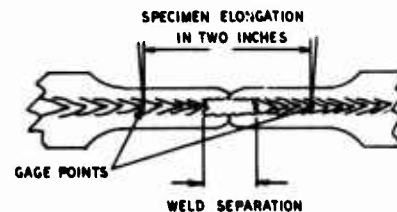
The testing equipment employed on the 1/2 inch thickness was a 400,000 pound Tinius Olson equipped with extensometers, a similar machine with 120,000 pound capacity was used on 3/8 inch material. The 1/4 inch tests were run on a 60,000 Baldwin tensile testing machine.

Base metal test specimen designs followed similar principles. Tests were made parallel to the rolling direction and transverse to the rolling direction.

The objective of these tests was to determine the weld joint efficiency of heat-treated welds in transverse tension with the crown and root intact (except for the crown and root of 3/8 inch welds). Additionally, longitudinal test welds were broken and examined after testing to determine whether the weld, the heat-affected zone, or the base metal was the least ductile portion of the joint.

The resulting tensile yield strength and elongation values show that the weld performed much like the base metal. Table V-8 and Fig. V-37 weld strengths ranged from 155 - 159 KSI ULT. Joint efficiencies exceeded 98.7% in all cases. Occasionally, the reinforcement caused joint strength to exceed base metal strength. Failure in most transverse welds was in the weld. However, two specimens broke outside of the weld.

SPECIMEN			ELONGATION (%)			ULTIMATE STRENGTH (psi)		
Thick	Description	Ident.	(1") Weld* (2")			Tensile	Yield	
1/4"	Transverse Base Metal	TTB-1T	23.6		13.1	160.266	144.649	
		TTB-2T	21.0		13.3	161.971	148.669	
	Longitudinal Base Metal	LTB-1T	24.0		13.2	151.589	144.254	
		LTB-2T	22.1		13.3	152.343	145.263	
	Transverse Welded	ATT-1T	4.5		1.5	156.366	153.987	
		ATT-2T	5.0		1.3	156.347	156.154	
		ATT-3T	4.7		.8	155.879	155.651	
	Longitudinal Welded	ALT-1T	11.7	5.6	7.6	158.000	149.110	
		ALT-2T		6.4	8.3	159.058	148.246	
		ALT-3T		4.6	6.5	159.381	142.436	
	3/8"	Transverse Welded	ATT-4T	19.0		11.0	138.200	134.600**
	1/2"	Transverse Base Metal	TTB-5T	22.1		13.3	152.958	146.439
TTB-6T			22.5		15.0	153.740	150.602	
Longitudinal Base Metal		LTB-5T	22.5		14.6	154.603	148.297	
		LTB-6T	21.8		13.5	153.232	149.738	
Transverse Welded		ATT-7T	25.0		13.3	157.165	148.158**	
		ATT-8T	11.0		8.2	157.476	146.852	
		ATT-9T	24.5		13.7	156.811	147.497**	
Longitudinal Welded		ALT-7T	16.1	7.8	9.5	157.987	148.548	
		ALT-8T	20.8	10.5	12.0	157.858	147.854	
		ALT-9T	19.8	10.1	12.0	159.115	148.052	
* Measurement of weld metal ductility when supported by the base metal and forced to yield at the same rate as the base metal. This determination of ductility is not affected by base metal weld strength differences. See Sketch.								
** Base metal failure.								



$$\text{WELD METAL ELONGATION}(\%) = \frac{\text{SPECIMEN ELONG} - \text{WELD SEPARATION}}{\text{ORIGINAL DISTANCE BETWEEN GAGE POINTS}} \quad (\text{TYPICALLY } 2")$$

Table V-8. TITANIUM ALLOY TENSILE RESULTS

Much of the plastic strain was absorbed by the relatively narrow welds. Therefore, elongation measured over two inches appeared to be low. When a one inch length was used, it increased the volumetric influence of the strain-absorbing characteristics of the weld. The elongation values based on a one inch gauge length in 1/2 inch welds approached those of the base metal specimens (i.e., 21-24% for base metal vs. 11-24% for welds). The ductility of the 1/4 inch welds was considerably lower (5-11%) suggesting a proportionally greater effect from the bands of contamination discussed under the section on titanium alloy weldability.

An analysis of the broken longitudinal welded specimens (Table V-8) showed that the weld had taken nearly as much strain as the heat affected zone or the base metal. Weld failure and the adjacent fracture faces showed a ductile mode except where the zones of contamination existed on welds that had been shielded by a jet trailer with an erratic jet.

b. Axial Fatigue Tests

Welded fatigue specimens equalled base metal performance in these tests on titanium alloy.

Procedure. The transverse axial fatigue specimens were designed to place the maximum amount of laser weld under test. This amount was limited by available testing machine capacity and the length of specimens that could be removed from the weld test panel. The selected gauge sections were:

1/4 inch thick x 0.75 inch wide

1/2 inch thick x 1.00 inch wide

Specimen designs are listed in Appendix E.

The testing equipment employed was a 165 KIP capacity electrohydraulic fatigue machine using MTS pre-aligned mechanical grips. Testing was conducted at a minimum/maximum stress ratio of 0.1 and at a frequency of 3 hertz.

The objectives of this limited testing program were to:

- 1) Compare base metal and laser weld performance.
- 2) Reveal defects that were not detected by prior non-destructive examination and consider the implications in terms of process control.

The determination of a definitive endurance limit for either base metal or welds was not attempted. Some reference data is shown for comparison.

The results are shown in Fig. V-38. Table V-9 lists stress and time to failure and correlates these with post-test observation of the fracture face. The principle observation is that the welds can be almost as strong as the base metal in axial fatigue. Both weld and base metal exhibited strengths slightly lower than comparative data for wrought material. Since the base metal followed this trend, as well as the welds, it appears that the relationship between the reference data and the data from this program does not come about as a result of the act of welding with a laser (i.e., the laser has no unusual effect on weld performance).

Failure site observation indicates that internal pores (Fig. V-38a) had little influence on fatigue behavior. For example, the specimen shown in Fig. V-38a tested in the upper region of the data band of Fig. V-38. The effect of a shallow surface crack (Fig. V-38b) is much more serious. Normally, the 50 KSI stress level on the specimen in Fig. V-38b would have resulted in a run out. All fracture faces are shown at a lower magnification in Figures V-39 and V-40.

c. Fracture Testing

Laser welds in titanium performed better than the base metal in fracture testing. A comparison between the laser weld data (K_Q) and handbook data (K_{IC}) suggests an equivalence in toughness.

Test Procedure. Tests were conducted and evaluated in accordance with ASTM E 399-74. The specimen configuration is described in VC 008251 in Appendix E. ASTM E 399-74 requires that the pre-crack front be essentially flat upon post-test examinations (e.g. that crack front measurements $L_{2,3,4}$ in the sketch on Table V-10 not vary more than 5%).

Fig. V-41 shows the profile of the fracture faces of the specimens. The crack front profiles do not meet the ASTM E 399-74 criteria. This limited analysis to a determination of K_Q , the

stress intensity at the tip of the crack. Under these conditions, K_Q is slightly higher than the K_{IC} value would have been. Table V-10 shows how the stress intensity factor at the tip of each crack (K_Q) was determined from the crack front dimensions. For information, the K_{max} fatigue loads are also shown in Table V-10.

The equipment used for pre-cracking was a Krause lever arm fatigue testing machine. Crack growth was monitored by a 16X optical scope. The pre-crack specimen was then placed in a Riehle 30,000 pound machine equipped with an MTS compliance gauge. The notch and crack were centered in the fused portion of the weld cross section on the welded samples.

The objective of these tests was to compare the toughness of base metal with the toughness of a laser weld.

The results of the stress intensity (K_Q) calculations for welds, are plotted with respect to the base metal performance in Fig. V-42. Available handbook data for the same alloy is also shown. The handbook data is in terms of K_{IC} . The stress intensity which the weld withstood is greater than that of the base metal from which the weld was made and is also quite attractive when compared to the reference (K_{IC}) data.

d. Notched Stress Corrosion Test (K_{ISCC})

The threshold stress intensity for stress corrosion to occur (K_{ISCC}) in titanium alloy welds appeared to be 40% of the K_Q value. This is considered a normal relationship between weld and base metal. Certainly the laser did nothing to increase the sensitivity of the weld to stress corrosion.

Procedure. There is no established test method for notched stress corrosion. Therefore, test specimens were pre-cracked and evaluated essentially in accordance with ASTM-E 399-74 which generally describes fracture toughness testing. The specimen configuration is VC 008951 described in Appendix E, and is identical to that used for fracture toughness determination.

Table V-11 indicates the method of determining the stress intensity K_Q for each specimen. Fig. V-41 shows the failed specimens and crack profile. Fig. V-42 relates stress intensity

Specimen		Ident.	Stress KSI	Cycles to Failure	Post Test Examination								
					Type of Defect at Origin				Initiation Point				
Thk.	Condition				None	Pores	Crack	Other	Surface	Subsurf.	Corner	Weld	Base Metal
1/4"	Base Metal	B-1	120	6x10 ³				X	X				X
		B-2	110	3x10 ⁴									X
		B-3	110	2.7x10 ⁴									X
	Welded	W-1	110	1.5x10 ⁴	X				X			X	
		W-2	110	6x10 ³	X				X			X	
		W-3	90	1x10 ⁴				X	X			X	
		W-4	90	3.9x10 ⁴		X						X	
		W-5	70	4.4x10 ⁴		X				X		X	
		W-6	50	3.6x10 ⁵				X		X		X	
		W-13	80	2.5x10 ⁵							X	X	
		W-14	80	5.3x10 ⁵		X				X		X	
		W-15	60	1.7x10 ⁶		X				X		X	
		W-16	60	6.9x10 ⁵		X				X		X	
1/2"	Base Metal	B-4	80	5.7x10 ⁴	X						X		X
		B-5	70	1.2x10 ⁵	X					X			X
		B-6	70	1.2x10 ⁵	X				X				X
	Welded	W-8	70	1.39x10 ⁵		X				X		X	No failure
		W-10	80	6.5x10 ⁴		X				X		X	
		W-11	60	6.17x10 ⁵	X							X	
		W-12	70	1.1x10 ⁵		X				X		X	No failure
		W-7	50	5.8x10 ⁵	X							X	
		W-7	80	4.7x10 ⁴	X				X			X	

Table V-9. TITANIUM ALLOY AXIAL TENSION
FATIGUE RESULTS

MATERIAL — 6AL-4V TITANIUM PLATE

STRESS RATIO — +0.1

TEST TEMPERATURE — AMBIENT (R.T.)

- WELD SPECIMEN 1/4" THICK
- BASE METAL 1/4" THICK
- ▲ WELD SPECIMEN 1/2" THICK
- △ BASE METAL 1/2" THICK

SEE APPENDIX C FOR FRACTURE
FACE CHARACTERISTICS.

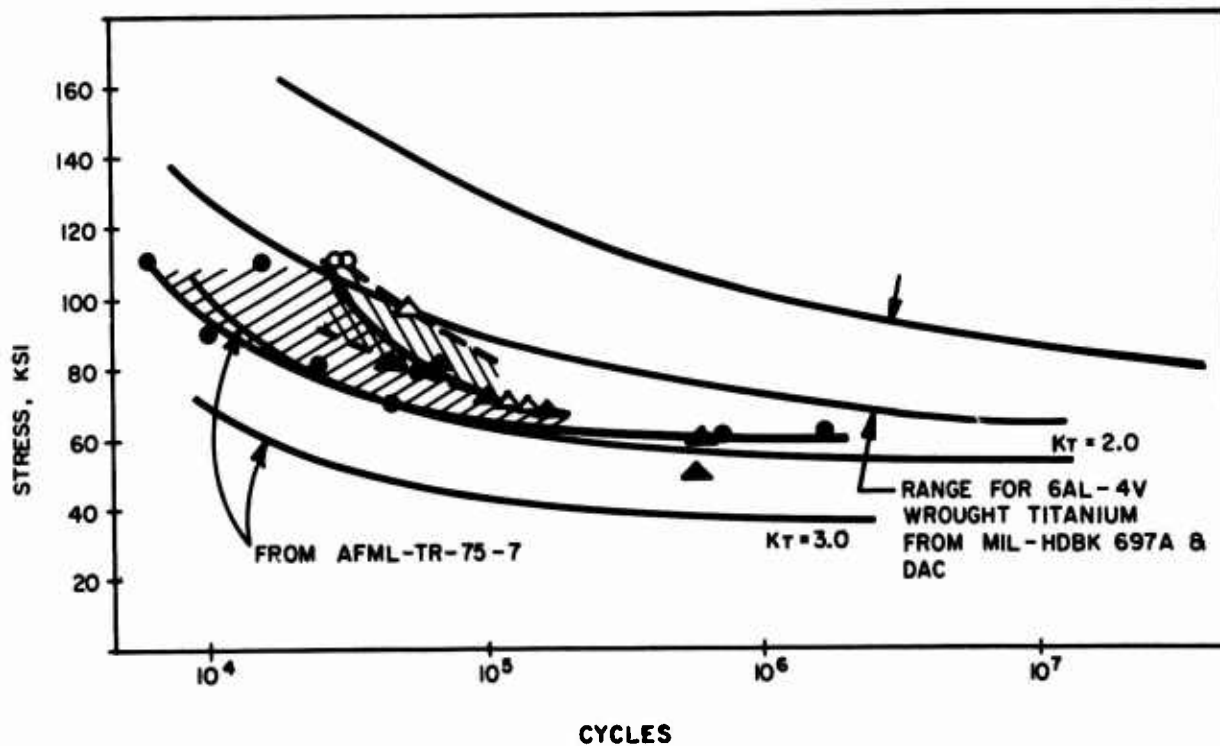
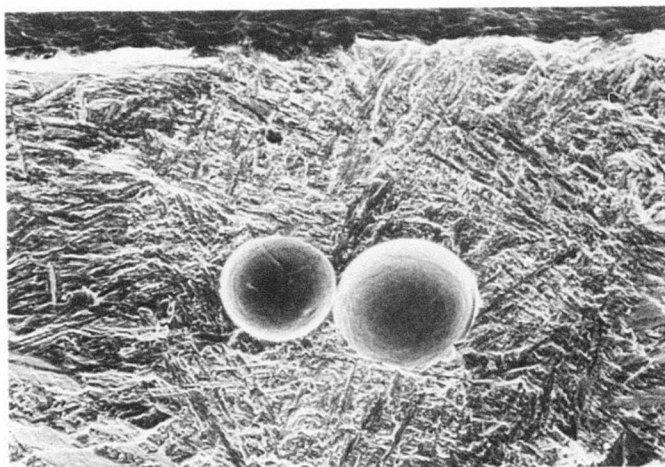


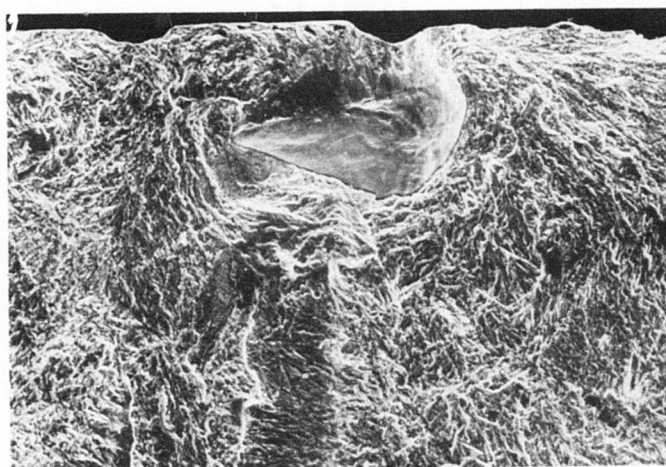
Figure V-38. AXIAL TENSION FATIGUE RESULTS (TITANIUM)



Negative No. SQ-1176

Mag. 327X

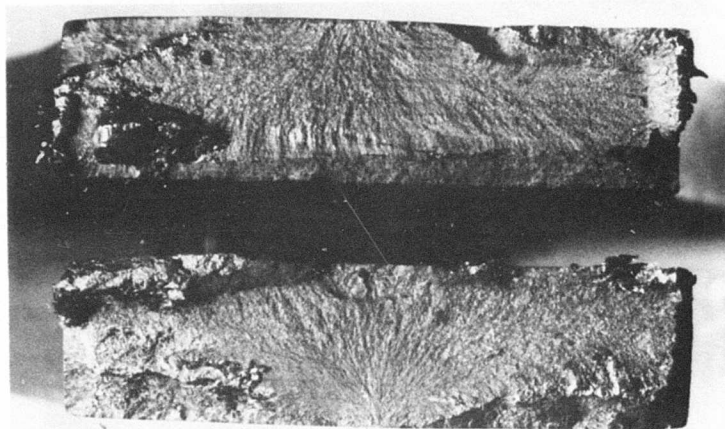
Figure V-38-a. FAILURE INITIATION SITE, SPECIMEN W-4
(PORES - TITANIUM)



Negative No. SQ-1181

Mag. 300X

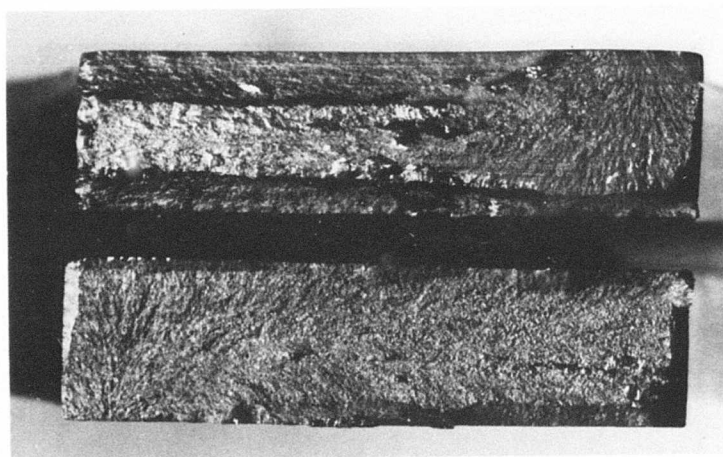
Figure V-38-b. FAILURE INITIATION SITE, SPECIMAN
W-6 (CRACK - TITANIUM)



Negative No. IQ-1078

Mag. 4.5X

Top: Specimen FTW-2T
Bottom: Specimen FTW-2T

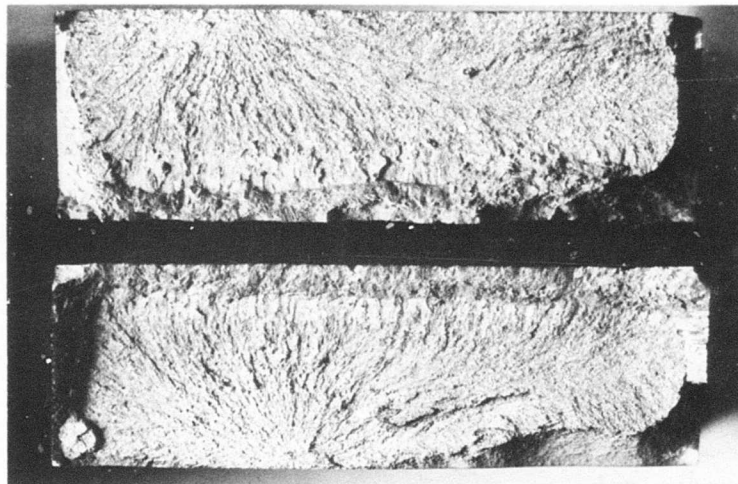


Negative IQ-1079

Mag. 4.5X

Top: Specimen FTW-3T
Bottom: Specimen FTW-4T

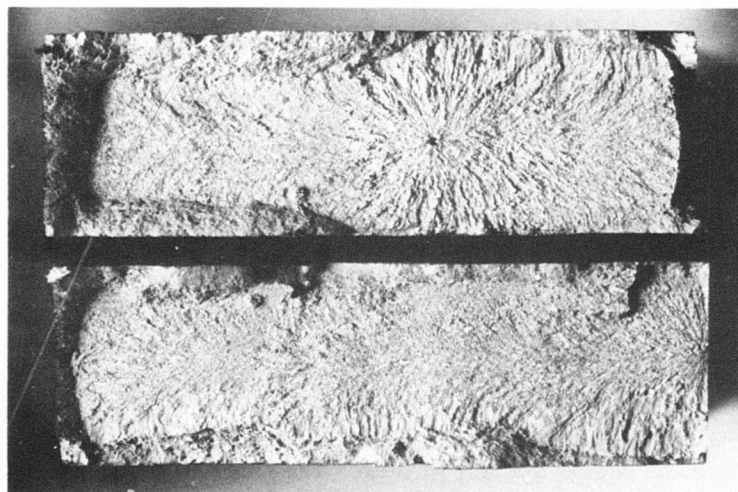
Figure V-39. FATIGUE TEST SPECIMENS (1/4 INCH TITANIUM)



Negative No. LR-499

Mag. 2.8X

Top: Specimen FTW-7T
Bottom: Specimen FTW-8T



Negative No. LR-500

Mag. 2.8X

Top: Specimen FTW-10T
Bottom: Specimen FTW-12T

Figure V-40. FATIGUE TEST SPECIMENS (1/2 INCH TITANIUM)

to time of failure. Therefore, Fig. V-42 indicates the threshold value of stress intensity below which, (in spite of the presence of salt water) a defect such as a crack would not be expected to progress. The value K_{max} has been calculated and is shown in Table V-11 for information.

The equipment used for both pre-cracking and final fracture was a Krause lever arm fatigue tester. Crack growth was monitored by an auto-collimator at 16X. Final breakage was accomplished by manually applying pre-load through a load cell. The load cell output was monitored by cathode ray tube and adjustments made as needed. The corrosive media was substitute sea-water (ASTM 1141-52, pH 7.8-8.2, specific gravity 1.02 - 1.03). The solution is fed to the crack through a gauze wick.

The objectives of this test were to compare the toughness of laser welds to the toughness of the base metal under corrosive conditions.

The test results in Fig. V-42 suggest that the stress intensity threshold, termed K_{ISCC} , is 19.7 KSI in. for titanium alloy welds.

Electron microscopic examination (Fig. V-43) of the fracture face of a typical titanium weld specimen (SCK-6T) indicates a characteristic flat-cleavage, transgranular stress corrosion failure mode. The presence of this mode supports the validity of the above K_{ISCC} value.

e. Microhardness Examination

As-welded hardness approximated base metal hardness. The limited contamination described under the welding subsection was not detectable.

The test procedure employed a Knoop Microhardness tester. Hardness impressions were uniformly spaced 0.014 inches apart.

Test objective - These tests sought to verify as-welded hardness to assure freedom from gross contamination.

Test results - Microhardness surveys of the weld metal and heat-affected zones of selected, representative sections of laser welds were made. These are shown in Figures V-46, V-47, V-48 and V-49. Variations in or near the weld may

represent the effect of cast structures as opposed to wrought structures. There is no clear indication of contamination throughout the weld or alongside the bead - although contamination was observed metallographically on some specimens that broke in straightening.

D. LASER WELDS IN NICKEL BASE ALLOY

As noted in Section III, this material was selected as representative of the age hardenable, high temperature alloys with good weldability.

1. Base Metal Characteristics

The trade name of the alloy is Inco 718. The material for the program was procured from the Stellite Division of the Cabot Corporation as AMS 5596. The supplier refers to the material as Haynes Alloy No. 718. The nominal composition (%) is:

	Cr	C	Si	Co	Ni+Co	Mn	Cb+Ta	Mo	P+S	Al	Ti	B	Cu
Min:	17	-	-	-	50.0	-	4.75	2.80	-	.2	.65	-	-
Max:	21.08	.35	1.00	55.0	.35	5.50	3.30	.35	.8	1.15	.006	.3	

The program material represented six heats. The composition of each heat is given in Table V-12. The required tensile properties of the material as received from the supplier are:

	Uti.	Yld.	Elong.
Solution Treated	150 KSI	90 KSI	30%
Precipitation Hardened 1200°F	145 KSI	120 KSI	5%

The material should not rupture in less than 23 hours when loaded at 1200°F to 100 KSI and should elongate at least 4% at rupture. All heats met this requirement. Table V-13 lists the test results by heat.

Type	Ident. No.	Thickness Inches B 1, 2, 3	Depth* Inches W 1, 2	CRACK FRONT DIEMNSIONS, INCHES*						K _{Max}	Ult. Load Lbs.	*** K Q	K 1C
				L ₁	L ₂	L ₃	L ₄	L ₆	L _{2,3,4}				
Base Metal	FBM-4T	.4968	1.0018	CATASTROPHIC FAILURE									
	FBM-5T	.4970	1.0016	.5590	.5878	.5906	.5818	.5486	.5867	27.3	1295	37.2	****
	FBM-6T	.4971	1.0020	.5596	.5912	.5956	.5940	.5484	.5936	27.9	1385	40.7	****
Welded	FAW-4T	.4967	1.0020	.5496	.5768	.5948	.5880	.5564	.5865	27.2	1805	51.7	****
	FAW-5T	.4970	1.0008	.5550	.5902	.6062	.6010	.5738	.5991	28.6	1650	49.7	****
	FAW-6T	.4965	1.0020	.5552	.5816	.5912	.5788	.5488	.5839	27.0	1770	50.3	****

NOTE: Testing and calculations performed in accordance with ASTM specification E399-74.

- * See sketch of specimen dimension.
- ** Calculation: $K_{max} = \frac{(\text{Fatigue Load}) W}{B (W-L)^{3/2}} [f(a/w)]$
- *** Calculation: $K_Q = \frac{(\text{Ultimate Load}) W}{B (W-L)^{3/2}} [f(a/w)]$
- **** Pre-crack front not in compliance with ASTM requirements for valid test. (Variation of crack front measurements more than 5% of $L_{2,3,4}$).

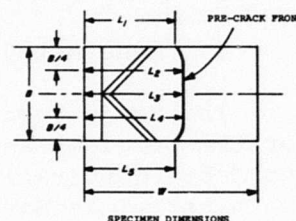
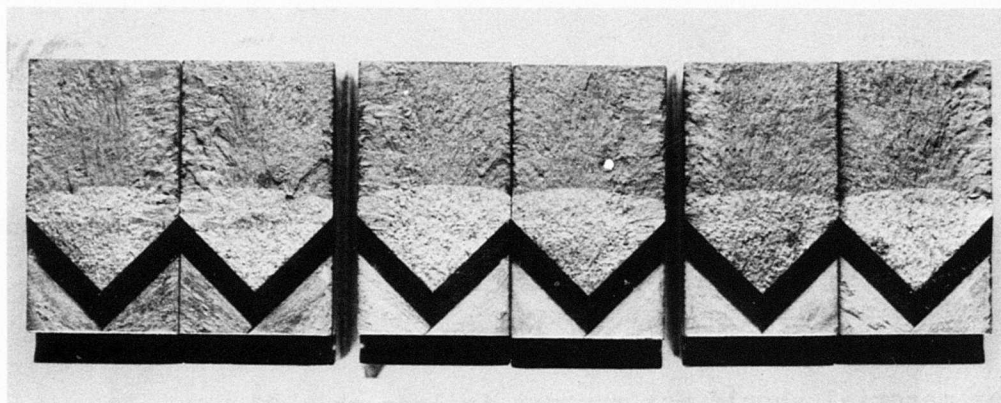


Table V-10. TITANIUM FRACTURE TOUGHNESS RESULTS



Negative No. LR-585

Mag. 2X

Left: Specimen FAW-4T
Middle: Specimen FAW-5T
Right: Specimen FAW-6T

Figure V-41. WELD TOUGHNESS SPECIMENS (TITANIUM)

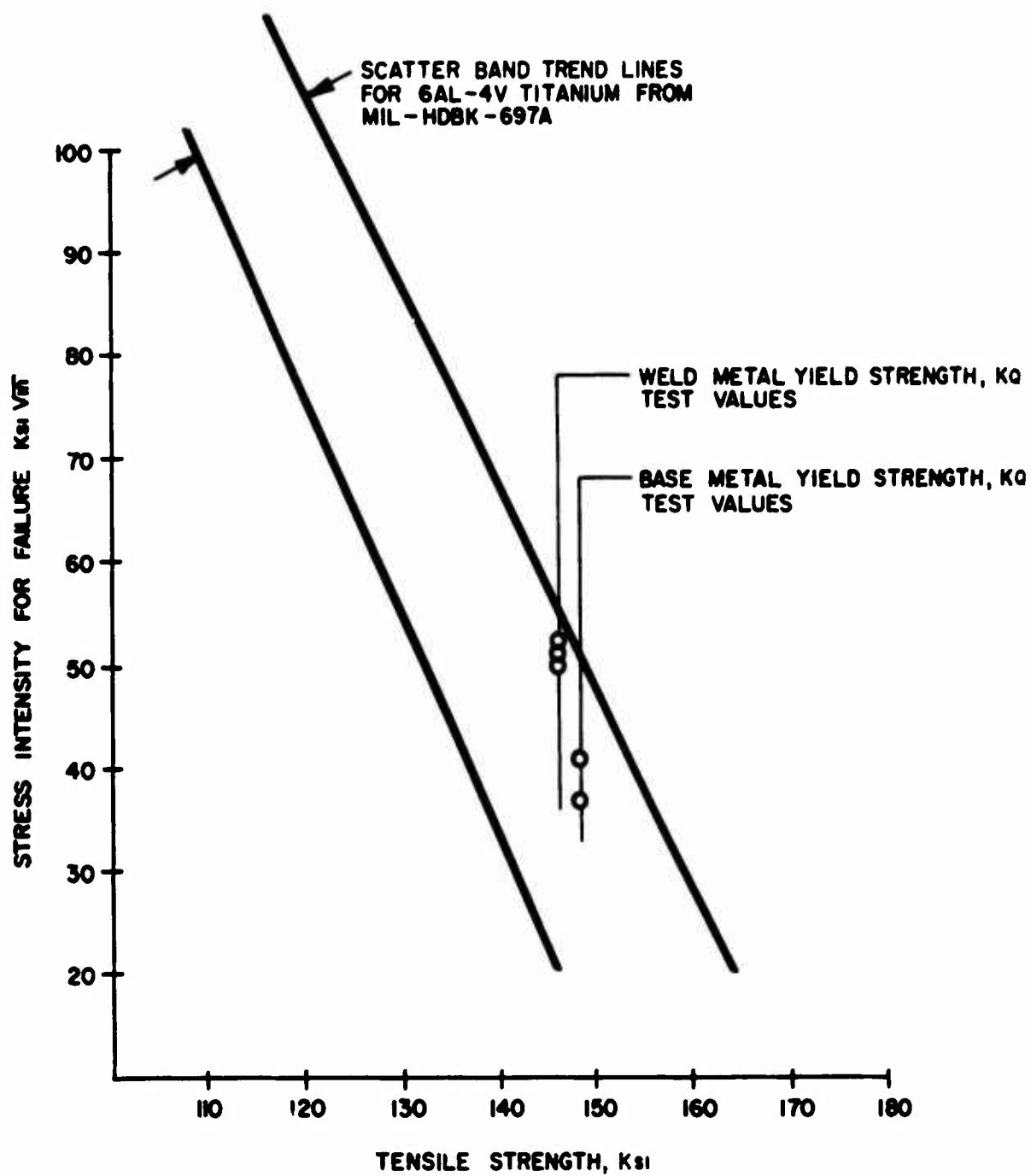
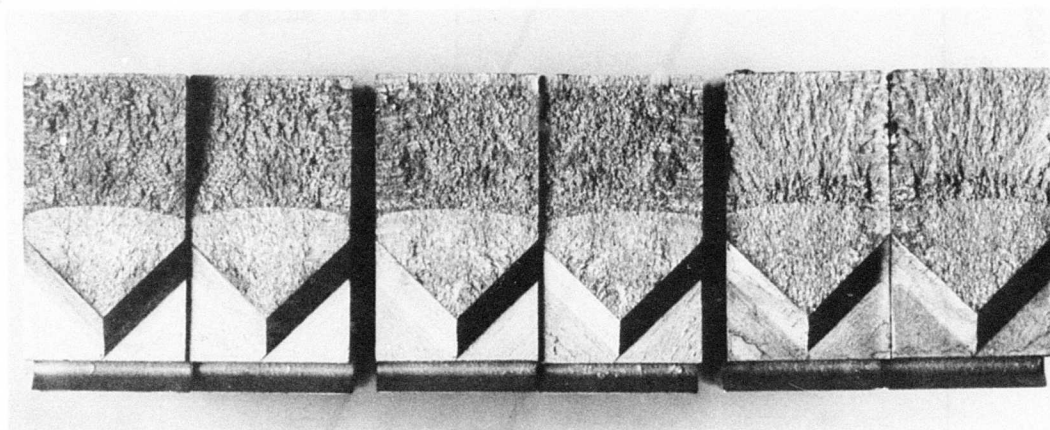


Figure V-42. FRACTURE TOUGHNESS RESULTS (TITANIUM)

Ident. No.	Thickness (Inches)	Depth (Inches)	CRACK FRONT DIMENSIONS						K_{Max}	Load (lbs.)	K_Q	Life Minutes
			L 1	L 2	L 3	L 4	L 5	L 2,3,4				
SCK4-T	0.489	1.001	.555	.587	.588	.577	.548	.584	27.0	1000	28.4	15
SCK5-T	0.497	0.999	.544	.564	.578	.578	.551	.573	27.1	750	21.4	745
SCK6-T	0.496	0.999	.557	.586	.594	.587	.565	.589	27.7	600	17.5	2880
SCK6-T	Same	Same	Same	Same	Same	Same	Same	Same	Same	675	19.7	2780

Table V-11. TITANIUM ALLOY NOTCHED
STRESS CORROSION RESULTS



Negative No. LR-437

Mag. 2X

Left Specimen - SCK-4T
Center Specimen - SCK-5T
Right Specimen - SCK-5T

Figure V-43. NOTCHED STRESS CORROSION SPECIMENS (TITANIUM)

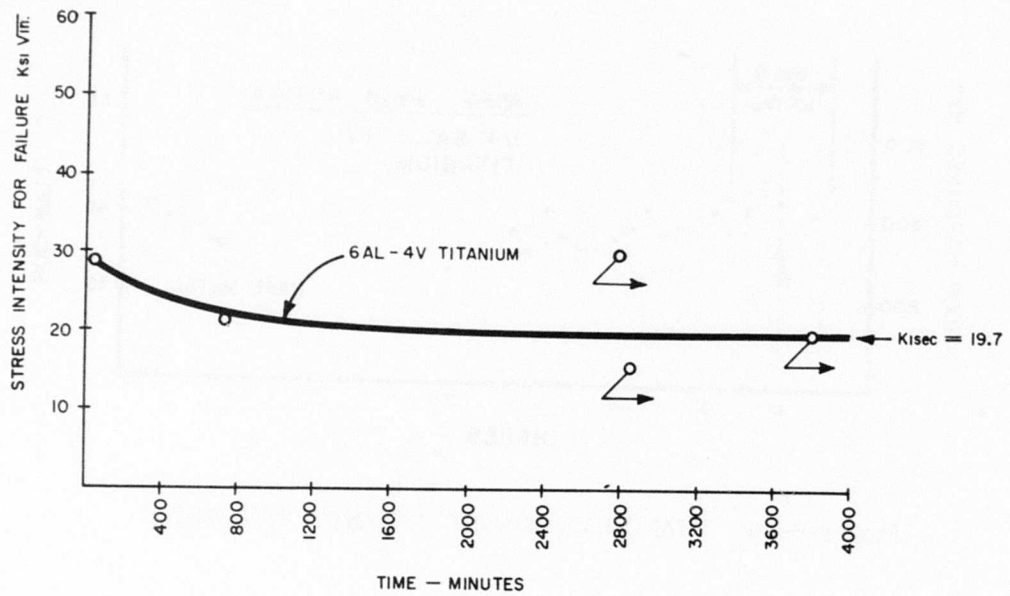
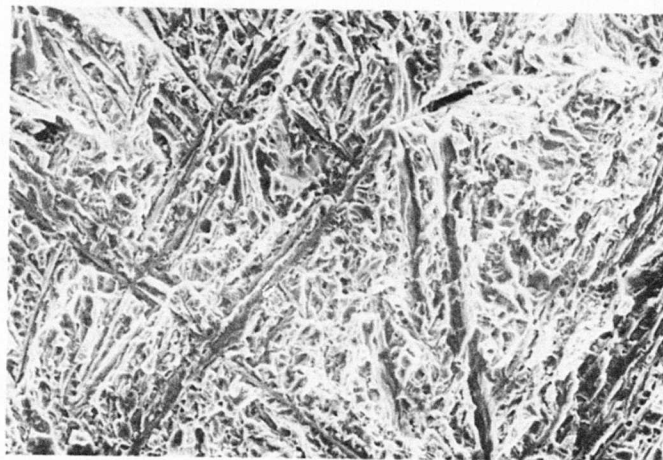


Figure V-44. NOTCHED STRESS CORROSION RESULTS (TITANIUM)



Negative No. SR-809

Mag. 560X

Figure V-45. STRESS CORROSION FAILURE MODE (TITANIUM)

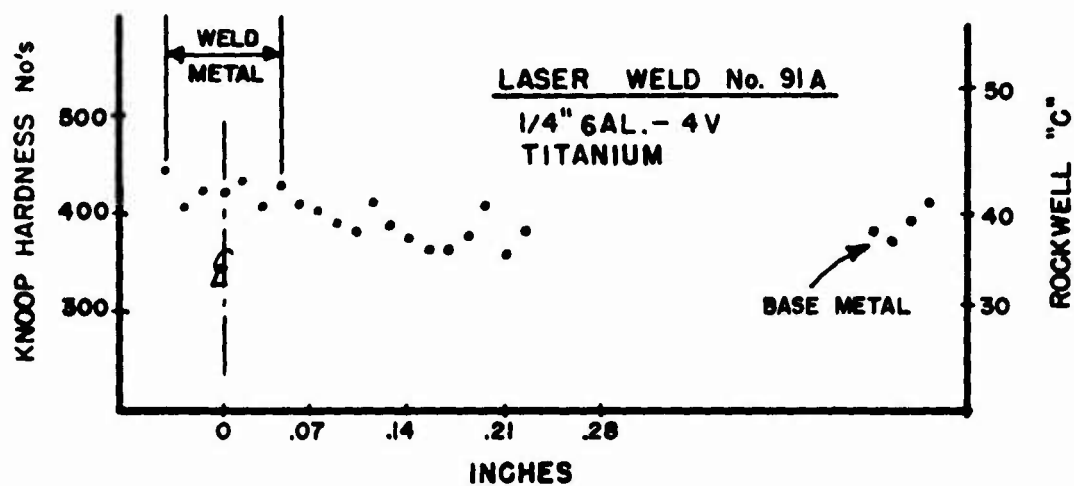


Figure V-46. HARDNESS SURVEY (1/4 INCH TITANIUM)

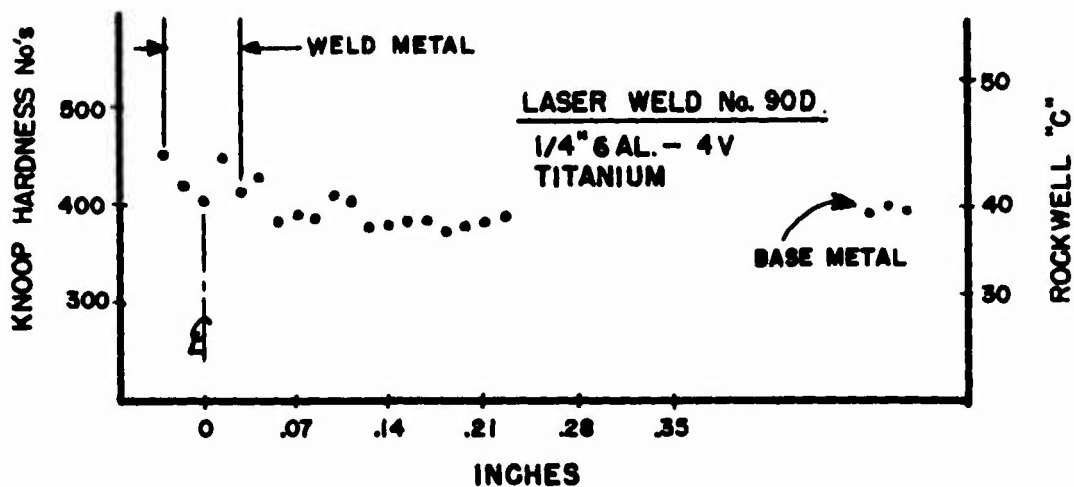


Figure V-47. HARDNESS SURVEY (1/4 INCH TITANIUM)

Thickness (inches)	Heat No. 2180-3	ANALYSIS (%)												
		Cr	C	Si	Co	Ni	Mn	Cb+Ta	Mo	(P&S)	Al	Ti	B	Cu
0.250	9427	18.00	.055	<.02	.04	52.30	.14	5.06	3.08	(<.005)	.48	.97	.004	.01
0.375	9417	18.27	.05	.11	.15	51.20	.25	5.12	2.98	(<.005)	.60	1.06	.005	.02
0.500	9422	18.07	.06	.12	.24	52.42	.10	5.02	3.11	(<.005)	.46	1.01	.003	<.01
0.500	9426	18.08	.05	.06	.51	52.59	.09	5.05	3.17	(<.005)	.49	1.06	.003	.02
0.350	9419	18.23	.05	.11	.55	51.69	.20	5.08	3.01	(<.005)	.49	.98	.005	.02

Table V-12. COMPOSITION OF NICKEL BASE MATERIALS
TESTED IN PROGRAM

Thickness (inches)	Heat No. 2180-3	TENSILE TESTS (RT)			TENSILE TESTS (1200°F)			STRESS RUPTURE (1200° F)			
		ULT (KSI)	.2% Yld. (KSI)	Elong. (% 4D)	Ult. (KSI)	.2% Yld. (KSI)	Elong. (%)	Stress (KSI)	Hr.	Elong. % 4D	Hardness
0.250	9427	*121 **192	<u>70.5</u> 171	<u>43.5</u> 19.5	*155.5	132.5	18.5	100	145.8	7.8	*98 Rb **42 Rc
0.375	9417	*126.8 **196.1	<u>58.2</u> 153.8	<u>46.5</u> 22.5	**159.3	130.9	13.5	105	61.4	6.2	*98 Rb **42 Rc
0.500	9422	*122 **198.5	<u>59.5</u> 162	<u>49.0</u> 20.5	**161.5	143	19	100	195.7	8.3	*92 Rb **42 Rc
0.500	9426	*126 **199	<u>56.5</u> 162.5	<u>48.4</u> 22.0	**172.5	148.5	20	105	125.3	7.0	*97 Rb **42 Rc
0.750	9419	*125.2 **198.0	<u>70</u> 173.7	<u>44.6</u> 18.5	**158.4	127.2	17	105	92.6	7.0	*91 Rb **42 Rc

* Annealed
** Aged

Table V-13. MECHANICAL PROPERTIES OF NICKEL
BASE MATERIALS TESTED IN PROGRAM

2. Panel Welding

Table V-14 summarizes the nickel base alloy test panel welding procedures which included wire brush and acetone rinse as a preweld cleaning procedure. Figure V-6 sets forth the details of shield set-up. Figure V-7 shows the tooling that was used to hold the panels for welding.

The welding set-up tests used to establish the procedures employed to weld the nickel base alloy panels and photographs of the resulting development welds are shown in Appendix E.

The quality of the resulting test panels was high (see Figure V-5) and is described for each welded test panel in Appendix D. Appendix B reports the following experimental detail:

Panel Identification Size Orientation and Shape

Identification Orientation and Location of Each Weld in the Panel

Procedure Details for each Weld in the Panel

Location of all Non-Destructive Indications in Each Weld

Location of Test Specimen Coupons in Each Weld

Relationship between NDT indications and Test Specimen Location

Test Specimen Location

3. Welding Characteristics

Behavior during welding that sets the nickel base alloys apart from other program materials was noted throughout the program and is summarized here.

The nickel base alloy (AMS 5596) is readily welded by laser in thicknesses up to 3/8 inch. However, over-all weldability was limited, because acceptable welding procedures could not be developed in the 1/2 inch thickness - even though this thickness was readily penetrated by the laser.

Welding Parameters	PANEL THICKNESS	
	1/4 Inch	3/8 Inch
Power, Beam On Work (kW)	11.0 7.7	16.0 11.2
Process Speed (ipm) Optics (F/No) Focal Distance (in.)	100 7 28-1/16	70 Same Same
Surface Preparation	Deburr, Wirebrush Rinse w/Acetone	Same
Shielding Gas (Type/CFH) Jet Trailer Hood Underbead	Helium / 100 Argon / 25 Helium / 10*	Same Same Same
Shield Position Set Back (in.) Lift Off (in.)	7/16 0.03	Same 0.04**
Gap	002*	Same
Mismatch	005*	Same
Tooling	Figure V-7	Same
Filler Wire	Not Used	Same

* Unless noted for a specific panel in Appendix D.

** In some panels, surface height varied 0.062 inches such that hood lift-off approached 0.1 inches. This is excessive at the nominal 25 CFH flow rate but appeared to be acceptable if the flow rate was raised to 50 - 60 CFH.

Table V-14. NICKEL-BASE ALLOY WELDING PROCEDURES

SPECIMEN			ELONGATION (%)			ULTIMATE STRENGTH (PSI)	
Thk.	Description	Ident.	(1")	Weld*	(2")	Tensile	Yield
1/4"	Transverse Base Metal	TTB-1N			16.4	201.076	175.717
		TTB-2N			16.4	201.020	177.551
	Longitudinal Base Metal	LTB-1N			17.0	204.092	177.859
		LTB-2N			20.0	204.295	178.628
	Longitudinal Welded	ALT-1N		4.2	5.2	200.214	174.586
		ALT-2N		8.1	10.5	200.000	173.228
		ALT-3N		3.8	6.0	198.533	170.246
	Transverse Welded	ATT-1N	5.7		3.9	198.840	179.325
		ATT-2N	3.1		2.2	194.920	180.930
		ATT-3N	5.0		3.2	197.250	180.357
3/8"	Transverse Welded	ATT-4	5.0		4.0	190.600	173.400
		ATT-5	11.0		8.0	199.300	169.000

* Measurement of weld metal ductility when supported by the base metal and forced to yield at the same rate as the base metal. This determination of ductility is not affected by base metal weld strength differences. See sketch.

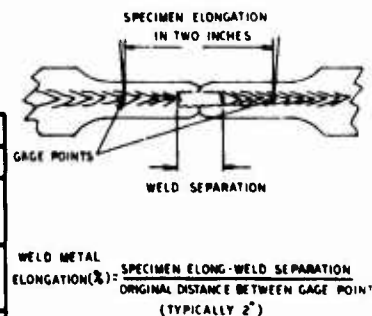


Table V-15. NICKEL BASE ALLOY TENSILE RESULTS

If just enough power was used in the 1/2 inch weld to form a continuous underbead, X-rays of the weld revealed a string of spherical voids. The appearance of the regularly spaced voids in a beam weld suggests incomplete penetration of the beam cavity that forms the weld. They are often observed in partial penetration welds.

If power into the 1/2 inch weld was increased to encourage full-penetration and a stable cavity, the greater amount of melting that resulted caused the heavy molten alloy to pour out and solidify in a series of drops hanging from the underbead. The upper bead fell below the plate surface as a consequence of the metal drop out.

No intermediate range of power input could be found between a "cold" weld with spherical voids and an over-welded joint with metal drop through. Both conditions exist on all materials but are separated by a broad intermediate range of power where neither condition is evident.

Chills were placed directly under the bottom bead in order to catch and freeze the drop out. This is contrary to the guidelines given for chills in Section IV but appeared to be needed to avoid the hanging drops of metal. The direct chills were not successful. If the chill was of copper, energy exiting from the bottom of the cavity melted the chill and contaminated the underbead. Nickel base alloy chills welded to the underside of the joint and the weld contained voids which extended into the joint after the chill was torn, or machined, loose.

Two beam geometries were attempted as follows:

F-21 optics (run 82H), 30 IPM, 13.5 kW on work,
Jet Trail Shield (100 He/25A).
F-7 optics (run 291B), 20 IPM, 13 kW on work,*
Jet Trail Shield (100 He/25A).

Penetration was easily achieved with the F21 optics but no intermediate welding range could be observed with either power or speed variations. Welds had either spherical voids (low heat input) or drop through (high heat input). The above F/21 procedure exhibited the least number of underbead drops (3-6 per inch).

*Power tapered to 9.45 during run to control melting.

The F/7 optics were employed for their small focal spot. Interest in a small intense spot was generated by the observation that the electron beam readily welds 1/2 inch nickel base alloy. It was not possible to confirm the value of the small spot in this program. The highly divergent F/7 beam did not penetrate the 1/2 inch plate at normal welding speeds of 30 - 40 ipm. Conduction melting and metal fallout had begun to dominate cavity action at the 20 ipm speed which was required for full penetration with F/7. Reducing power during the welding process did not prevent metal fallout. Power reduction was continued until penetration was lost.

What appeared to be needed was more efficient penetration with less melting. This might occur with different power distribution. (Rev. V-4). Straight beam sides that were better adopted to thick plate might also help. Straight sides imply an F/Number that is intermediate between F/7 and F/21. A laser with a wave length other than 10.6 microns could also be considered. All of these approaches are beyond the scope of this program.

One observation that came out of this extensive procedure development is that the ability of a laser to penetrate a given thickness does not mean that the laser can produce a weld in that thickness. Other factors enter into making a weld. In this case it appeared that the two beam geometries available to the program were not capable of establishing an efficient, penetrating procedure without overwelding the part and causing metal dropout as soon as the cavity penetrated the underside of the plate.

4. Specimen Preparation

Once nickel base alloy panel weldments in thicknesses up to 3/8 inch were completed at the Avco Everett Research Laboratories, Everett, Massachusetts, they were identified and shipped to the Long Beach, California plant of the Douglas Aircraft Corporation for weld evaluation. At that site, the following steps were implemented in processing the material from the welded panel form to finished test specimens:

- A. Receive test panels
- B. Non-destructive evaluation, welded plates only
- C. Specimen location and layout in areas with no NDT indications
- D. Remove coupons from plates (band saw)
- E. Check and straighten
- F. Machine to finish dimensions (3/8 inch specimens had both bead and crown removed)
- G. Age harden at 1325°F for 8 hours to a hardness of Rc36 minimum
- H. Inspect

5. Mechanical Behavior

As a final task in the program, nickel base alloy weld specimens were subjected to the following tests:

Tensile (including tests of repaired welds)
Microhardness

Each of these tests are described in the following sections in terms of:

Test procedure
Test objective
Results

a. Tensile Tests

After welding and aging specimens exhibited slightly reduced tensile behavior when compared to wrought, aged specimens.

Procedure - The transverse tensile weld specimens were designed to place the maximum length of laser welded joint under test. This amount was limited by available testing machine capacity and the length of specimens that could be removed from the weld test panel. The width at the gauge section of the longitudinal samples was also selected within the above constraints to provide the maximum amount of wrought

metal on either side of the fused metal-plus-heat-affected-zone of the weld. This practice makes for easier delineation of the relative ductility of the true elements of a weld cast metal, heated metal, or supporting base metal.

The selected gauge sections for longitudinal and transverse specimens were:

1/4 inch thick x 0.75 inch
3/8 inch thick x 0.75 inch

Base metal test specimen designs followed similar principles. Tests were made parallel to the rolling direction and transverse to the rolling direction.

Specimen designs are listed in Appendix E.

The Testing Equipment employed on the 3/8 inch thickness was a 120,000 lb. Tinius Olson equipped with extensometers. The 1/4 inch tests were run on a 60,000 Baldwin tensile testing machine.

The Objective of these tests was to determine the weld joint efficiency of heat treated welds in transverse tension with the crown and root intact. Additionally, longitudinal tests of welds could be examined after testing to determine whether the weld, the heat-affected zone, or the base metal was the least ductile portion of the joint.

Results - The resulting ultimate tensile strengths, yield strengths and elongation values show that the welds do not perform as much like the wrought base metal as do titanium or steel (Table V-15 and Figure V-50). Weld strengths ranged from 195 - 200 KSI ult. joint efficiencies exceeded 95.5% in all cases. This is slightly lower than the 98 - 99 per cent efficiencies observed in low alloy steel and titanium. Failure in all transverse welds was in the weld.

Elongation values were considerably lower than those observed in the wrought material, even when elongation was measured in longitudinal specimens where strength differences between weld and base metal have no effect (see sketch on table V-15) on weld performance.

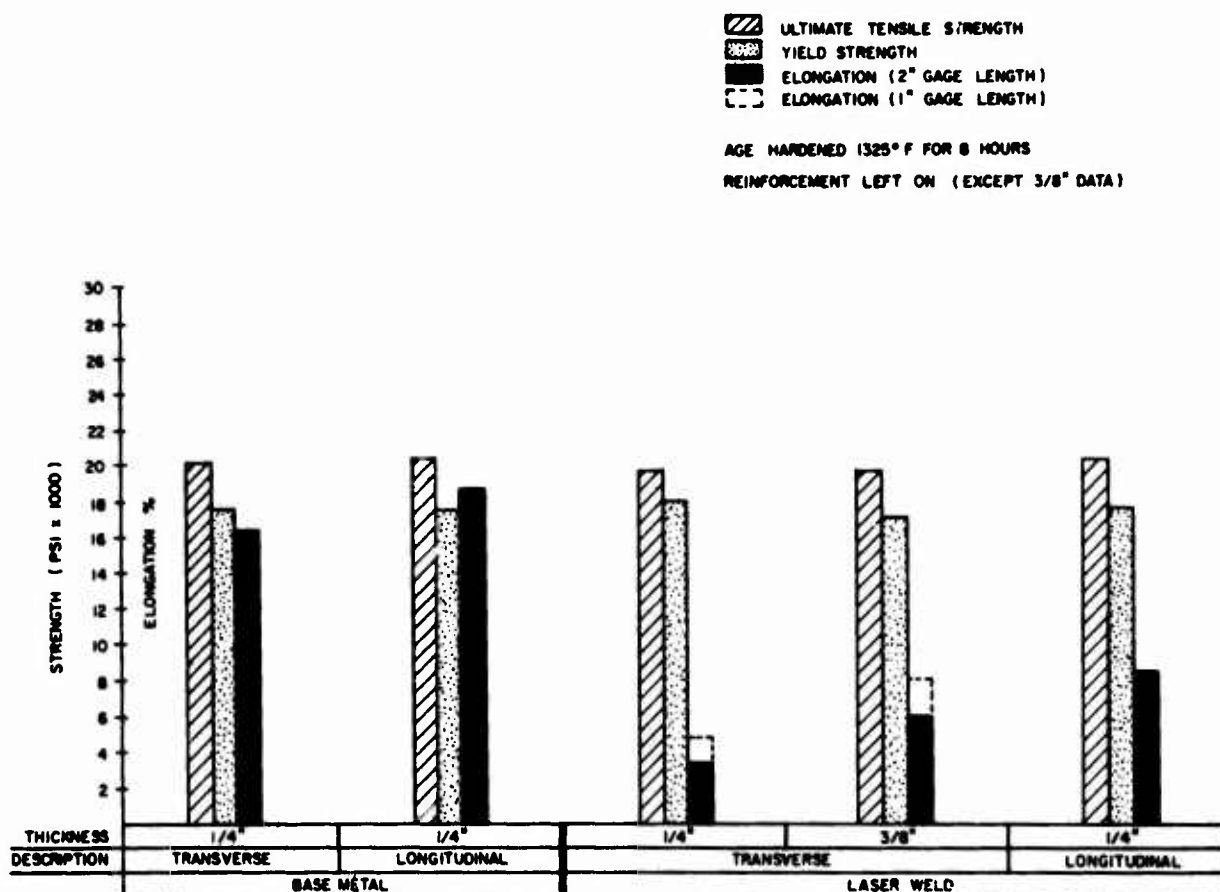


Figure V-50. TENSILE RESULTS (NICKEL BASE ALLOY)

b. Microhardness Examination

Laser welds in this age hardening nickel base alloy responded fully to heat treatment.

Procedure - A Knoop hardness tester was used. Hardness impressions were uniformly spaced 0.014 inches apart.

Objective - These tests established the effects of the aging treatment on the weld structure and material immediately adjacent to it.

Results - After aging the hardness of this weld (93E) and the adjacent base metal are very similar (Figure V-51).

The laser does not seem to have reduced the amount of the hardening elements in the weld metal (principally titanium, aluminum and to a lesser extent-columbium). This particular weld performed quite well in tensile tests. It was longitudinal test ALT-20 (Table V-15). Its ultimate strength equalled base metal. Ductility was about half of the wrought base metal.

Tests from 94D were not as strong. They were transverse test ATT 1, 2 and 3 (Table V-15). There appears to be some slight auto hardening from welding which may have reduced the ability of the joint to respond to the post weld furnace treatment. The weld approached Rc 30 while the base material hardness was closer to Rc 20.

E. LASER WELDS IN ALUMINUM ALLOY

As noted in Section III, this material was selected because a large background of welding information existed. It also has good strength at moderately elevated temperatures and has demonstrated good resistance to stress corrosion cracking.

1. Base Metal Characteristics

This material was purchased against a certificate of compliance to Mil-A-8920. The commercial designation is 2219-T87.* The designation T87 indicates coldwork following solution treatment and then aging.

*Superseded by QQ-A-250/30

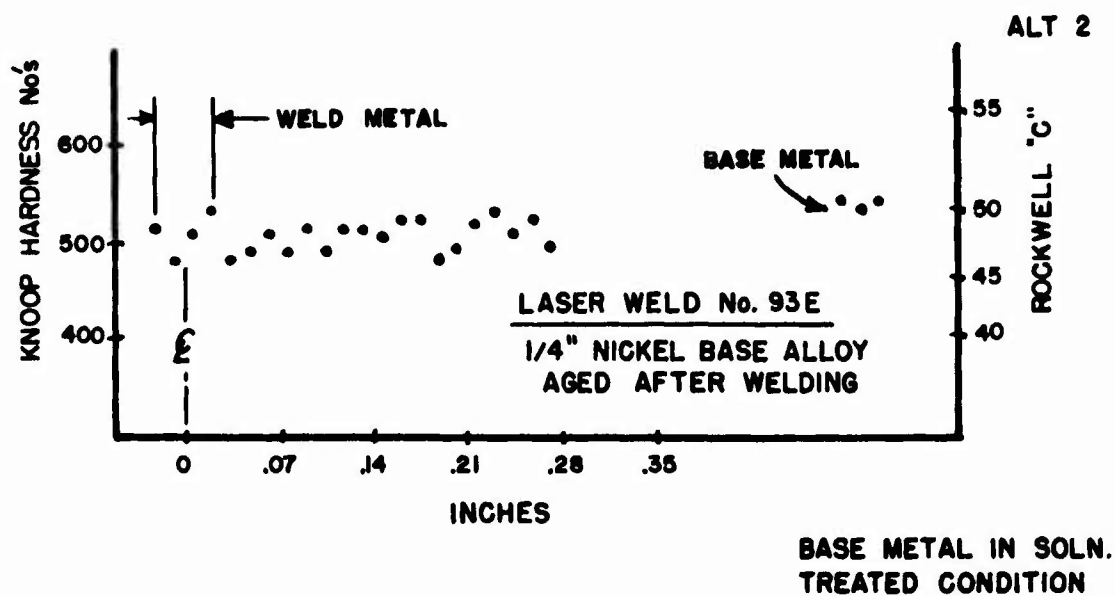
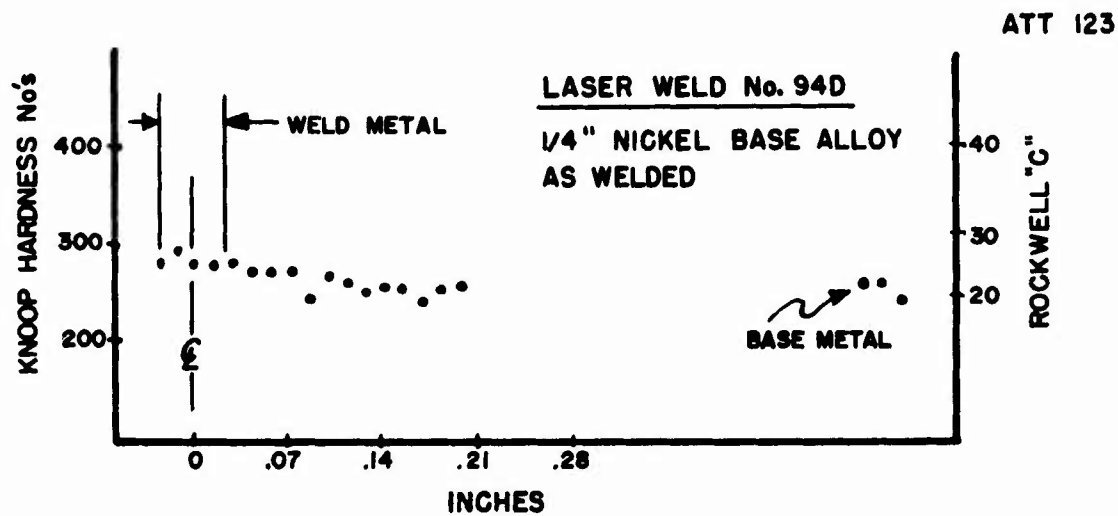


Figure V-51. HARDNESS SURVEY, (NICKEL BASE ALLOY)

The nominal composition is:

	Si.	Fe	Cu	Mn	Mg	Zn. Al	Ti	V	Zr	Other
Min	-	-	5.8	.2	-	-	.02	.05	.7	.05 each
Max	.2	.3	6.8	.4	.02	.1	.10	.15	.25	.15 total

The tensile properties of the material as received from the supplier are - in the T-87 condition:

Ult	64,000
Yield	51,000
Elong	7%

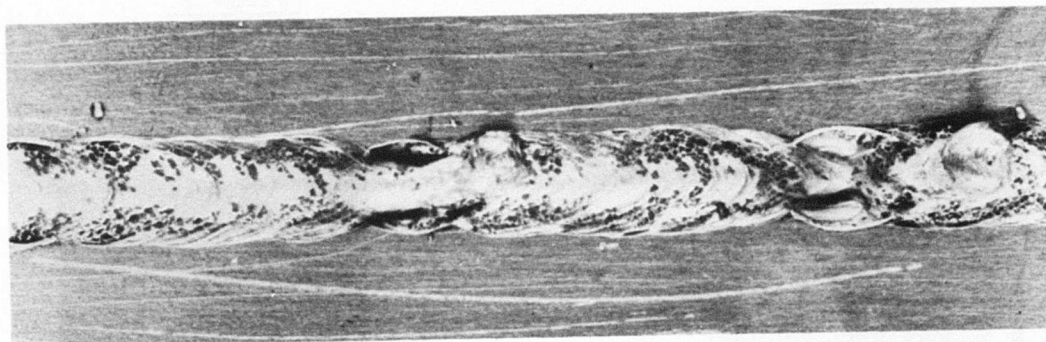
2. Panel Welding

All welds in aluminum were made on surfaces from which all oxide had been removed. Contrary to expectations, penetration in this highly reflective metal was easily achieved in aluminum. Therefore, extensive procedure optimization was possible. Speed, focus, power, gas shielding, types of telescope, special underbead pressure control, special plasma manipulation and special metal chills were all carefully evaluated without achieving a procedure that would be applicable to the welding of test panels.

Short sections of weld could be produced without excessive porosity. When welds of more than a few inches length were attempted, a periodic instability would occur as metal dropped out of the weld bead at a particular point. The result might be a depression in the bead (Figure V-52), or a hole completely through the bead.

3. Welding Characteristics

Figure V-53, frame 1, shows the sequence of events that appear to lead to periodic instabilities in the laser process for aluminum welding. Initially, the beam - metal interaction is confined to a relatively narrow band. This is the conventional welding mode for the beam with a nominal specific energy level of 7.9×10^6 watts/inch.



↑
TYPICAL INSTABILITY
CAVITY

↑
TYPICAL INSTABILITY
CAVITY

PROCEDURE

MATERIAL: ALUMINUM
POWER/SPEED: 10 KW AT 60 IPM
F NUMBER: 7
SURFACE CONDITION: SCRAPPED
SHIELDING: JET SET BACK MAXIMUM AMOUNT (.625")
HOOD RAISED MAXIMUM AMOUNT (.062")
(PRODUCED MAXIMUM PUDDLE OXIDATION)
TOOLING: MULTICHANNEL

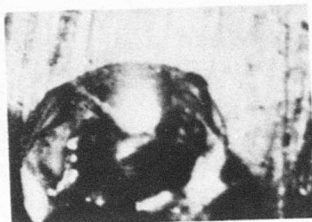
Figure V-52. PROCESS INSTABILITY IN ALUMINUM WELDS.



Frame 1
Normal Narrow Pool



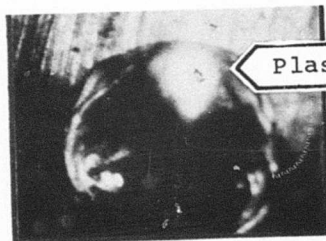
Frame 2
Melting Behind Beam



Frame 3
Forward Melting



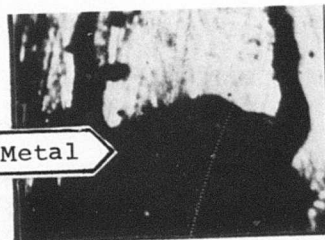
Frame 4
Drop Thru



Frame 5
Back Reflection

Plasma Plume

Ejected Metal



Frame 6
Expulsion

Frames 1-5 taken in order, but not in sequence, from series of 12 frames showing welding of 1/4 inch 2219-T87. 10.5 kW on work at 85 ipm. Magnification 7X (approximately). Film speed was 140 fps.

Figure V-53. HIGH SPEED MOTION PICTURE SEQUENCE
OF ALUMINUM CAVITY INSTABILITY

- 2) As the process moves, Fig. V-53, frame 2, melting to the side takes place behind the beam impingement point. At process speeds of 100 ipm it is unlikely that this is entirely due to conduction melting from the beam. The strong plasma plume that characterizes aluminum welding may be acting as a powerful, but diffuse, source of heat. The super heated aluminum at the rear of the cavity may be giving up enough energy to contribute to melting.
- 3) The extension of the melt zone may catch up to the impingement point and the melting condition may move ahead of the beam (Fig. V-53, Frame 3), surrounding the impingement point with a volume of molten metal.
- 4) The volume of metal surrounding the beam then disappears leaving a bowl shaped cavity. Often the cavity extends through the plate illumination that comes from below as the beam strikes the tooling (Fig. V-53, Frame 4). Momentarily the beam may drop through the drainage hole and all heating ceases. A post weld inspection of the underbead will show cascades of solidified metal slightly to the rear of the bowl. Thus drainage, not expulsion, is suggested as the principle action during bowl formation.
- 5) The wide, curved surfaces of the bowl appear to act as a reflector for the beam. As the process moves forward it reengages the front surface of the bowl. This surface turns the vertical beam 90° and directs it into the molten metal pool at the rear of the bowl (Fig. V-53, Frame 5). Frame 5 shows an unusually well directed impingement with the attendant plasma plume jetting forward from the rear face of the bowl. Radial pressure from these rearward beams occasionally blasts metal from a significant length of joint. (See Frame 6 which comes from a later series of events than Frames 1 - 5).

These observations were made in a chamber filled with still, pure helium. The procedures are shown in Table V-16.

In this program it was possible to determine that problems associated with the aluminum procedure stemmed from a basic cavity instability. Therefore, procedure development for aluminum was extended, within the scope of the contract, to determine if special, practical approaches to any of the common welding variables could reduce instability (without introducing other weld quality problems). The resulting observations are listed below.

Effect of Gasses - Helium increases the severity and frequency of the instability. The addition of up to 30% argon, reduces the frequency of the phenomenon but not the severity. Oxygen in the form of air or oxidizing gasses such as CO₂ produces a uniform bead. The mechanism appears to relate to the formation of an oxide film on the molten pool and at the underbead. No instabilities were observed in six inches of weld but it cannot be concluded that none would occur if several feet could have been welded. Air and CO₂ introduced severe random porosity suggesting the presence of moisture or other sources of hydrogen. Oxygen damaged hoods.

Power - Metal would stay in the weld if marginal power settings were used. However, such welds exhibited a large number of voids. The regular spacing of the voids, suggests that they are vapor pockets. These pockets are often observed in partial penetration joints.

Gas Purity - All gas piping was converted to brazed metal construction. This would eliminate moisture pickup as a result of diffusion through the walls of plastic hose. There was no change in the voids observed at low power levels. This points to vapor pockets from incomplete penetration as their source. The piping had no effect on instabilities.

Underbead Pressure - Pressure was reduced under the weld in an attempt to stabilize the lower opening of the cavity. This might permit welding at a lower total power. Low power welds did not seem as susceptible to instabilities. Additionally, it was hoped that the differential pressure would pull the plasma through the cavity. Accordingly 3/8 inch thick

	266A	266B	266C
Power (KW) (on work)	11.2	11.2 - 9.1	10.2
Focus (inches)	28-1/16	28-1/16	28-1/8 - 27-31/32
Optics	F/7	F/7	F/7
Speed (ipm)	80 - 90	87	87
Shielding ⁽¹⁾	He	He	He
Photography Camera Speed Lens Setting Lighting	Milichron 300 Frames F/8 Tungsten		

- (1) A vacuum pumped and backfilled chamber was used for these experiments. Visual examination of titanium test pieces welded just prior to the aluminum indicate a gas purity of 99.999 (approximately). The box was used so that footage for the motion picture report could be obtained and the weld would not be obscured by a local jet trailer or hood-type shield.

Table V-16. WELDING PROCEDURE FOR INSTABILITY
ANALYSIS OF ALUMINUM WELDING PROCEDURE

plates were welded with a 9.8 KW process at 55 ipm with a 15 psig pressure differential. A diffuse flow of 70/30 He/A shielding gas was used. The top surface of the weld was not narrowed. If its width is a function of the plasma intensity above the weld, then the plasma was not shifted into the weld by placing a pressure differential across the cavity. The undersurface was very uniform, but an excessive amount of metal had been forced below the plate as the pressure differential worked on the molten weld pool. Instabilities were eliminated compared to similar welds without the pressure differential. This solution is not a practical one however, because the metal is forced out of the joint, and thus does not fit into the context of this program.

Back Up Strip - A strip was tacked to the underside of the weld to support metal. All involved surfaces were scraped to remove oxide. Good set up was hard to achieve but 3/8 inch thick plates were welded at 40 ipm using maximum available power on the surface (12.6 KW for the F/7 optical system). Contours improved but porosity formed in the weld just above the top of the strip. This approach might be improved for special applications where the underbead strip was not objectionable or could be machined away. It was too specific for this program.

Plasma Manipulation - An attempt was made to apply, within the hood type shield, a small jet. This jet would blast helium of the plasma plume as it emerged from the cavity and before it could cause melt back. There was some narrowing of the weld but the action of the jet of helium from a hypodermic needle inside the hood (or in a helium filled dry box) caused considerable turbulence, which masked observations dealing with the instabilities. Uniform beads were obtained when operating the jet without a shield. However, the color of the weld indicated that the principle effect was from oxide formed by inspired air. Proper conduct of jet experiments would require design of a nozzle and shield that were compatible. Shield design is not part of procedure development and is therefore beyond the scope of the program.

Focus - During several of these tests careful evaluation of the optimum focus occurred. As focus was moved out of the work it appeared that the frequency of the instabilities decreased slightly. However, the number was still excessive within any useable focal range.

The extended investigation of procedure variables failed to eliminate the incidence of instabilities in aluminum welds. The problem appears to relate to the interaction between the beam and the aluminum. It has some of the characteristics of the overwelding, intermittent dropout problem encountered in thick nickel base alloys. Because of the characteristic behavior of aluminum, no procedure could be developed with which to make tests.

SECTION VI

CONCLUSIONS

As a result of this program, laser CO₂(CW) welding appears to be a high-speed, low-distortion process that should be considered for the manufacture of aerospace structures wherever the special capabilities of laser are called for. This conclusion is supported by a number of program findings and is subject to certain limitations that also came out of the program.

A. ADVANTAGES

Twelve procedure development efforts were included in the program. Where procedures could be developed to produce sound welds, the following conclusions can be drawn in support of CO₂(CW) welding.

- 1: Low levels of porosity were achieved wherever proper shielding was applied. Distance between detachable pores ran from 6 inches for thick plates to 24 inches (or more) for 1/4 inch plates.
- 2: Useable thicknesses of 0.5-0.6 inch could be penetrated in a single pass.
- 3: Welding speeds were high compared to arc or plasma welding. They were typically:
 - 30 ipm on 1/2 inch thick joints
 - 60 ipm on 3/8 inch thick joints
 - 100 ipm on 1/4 inch thick joints
- 4: Distortion was low. When measured on welds made between flat ground 1/4 inch thick stock (carbon steel):
 - Transverse Distortion - 0.30°
 - Longitudinal Distortion - 0.01°

- 5: Upon mechanical testing, sound laser weld performance was very close to that of base metal reference tests. Laser welds tested for their fracture toughness exceeded base metal performance and fell in the upper portion of the data taken from other experiments.
- 6: Laser welds in carbon steel were tested for resistance to fracture in the presence of a precracked notch and exhibited unusually high K_{ISCC} values.
- 7: Laser welding had some attractive operational features:
 - Tolerance for gaps as large as 0.02T
 - Ability to be repaired by simple refusion
 - Need for only simple butt weld geometry

B. LIMITATIONS

In the course of process development some limitations were observed. These were:

- 1: Failure of the aluminum alloy to respond to development effort. A number of special variables were explored including:
 - Mechanical scraping to lift oxide off surface
 - Use of metal gas delivery lines
 - Application of underbead pressure
 - Back up strip
 - Plasma manipulation through jets
 - Critical control of power, speed, and focus
 - Use of Argon rich helium gas mixtures
 - Use of Oxidizing gasses air, CO_2 and O_2

Many elements of the problem were eliminated by the argon rich shielding gas mixture applied so as to minimize disturbance of molten metal. Conventional gas metal reaction porosity was prevented by the metal gas delivery lines and scraping. None of the above could prevent excessive melting to produce a

puddle and periodic loss of puddle to produce a void in the bead (when weld length is defined as greater than 12 inches).

- 2: Failure of the 1/2 inch thick nickel base alloy to respond to extensive procedure development though all other program thicknesses responded readily. Several special procedure variables were explored including:

- Critical control of power, speed and focus in order to find a welding procedure that fell between marginal penetration (on one hand) and metal drop-out on the other. No such range was observed for this particular thickness of nickel base alloy though it was readily obtained in 3/8 inch and 1/4 inch alloy (and in all other program materials except aluminum).
- Chills did not alleviate the metal drop-out problem. In the overwelding situation, where drop out is observed, enough energy from the beam exits from the bottom of the cavity to interact with the chill material if it is placed so as to catch and support the molten metal.

- 3: Requirement of full hood shielding for titanium alloys. Careful post welding analysis of titanium welds shielded by helium jets and argon trailers revealed evidence of micro contamination in a region of the weld cross section which represented the upper lip of the cavity.

No other significant limitations on the CO₂(CW) process were observed.

C. ELEMENTS OF TECHNOLOGY

A number of practical welding variables were systematically reviewed and certain conclusions as to their use in a welding procedure can be drawn as follows:

1: Reflectivity as a Factor in Multikilowatt Welding

The effectiveness of the cavity as a light trap is suggested by the 7% reflectance measurements observed for all program materials except aluminum, which exhibited 14% reflectivity.

2: Surface Finish as a Factor in Multikilowatt Welding

It did not appear that the condition of the surface of a plate had a significant affect on the ability of the plate to absorb beam energy.

3: Shielding Gasses for Laser Welding

Helium permitted the best penetration - twice the penetration observed in still air for a given set of welding conditions. Argon seemed to react with the beam (perhaps by formation and maintenance of a plasma) and inhibited penetration. Helium did not provide perfect blanketing of the weld in difficult shielding situations. When shielding was less than perfect, additions of 10% argon improved blanketing with no significant loss of penetration. Mixtures of 30% argon with helium usually resulted in some loss of penetration.

At 50% argon concentration (in helium), shield damage was frequent unless welding speed kept the welding cycle very short. Thus, the limiting amount of argon seemed to fall between 30 and 50% with little to be gained from concentrations over about 10%.

Other gasses such as CO_2 , O_2 , and H_2 were evaluated and the results reported.

4: Gas Shield Tooling for Laser Welding

The following methods for delivery of gas to the upper surfaces of the weld were explored and their recommended use determined:

- Off-Axis GTA Nozzle - Low speed welding in nickel base alloys and carbon steel alloys
- Jet-Trailing Hood Shields - High speed welds in nickel base and carbon steel alloys.
- Full Diffusion Shield - Required for all aluminum and titanium welding
- Manifold Shielding - Potentially useful in restricted areas for all materials in the program.

5: Methods for Controlling Underbead Geometry and Drop Through

Full penetration laser welding procedures for 1/4 inch thick plates of aluminum, nickel base alloy, titanium, stainless steel, and carbon steel resulted in an underbead that was 0.05-0.75 inches wide (except aluminum which was 0.1 inches wide). Typically this underbead projected 0.02 inches below the plate.

5a: Chill Spacing

Chill contact spacing at least 250-350% wider than the underbead reduced the angle between the plate and the underbead projection to about 30°.

Carbon and stainless steels exhibited sharper angles as chill spacing was increased to 500% of plate thickness. Materials such as the aluminum, nickel base alloys, and titanium maintained a 30° angle between plate and underbead regardless of chill spacing as long as the chills were spaced at least 250-350% of the plate thickness. Proper chill spacing definitely results in reduced mechanical notch effects, as defined by angle, for laser welds.

Changing the position of the focal point in the plate did not change the angle between the underbead and the plate.

5b: Backstop Tooling

Backstop tooling appeared to represent a means for protecting other workpiece surfaces from the exiting beam but otherwise exercised no effect on underbead size or contour. Surfaces within 1/8 inches of the underside of welds should be protected against molten metal exiting from the underside of the weld. In the presence of a beam stop material placed closer than 1/8 inch, focus becomes more critical and this should be taken into account when considering tooling changes that will effect the placement of beamstops.

5c: Underbead Gas Pressure

Underbead gas pressure will control underbead contour. Aluminum is very sensitive to underbead pressure. If pressure is varied far enough, the metal will be blown upward out of the joint and under fill would result. If gas pressure was controlled by the tooling, drop through could be eliminated.

6: Selection of F/No., Focus, Speed, Power and Incidence Angle

When the latitude for focal position within the workpiece was compared with respect to F/7 and F/21, the latter telescope (high F/No.) was observed to have more than twice the latitude. Within this range, cross-sections of those welds made at slight underfocus have the straightest sides. Welds with curved sides and with a pinched cross-section often result in cracking during solidification.

There was no evidence that changing the impingent angle of the beam on the plate affected the penetrating ability of the beam.

When welding speeds were forced below about 30 ipm in order to penetrate 1/2 inch material, the welding process became conduction dominated and began to approach an arc weld in appearance.

7: Maximum Single Pass Thickness

The following joint thicknesses represent the current maximum penetrating capability of the HPL industrial laser at 15 Kw (13.5 Kw on the work) when an F/21 optical system is used:

Carbon Steel:	$0.6 \pm .005$ inches
Titanium:	$0.6 \pm .005$ inches
Nickel Base Alloy:	$0.57 \pm .005$ inches
Stainless Steel (AISI 321):	$0.544 \pm .005$ inches

Aluminum was tested at slightly lower power (13 Kw on the work) to conserve the diffuser hood. The maximum thickness penetrated at 50 ipm was:

Aluminum:	$0.5 \pm .005$ inches
-----------	-----------------------

SECTION VII

RECOMMENDATIONS

The success achieved during this program suggests that applications be identified for laser welding in aerospace structures. Any one, or a combination of, the following characterize a candidate application:

- . Need for fast single pass fusion welding
- . Emphasis on low distortion in large weldments
- . Special access problems during welding
- . Critical toughness or corrosion requirements
- . Possibility for sharing any of the above advantages over several operations in one shop.
- . Possibility for more cost effective components by redesigning to take advantage of one of the above characteristics

Techniques that employ the low angle reflection of laser beams should be developed for welding stiffeners, flanges and couplings rapidly, with a minimum of distortion, and with high reliability.

Additionally, programs should be developed to lift the process limitations observed in this program so as to extend the benefits of welding to all aerospace structures and materials.

1. The highest priority should be placed on overcoming the inability of aluminum to respond to high power welding beams. What is required is improved penetrating efficiency for the laser beam with less melting.

2. Similar, advanced, optics should be applied to the nickel base alloy to place greater emphasis on penetration and less on melting. Again, the program should emphasize thick plate where the problem of excessive melting and metal drop-out is most severe.

Small programs aimed at isolating and confirming some of the observations in this program should be undertaken. These include:

1. Statistical confirmation of the apparently attractive toughness and corrosion properties of laser welds. Such programs should consider the use of several heats of the base metal, testing in more than one facility to obtain reference data useful to the designer in critical applications if the full advantage of laser welds is to be realized.
2. Moving-beam focus stability studies, as opposed to the single point studies of weld cross-sections applied in the early part of this program.

REFERENCES

- IV-1 Woods, R.A., Porosity & Hydrogen Absorption in Aluminum, Welding Research Supplement, Welding Journal, March, 1974, p. 97-S.
- IV-2 Gorman E.F., "New Developments in Gas Shielding", Welding Journal, October, 1972.
- IV-3 Hella, Locke, and Ream "Industrial Laser Welding Evaluation Study" prepared by Avco Everett Research Laboratory, Everett, Mass., NASA Contract NAS8-28610 Marshal Space Flight Center, Nov., 1974.
- V-1 "Results of Fatigue Tests on Steel", Communication AFML/LTM to F. Seaman 26/FEB/76.
- V-2 "Effects of Processing Variables on Stress Corrosion Cracking in 9Ni-4Co Steel Alloy", AFML-TR-66-388, December, 1966.
- V-3 Swift-Hook and Gick, "Penetration Welding with Lasers", Welding Journal, Research Supplement, Nov., 1973, p.492.
- V-4 Breinan and Banas "Evaluation of Basic Laser Welding Capabilities", Office of Naval Research, Contract N00014-74-C-0423, United Technologies Research Center, East Hartford, Conn. 06108.

APPENDIX A

MILITARY SPECIFICATION
(TENTATIVE) WELDING,
FUSION, LASER BEAM,
(WITH ATTACHED SAFETY
AND MAINTENANCE
REQUIREMENTS FOR A
MULTIKILOWATT LASER)

MILITARY SPECIFICATION (TENTATIVE)

WELDING, FUSION, LASER BEAM, PROCESS FOR

PART I

1. SCOPE. This specification establishes processing requirements for the use of continuous wave CO₂ laser beam for fusion welding of metals and alloys.

1.1 Applicability. Processing requirements defined by this specification will result in welds or weldments joined by laser beam fusion welds of the quality specified herein. Processing does not include any subsequent thermal or other treatment required to optimize weldment mechanical properties.

2. APPLICABLE DOCUMENTS. The following documents of the issue in effect on the date of invitation for bids or request for proposal form a part of this specification to the extent specified herein.

2.1 Government Documents

MILITARY SPECIFICATIONS

MIL-S-5002	Surface Treatments and Metallic Coatings for Metal Surfaces of Weapon Systems
MIL-T-5021	Tests; Aircraft and Missile Welding Operators' Qualification
MIL-I-6866	Inspection, Penetrant, Method of
MIL-I-6868	Inspection Process, Magnetic Particle
MIL-I-6870	Inspection Program Requirements, Non-Destructive Testing for Aircraft and Missile Materials and Parts
MIL-H-6875	Heat Treatment of Steels (Aircraft Practice), Process for
MIL-A-18455	Argon, Technical
MIL-P-27407	Propellant Pressurizing Agent, Helium
MIL-I-25135	Inspection Material, Penetrant (ASG)
MIL-H-81200	Heat Treatment of Titanium and Titanium Alloys

2.1 (Cont'd)

MILITARY STANDARDS

MIL-STD-105	Sampling Procedures and Tables for Inspection by Attributes
MIL-STD-453	Inspection, Radiographic
MIL-STD-779	Reference Radiographs for Steel Welds

(Copies of specifications, standards, drawings, and publications required by suppliers in connection with specified procurement functions should be obtained from the processing activity or as directed by the contracting officer.)

2.2 Non-Government Documents

American Society for Testing and Materials

ASTM-164	Ultrasonic Contact Inspection of Weldments
ASTM-273	Ultrasonic Inspection of Longitudinal and Special Welds of Welded Pipe and Tubing

American Welding Society

AWS A 3.0	Definitions - Welding and Cutting
-----------	-----------------------------------

ANSI-Z-136.1	American National Standard For the Safe Use of Lasers
--------------	---

(Technical society and technical association specifications and standards are generally available for reference from libraries. They are also distributed among technical groups and using Federal agencies.)

3. REQUIREMENTS

3.1 EQUIPMENT: The source of beam energy shall be a CO₂ continuous wave laser. The power of the beam shall be controlled by a closed loop system which continuously monitors output power during the entire welding cycle. Power shall be maintained to $\pm 3\%$ of the preset value. Equipment shall be constructed to existing federal and state regulations.

3.1.1 The operation of the laser system, including tooling and beam handling sub-systems shall comply with existing state and federal regulations. Where such regulations have not been enacted, operation shall be in accordance with ANSI Standard, ANSI-Z-136.1

3.1 (Conf'd)

3.1.2 Qualification. The operating capability of the welding equipment shall be established by demonstration of acceptable welding performance. Establishment of production welding procedures and equipment schedules in accordance with requirements of the applicable paragraphs shall be considered a suitable demonstration of acceptable welding performance.

3.1.2.1 The welding equipment shall be requalified after any significant repair or maintenance service involving those parts of the equipment used for the generation (i.e. laser cavity), alignment (i.e. mirrors, or any instrumentation used in the control or concentration of the laser beam power.

3.1.3 Jigs and Fixtures. All work piece holding fixtures shall be capable of holding parts in proper alignment, maintaining desired configuration and tolerances during welding, and providing back-up as required. "Back up" material used to absorb residual laser beam energy shall be of the same alloy (nominal chemical composition) as the part being welded.

3.2 Materials

3.2.1 Welding Shield Gases. Gas used for weld joint shielding shall be in accordance with the following:

Argon MIL-A-18455
Helium MIL-P-27407

3.2.2 Equipment (Laser) Gases. Gases used for the purpose of generation of the laser shall be in accordance with manufacturer's instructions.

3.2.3 Welding Filler Metal. Welding filler metal shall be in accordance with requirements specified on the applicable engineering drawing.

3.3 Equipment Operators. Laser beam welding equipment operators shall be qualified in accordance with procedures established in MIL-T-5021.

3.4 Classification of Weld Joints. The responsible weldment design contractor shall classify and grade each laser beam weldment or weld in accordance with requirements established by MIL-I-6870.

3.4.1 Class.* Class refers to functional reliability requirements of the weldment or weld and implies a confidence level requirement for non-destructive testing. A high reliability class may require redundant testing to assure an adequate NDT confidence level.

*From MIL-I-6870C

3.4 (Cont'd)

3.4.2 Grade.* The grade of a weldment or weld is a measure of quality level and implies a defect sensitivity requirement for NDT. The grade is defined in terms of defect size, location, type, and frequency which are acceptable. High and low stress areas on the same weldment or component can have different grade levels. The grade level shall be based on the acceptable defect limits.

3.5 Weld Joint Design. Unless otherwise specified by the applicable engineering drawing, laser beam welding joint design shall be in accordance with the following: See Figure 1 for descriptive illustration.

3.5.1 Joint Details. Mating surfaces of joint details shall have a surface finish not rougher than 125 rms.

3.5.2 Joint Gap. Mating surfaces of joint details shall fit together so that open gaps in the joint, assembled for welding will not exceed 2 per cent of the joint thickness.

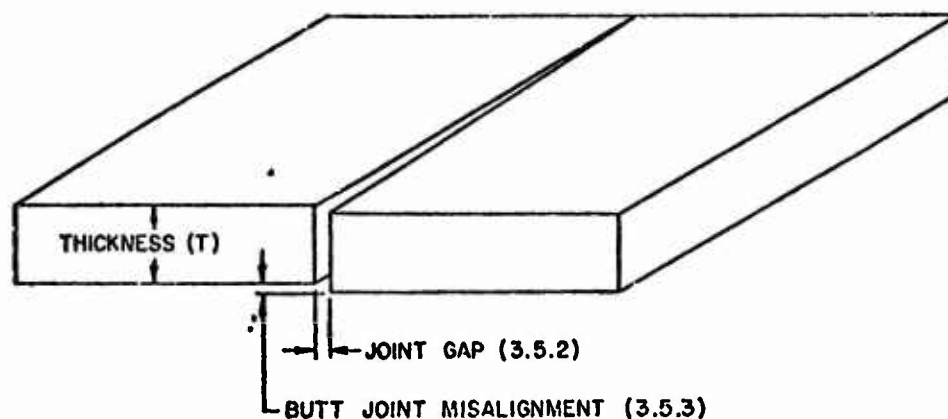


FIGURE 1. JOINT DESIGN DETAILS

*From MIL-I-6870C.

3.5 (Cont'd)

3.5.3 Misalignment of Butt Joints. Misalignment of the butting edges of sheet or plate in a butt weld shall not exceed the following where "T" is the thickness of the thinnest member.

- (1) Material thickness .010" to .100"
0.004" or 15% T whichever is greater
- (2) Material thickness .101" to .199"
0.020" or 15% T whichever is smaller
- (3) Material thickness .200" and thicker
0.030 or 10% T whichever is smaller

3.5.4 Weld Penetration of Butt and Lap Joints. Weld joint penetration shall be a minimum of 100 per cent of the material thickness for all butt and lap type joints.

3.6. Required Procedures and Operations

3.6.1 Cleaning

3.6.1.1 Equipment and Fixtures. Equipment and fixtures adjacent to or directly influential in the resulting compositional quality of a laser weld shall be cleaned to remove all oils, greases, dirt, or any other contaminating substances prior to welding assembly and so maintained until completion of the welding operation.

3.6.1.2 Joint Details. Detail joint components shall be cleaned in accordance with requirements specified in MIL-S-5002 before assembly for welding and so maintained until the completion of the welding operation.

3.6.2 Assembly for Welding. Joint detail components shall be assembled as required by the applicable engineering drawing.

3.6.2.1 Tack Welding. Tack welding (any welding process) to maintain joint component alignment is permissible provided all effects of the tack weld are obliterated by subsequent laser beam welding and is a required operation of the authorized welding procedure.

3.6 (Cont'd)

3.6.3 Production Welding. Production laser beam welding shall be performed in accordance with an authorized welding procedure established by procedures specified in 3.6.4.1. The authorized welding procedure shall specify the sequence of each application of laser beam power, the specific schedule of equipment adjustments (3.6.4.2) for each application, as well as all other parameters influential in the resulting weldment quality, metallurgical structure, and/or mechanical properties. Figure 2 is a suggested format for the recording of a laser beam welding procedure.

3.6.4 Establishing Welding Procedures and Equipment Adjustments

3.6.4.1 Welding Procedure. A laser beam welding procedure shall be established by demonstration of acceptable manufacture. The welding procedure shall be considered approved if two consecutive production weldments made in accordance with all details of the procedure are in compliance with the requirements of the engineering drawing and this specification (3.7), when inspected at levels specified for Class 1A weldments (see 4.1.1) and the applicable quality grade level.

LASER BEAM WELD PROCEDURE No. 307

PAGE 2 OF 2 PAGES

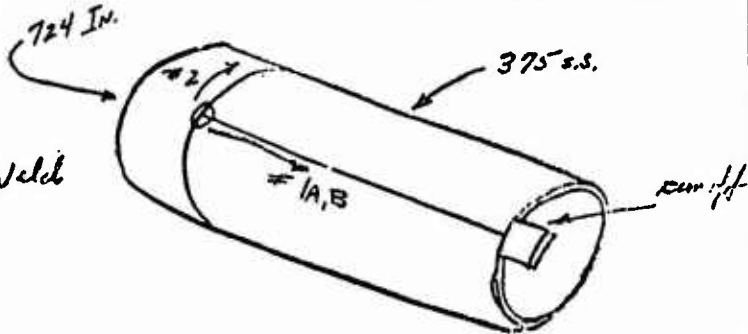
WELDMENT Blanching
 ENG. DWG. NO. 116C-301
 MATERIAL 705 SS - 92.4
 HEAT TREATMENT None
 LASER EQUIPMENT CW/02 Seely 8.15 X8
 SERIAL NO. 11601
 STATION NO. 007 (F-7)
 TELESCOPE SERIAL NO. 11601
 GAS SHIELD SERIAL NO. 11601
 WELD FIXTURE DWG NO. 11601

DATE September 9, 1975
 OPERATOR W. J. 9-9-75
 SUPERVISOR W. J. 9-9-75
 QUALITY ASSURANCE W. J. 9-9-75

WELD SEQUENCE SKETCH & DETAILS:

START	DIRECTION
WELD	POSITION
1	1
2	2
3	3

note: TIG tack weld before laser weld
 1/2" tack on 12" center
 no filler wire



LASER WELD PASS NO. 1A 1st
 PURPOSE: TACK WELD, PENETRATION, COSMETIC,
 PRE-HEAT, POST-HEAT, FILLER,
 OTHER
 EQUIPMENT ADJUSTMENTS:
 LASER POWER START DELAY 2.00 SECS.
 START 12.5 SLOPE TIME 0.5 SECS.
 RUN 9.1 10% TACK WELD TIME 11 SECS.
 STOP 2.5 DECAY TIME 2.5 SECS.
 FOCUS DIMENSION 2.5 INCHES

JOINT THICKNESS 0.375 HEATING METHOD
 PREHEAT TEMP. < 100 F
 INTERPASS TEMP. None
 POSTHEAT TEMP. None
 JET GAS TYPE Helium CFM 4.0
 SHIELD GAS TYPE Helium CFM 1.0
 TRAVEL SPEED 0.5 INCHES/MIN.
 TRAVEL START DELAY 0.5 SECONDS
 WIRE FEED MATERIAL None
 WIRE DIAMETER None INCHES
 FEED RATE None INCHES/MIN.

LASER WELD PASS NO. 1B 2nd
 PURPOSE: TACK WELD, PENETRATION, COSMETIC,
 PRE-HEAT, POST-HEAT, FILLER,
 OTHER
 EQUIPMENT ADJUSTMENTS:
 LASER POWER START DELAY 2.00 SECS.
 START 12.5 SLOPE TIME 0.5 SECS.
 RUN 9.1 10% TACK WELD TIME 11 SECS.
 STOP 2.5 DECAY TIME 2.5 SECS.
 FOCUS DIMENSION 2.5 INCHES

JOINT THICKNESS 0.375 HEATING METHOD
 PREHEAT TEMP. < 200 F
 INTERPASS TEMP. None
 POSTHEAT TEMP. None
 JET GAS TYPE Helium CFM 4.0
 SHIELD GAS TYPE Helium CFM 1.0
 TRAVEL SPEED 0.5 INCHES/MIN.
 TRAVEL START DELAY 0.5 SECONDS
 WIRE FEED MATERIAL None
 WIRE DIAMETER None INCHES
 FEED RATE None INCHES/MIN.

LASER WELD PASS NO. 1C 3rd
 PURPOSE: TACK WELD, PENETRATION, COSMETIC,
 PRE-HEAT, POST-HEAT, FILLER,
 OTHER
 EQUIPMENT ADJUSTMENTS:
 LASER POWER START DELAY 2.00 SECS.
 START 12.5 SLOPE TIME 0.5 SECS.
 RUN 9.1 10% TACK WELD TIME 11 SECS.
 STOP 2.5 DECAY TIME 2.5 SECS.
 FOCUS DIMENSION 2.5 INCHES

JOINT THICKNESS 0.375 HEATING METHOD
 PREHEAT TEMP. < 200 F
 INTERPASS TEMP. None
 POSTHEAT TEMP. None
 JET GAS TYPE Helium CFM 4.0
 SHIELD GAS TYPE Helium CFM 1.0
 TRAVEL SPEED 0.5 INCHES/MIN.
 TRAVEL START DELAY 0.5 SECONDS
 WIRE FEED MATERIAL None
 WIRE DIAMETER None INCHES
 FEED RATE None INCHES/MIN.

FIGURE 2 : WELD PROCEDURE FORMAT WITH EXAMPLE PROCEDURE

3.6.4 (Cont'd)

3.6.4.2 Equipment Adjustments. A schedule of equipment adjustments shall consist of a tabulation of all adjustments directly involved in the generation, concentration, and quantity of power and/or temperature imposed on the workpiece. An allowance of ± 10 per cent of the power contained in the laser beam shall be available to compensate for processing variables. Equipment schedules for an authorized laser beam welding procedure shall be established in accordance with the following:

3.6.4.2.1 Test Specimen. A laser beam weld joint test specimen, using the same material (nominal chemical composition and heat treatment) as the production pass shall be produced for each separate application of laser beam power required to produce the desired weldment. If an application of laser power is to be imposed on top of a previous pass, the specimen representing the second application shall include the previous laser weld pass or passes. If tack welding (by any welding process) is required to produce the production weldments, the specimens shall include the tack welds.

3.6.4.2.2 Specimen Configuration. The specimen weld joint shall be no less than 16 inches in length. Specimen dimensions shall not be less than 18 inches long by 4 inches wide by the thickness of the joint to be welded. The weld length and test specimen dimensions may be reduced to the dimensions of the production weldment if it is smaller. Duplication of curvature or configurational detail is optional unless those features are influential in the determination of the equipment settings.

3.6.4.2.3 Specimen Requirements. A schedule of equipment adjustments shall be approved for an authorized welding procedure if the test specimen weld is in compliance with all applicable requirements (3.7) of this specification when nondestructively inspected at levels established for Class 1A weldments (4.1.2), the applicable quality grade level, and 3.6.4.2.4, 3.6.4.2.5, and 3.6.4.2.6, if applicable.

3.6.4.2.4 Specimens Thicker than 3/8 Inch. Test specimens representing weld joint thicknesses greater than 3/8 inch shall also be destructively inspected for compliance with applicable requirements. Destructive evaluation shall be in accordance with procedures specified in 4.3.

3.6.4.2 (Cont'd)

3.6.4.2.5 Heating Pass Specimens. Test specimens representing the application of a laser beam for heating purposes shall show no evidence of melting, phase changes, recrystallization or crystallographic growth. Visual inspection methods (4.1.2.1) shall be used to establish the presence or absence of melting. Metallographic polishing and acid etching of the specimen surface shall be used to aid in establishing whether metallurgical changes have occurred.

3.6.4.2.6 Weld Penetration and Configuration. Specimens representing weld requirements (less than 100% or special configurations) not inspectable except by destructive sectioning, shall be evaluated as required by 4.3.2.

3.7 Weld Joint Attributes. Unless otherwise specified by the applicable engineering drawing, laser beam welds shall be in compliance with the following: See Figure 3 for descriptive illustration.

3.7.1 Weld Bead Widths. The width of a laser weld bead shall not exceed the following:

WELD PENETRATION DEPTH (P) OR PART THICKNESS (T) FOR THRU WELDS	WELD BEAD WIDTH		
	PENETRATION BEAD	COSMETIC BEAD	FILLER BEAD
LESS THAN 0.125"	1 X (P OR T)	3/2 X (P OR T)	3/2 X (P OR T)
0.125" TO 0.250"	1/2 X (P OR T)	1 X (P OR T)	1 X (P OR T)
GREATER THAN 0.250"	2/3 X (P OR T)	3/2 X (P OR T)	3/2 X (P OR T)

3.7.2 Weld Reinforcement

3.7.2.1 Face Side of Weld. Weld reinforcement on the face side of the weld bead shall not exceed 25 per cent of the weld bead width.

3.7.2.2 Root Side of Weld. Weld reinforcement on the root side of the weld bead shall not exceed 1.0 times the width of the bead at the root.

3.7.2.3 Cosmetic and Filler Weld Beads. Weld reinforcement for any cosmetic or filler pass weld beads shall not exceed 20 per cent of the joint thickness or .060 inch whichever is the smaller.

3.7 (Cont'd)

3.7.3 Undercut or Underfill Undercut or underfill are acceptable if not in excess of 10 per cent of the joint thickness or 0.010" whichever is the smaller and all edges of the weld or undercut are not sharp. This definition is applicable to both face and root side of the weld joint cumulatively (10% total).

i.e. If maximum allowable undercut is measured on one side of joint, no undercut is permissible on the other side.

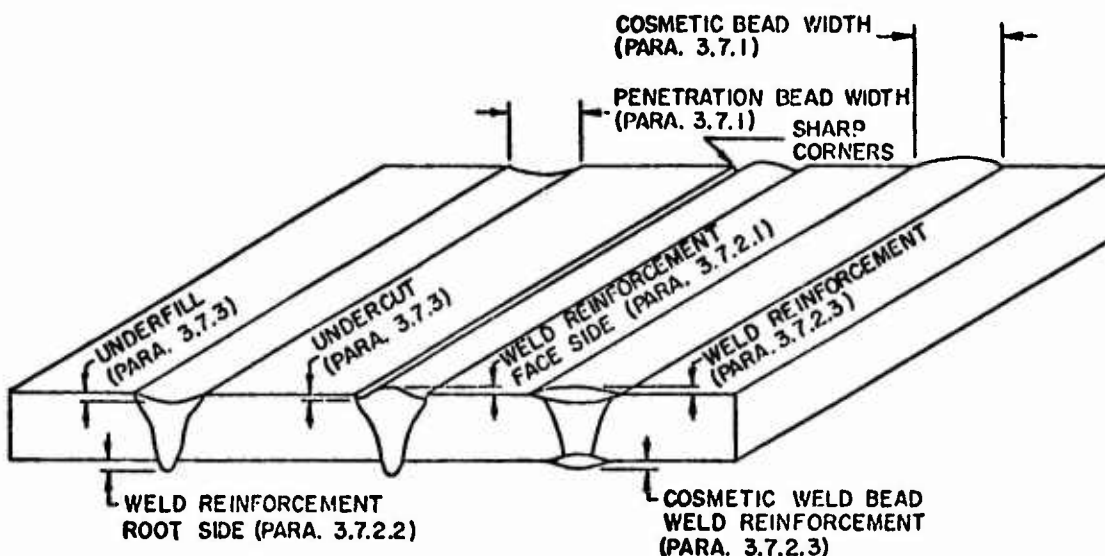


FIGURE 3. WELD JOINT CHARACTERISTICS

3.7.4 Weld Coloration for Titanium Welds. The weld bead and adjacent base metal heat affected zone shall be a bright silver to a light straw color. Darker coloration from a dark straw to dark blue or blue black is not acceptable. The presence of gray scale is also not acceptable.

For purposes of determination of titanium weld and heat affected zone coloration, the heat affected zone shall be considered as starting at the fusion line of the weld and extending 1/64 inch or 15 per cent of the weld bead width whichever is the larger.

Titanium welds that have been wire brushed, buffed, rewelded, sanded, filed, etched, etc. before evaluation of weld coloration shall be rejected.

3.7 (Cont'd)

3.7.5 Cracks. Cracks are not acceptable in the weld, heat affected zone, or adjacent base metal.

3.7.6 Laps or Cold Shuts. Laps or cold shuts are not acceptable.

3.7.7 Lack of Fusion. Lack of fusion is not acceptable.

3.7.8 Lack of Penetration. Lack of penetration is not acceptable.

3.7.9 Porosity, Voids and Inclusions. Acceptable or rejectable levels of porosity, void, or inclusion type of internal discontinuities shall be established by the grade of weld or weldment required. The grade shall be established in accordance with 3.4. Table I is a tabulation of four (4) grade levels of quality. Unless otherwise specified, porosity, voids, or inclusion type discontinuities occurring in the weld metal shall not be in excess of the occurrence and frequency shown by the referenced radiographic standards specified for Grade B welds. Porosity, voids, and inclusions on the surface of the weld metal are not acceptable.

TABLE I
MAXIMUM ALLOWABLE INTERNAL WELD DEFECTS
Notes (1), (2)

Defect (Internal)	Grade A	Grade B	Grade C	Grade D
Porosity ⁽³⁾				
Fine, scattered	1	1	2	3
Coarse, scattered	1	1	2	3
Linear	None	None	1	2
Clustered	None	None	1	2
Inclusion, more dense ⁽³⁾	None	None	2	2
Inclusion, less dense ⁽³⁾	None	1	2	2

- Notes: (1) See reference radiographs in MIL-STD-779 (ASTM E390).
(2) Defects that will be removed by a subsequent machining operation shall not be a basis for rejection of the weldment.
(3) Porosity or inclusions with sharp tails shall be treated as cracks.

3. (Con't)

3.8 Repair Welding

3.8.1 Defects that will be removed by a subsequent machining operation shall not be a basis for repair welding.

3.8.2 Defects confined entirely within the fused weld metal, visually detected, may be reworked by rewelding once, using the established production welding procedure provided no further processing has been accomplished.

3.8.3 All parts which have defects in the base metal or at the base metal fusion line and those parts in which rejectable defects are detected by one or more nondestructive test methods shall be rejected and submitted to Engineering for disposition.

3.8.4 Discolored titanium weld beads shall not be rewelded for repair or any other purpose. The discoloration is a surface effect only, but indicates a contaminating condition during the welding operation. Once a titanium weld has been contaminated, the impurities cannot be removed regardless of the coloration of the weld after any subsequent treatment. Such welds shall be rejected for Engineering disposition.

3.9 Post Weld Thermal Processing. Post Weld thermal processing or heat treatment shall be in accordance with requirements specified on the applicable engineering drawing. If post weld heat treatment is not specified or specifically excluded, laser beam weldments will be processed as follows:

<u>Alloy Type</u>	<u>Post Weld Heat Treatment</u>
Titanium and alloys	Stress relieve at 1050 - 1100°F per MIL-H-81200A
Heat treat hardenable low alloy steels	Stress relieve at 1100 - 1150°F per MIL-H-6875
Unstabilized stainless steels	Anneal per MIL-H-6875

Note: Metals and alloys not included in this tabulation do not require any additional thermal processing except as specified by applicable engineering drawing.

4. QUALITY ASSURANCE PROVISIONS

4.1 Responsibility for Inspection. Unless otherwise specified in the contract or order, the supplier is responsible for the performance of all inspection requirements as specified herein. Except as otherwise specified, the supplier may utilize his own facilities or any commercial laboratory acceptable to the Government. The Government reserves the right to perform any of the inspections set forth in the specification where such inspections are deemed necessary to assure supplies and services conform to prescribed requirements.

4.1.1 Inspection. Laser beam welds and/or weldments shall be inspected as specified in an inspection program established in accordance with applicable requirements shown in MIL-I-6870.

4.1.2 Nondestructive Inspection. Laser beam welds or weldments shall be nondestructively inspected by the following inspection processes as required by Table II. If classification of a weld is not specified by applicable engineering drawing or the inspection program (see 4.1.1), non-destructive inspection shall be in accordance with requirements specified in Table II for Class IA welds.

4.1.2.1 Visual Inspection. Visual inspection consists of examination and/or measurements of surface attributes of the weld with or without the aid of magnification.

4.1.2.2 Magnetic Particle Inspection. Ferromagnetic welds or weldments shall be inspected for surface and near surface discontinuities in accordance with MIL-I-6868. Magnetizing by current carrying prods is forbidden.

4.1.2.3 Penetrant Inspection. Nonmagnetic and slightly magnetic alloy weldments shall be inspected for surface discontinuities in accordance with MIL-I-6866 and MIL-I-25135.

4.1.2.4 Radiographic Inspection. Inspection for internal discontinuities shall be performed by radiographic inspection in accordance with MIL-STD-453.

TABLE II
MINIMUM INSPECTION REQUIREMENTS (Per Cent of Weldments Inspected)

Inspection Method	Weld Class, Note (1)			
	Class IA (2)	Class IB	Class IIA	Class IIB
Visual	100	100	100	100
Magnetic Particle ⁽³⁾	100	100	2.5 AQL	4.0 AQL
Penetrant ⁽³⁾	100	100	2.5 AQL	4.0 AQL
Radiographic	100	2.5 AQL	4.0 AQL ⁽⁴⁾	---
Ultrasonic	100	2.5 AQL	(4)	---
Other Tests	100	2.5 AQL	---	---

Notes: (1) Classifications shown from MIL-I-6370. Where 100 per cent inspection is specified, each weld in all assemblies shall be inspected throughout its entire length. When AQL is specified, sampling shall be in accordance with MIL-STD-105 except that when a rejectable weld is found in a "lot" of assemblies, all welds in that lot shall be inspected.

(2) Applicable inspections shall be repeated after proof tests.

(3) Ferromagnetic parts shall be magnetic particle inspected. Slightly magnetic and nonmagnetic parts shall be penetrant inspected. Heat affected zones in parts showing magnetic particle indications shall be penetrant inspected to confirm external defects.

(4) Based on the geometry of the assembly, either ultrasonic or radiographic inspection, whichever will best reveal any critical defects, shall be used.

4.1.2.5 Ultrasonic Inspection. Manual contact, pulse echo, ultrasonic inspection of weldments with pertinent dimensions of 0.25 to 8.0 inches shall be performed in accordance with ASTM E164, where applicable. Contact or immersion inspection of longitudinal or spiral welds of welded pipe or tubing having nominal outside diameters from 2 to 36 inches and nominal thicknesses of 0.12 to 0.80 inches shall be performed in accordance with ASTM E273.

4.1.2 (Cont'd)

4.1.2.6 Other Nondestructive Tests. Other nondestructive tests may be specified where applicable, e.g., leak test, load or proof test, or acoustic emission monitoring test. When required, the test method and criteria for acceptance shall be defined on the component drawing or in the applicable document. Leak testing, if required, shall be performed prior to penetrant, magnetic particle, ultrasonic, or hydrostatic proof tests.

4.2 Equipment Calibration. All recording or indicating instrumentation involved in the control, generation, or concentration of the power contained in the laser beam shall be calibrated at intervals based on accumulated records of performance. The intervals between calibrations not to exceed 6 months.

4.3 Destructive Inspection of Test Specimens

4.3.1 Weld Thickness Greater than $3/8$ Inch. Section the test specimen as shown in Figure 4 to obtain six (6) randomly located $1/2$ inch wide test strips. Radiographically inspect each test strip axially through the weld to determine compliance with requirements specified in 3.7.5 through 3.7.9.

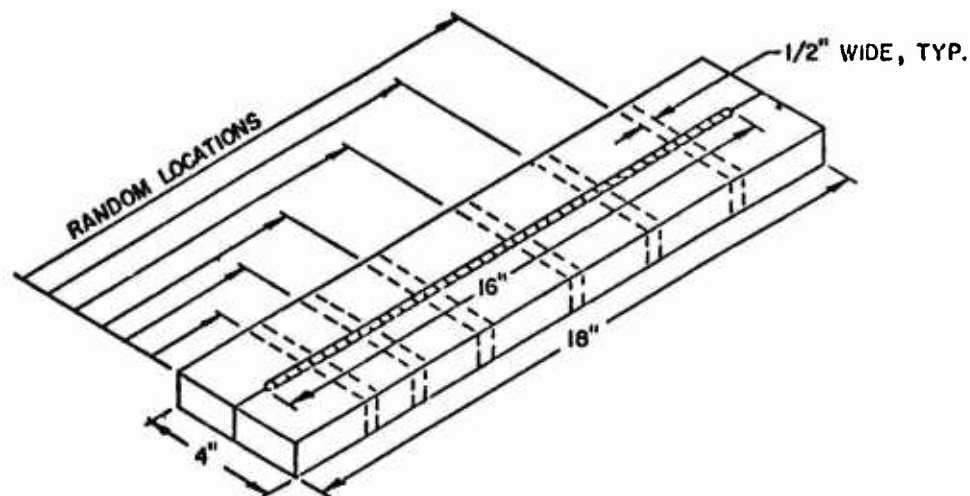


FIGURE 4. TEST SPECIMEN SECTIONING

4.3 (Cont'd)

4.3.2 Penetration and Configuration. Section the test specimen as shown in Figure 4 to obtain six (6) randomly located test strips (1/2" wide). Polish and etch one side of each test strip (one weld cross section) for macroscopic examination. Measure or examine to determine compliance with applicable requirements. For specimens requiring more than 3/8 inch or more depth of penetration, shall also be radiographically inspected axially through the weld to determine compliance with 3.7.5 through 3.7.9.

5. Definitions. Definition of all welding terms shall be as defined by American Welding Society Specification number AWS A3.0.

PART II

I LASER SAFETY STANDARDS

A) Light Emission Safety Standards

A review of laser safety standards has been undertaken with the following result: The Department of Labor - Occupational Safety and Health Administration (OSHA) has indicated that they will be publishing their Laser Use Standards in the Federal Register before January 1976, with the intention of these standards becoming a law effective about August 2, 1976. This will be the appropriate set of standards which must be met by any user of laser equipment. They further indicated that the content of this Laser Use Standard will be the safety standards established by the American National Standards Institute (ANSI) Z136.1, published in 1973. This is a laser safety standard which has been established for use of lasers which operate between 0.2 μ m and 1mm. Since this safety standard is the most likely standard to be incorporated into law, it is the one that has been analyzed for this report. The following summary of that report contains the salient features for CO₂ lasers.

1. Classification of Lasers

Class 1 - Exempt Lasers and Laser Systems

CO₂ Lasers which operate at a power level below 0.8×10^{-3} watts are in this category.

Class 2 Lasers - Low Power Visible Lasers and Laser Systems

Not applicable to CO₂ Lasers.

Class 3 - Medium Power Lasers and Laser Systems

CO₂ Lasers which can emit power less than 0.5 watts fall into this category.

Class 4 - High Power Lasers and Laser Systems

Any CO₂ laser system which emits power in excess of 0.5 watts is labeled as a class 4 laser.

Class 5 - Enclosed Lasers and Laser Systems

Any class 3, or 4 CO₂ laser or laser system which by virtue of appropriate design or engineering control cannot directly irradiate the eye with levels which are in excess of 0.1 watt/cm² falls into this category. For all practical purposes a class 5 laser system, since it does not produce any laser radiation outside of the enclosure, does not have to satisfy any other safety requirements nor are medical surveillance requirements necessary for their operation. However, to insure the safe operation of such a system, there are a number of requirements which must be met.

2. Requirements for a Class 5 Laser System

a. Protective Housing

The laser system shall have a protective housing that prevents emission of radiation at levels above 0.1 watt/cm². The protective housing must prevent human access during normal operation. No special control measures shall be required for personnel outside of the protective housing.

Personnel who require access to the protective housing for the purpose of maintenance shall comply with the control measures specified for the laser class or laser system contained therein.

b. Safety Interlocks

Each laser or laser system shall be provided with safety interlocks for any portion of the protective housing which when removed or displaced allows human access to radiation in excess of the applicable 0.1 watt/cm² limit.

A minimum of two operative safety interlocks, one of which must be consealed, shall be provided for any portion of the protective housing which by design can be removed or displaced during normal operation and thereby allow access to radiation in excess of the 0.1 watt/cm^2 limit. Interruption of these safety interlocks shall insure that the beam cannot leave the laser enclosure at powers above this limit. Failure of any single mechanical or electrical component in the redundant interlock system shall not prevent the total interlock system from functioning.

Service adjustments or maintainance procedures on the laser contained within the enclosure shall not cause safety interlocks to become inoperative or the radiation levels outside of the enclosure to exceed the allowable limit unless performed in a temporary controlled area.

c. Fail Safe System

Adjustments or failure of any part of the laser or the enclosure containing a laser or laser system shall not foreseeably cause the laser or laser system to be in uncompliance with the requirements of an enclosed laser operation.

d. Viewing Windows

All viewing windows incorporated into an enclosed laser shall employ a suitable filter material which attenuates the laser radiation transmitted through the window to levels below the specified 0.1 watt/cm^2 level under any conditions of operation of a laser or laser system. At the 10.6 micron level, the use of plexiglass or lexan entirely fulfills this attenuation requirements.

e. Warning Signs

Warning labels shall not be required on the exterior protective enclosure of a class 5 laser system. However, the appropriate warning signs or label which designate the class of laser contained within the enclosure shall be prominently and permanently attached to the inside of the enclosure in a manner to be instantly viewed upon removal of any of the interlock access panels or removal covers which allow exposure to the laser beam.

f. Safety Instructions

Manufacturer of laser equipment shall prepare adequate safety instructions covering the use and operative maintenance of their equipment.

The management shall establish and maintain an adequate program for the control of laser hazards. The program shall include provision for education of authorized operators.

3. Applicability to the Avco HPL Laser Welding System

For the welding tests performed under this contract, the entire laser system including welding interaction point, were completely enclosed in a material that does not transmit the infrared energy. Measurements of laser energy which escapes the enclosure entirely, were below the required 0.1 watt/cm^2 flux level. Thus lasers which use a complete enclosure around the work piece clearly fall into the class 5 category and need no warning signs, operator medical examinations, bells or alarms or any of the other safety requirements for laser systems.

If an extended piece of material is to be laser welded and it is no longer practical to enclose that piece in an enclosure, then the situation changes, but only slightly. In such a system, the beam would be enclosed all the way down to the shielding hood, providing the required enclosure around the entire system. However, a slight amount of laser radiation that was not absorbed in the work piece would be diffusely scattered under the shielding hood and would escape from the small gap between the shielding hood and the work piece. Calculations indicate that if 10% of the incident beam is not absorbed in the work piece and is diffusely scattered, the power density would be down below the required 0.1 watt/cm^2 at points that are approximately three feet radially away from the weld point.

A measurement of the actual radiation level for a particular system would have to be undertaken at various locations to determine the distance beyond which the radiation is sufficiently low, and adequate barriers provided to prevent operators from positioning themselves closer to the weld point.

B) Electrical and X-Ray Safety Standards

Design and assembly of electrical control and power in the HPL laser system is in accordance with the American National Standard Electric Code, C1-1971 (NFPA 70-1971), Articles 300 and 400.

The HPL system also adheres to the Electrical Standard set up by the Joint Industrial Council. (JIC Electrical Standards for Mass Production Equipment EMP-1-67.) This standard provides detailed specifications for the application of electrical systems to production industrial equipment.

The provisions of this standard apply to all electrical systems, which operate from a supply voltage of 600 volts or less. Compared to standard engineering practices, this standard provides for larger conductor sizes, higher temperature insulation, oil and dust tight enclosures and distribution, and mechanically interlocked enclosures inaccessible to other than authorized personnel.

The mechanical design and material selection insures that no detectable X-radiation is present outside the HPL lasing chamber. Detailed Geiger counter measurements have been made to verify that this is the case.

II MAINTENANCE

A) Maintenance History

The following expected lifetimes have been determined from over three years of experience with HPL Laser systems.

Optics

Internal:

During a 6 month period, the cavity optics develop a slight coating, or tarnishing which results in a slight (5%) decrease in laser efficiency. They are changed once every 6 months and are reworked and available for use again.

External:

Most external mirrors can be used for several years. The exceptions are:

- a. Mirrors close to work piece. These mirrors may be contaminated by splatter from the work piece, and should be protected by a purge system which directs a gas jet across the mirror surface. The service time for such mirrors depend on the severity of the environment. However, no HPL Mirror has been destroyed due to hostile environment operation. Some of the mirrors have been damaged on the surface but were able to be re-ground and polished.
- b. Mirrors which point in the upward direction are susceptible to damage caused by dust settling on the surface. Even if a protective purge is provided, these up-hand mirrors usually have to be reworked once every 6 months.

E-Beam

There are three types of failures which may occur in the HPL E-Beam;

1) Foil Failures, 2) Filament Failures, and 3) High Vacuum Feed Through Failures.

1. Foil Failure:

Foil failure has occurred approximately once every 6 months. The down time is usually only a few hours.

2. Filament Failure:

Filaments will last about a year. Down time is a day.

3. Feed Through Failure:

At most, feed throughs will fail once every 2 years, with a down time of 2-3 days.

Sustainer Electrodes:

The electrodes are routinely replaced every year.

Blowers:

The limitation on the HPL system blowers is bearing lifetime. It has been found that a set of bearings will last at least 1000 hours. Thus, all blowers are replaced every 1000 hrs with rebuilt units containing new bearings.

Electrical and Electronic Equipment:

When the blowers are replaced, the electrical equipment is checked (including waveform patterns), and filters are serviced.

Vacuum Equipment

The pumps for both the E-Beam vacuum chamber and the main wind tunnel chamber should be serviced every year, and the bearings replaced. If the blank off pressure exceeds the level described below, service should be initiated immediately to remedy the situation.

The E-Beam blank off pressure should not exceed 3×10^{-5} torr when operating at the 10 kw power level. Operation at higher pressures may lead to premature foil failures.

For the main vacuum chamber, experience indicates a blank off pressure of 0.5 torr must be achieved. Based on measurements of the quantity of air needed to significantly degrade the laser performance (reported in the Appendix) the corresponding blank off pressure would be substantially greater, in the range of 2-3 torr. This is probably explained by the fact that water vapor contamination due to slight leaks (i.e., from sustainer electrode, or optics) is more significant than air contamination. If the blank off pressure exceeds this 0.5 torr level, the system should be serviced.

B) Maintenance Schedule

Based on the maintenance history cited above the following preventative maintenance schedule is recommended for the HPL Laser System:

1. Cavity Optics

Change every 6 months

2. External Mirrors

Inspect each year, refurbish as required. Upward facing mirrors, and mirrors close to the work piece should be inspected at shorter intervals.

3. E-Beam

- a) Filaments - replace as needed, typically once a year.
- b) Foil - replace as needed.

4. Sustainer Electrodes

Replace every year.

5. Blowers

Replace with refurbished blowers with new bearings and rebalance after 1000 hours of operation.

6. Vacuum Equipment

Inspect every 6 months, and replace bearings every year.

7. Electrical and Electronic Equipment

Check waveforms and service filters every 1000 hours.

APPENDIX

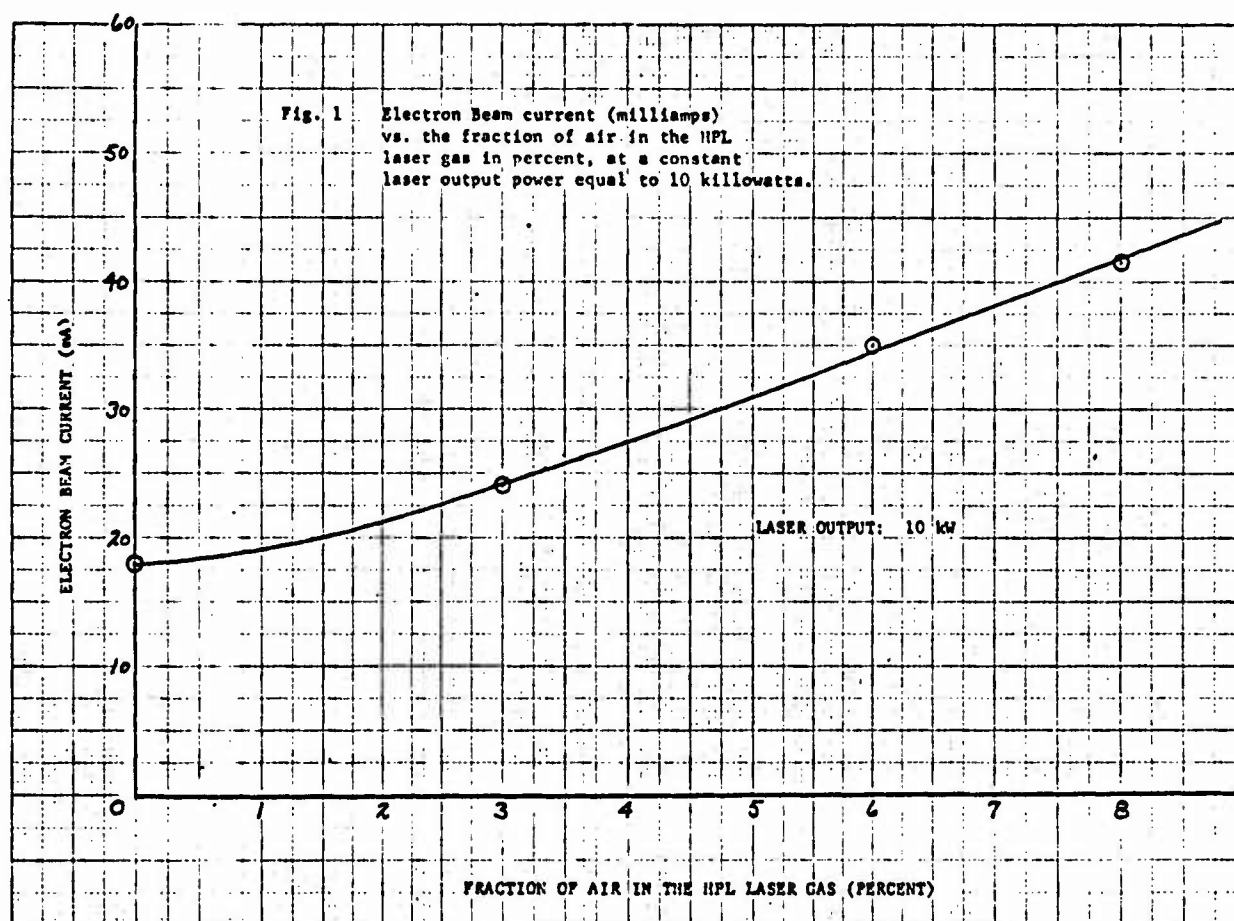
SENSITIVITY OF HPL LASER SYSTEM TO AIR LEAKAGE INTO LASER CAVITY

In considering the maintenance characteristics of the HPL laser systems, it is important to determine the maximum concentration of air inside the laser cavity which will cause no significant degradation in laser performance.

The closed loop power control system on the HPL is designed to maintain a constant output power. If the power begins to drop, the closed loop system senses this drop, and increases the electron beam current (which in turn causes the laser power to increase) until the preset value is reached. However, this increase must not exceed the power supply limitations, which will be 20-30% above the nominal operating point in a production HPL system.

Tests were conducted in which the increase in electron beam current was measured for various values of air concentrations inside the laser cavity at an output power level of 10 kw. The air concentrations were controlled by introducing air into the laser cavity through flow meters. The air contamination level is then determined by dividing the air flow rate by the laser make up gas flow rate.

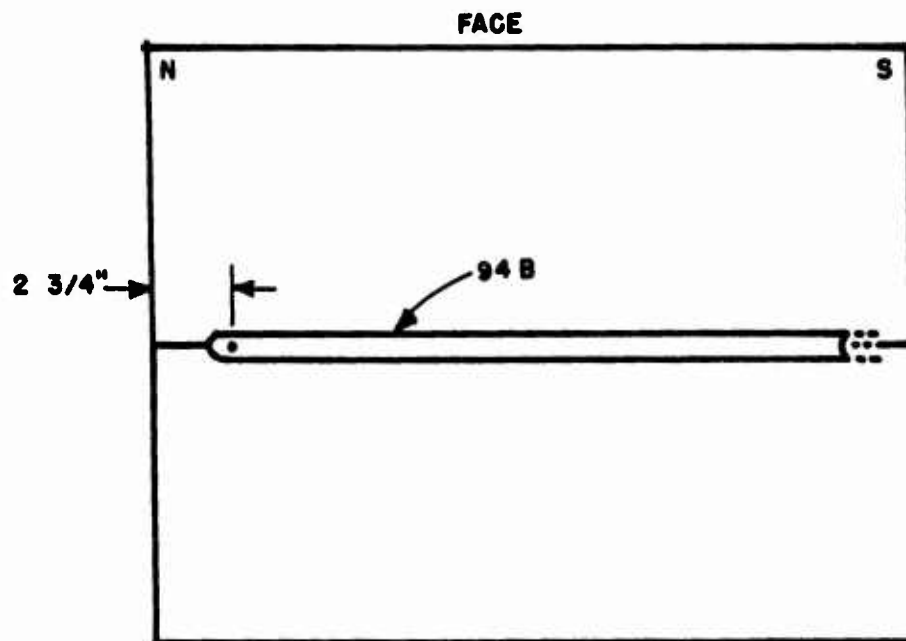
The conclusions of the test results shown in Fig. 1 were that the air concentration must be 2% to 3% to require an additional 20 - 30% electron beam current. If a leak of this magnitude were to occur, the blank-off pressure for the laser cavity would correspondingly be 2-3% of the operating pressure of 76 torr, or 1.5 - 2.3 torr.



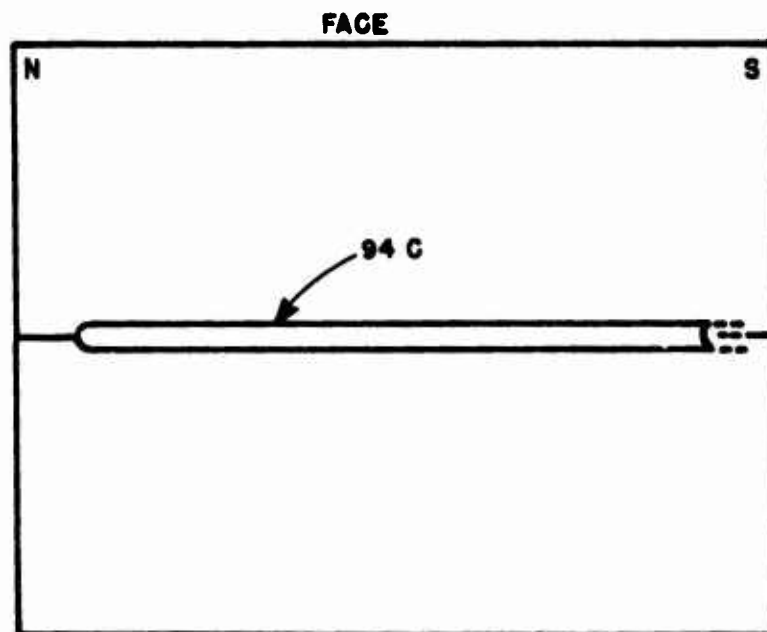
APPENDIX B

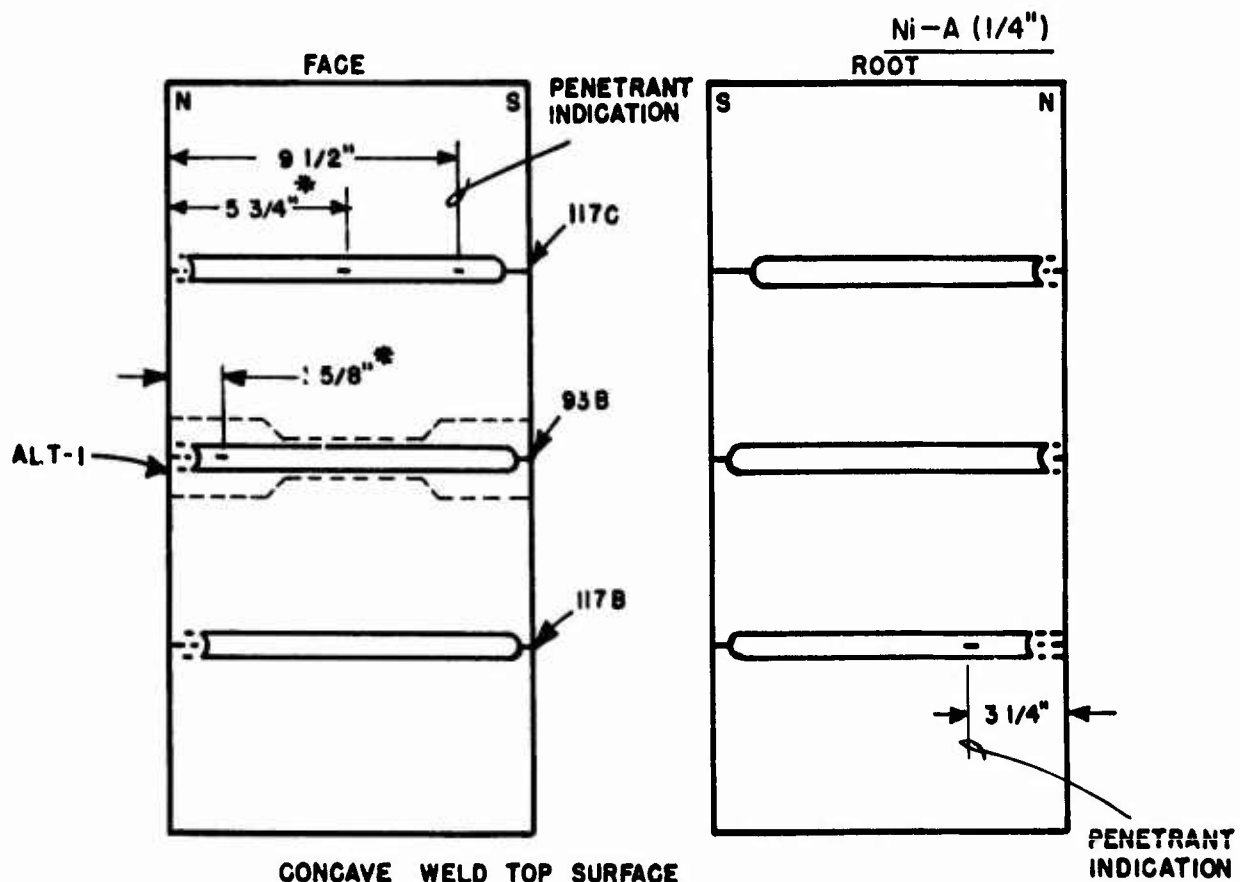
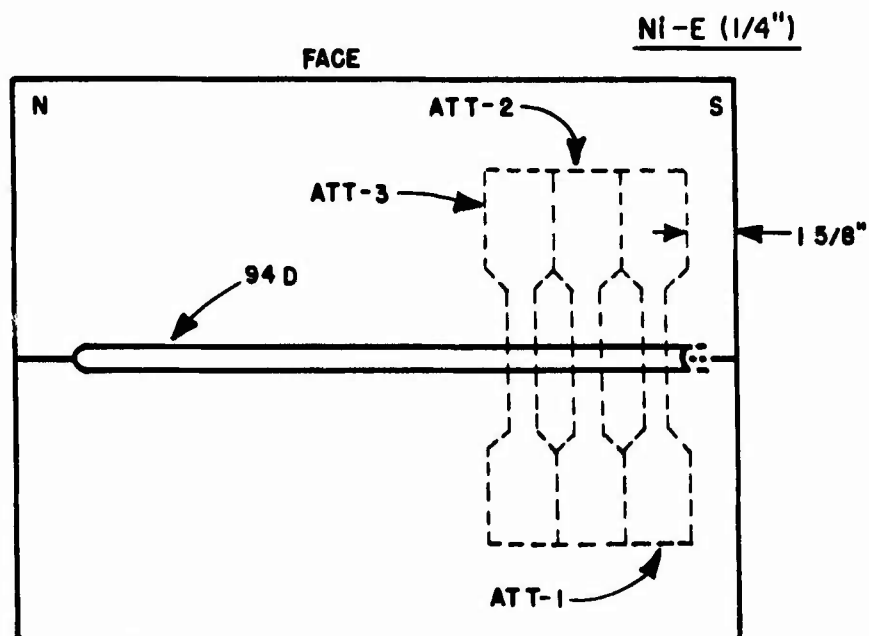
RESULTS OF NONDESTRUCTIVE EVALUATION OF "AS WELDED" MATERIAL

Ni-C (1/4")



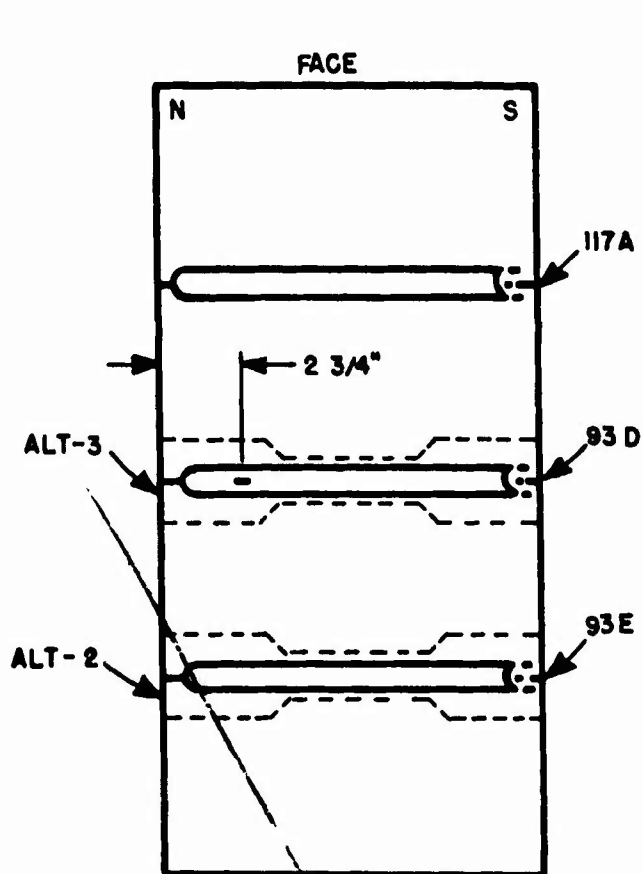
Ni-D (1/4")



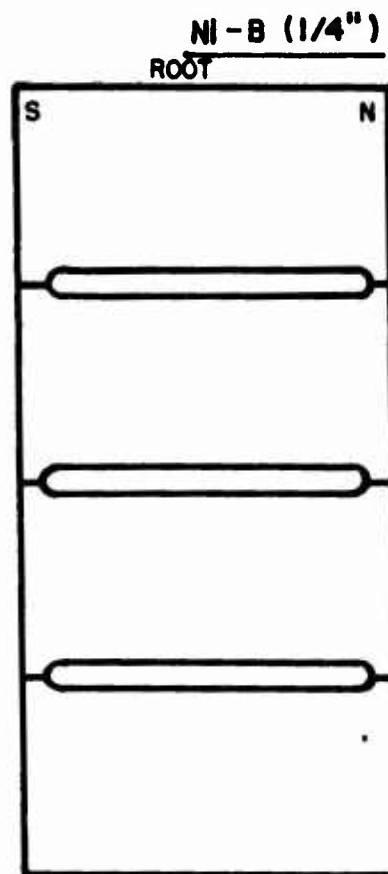


CONCAVE WELD TOP SURFACE

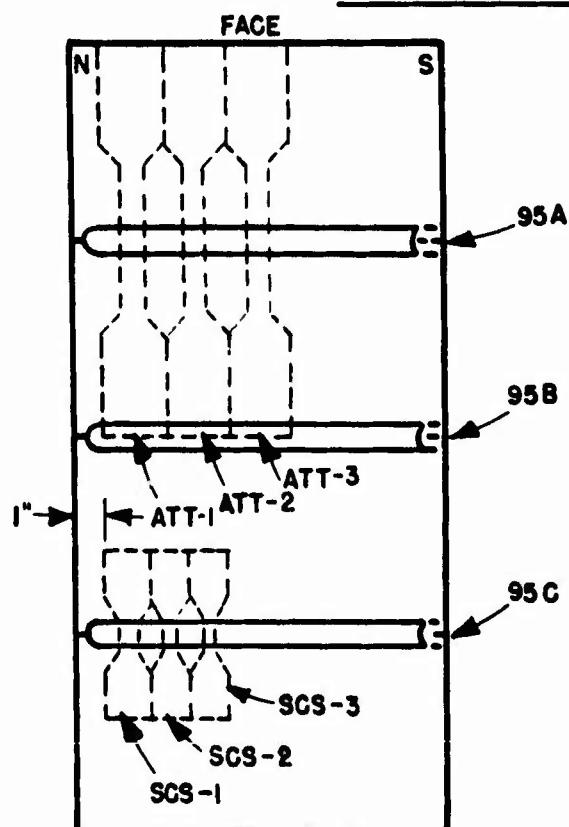
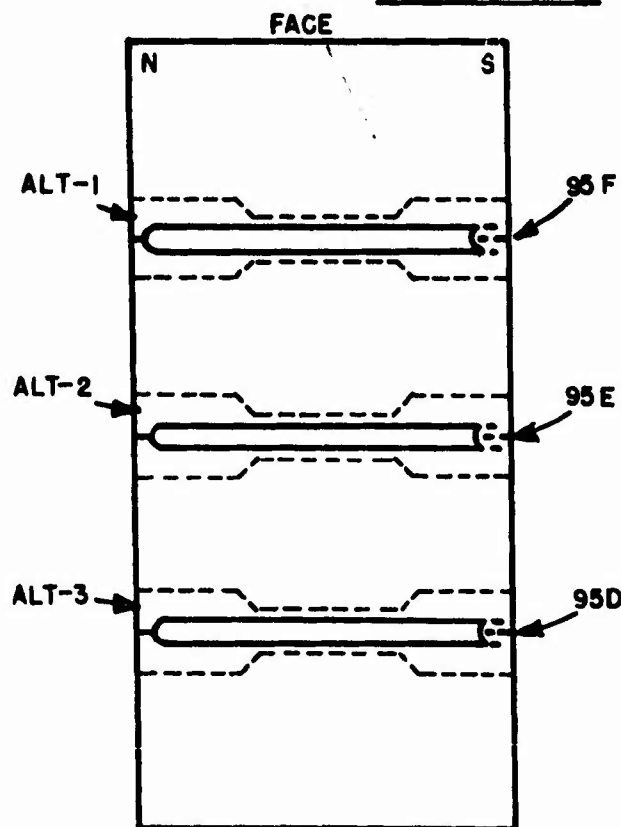
* ULTRASONIC INDICATION MAY BE SURFACE CONCAVITY



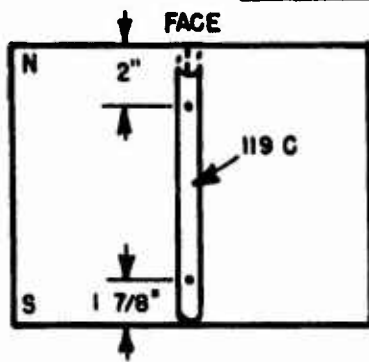
C/S-C II (1/4")



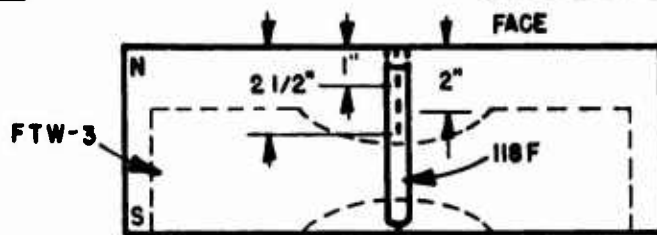
C/S-D (-) (1/4")



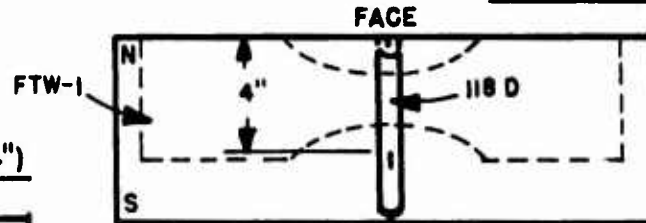
C/S-E (1/4")



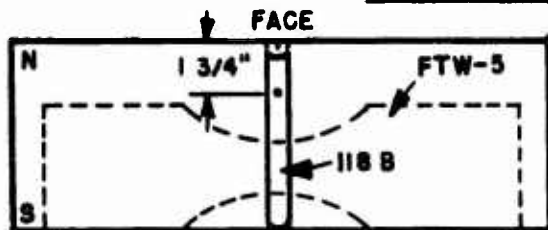
C/S-F (1/4")



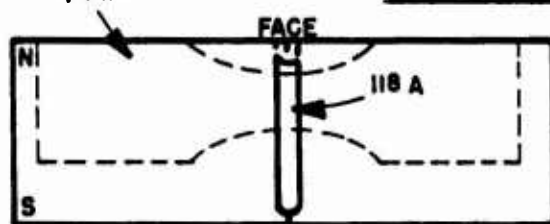
C/S-G (1/4")



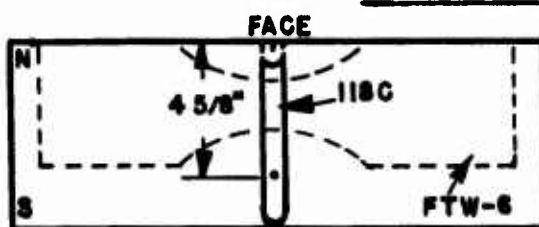
C/S-H (1/4")



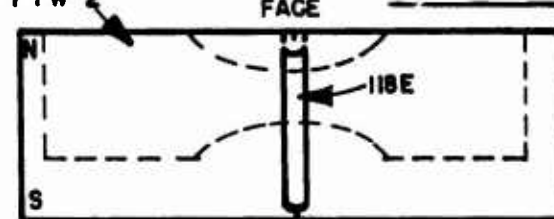
C/S-J (1/4")

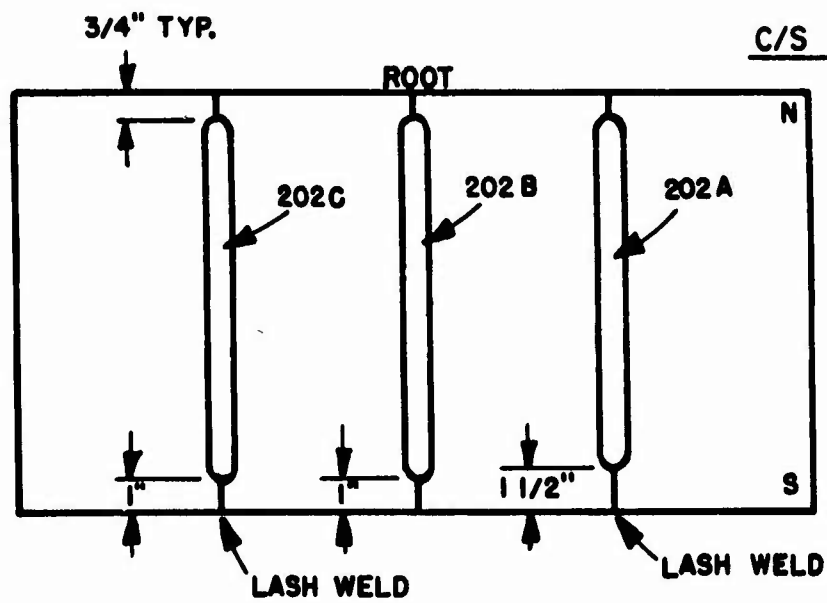
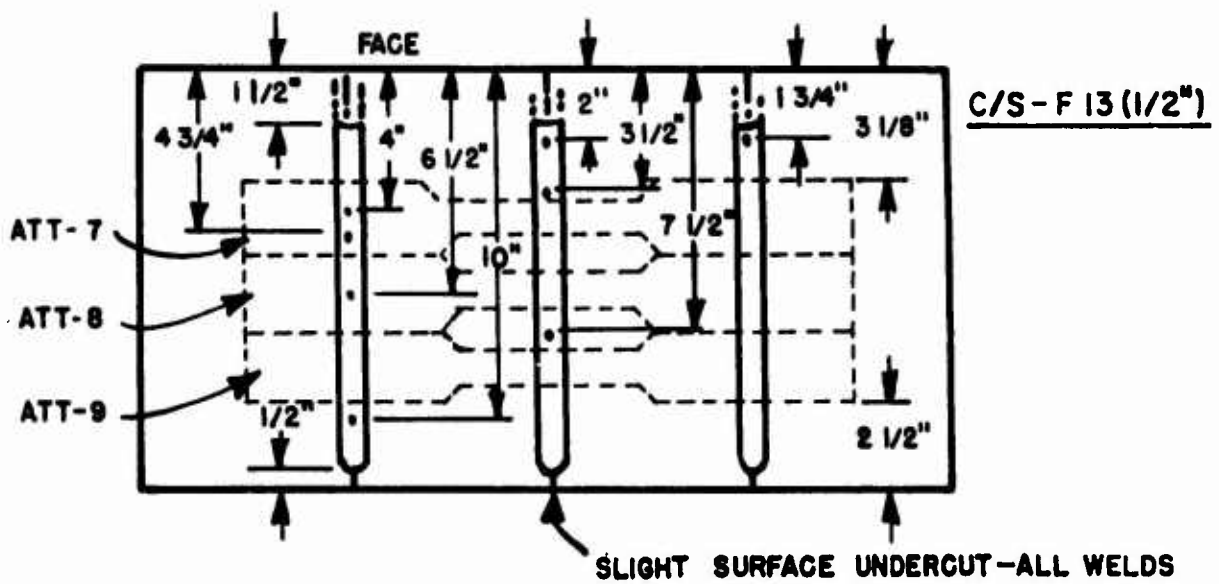


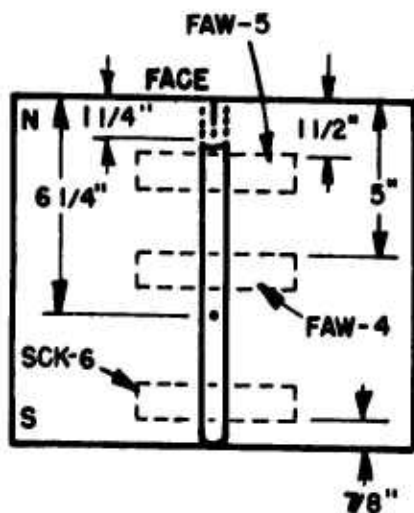
C/S-I (1/4")



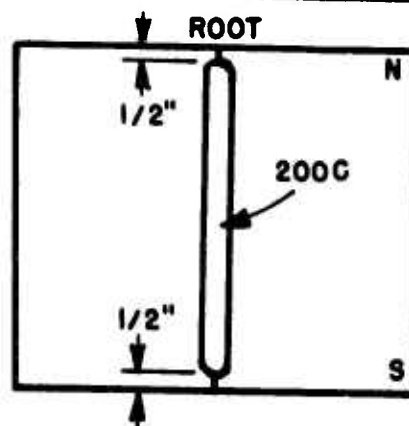
C/S-K (1/4")



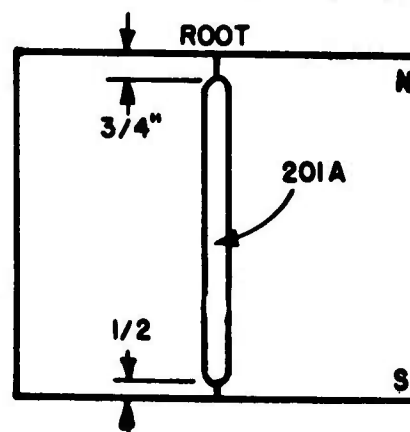
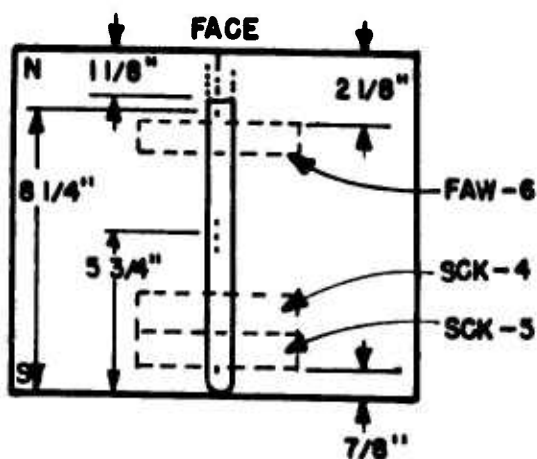




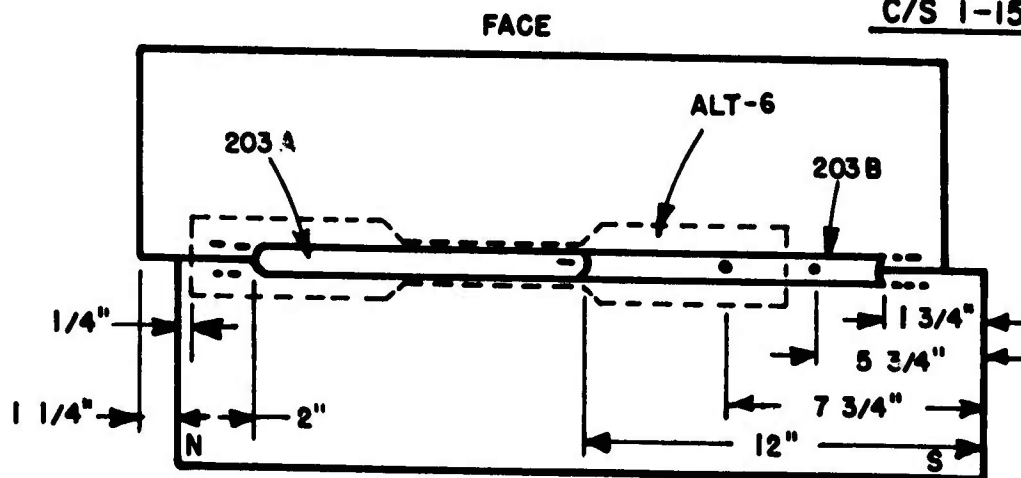
C/S G-10 (1/2")



C/S - H 11 (1/2")

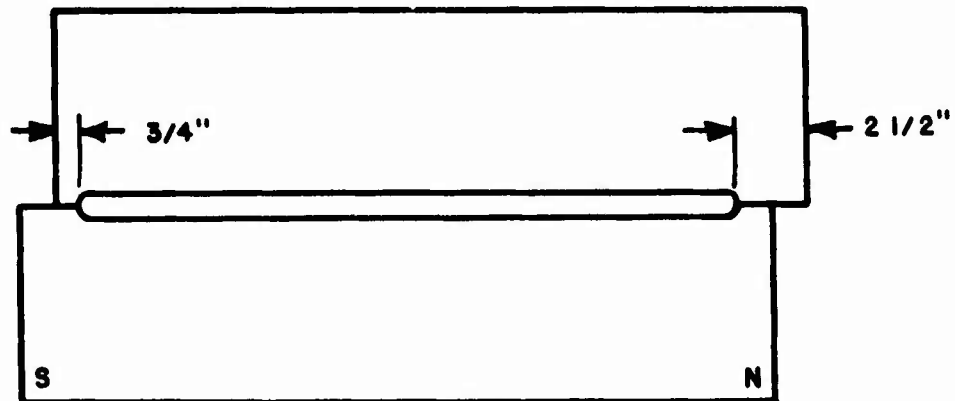


C/S 1-15 (1/2")

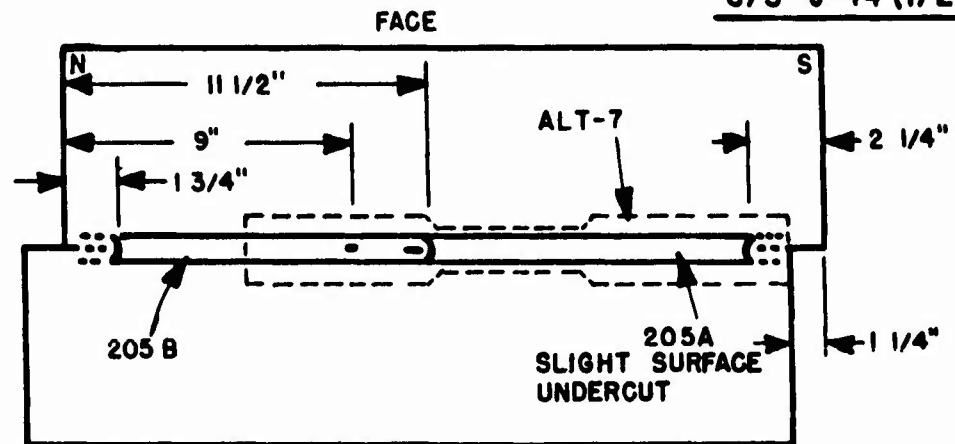


SLIGHT SURFACE UNDERCUT NORTH
END OF 203A - 203 B WHOLE LENGTH

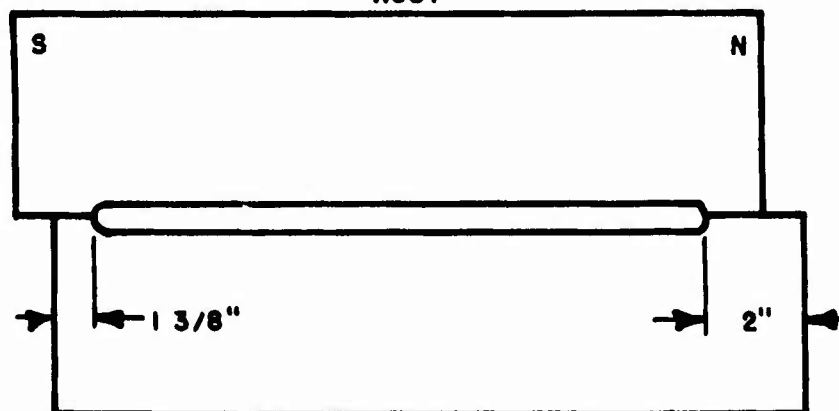
C/S 1-15 (1/2")



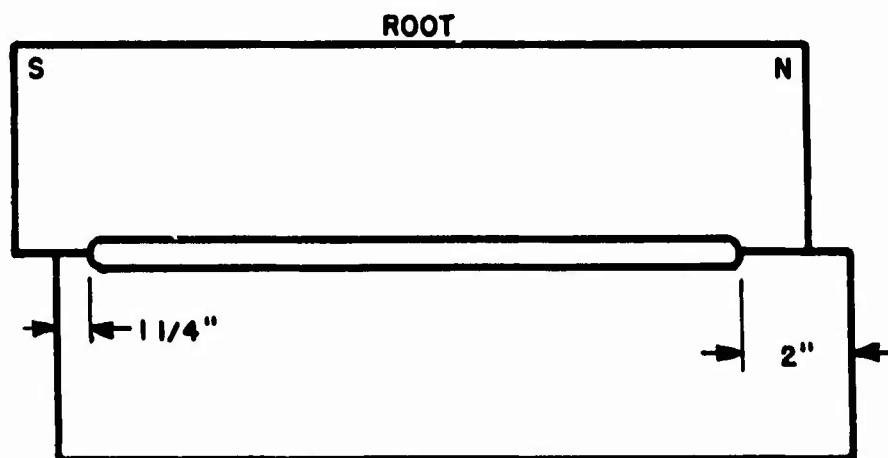
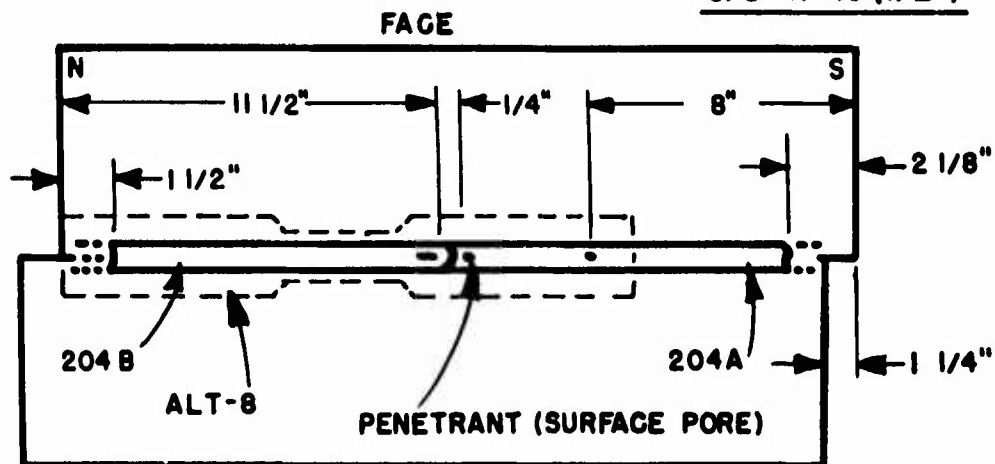
C/S J-14 (1/2")



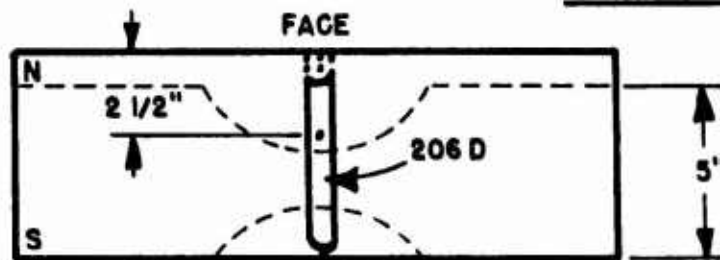
ROOT

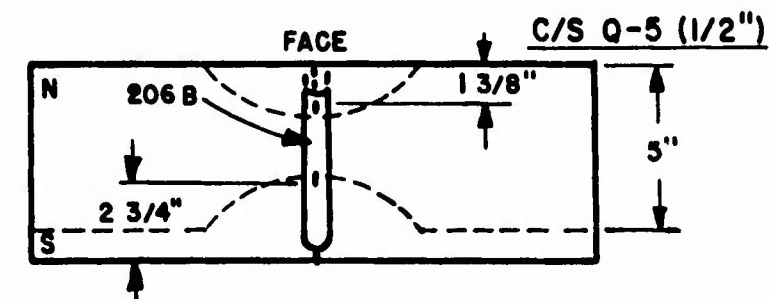
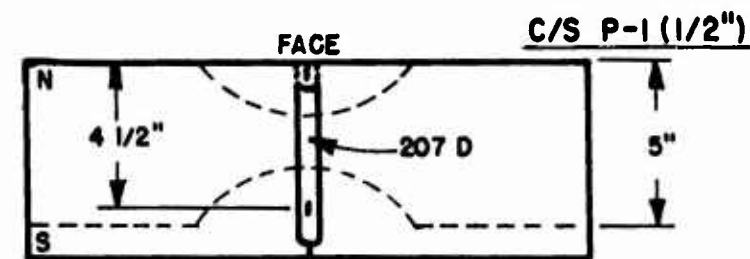
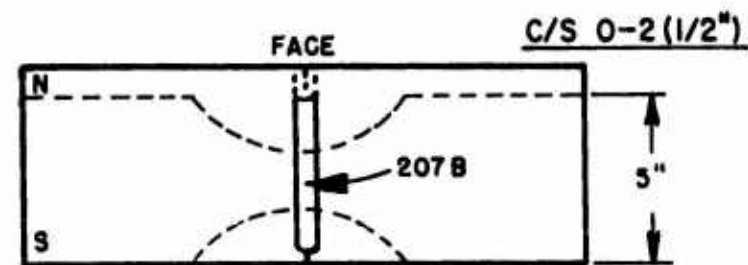
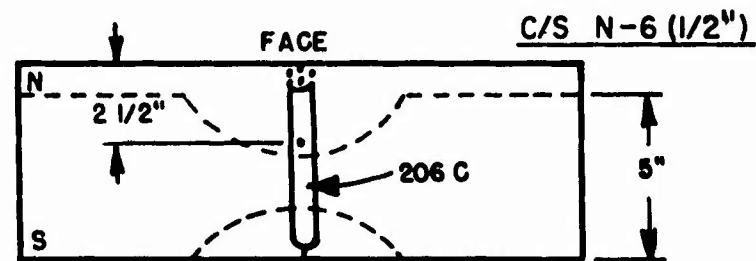
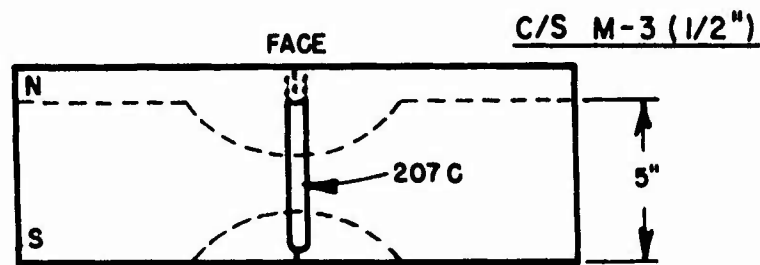


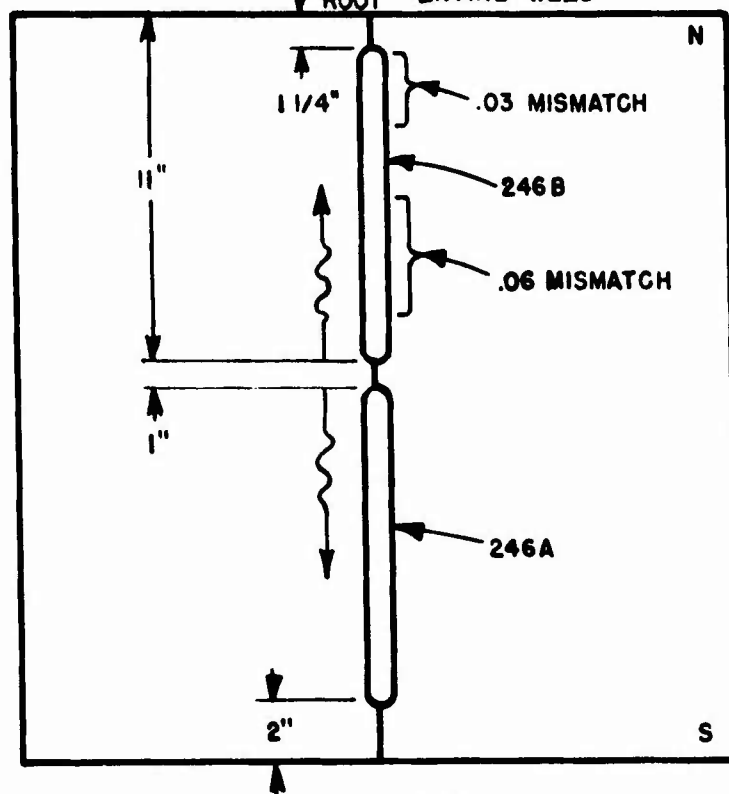
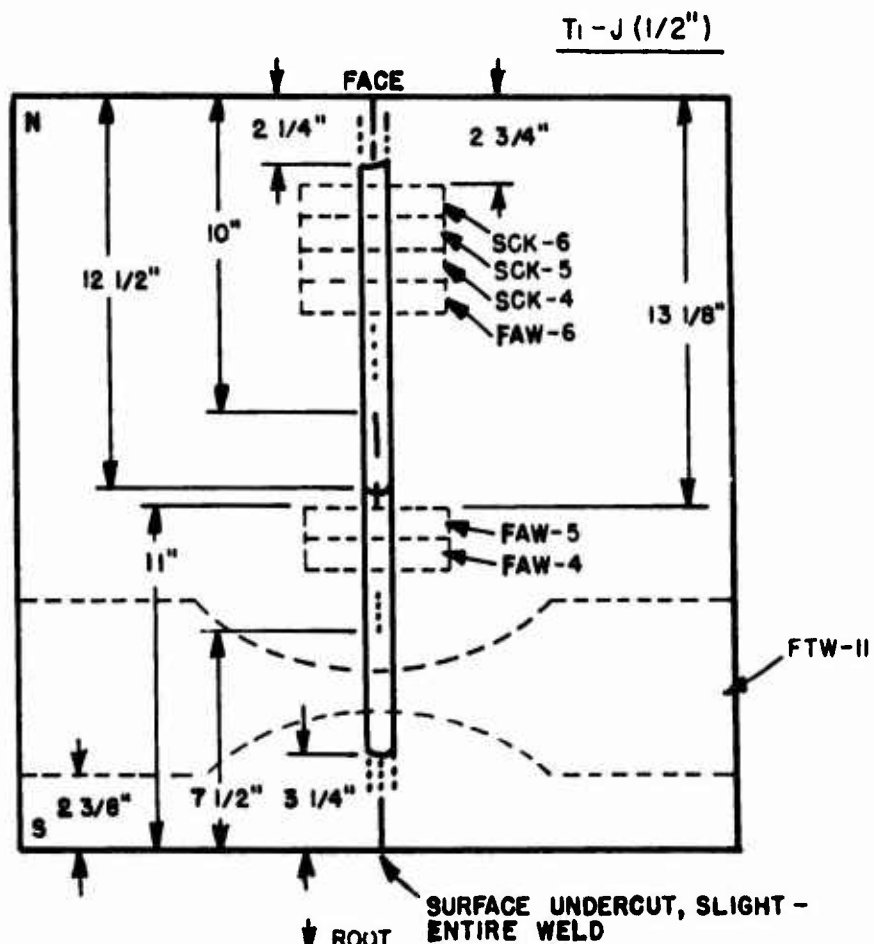
C/S K-16 (1/2")

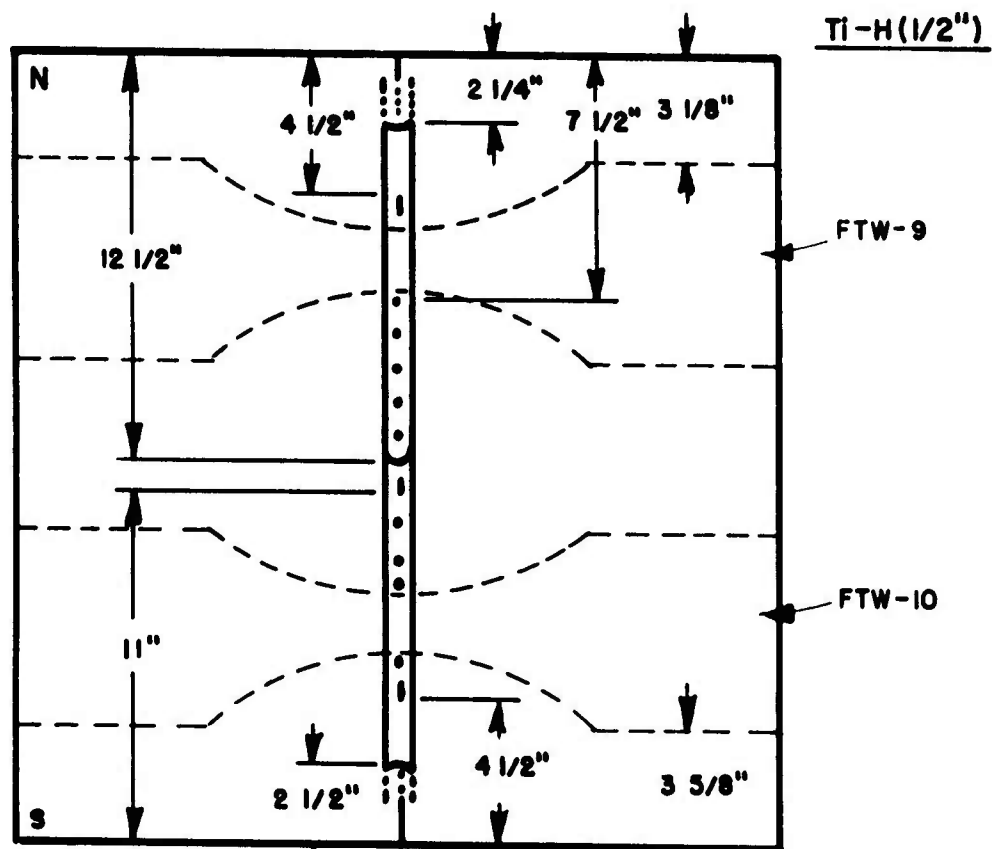


C/S L-7 (1/2")

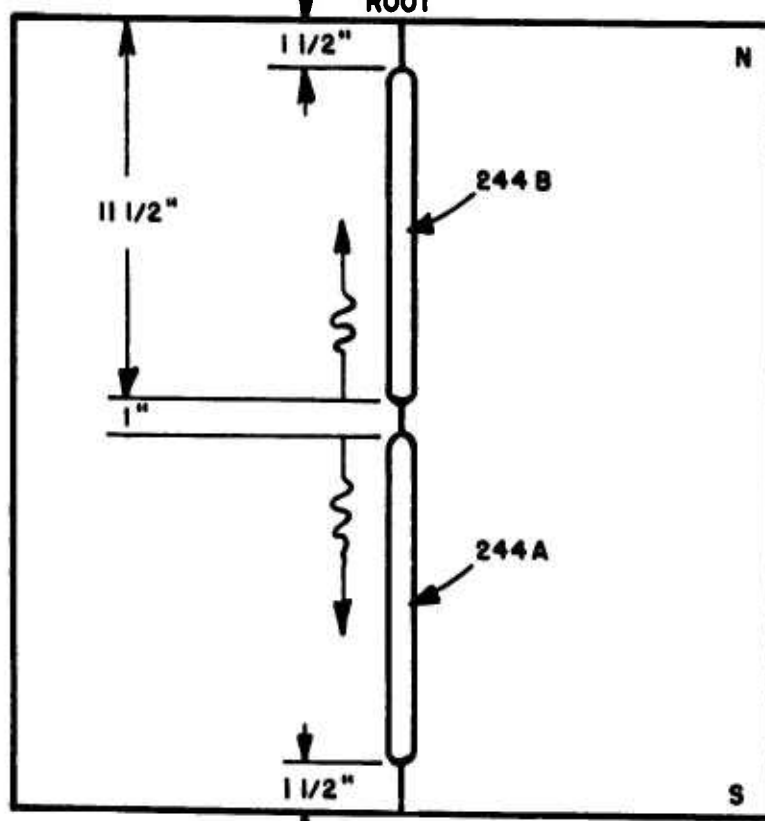




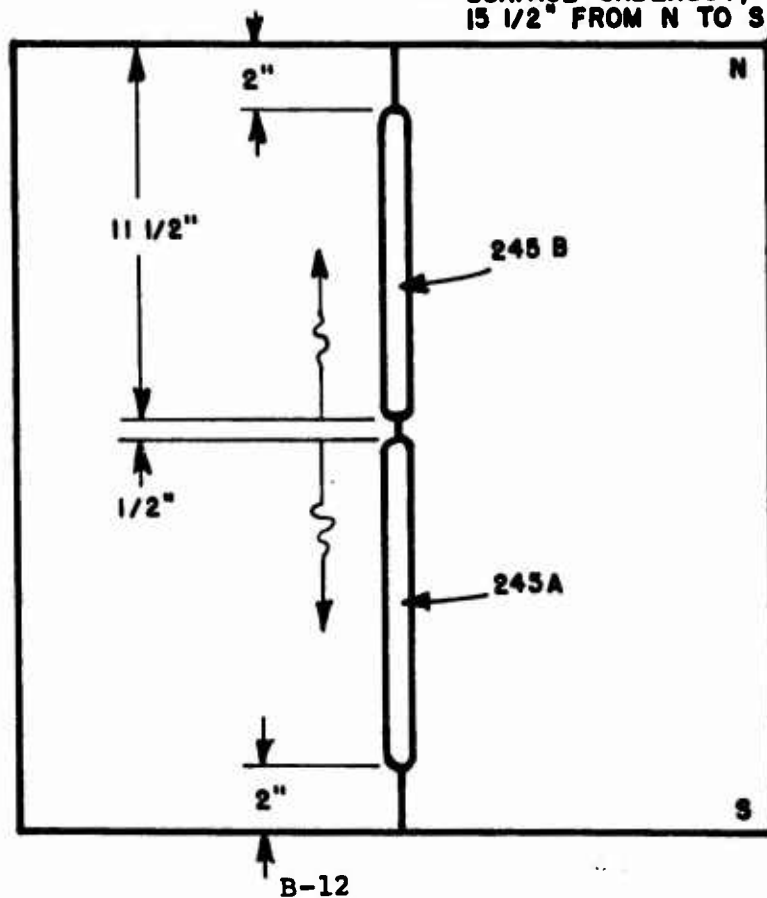
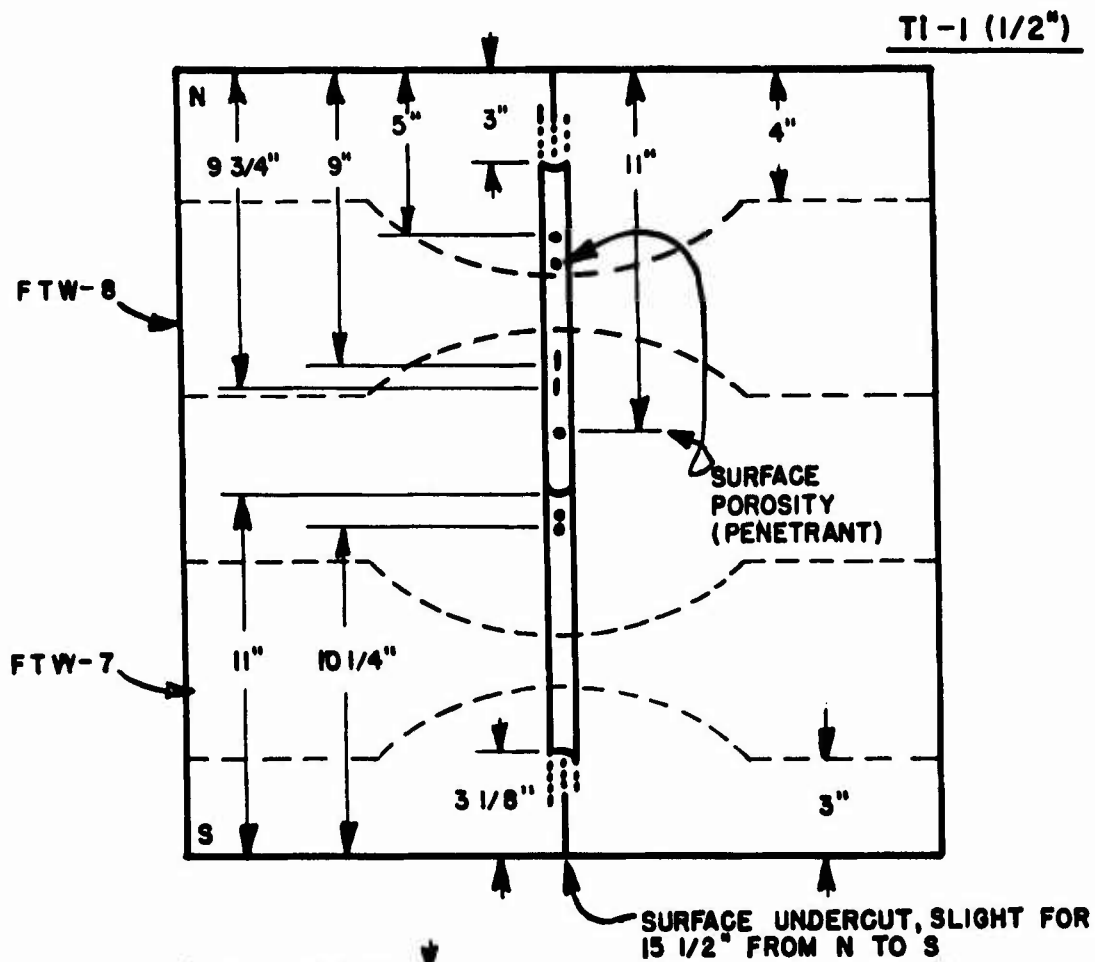


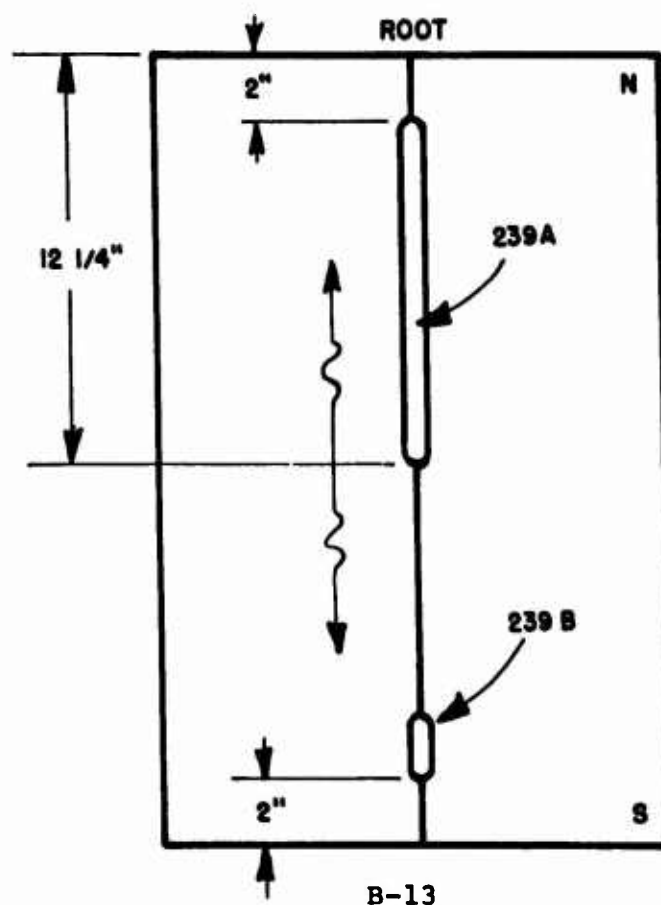
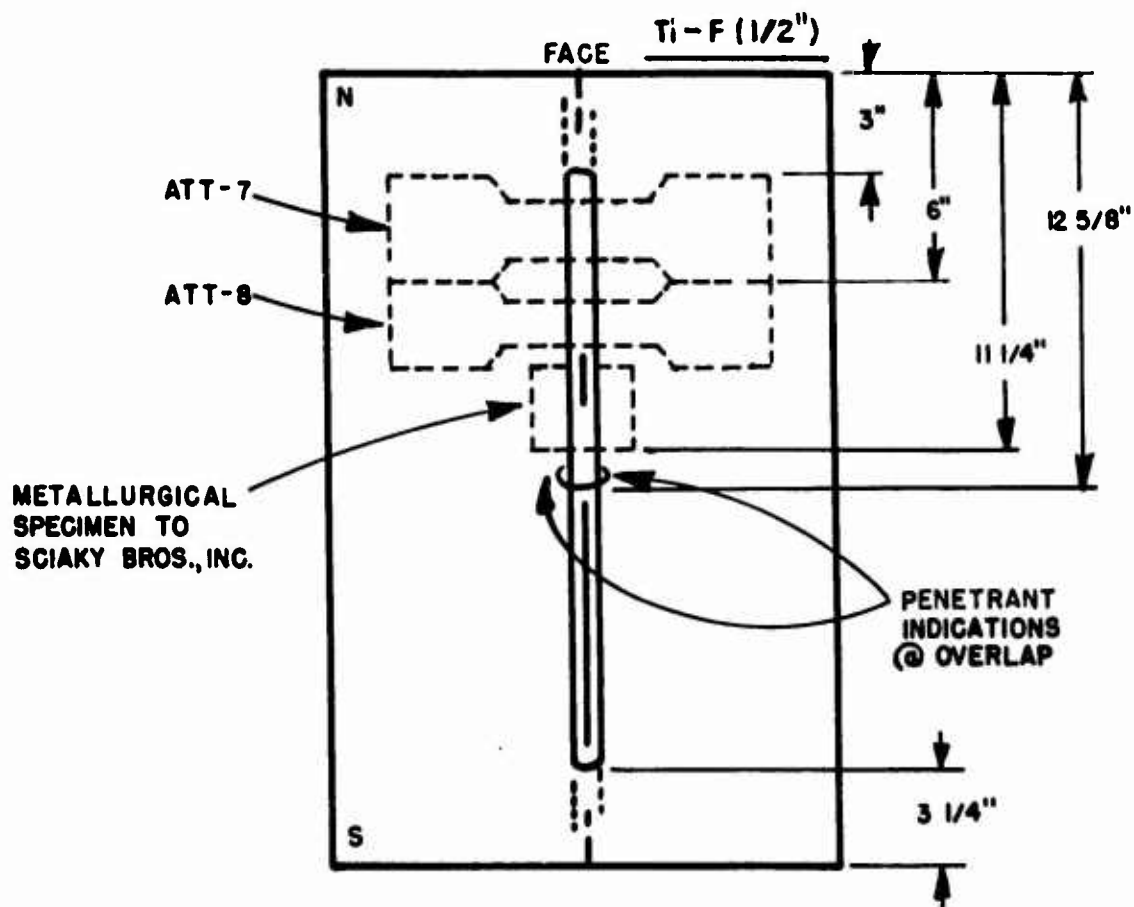


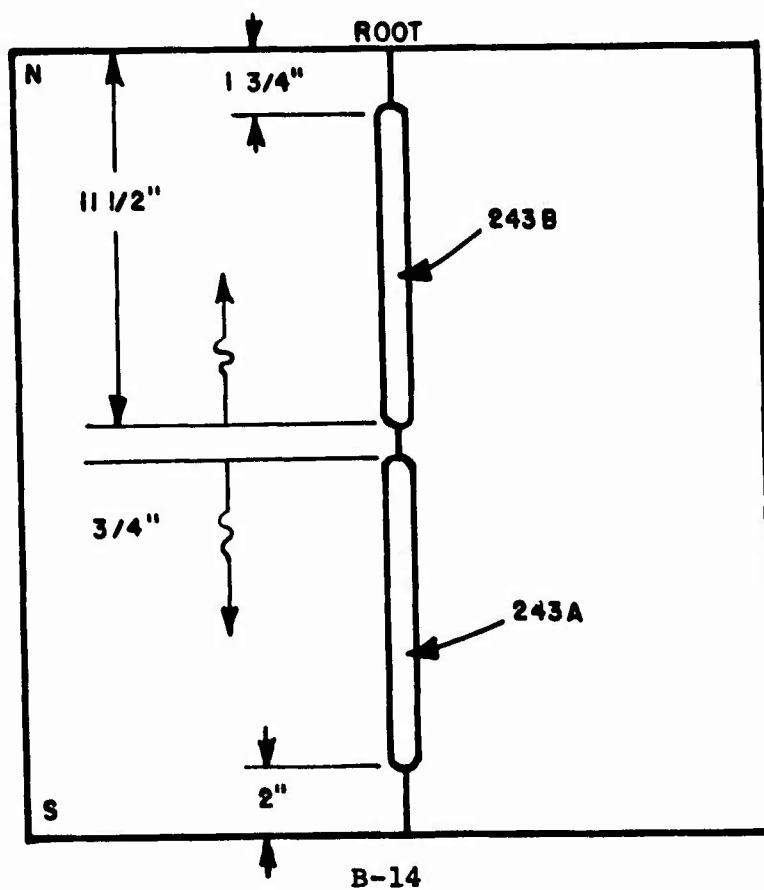
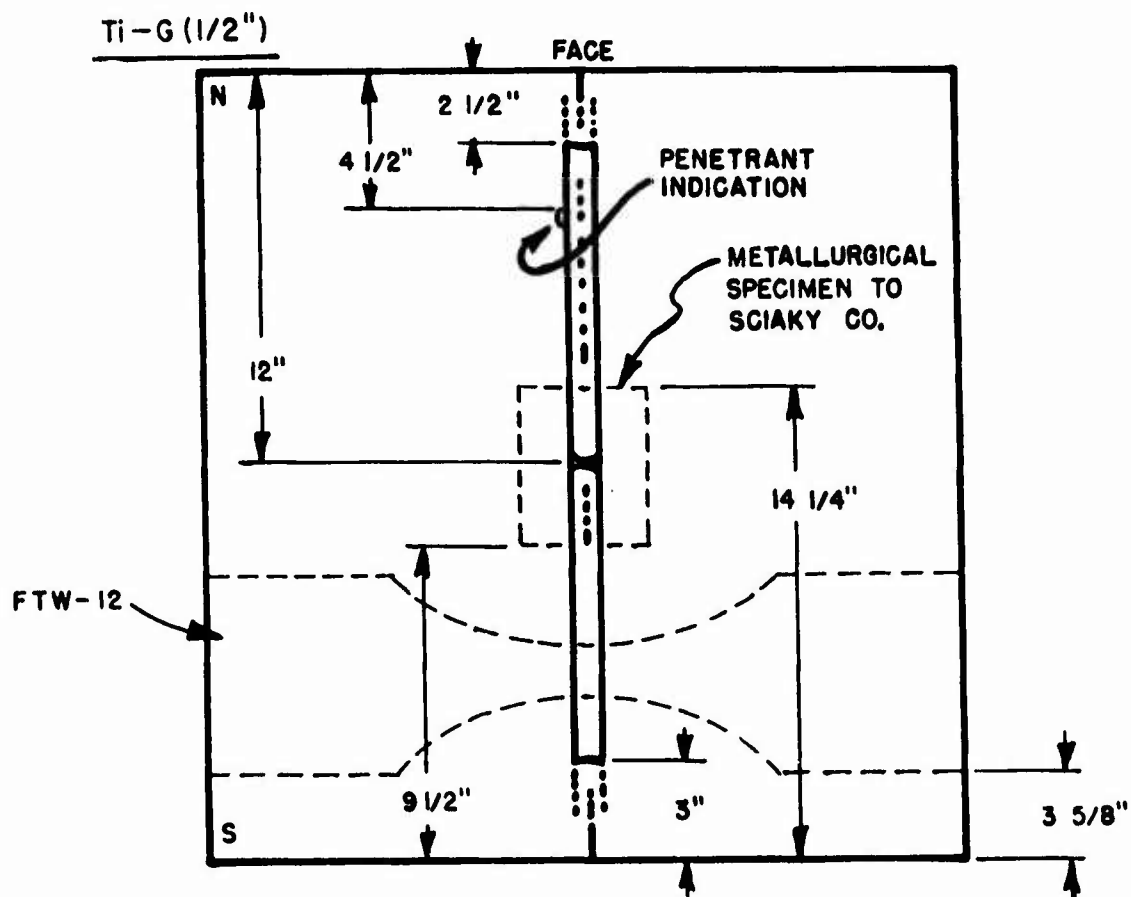
SURFACE UNDERCUT, SLIGHT-ENTIRE WELD



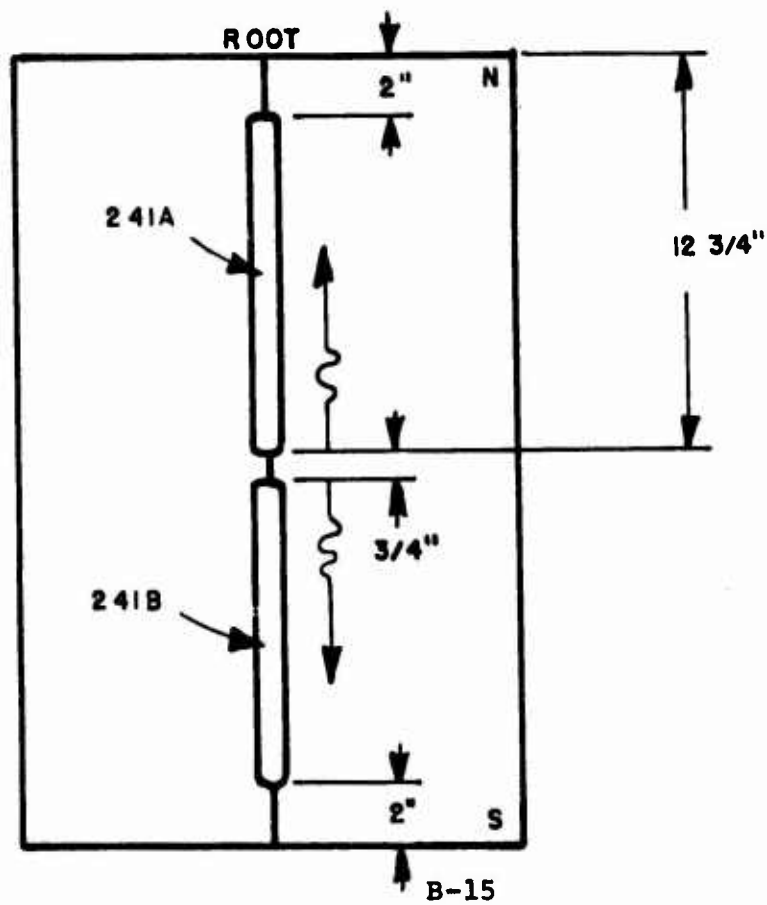
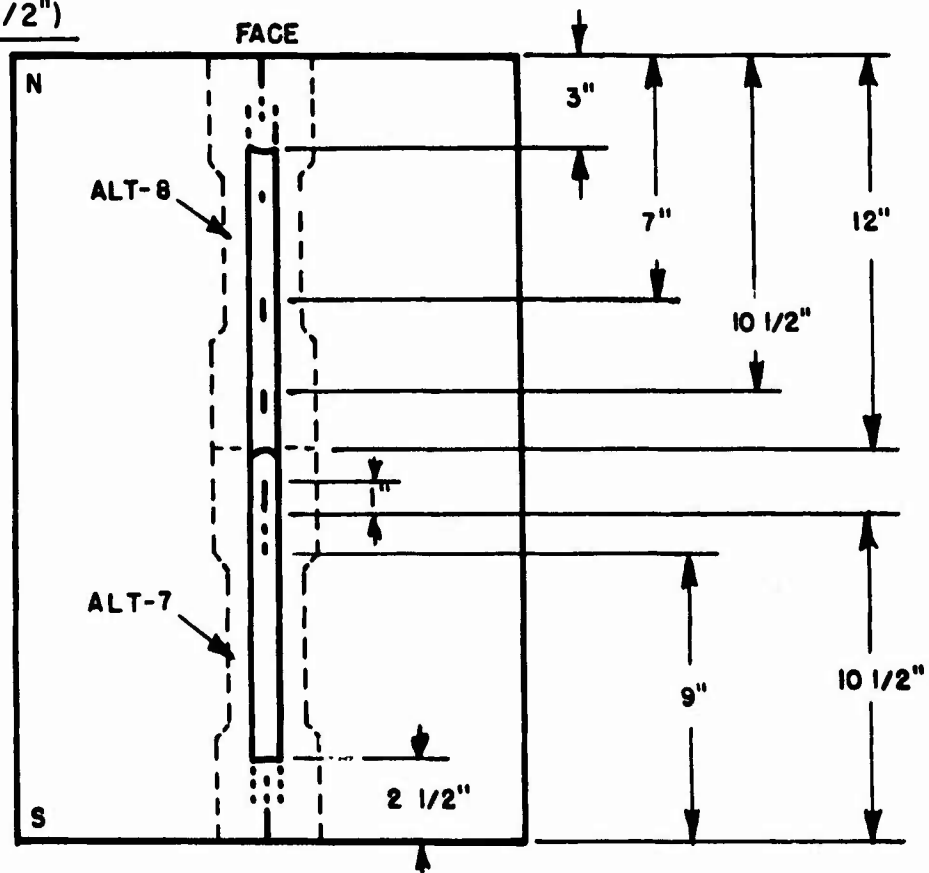
B-11



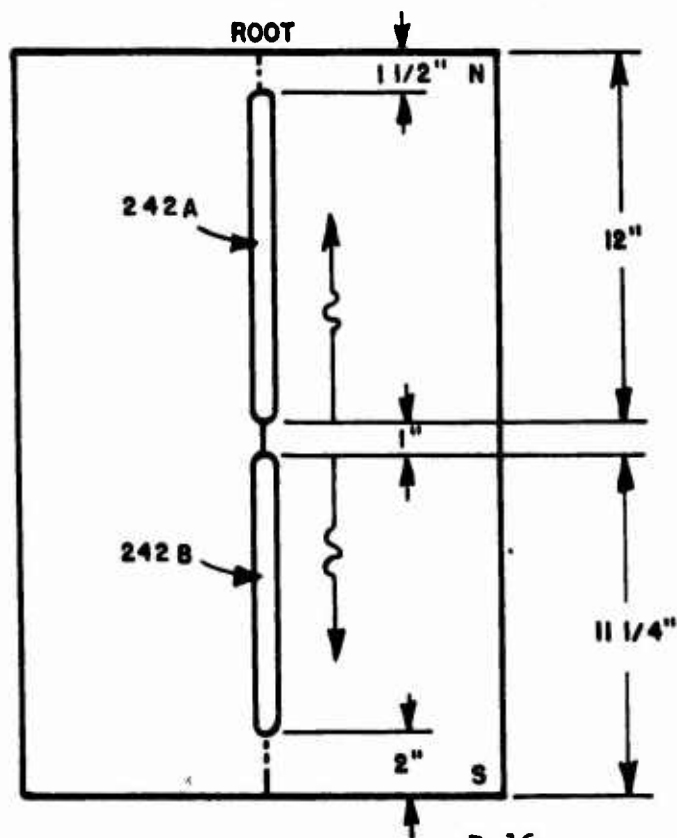
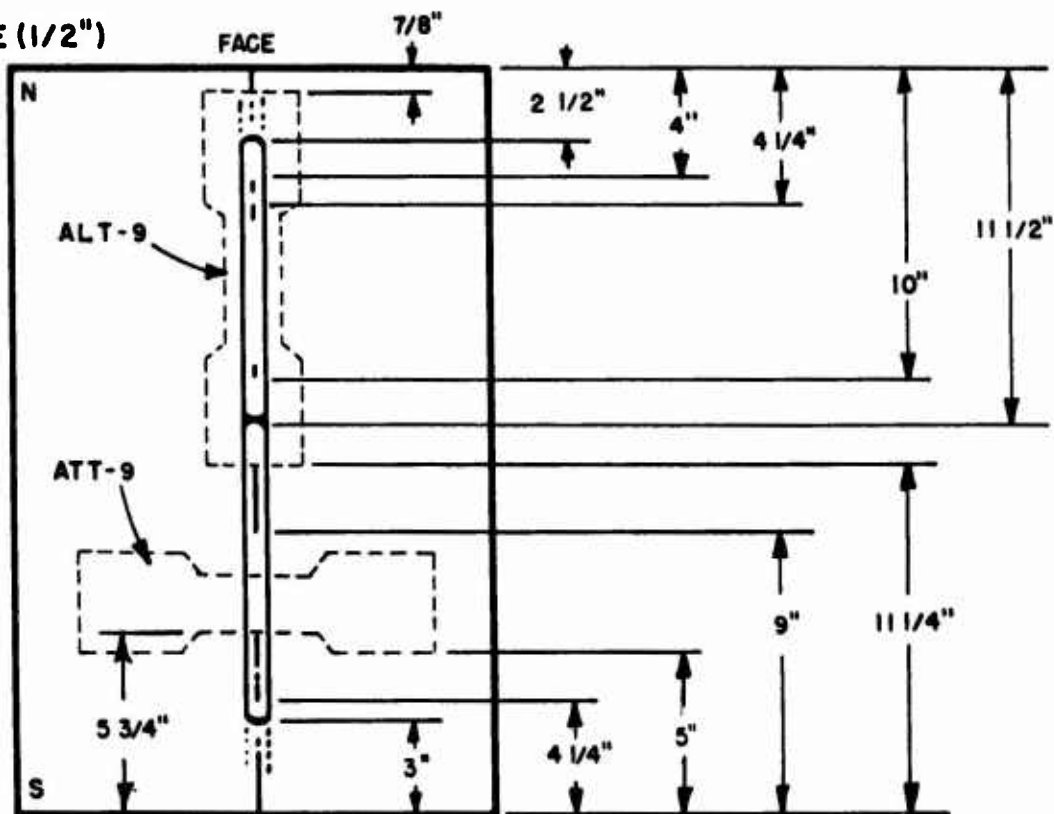




Ti-E (1/2")



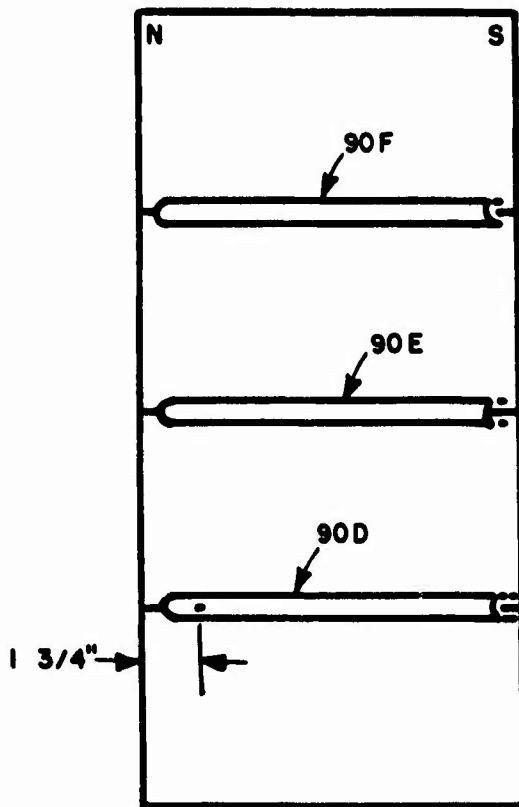
TI-EE (1/2")



B-16

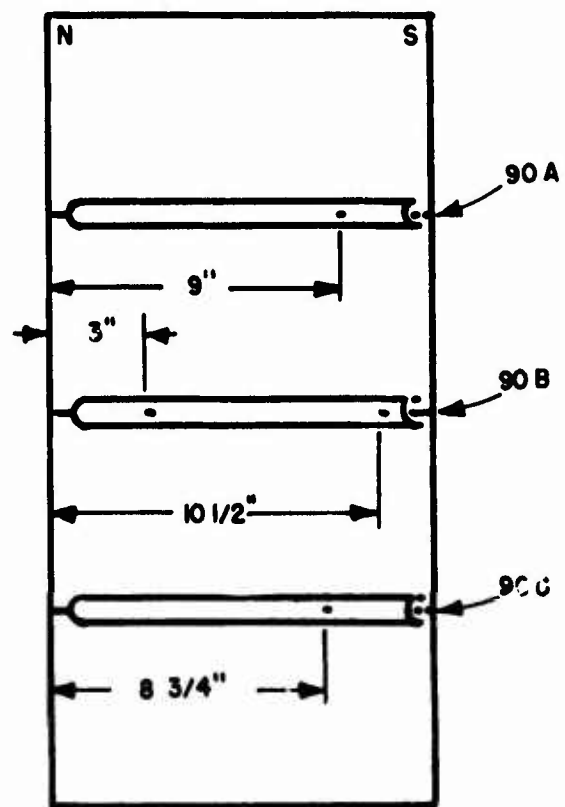
TI-AA (5) 1/4"

FACE



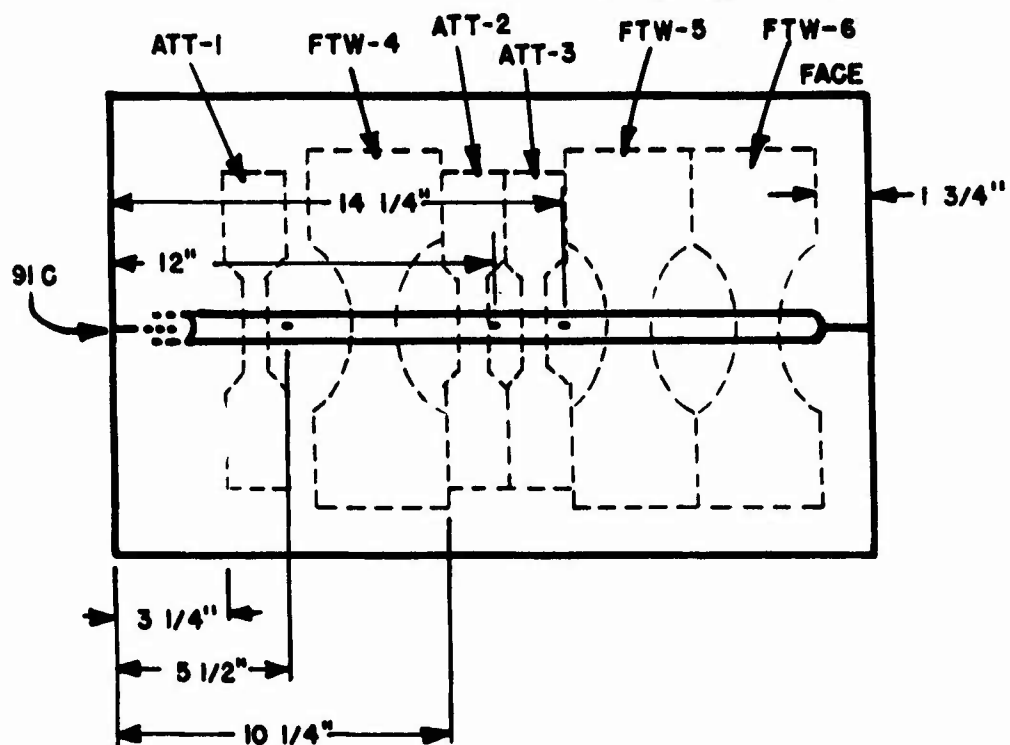
TI-BB(6) 1/4"

FACE

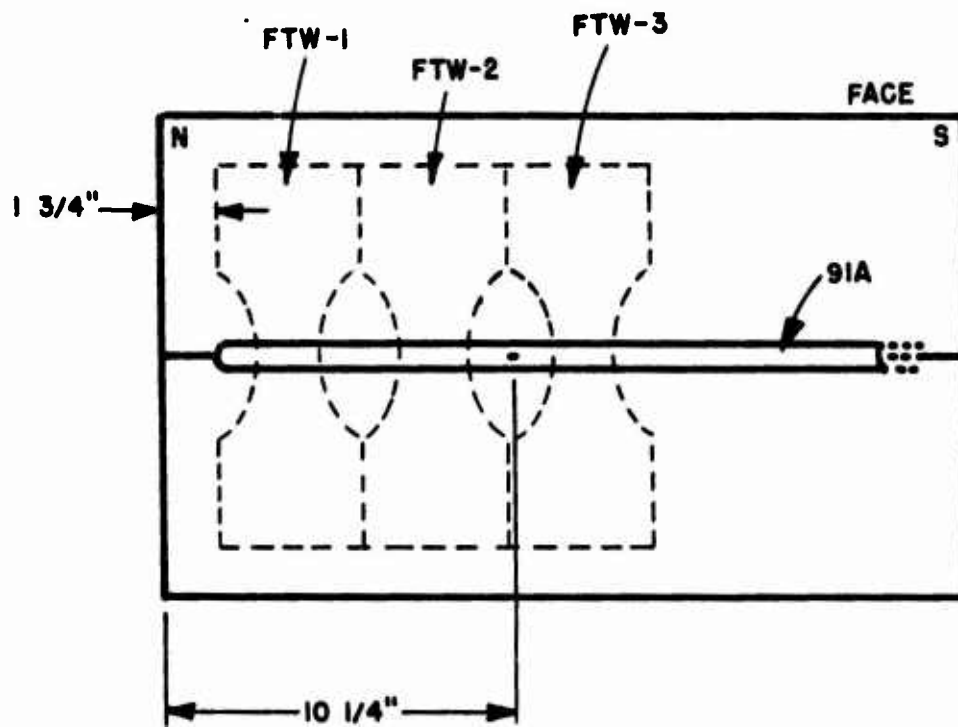


Ti-C (4) 1/4"

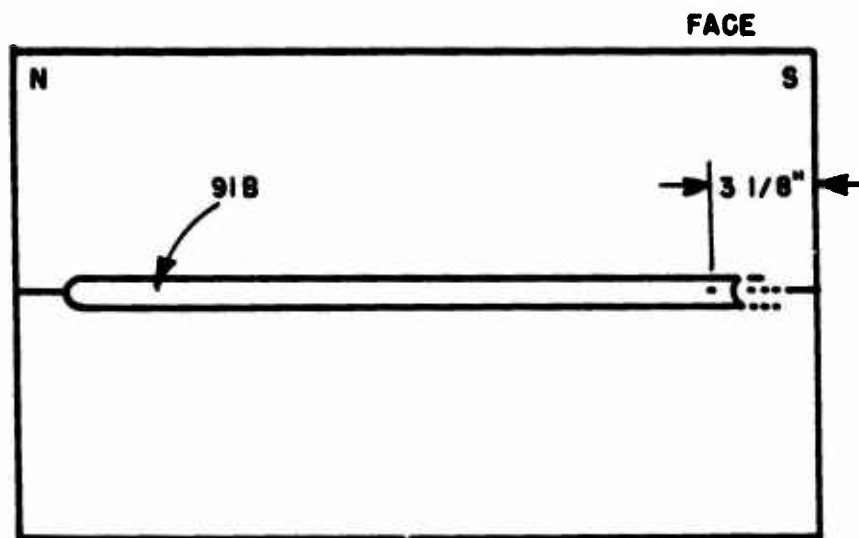
FACE



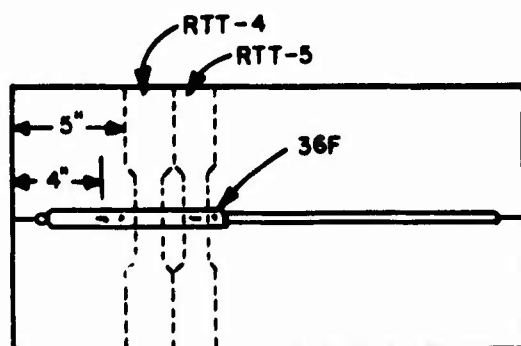
TI - D(1) 1/4"



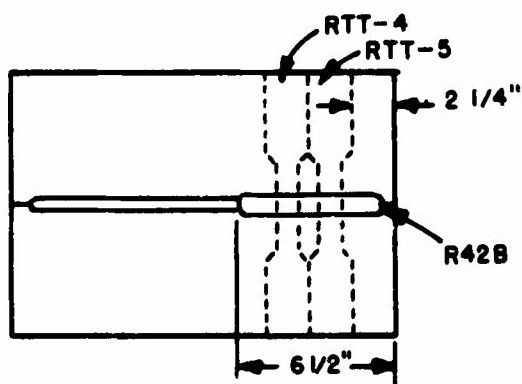
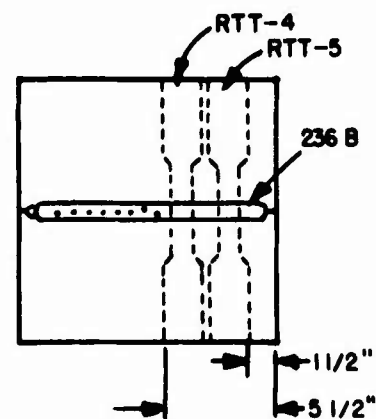
TI - E (2) 1/4"



300H ALLOY STEEL REPAIR PLATE - 3/8"



718 INCONEL REPAIR PLATE - 3/8"



6AL-4V TITANIUM REPAIR PLATE
(3/8")

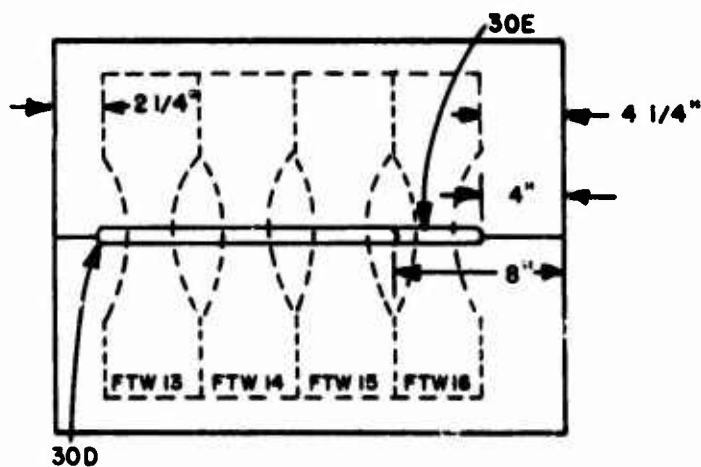


PLATE RAAA TITANIUM - 1/4"

APPENDIX C

**CORRELATION OF
FRACTURE FACE
OBSERVATION,
WELDING PROCEDURE**

TEST WELD CROSS-SECTION

FRACTURE FACE EXAMINATION & WELD PROCEDURE

Tables C-1 and C-2 are tabulations of the results of macroscopic examination of the fracture faces of all the specimens used for mechanical properties determination. Except where noted, all weld discontinuities observed and recorded in the tables are pores and have characteristic spherical shapes. They are tabulated in columns to indicate their number and approximate size. It should be noted that most of the pores observed were less than 2 percent of the joint thickness which would not be easily identified using conventional radiographic inspection methods. Shrink tears discovered in some specimens are noted in the comment column. These tears were not included in the measurement column because of irregular shapes.

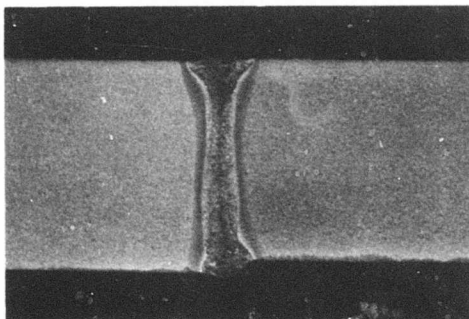
Representative cross sections of the test panel weld procedures tabulated below will be found on the following pages:

IDENTIFICATION					WELDING PROCEDURE							Porosity Size (inches)					REMARKS
Matl.	Thk.	Test	Spec. #	Weld #	kW	Speed	Focus	Shield Gas	Ar	Sb	L	.003"	.005"	.010"	.018"	.018"	Failure Location and/or Comment
300M Alloy Steel	1/4"	Tensile	ATT-1S	95A	7.7	100	28.1	100	25	7/16	.03						Fusion Line
			ATT-2S														Fusion Line
			ATT-3S														Fusion Line
			ALT-1S	95F													Shrink Tear
			ALT-2S	95E													Shrink Tear
			ALT-3S	95D								1					Shrink Tear
		Fatigue	FTW-1S	118D	8.0												Base Metal
			FTW-2S	118E	8.0												Base Metal
			FTW-3S	118F	7.7												
			FTW-4S	118A	8.0							1					Shrink Tear
			FTW-5S	118B								5	1				Base Metal
			FTW-6S	118C													
		Stress Corr.	SCS-1S	95C													
			SCS-2S														Shrink Tear
			SCS-3S														
	3/8"	Tensile	ATT-4S	256C	11.2	65	28.1	100	25	7/16	0.04						Shrink Tear
			ATT-5S	256C													Shrink Tear
			RTT-4S	R36F		58			0	NA	NA						Shrink Tear
			RTT-5S	R36F		58			0	NA	NA						Shrink Tear
	1/2"	Tensile	ATT-7S	202B	13.5	30	32.5	100	25	3/8	.03				1		
			ATT-8S														
			ATT-9S														Shrink Tear
			ALT-7S	205A											1		
			ALT-8S	204B													
			ALT-9S	203B													
		Fracture Tough.	FAW-4S	200C								7	1				
			FAW-5S	200C								2					
			FAW-6S	201A								1					
		Stress Corr.	SCK-4S														
			SCK-5S														
			SCK-6S	200C													
		Fatigue	FTW-7S	206D									3	1*			*Origin
			FTW-8S	206C								10	2				
			FTW-9S	207D								8		1	1*		*Origin
			FTW-10S	207C													
			FTW-11S	207B								2*/14	1				*Origin
			FTW-12S	206B								7	1				Shrink Tear

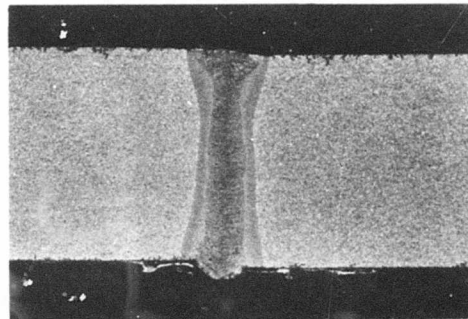
Table C-1: Fracture Face Examination

IDENTIFICATION					WELDING PROCEDURE								Porosity					REMARKS
Matl.	Thk.	Test	Spec. #	Weld#	Variables			Shield Gases		Trailer Shield		L	Size (Inches)					Failure Location and for Comment
					kW	Speed	Focus	He	Ar	Sb	L		.003"	.005"	.010"	.018"	.018"	
718 Inconel	1/4"	Tensile	ATT-1N	94D	7.0	100	28.1	100	25	7/16	.03							
			ATT-2N															
			ATT-3N															
			ALT-1N	93B														
			ALT-2N	93E														
			ALT-3N	93D														Shrink Tear
	3/8"	Tensile	ATT-4N	254B	11.2	70	28.1	100	25				7					
			ATT-5N	254B	11.2	70	28.1						8	2				
			RTT-4N	R36B	10.5	67.5	28.1	100	0	NA	NA		8	5				
			RTT-5N	R36B									5					
6Al-4V Titanium	1/4"	Tensile	ATT-1T	91C	7.0	100	28.1	100	25	3/8	.04							Fusion Line
			ATT-2T										1					Fusion Line
			ATT-3T															
			ALT-1T	90F														
			ALT-2T	90L														
			ALT-3T	90D														
		Fatigue	FTW-1T	91A										1*	2	3		*Origin, not Face
			FTW-2T															
			FTW-3T															
			FTW-4T	91C									5					
			FTW-5T										1		1			
			FTW-6T										4					
			FTW-13T	30D	8.4	100	28.1	100	NA	NA	NA		60					
			FTW-14T										23*					*Origin
			FTW-15T										17*					*Origin
			FTW-16T	30E									13*					*Origin
	3/8"	Tensile	ATT-4T	254F	11.2	70	28.1	100	25	7/16	0.04							Base Metal
			ATT-5T	254F														Base Metal
			RTT-4T	R42B	11.2	63	28.1	50	12	NA	NA							Base Metal
			RTT-5T	R42B														
	1/2"	Tensile	ATT-7T	239A	12.1	30	32.5	100	50	3/8	.03							Base Metal
			ATT-8T	239A	12.1								10			2		Base Metal
			ATT-9T	242B	13.1													
			ALT-7T	241B														
			ALT-8T	241A														
			ALT-9T	242A														
		Fracture Tough.	FAW-4T	246A									100	6	1			
			FAW-5T	246A									10	4				
			FAW-6T	246B														
		Stress Corr.	SCK-1T							65								
			SCK-2T															
			SCK-3T															
		Fatigue	FTW-7T	245A				140					10		1			
			FTW-8T	245B				100					1*	2*	5			*Origin
			FTW-9T	244B														
			FTW-10T	244A									10	1*				*Origin
			FTW-11T	246A														
			FTW-12T	243A									6	1		1*		*Origin

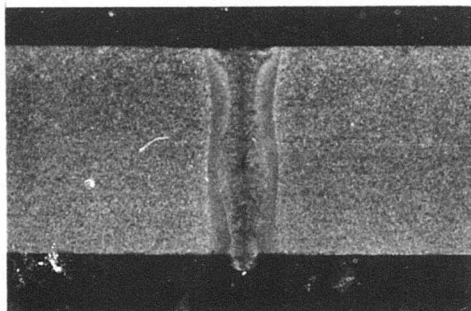
Table C-2: Fracture Face Examination



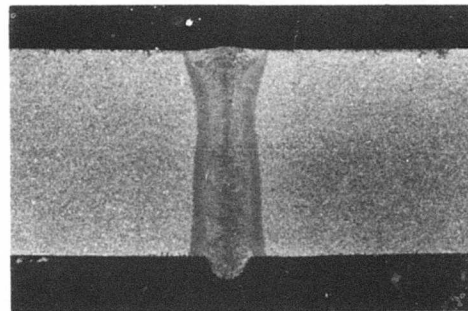
Negative No. LR-222 Mag. 4.7
(a) Weld No. 95A



Negative No. LR-219 Mag. 4.7X
(c) Weld No. 118E

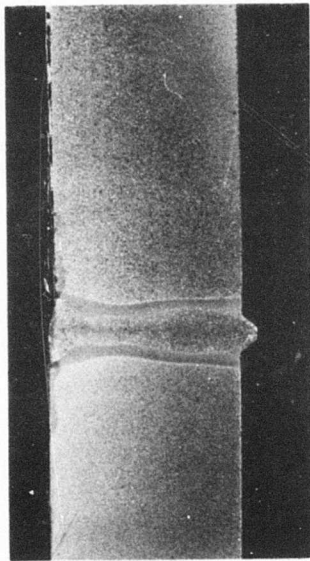


Negative No. LR-221 Mag. 4.7X
(c) Weld No. 118F

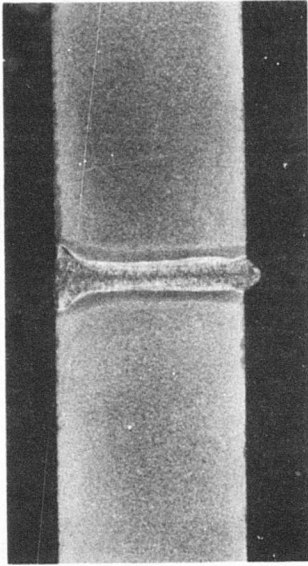


Negative No. LR-220 Mag. 4.7X
(d) Weld No. 118F

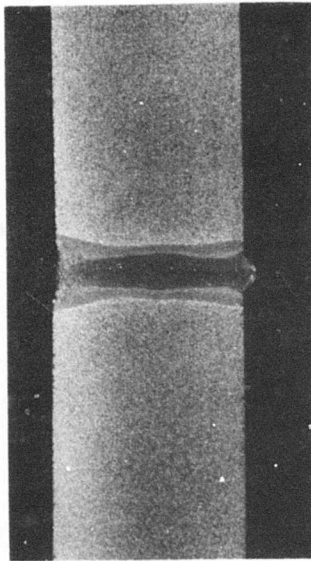
Figure C-1. WELD CROSS SECTIONS (LOW ALLOY CARBON STEEL)
1/4 INCH THICK



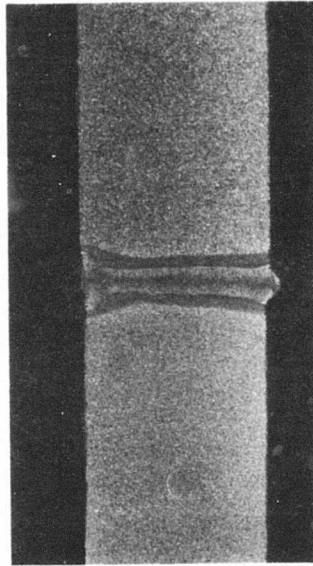
Negative No. LR-215
(a) Weld No. 118A
Mag. 4.9X



Negative No. LR-216
(b) Weld No. 118B
Mag. 4.7X

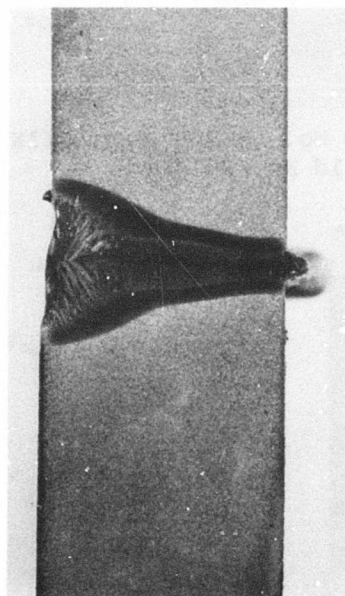


Negative No. LR-217
(c) Weld No. 118C
Mag. 4.7



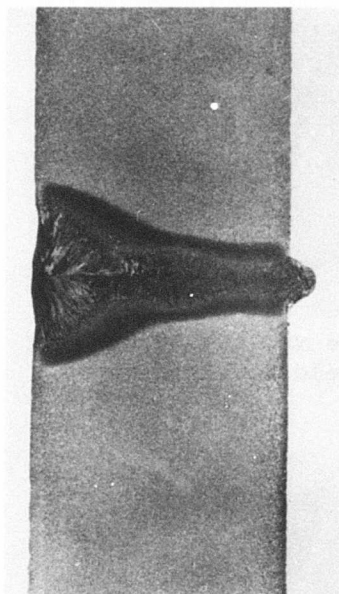
Negative No. LR-218
(d) Weld No. 118D
Mag. 4.8

Figure C-2. WELD CROSS SECTIONS (LOW ALLOY CARBON STEEL TEST SPECIMENS) 1/4 INCH THICK



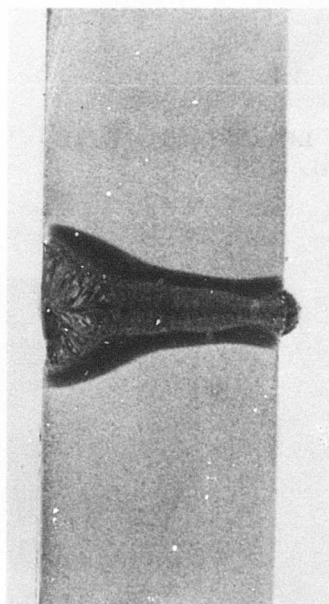
Negative No. LR-202
(a) Weld No. 206B

Mag. 3.1X



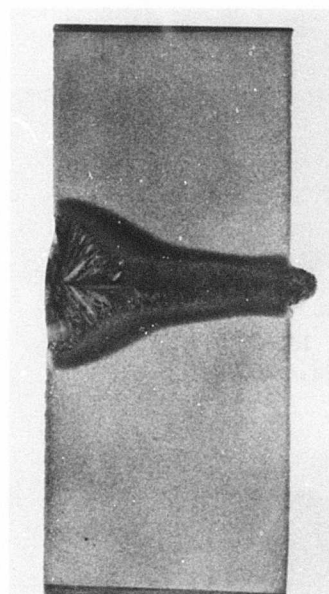
Negative No. LR-206
(b) Weld No. 207C

Mag. 3.2X



Negative No. LR-205
(c) Weld No. 207B

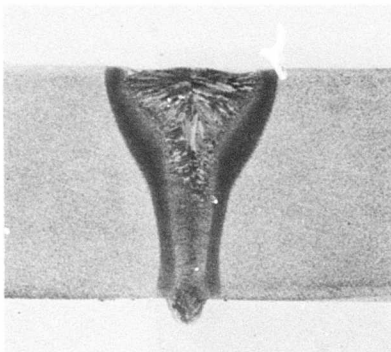
Mag. 2.9X



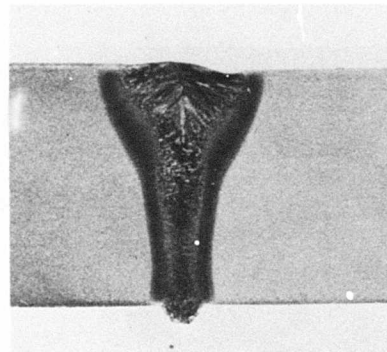
Negative No. LR-203
(d) Weld No. 206C

Mag. 3X

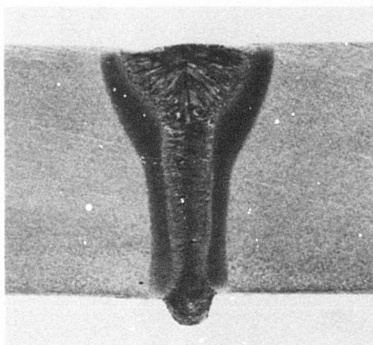
Figure C-3. WELD CROSS SECTIONS (LOW ALLOY CARBON STEEL
TEST SPECIMENS) 1/2 INCH THICK



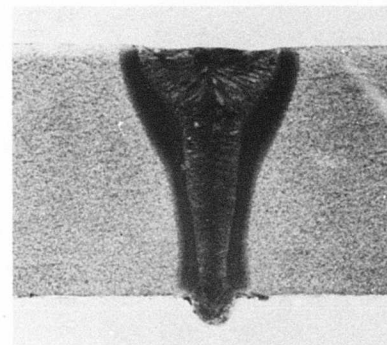
Negative No. LR-207 Mag. 2.9X
(a) Weld No. 207D



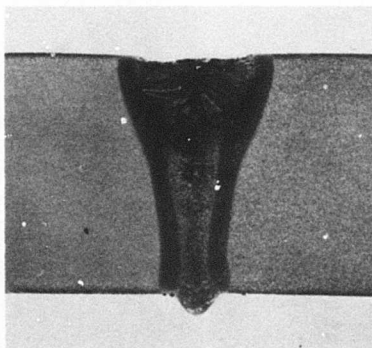
Negative No. LR-204 Mag. 3X
(b) Weld No. 206D



Negative No. LR-199 Mag. 3.1X
(c) Weld No. 200C

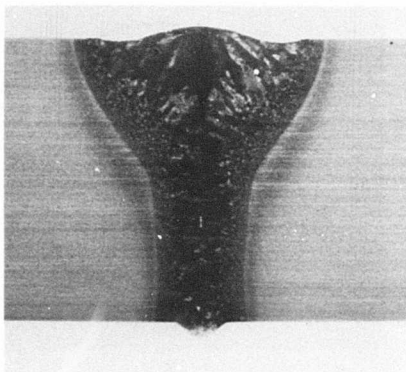


Negative No. LR-200 Mag. 3.1X
(d) Weld No. 201A

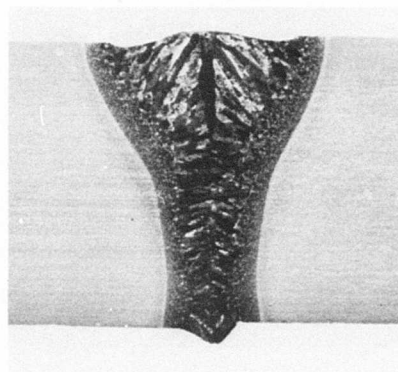


Negative No. LR-201 Mag. 3X
(e) Weld No. 202B

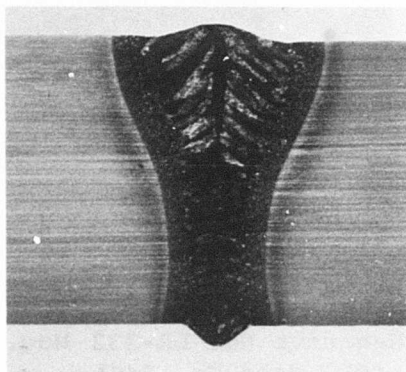
Figure C-4. WELD CROSS SECTIONS (LOW ALLOY CARBON STEEL)
1/2 INCH THICK



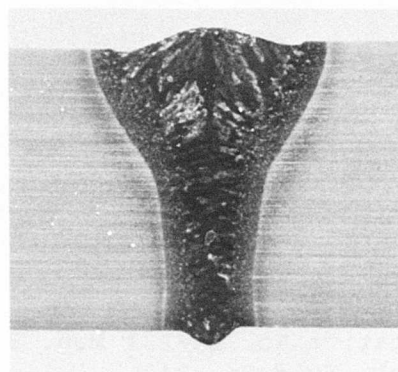
Negative No. LR-235 Mag. 3.3X
(a) Weld No. 246A



Negative No. LR-236 Mag. 3.3
(b) Weld No. 246B

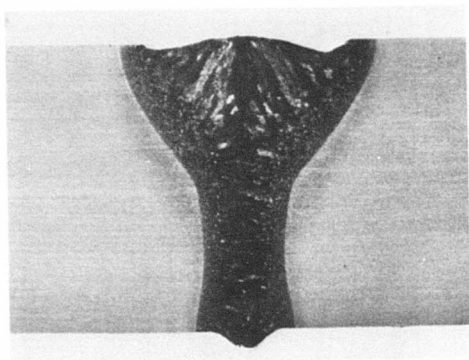


Negative No. LR-233 Mag. 3.3X
(c) Weld No. 245A

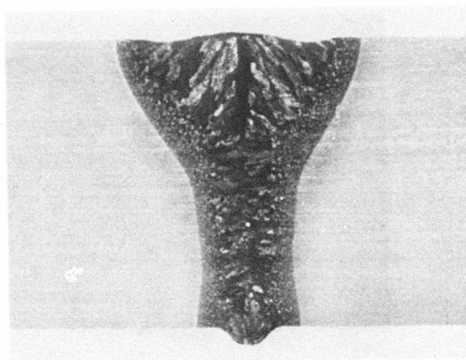


Negative No. LR-234 Mag. 3.3X
(d) Weld No. 245B

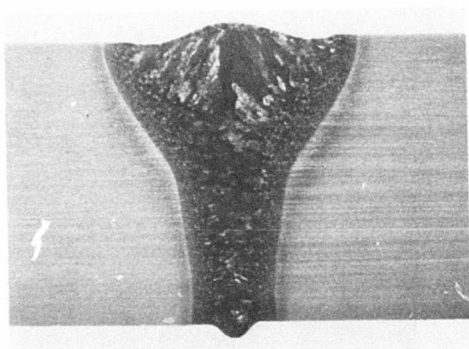
Figure C-5. WELD CROSS SECTIONS (TITANIUM ALLOY) TEST
SPECIMENS 1/2 INCH THICK



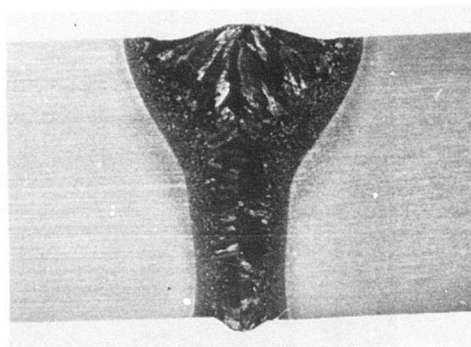
Negative No. LR-226 Mag. 3.3X
(a) Weld No. 239A



Negative No. LR-230 Mag. 3.3X
(b) Weld No. 242B

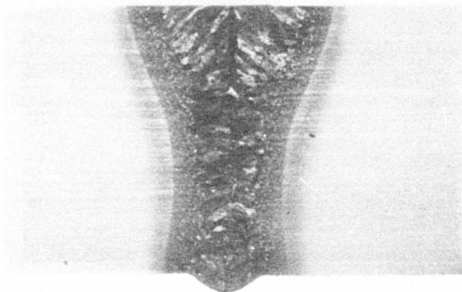


Negative No. LR-231 Mag. 3.3X
(c) Weld No. 243A

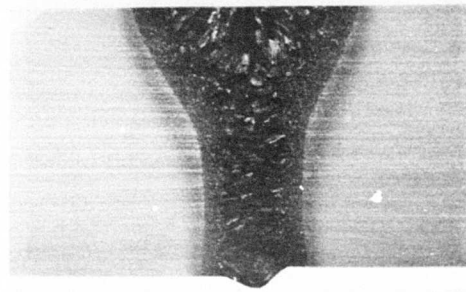


Negative No. LR-232 Mag. 3.3X
(d) Weld No. 244A

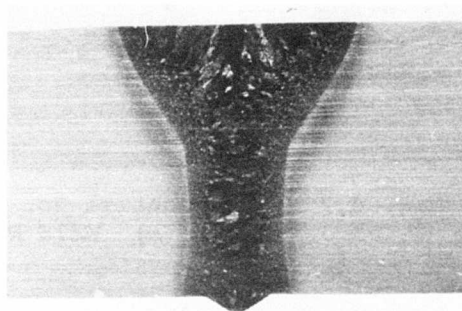
Figure C-6. WELD CROSS SECTIONS (TITANIUM ALLOY) TEST
SPECIMENS 1/2 INCH THICK



Negative No. LR-228 Mag. 3.3X
(a) Weld No. 241B

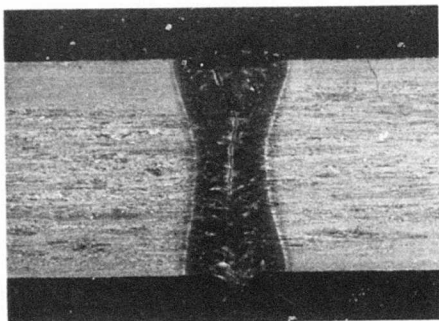


Negative No. LR-227 Mag. 3.1X
(b) Weld No. 241A

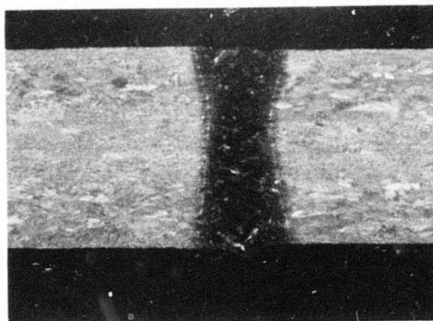


Negative No. LR-229 Mag. 3.3X
(c) Weld No. 242A

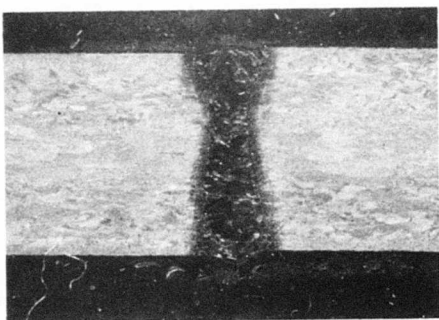
Figure C-7. WELD CROSS SECTIONS (TITANIUM ALLOY) TEST
SPECIMENS 1/2 INCH THICK



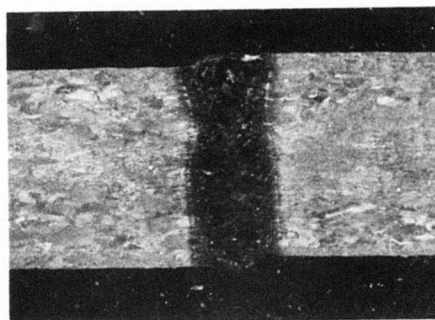
Negative No. LR-246 Mag. 4.5X
(a) Weld No. 91C



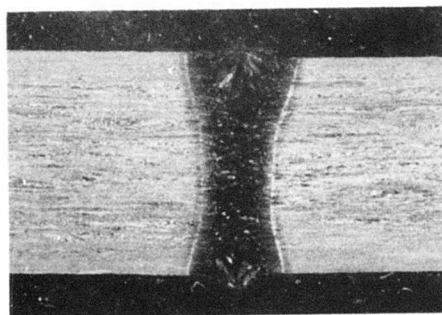
Negative No. LR-242 Mag. 4.2X
(b) Weld No. 90D



Negative No. LR-244 Mag. 4.2
(c) Weld No. 90F

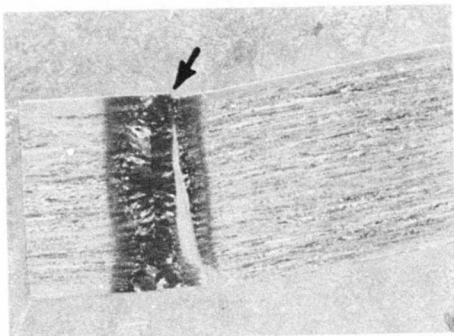


Negative No. LR-243 Mag. 4.4
(d) Weld No. 90E

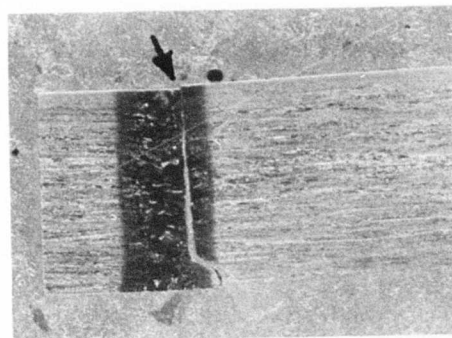


Negative No. LR-245 Mag. 4.6X
(e) Weld No. 91A

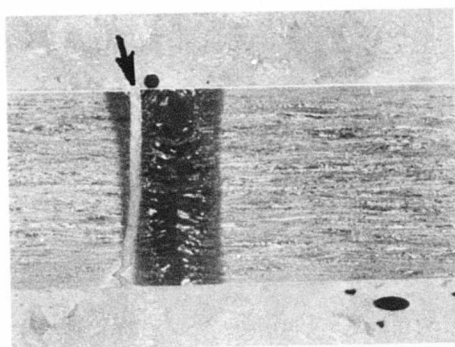
Figure C-8. WELD CROSS SECTIONS (TITANIUM ALLOY SPECIMENS)
1/4 INCH THICK



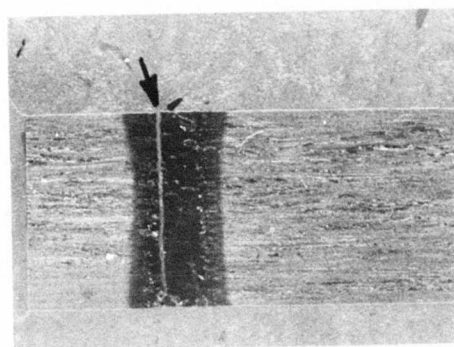
Negative No. LR-237 Mag. 4.8X
(a) Fatigue Spec. #FTW-2T



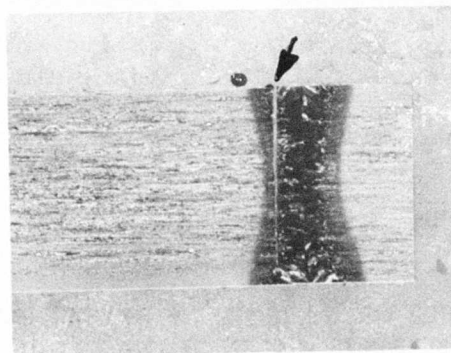
Negative No. LR-238 Mag. 4.8X
(b) Fatigue Spec. #FTW-3T



Negative No. LR-239 Mag. 4.7X
(c) Fatigue Spec. #FTW-4T

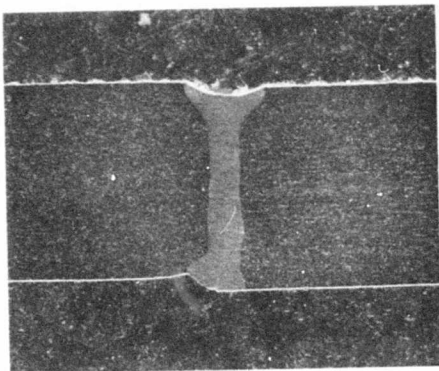


Negative No. LR-240 Mag. 4.7X
(d) Fatigue Spec. #FTW-5T

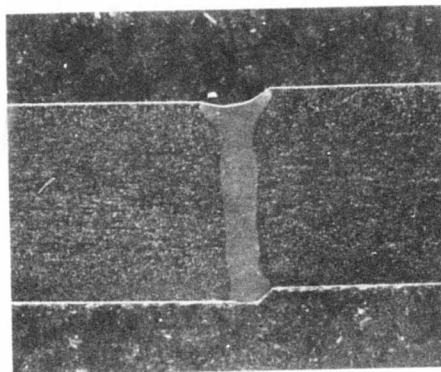


Negative No. LR-241 Mag. 4.7X
(e) Fatigue Spec. #FTW-6T

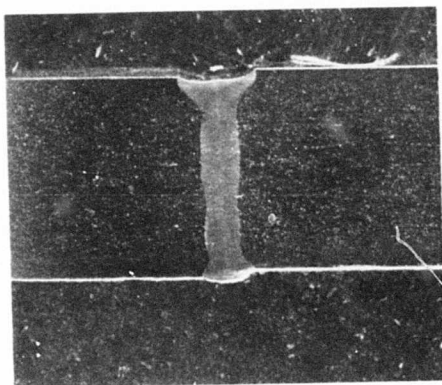
Figure C-9. WELDED FATIGUE SPECIMEN SECTIONS (TITANIUM ALLOY)
1/4 INCH THICK (ARROWS INDICATE CRACK INITIATION)



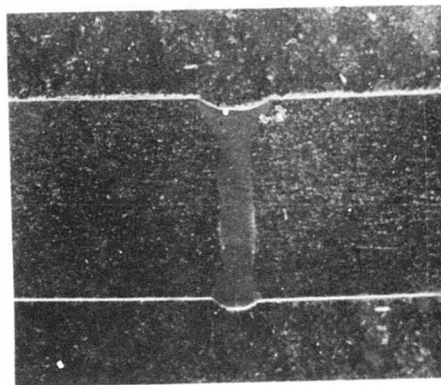
Negative No. LR-211 Mag. 4.7
(a) Weld No. 93B



Negative No. LR-212 Mag. 4.7
(b) Weld No. 93D

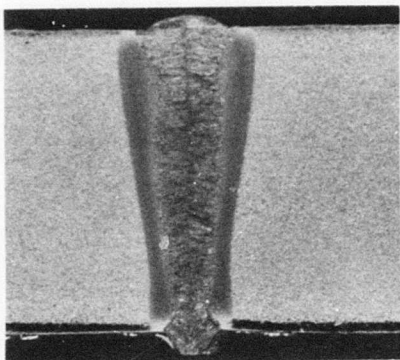


Negative No. LR-214 Mag. 4.7
(c) Weld No. 94D

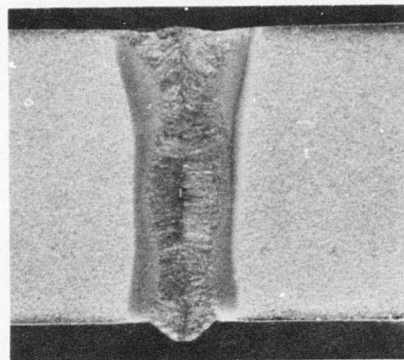


Negative No. LR-213 Mag. 4.7
(d) Weld No. 93E

Figure C-10. WELD CROSS SECTIONS (NICKEL BASE ALLOY) TEST SPECIMENS 1/4 INCH THICK

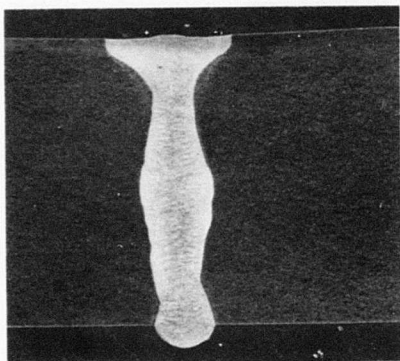


Neg. No. LR-526 Mag. 4.9X
(a) Tensile Specimen #ATT-5S

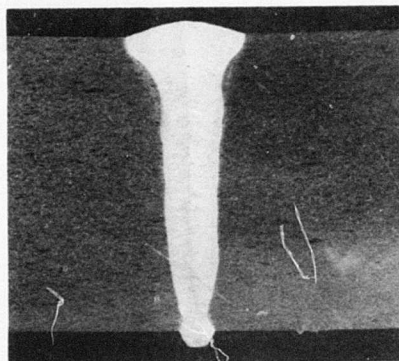


Neg. No. LR-527 Mag. 4.9X
(b) Weld No. 36F

Figure C-11. 300 M ALLOY STEEL WELD CROSS SECTIONS (3/8 INCH THICK)

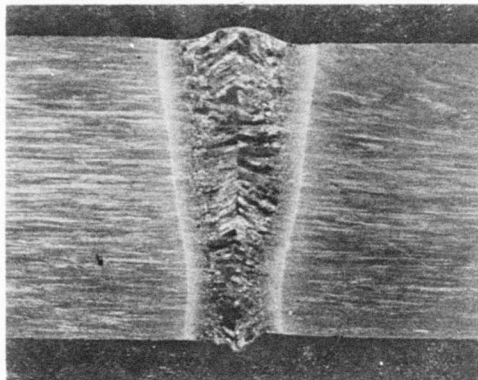


Neg. No. LR-521 Mag. 4.4X
(a) Weld No. R36B

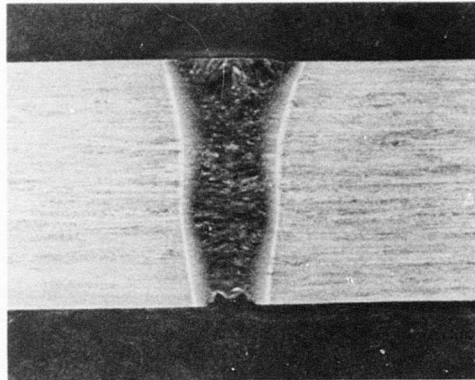


Neg. No. LR-522 Mag. 4.4X
(b) Weld No. 252C

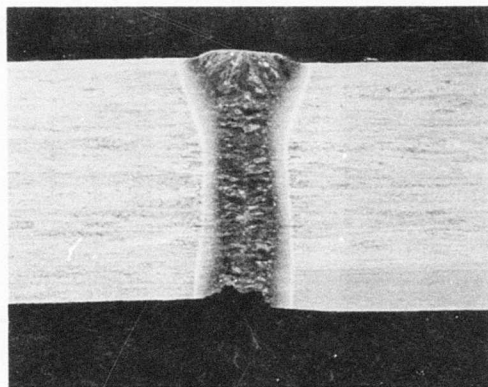
Figure C-12. INCONEL 718 WELD CROSS SECTIONS (3/8 INCH THICK)



Neg. No. LR-523 Mag. 4.4X
(a) Weld No. 254C



Neg. No. LR-524 Mag. 5.4X
(b) Weld No. 30D



Neg. No. LR-525 Mag. 5.4X
(c) Weld No. 30E

Figure C-13. 6Al-4V TITANIUM WELD CROSS SECTION (3/8 INCH THICK)

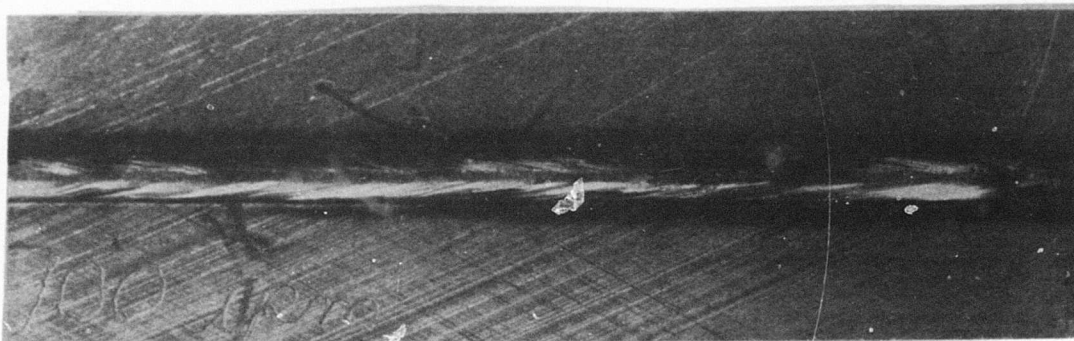
APPENDIX D

**CORRELATION OF
PROCESS SETTINGS**

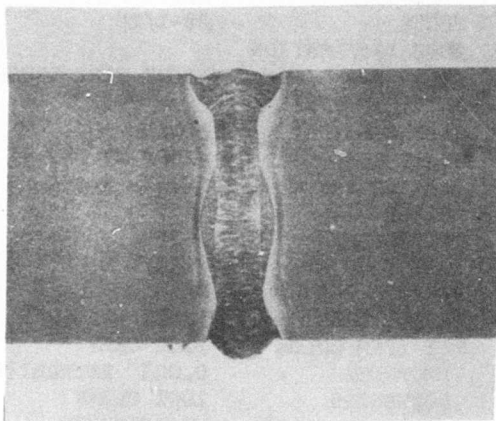
TEST WELD CROSS-SECTION

MATERIAL: LA C/S 300 M 1/4"

POWER RECORD: 72C



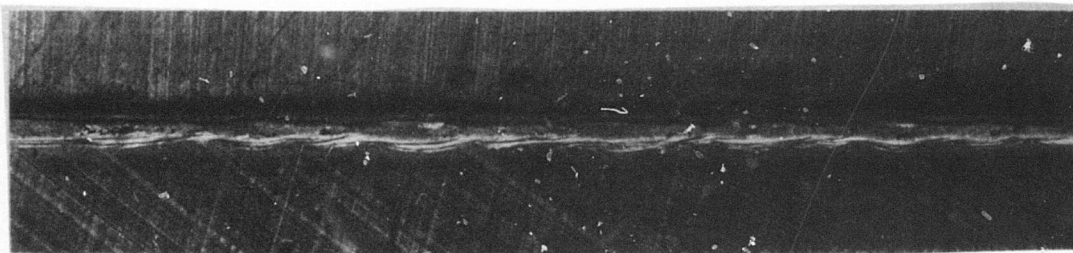
TOP BEAD 3X



6X

POWER ON WORK	8.4 KW
TRAVEL SPEED	100 IPM
TELESCOPE	f/7
FOCUS	28-1/8"
EDGE PREPARATION	
BLANCHARD GROUND-DEBURR-WIRE BRUSH-	
ACETONE RINSE	
WELD GAS (JET)	HELIUM 100 CFH
TRAIL GAS	ARGON 25 CFH
BACK-UP GAS	HELIUM 10 CFH
SHIELD	SR-7
STAND-OFF	.075"
SET-BACK	7/16"
FIXTURE	FDS
CHILL BAR	#210
TOP BEAD COLOR	METALLIC BLUE
UNDERCUT	0.005"*
SOUNDNESS	100% CLEAR
UNDERBEAD COLOR	WHITE
SHAPE	.05" WIDE X .025"***

*REMARKS	INTERMITTENT
**REMARKS	.020" MISMATCH



UNDER BEAD 3X

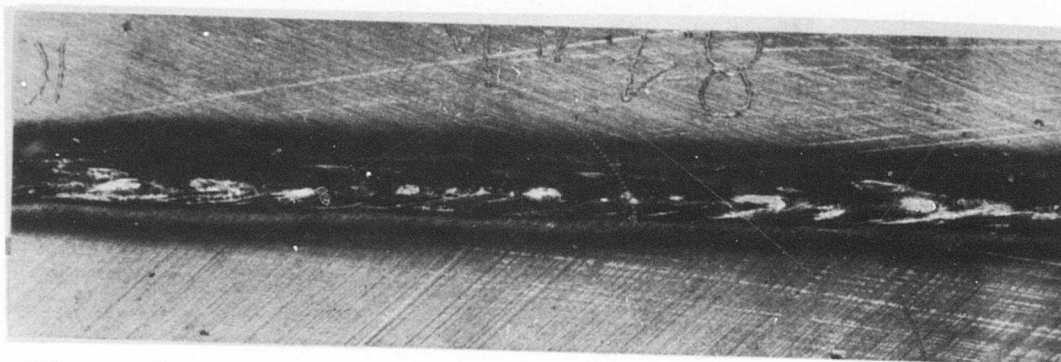
M-2650

L-2470

JUNE 1975

MATERIAL: LA C/S 300 M 1/4"

POWER RECORD: 72D



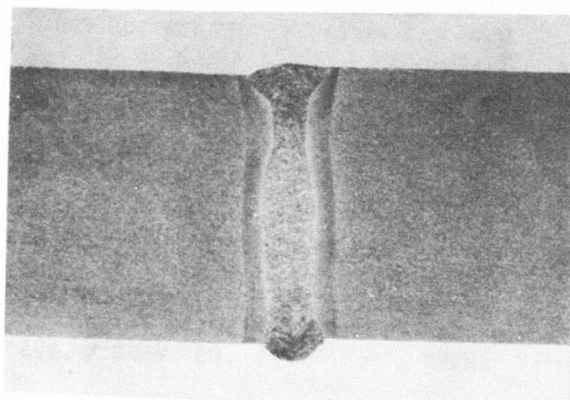
TOP BEAD 3X

POWER ON WORK 8.4 KW
TRAVEL SPEED 100 IPM
TELESCOPE f/7
FOCUS 28-1/2"

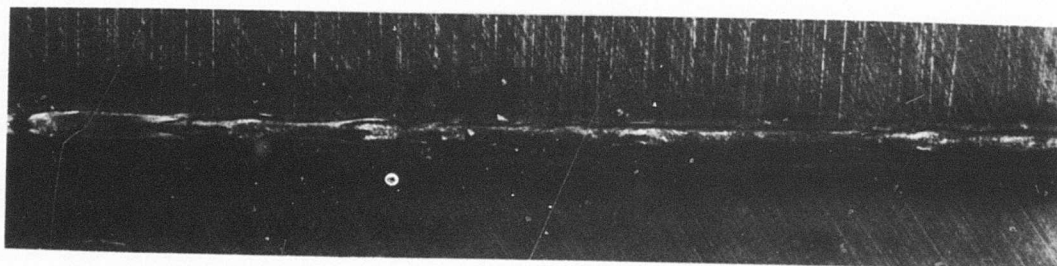
EDGE PREPARATION

BLANCHARD GROUND-DEBURR-WIRE BRUSH
ACETONE RINSE

WELD GAS (JET) HELIUM 100 CFH
TRAIL GAS ARGON 25 CFH
BACK-UP GAS HELIUM 5 CFH
SHIELD SR-7
STAND-OFF .075"
SET-BACK 7/16"
FIXTURE FDS
CHILL BAR #210
TOP BEAD COLOR BLUE-GREY
UNDERCUT 0.005" INTERMITTENT
SOUNDNESS 100% CLEAR
UNDERBEAD COLOR WHITE-BRUSH
SHAPE .05" WIDE X .025"



6X



UNDERBEAD 3X

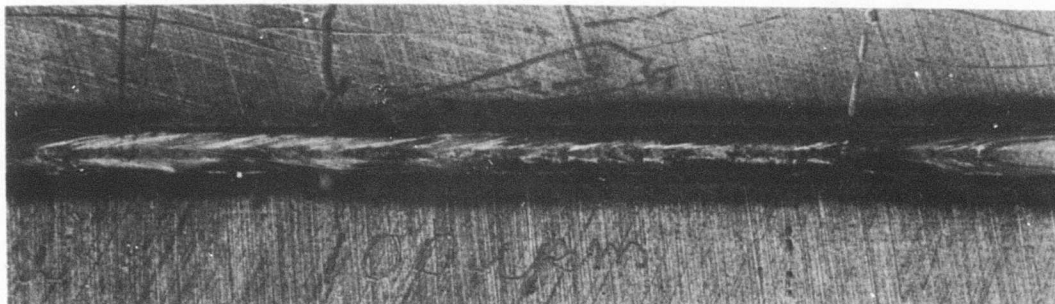
M-2651

L-2470

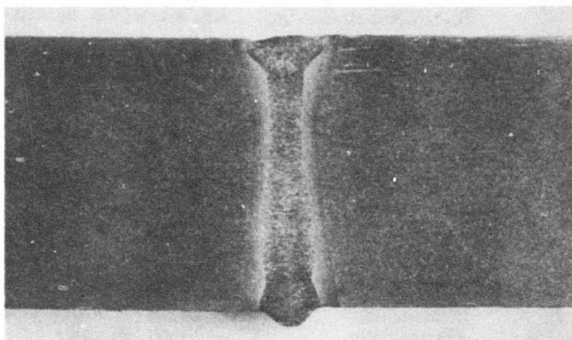
JUNE 1975

MATERIAL: LA C/S 300 M 1/4"

POWER RECORD: 72E



TOP BEAD 3X



6X

POWER ON WORK	8.4 KW
TRAVEL SPEED	100 IPM
TELESCOPE	f/7
FOCUS	28-1/8"
EDGE PREPARATION	
BLANCHARD GROUND-DEBURR-WIRE BRUSH -	
ACETONE RINSE-DETERGENT-ALCOHOL DRY	
WELD GAS (JET)	HELIUM 100 CFH
TRAIL GAS	ARGON 25 CFH
BACK-UP GAS	HELIUM 10 CFH
SHIELD	SR-7
STAND-OFF	.075"
SET-BACK	7/16"
FIXTURE	FDS
CHILL BAR	#210
TOP BEAD COLOR	BLUE GREY
UNDERCUT	NONE
SOUNDNESS	100% CLEAR
UNDERBEAD COLOR	WHITE
SHAPE	.05" WIDE X .025"*

*REMARKS VERY SMOOTH



UNDERBEAD 3X

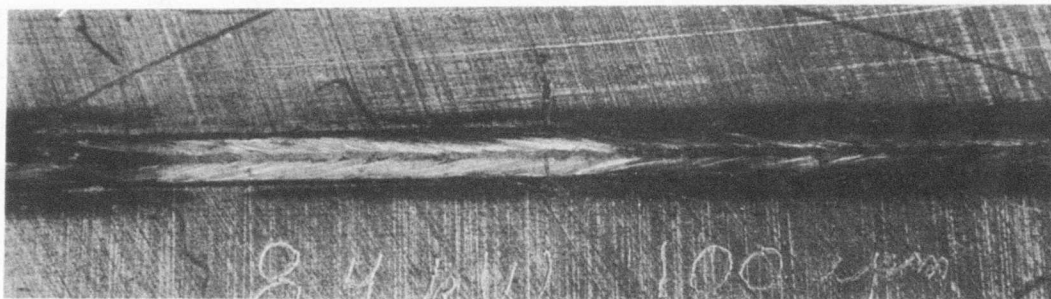
M-2649

L-2470

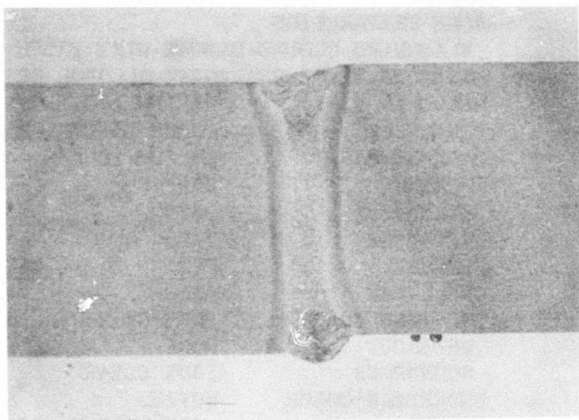
JUNE 1975

MATERIAL: LA C/S 300 M 1/4"

POWER RECORD: 72F

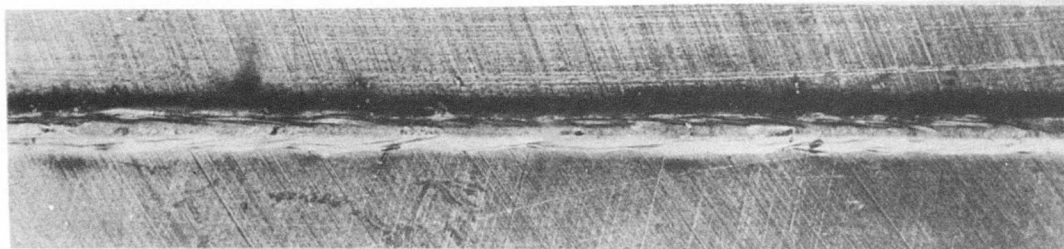


TOP BEAD 3X



POWER ON WORK	8.4 KW
TRAVEL SPEED	100 IPM
TELESCOPE	f/7
FOCUS	28-1/8"
EDGE PREPARATION	
	BLANCHARD GROUND-DEBURR-WIRE BRUSH-
	ACETONE RINSE-DETERGENT-ALCOHOL DRY
WELD GAS (JET)	HELIUM 100 CFH
TRAIL GAS	ARGON 35 CFH
BACK-UP GAS	HELIUM 10 CFH
SHIELD	SR-7
STAND-OFF	.075"
SET-BACK	7/16"
FIXTURE	FDS
CHILL BAR	#210
TOP BEAD COLOR	BLUE-GREY
UNDERCUT	NONE - VERY GOOD
SOUNDNESS	100% CLEAR
UNDERBEAD COLOR	WHITE
SHAPE	.06" WIDE X .025"

6X



UNDERBEAD 3X

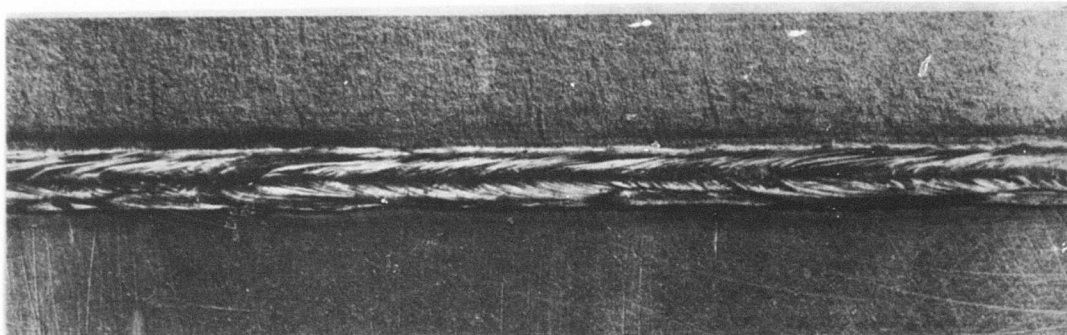
M-2648

L-2470

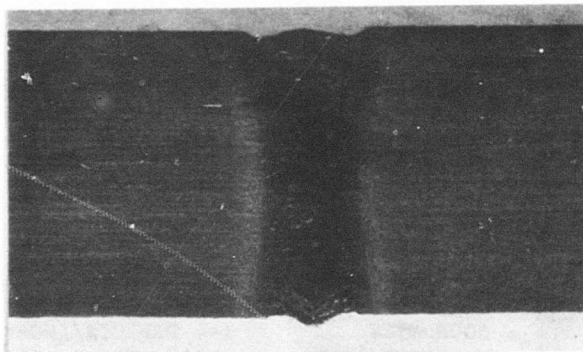
June 1975

MATERIAL: TITANIUM 6-4 1/4"

POWER RECORD: 75A

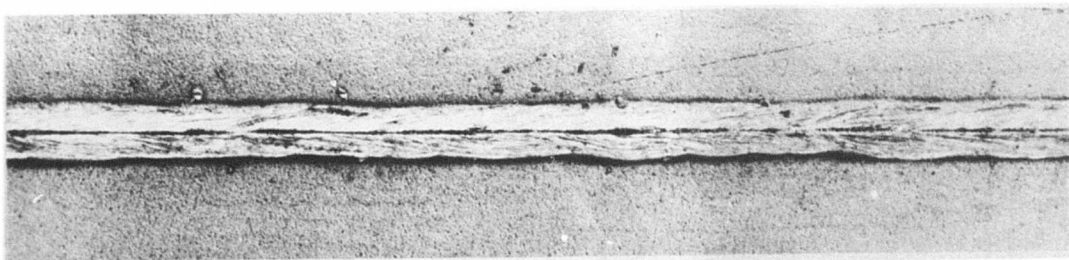


TOP BEAD 3X



6X

POWER ON WORK	7.0 KW
TRAVEL SPEED	100 IPM
TELESCOPE	f/7
FOCUS	28"
EDGE PREPARATION	
BLANCHARD GROUND-DEBURR-WIRE BRUSH	
ACETONE RINSE	
WELD GAS (JET)	HELIUM 100 CFH
TRAIL GAS	ARGON 25 CFH
BACK-UP GAS	HELIUM 10 CFH
SHIELD	SR-7
STAND-OFF	.07"
SET-BACK	7/16"
FIXTURE	FDS
CHILL BAR	#210
TOP BEAD COLOR	METALLIC
UNDERCUT	NONE
SOUNDNESS	1-4 DEFECTS/INCH
UNDERBEAD SHAPE	.100" WIDE X .015"



UNDER BEAD 3X

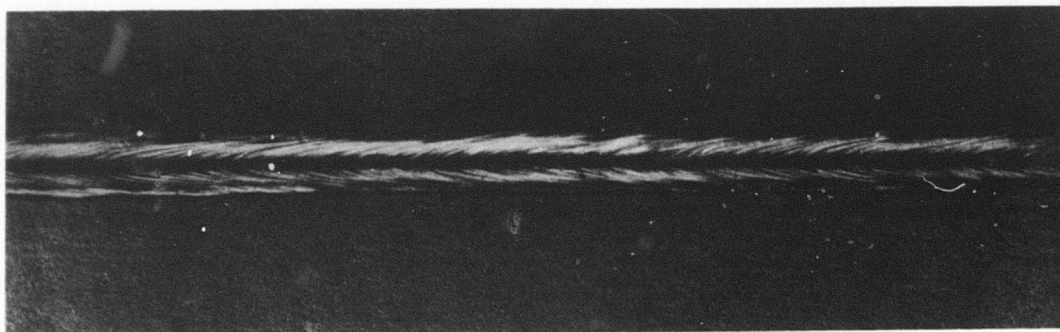
M-2638

L-2470

JUNE 1975

MATERIAL: TITANIUM 6-4 1/4"

POWER RECORD: 75B



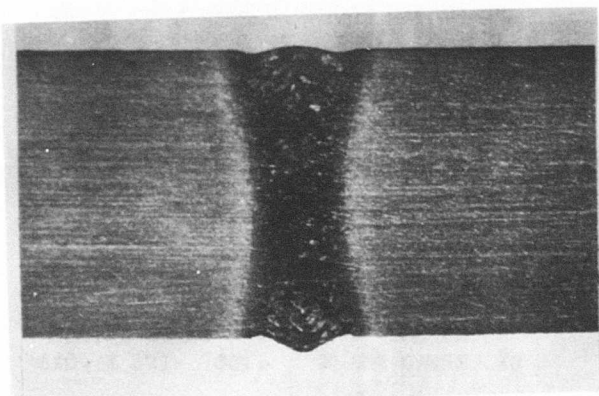
TOP BEAD 3X

POWER ON WORK 7.0 KW
TRAVEL SPEED 100 IPM
TELESCOPE f/7
FOCUS 28-1/4"

EDGE PREPARATION

BLANCHARD GROUND-DEBURR-WIRE BRUSH-
ACETONE RINSE

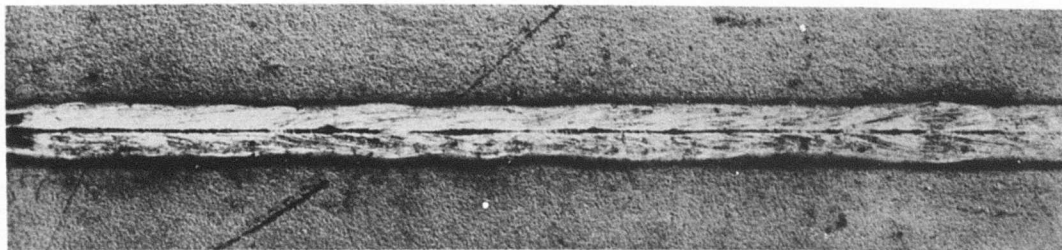
WELD GAS (JET) HELIUM 100 CFH
TRAIL GAS ARGON 25 CFH
BACK-UP GAS HELIUM 10 CFH
SHIELD SR-7
STAND-OFF .04"
SET-BACK 7/16"
FIXTURE FDS
CHILL BAR #210
TOP BEAD COLOR METALLIC
UNDERCUT NONE
SOUNDNESS 1-4 DEFECTS/INCH*
UNDERBEAD SHAPE .100" WIDE X .015"



6X

*REMARKS

LACK OF PENETRATION



UNDERBEAD 3X

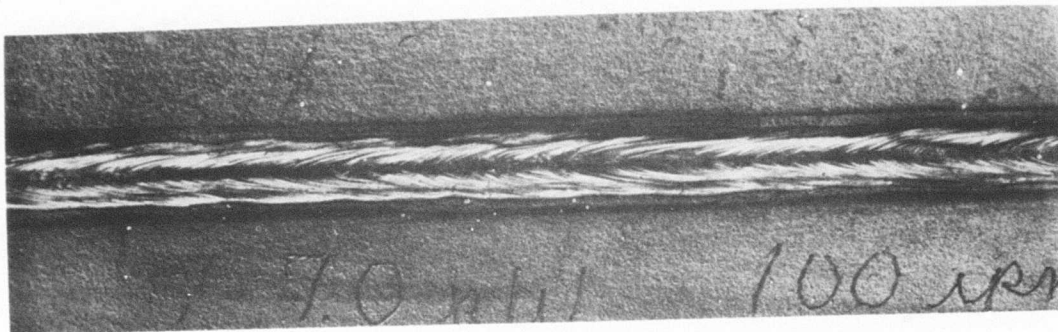
M-2639

L-2470

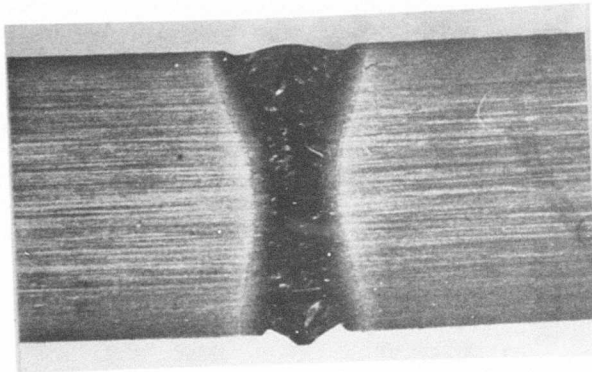
JUNE 1975

MATERIAL: TITANIUM 6-4 1/4"

POWER RECORD: 75C

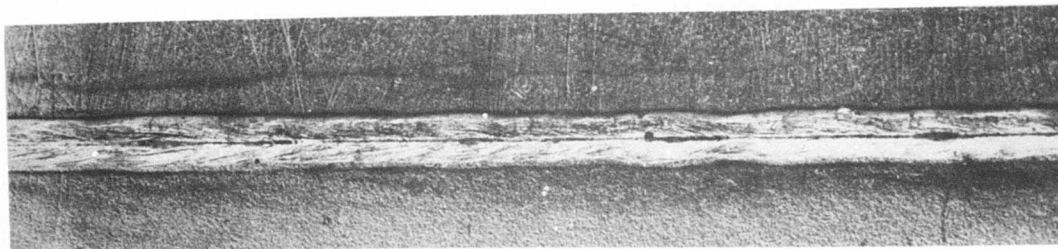


TOP BEAD 3X



6X

POWER ON WORK	7.0 KW
TRAVEL SPEED	100 IPM
TELESCOPE	f/7
FOCUS	28-1/8"
EDGE PREPARATION	
BLANCHARD GROUND-DEBURR-WIRE BRUSH-	
ACETONE RINSE-DETERGENT-	
HNO ₃ + HF + H ₂ O ETCH-	
WATER RINSE-ALCOHOL DRY	
WELD GAS (JET)	HELIUM 100 CFH
TRAIL GAS	ARGON 25 CFH
BACK-UP GAS	HELIUM 10 CFH
SHIELD	SR-7
STAND-OFF	.04"
SET-BACK	7/16"
FIXTURE	FDS
CHILL BAR	#210
TOP BEAD COLOR	METALLIC
UNDERCUT	NONE
SOUNDNESS	100% CLEAR
UNDERBEAD SHAPE	.100" WIDE X .015"



UNDER BEAD 3X

M-2640

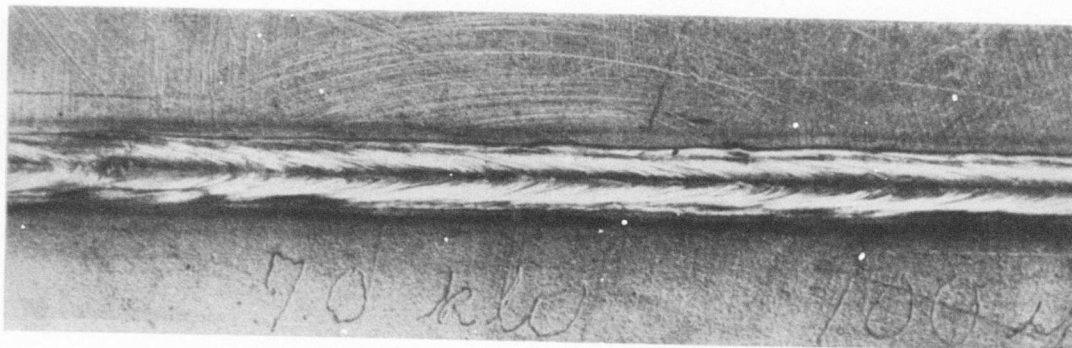
L-2470

JUNE 1975

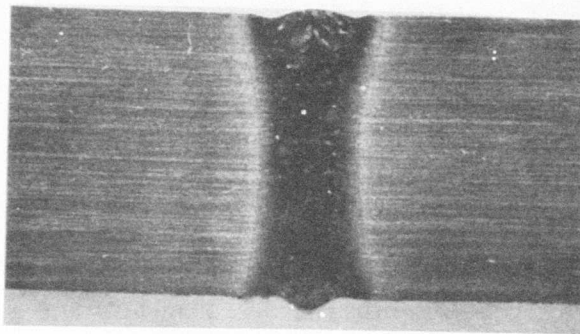
D-7

MATERIAL: TITANIUM 6-4 1/4"

POWER RECORD: 75D

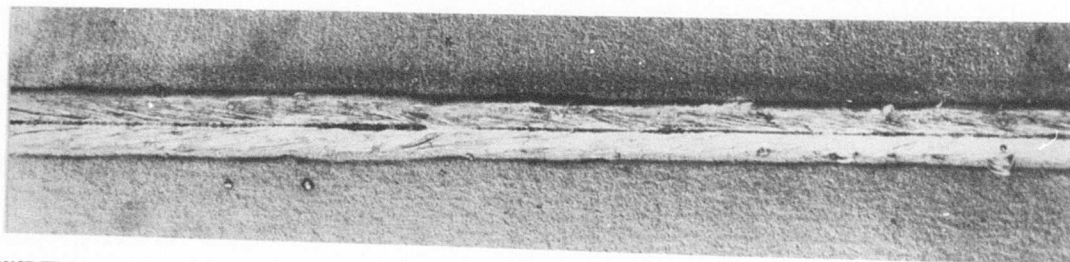


TOP BEAD 3X



6X

POWER ON WORK	7.0 KW
TRAVEL SPEED	100 IPM
TELESCOPE	f/7
FOCUS	28-1/8"
EDGE PREPARATION	
BLANCHARD GROUND-DEBURR-WIRE BRUSH -	
DETERGENT-ACETONE RINSE-	
HNO ₃ + HF + H ₂ O ETCH-	
WATER RINSE-ALCOHOL DRY	
WELD GAS (JET)	HELIUM 100 CFH
TRAIL GAS	ARGON 25 CFH
BACK-UP GAS	HELIUM 10 CFH
SHIELD	SR-7
STAND-OFF	.04"
SET-BACK	7/16"
FIXTURE	FDS
CHILL BAR	#210
TOP BEAD COLOR	METALLIC
UNDERCUT	NONE
SOUNDNESS	100% CLEAR
UNDERBEAD SHAPE	.095" WIDE X .015"



UNDER BEAD 3X

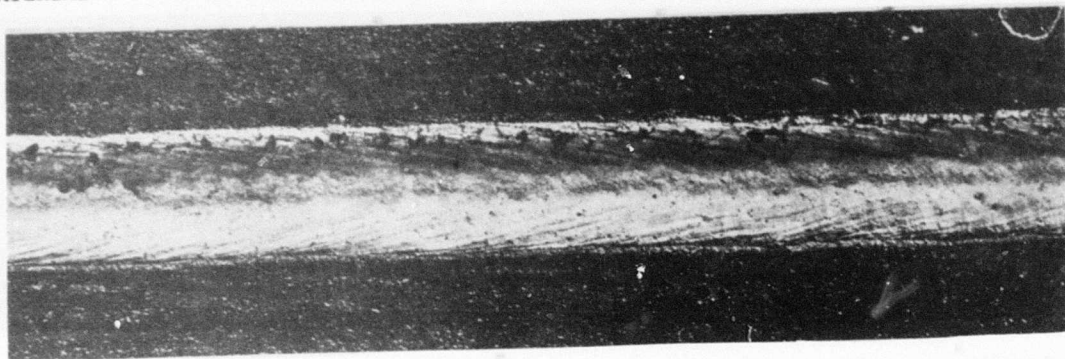
M-2641

L-2470

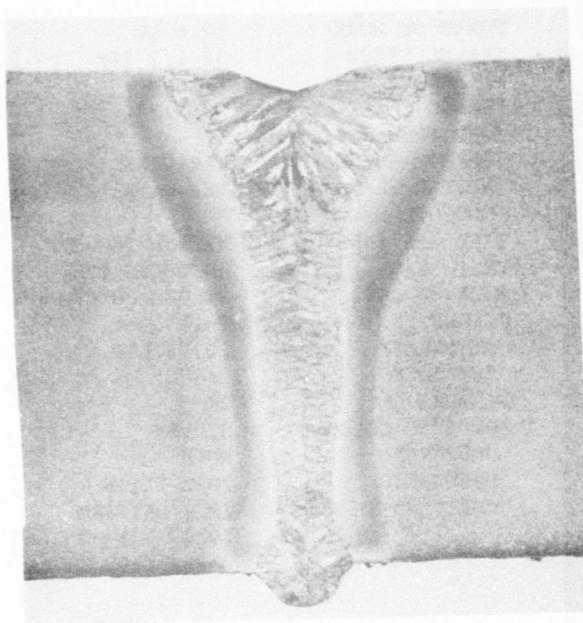
JUNE 1975

MATERIAL: LA C/S 300 M 1/2"

POWER RECORD: 80E

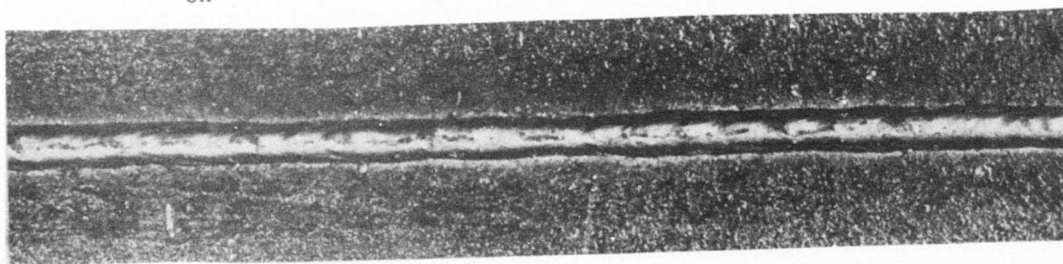


TOP BEAD 3X



6X

POWER ON WORK	13.5 KW
TRAVEL SPEED	30 IPM
TELESCOPE	f/20
FOCUS	32-1/2"
EDGE PREPARATION	
	BLANCHARD GROUND-DEBURR-WIRE BRUSH-
	ACETONE RINSE-DETERGENT-WATER RINSE-
	ALCOHOL DRY
WELD GAS (JET)	HELIUM 100 CFH
TRAIL GAS	ARGON 25 CFH
BACK-UP GAS	HELIUM 10 CFH
SHIELD	7-1
STAND-OFF	.03" FLAT
SET-BACK	1/4"
FIXTURE	24
TOP BEAD COLOR	SILVER
UNDERCUT	NONE
SOUNDNESS	100% CLEAR
UNDERBEAD COLOR	SILVER
SHAPE	VERY UNIFORM
	.086" WIDE X .045"



UNDERBEAD 3X

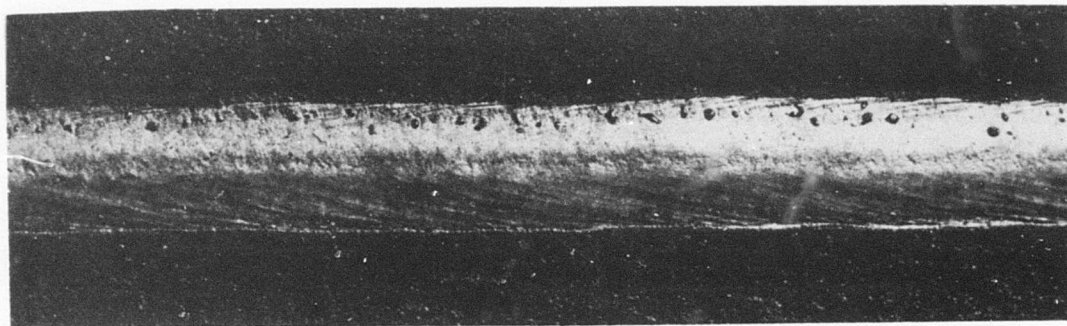
M-2647

L-2470

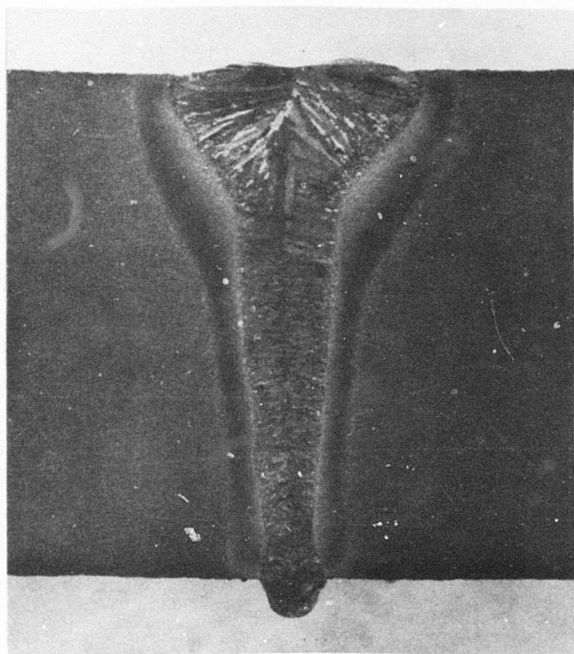
JUNE 1975

MATERIAL: LA C/S 300 M 1/2"

POWER RECORD: 80F

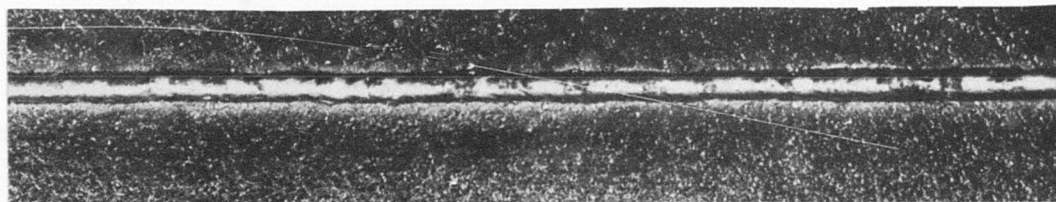


TOP BEAD 3X



6X

POWER ON WORK	12.6 KW
TRAVEL SPEED	32-1/2 IPM
TELESCOPE	f/20
FOCUS	32-1/2"
EDGE PREPARATION	
BLANCHARD GROUND-DEBURR-WIRE BRUSH-	
ACETONE RINSE-DETERGENT-WATER RINSE-	
ALCOHOL DRY	
WELD GAS (JET)	HELIUM 100 CFH
TRAIL GAS	ARGON 25 CFH
BACK-UP GAS	HELIUM 10 CFH
SHIELD	7-1
STAND-OFF	.03" FLAT
SET-BACK	1/4"
FIXTURE	24
TOP BEAD COLOR	SILVER
UNDERCUT	NONE
SOUNDNESS	100% CLEAR
UNDERBEAD SHAPE	VERY UNIFORM
	.050" WIDE X .045"



UNDER BEAD 3X

M-2646

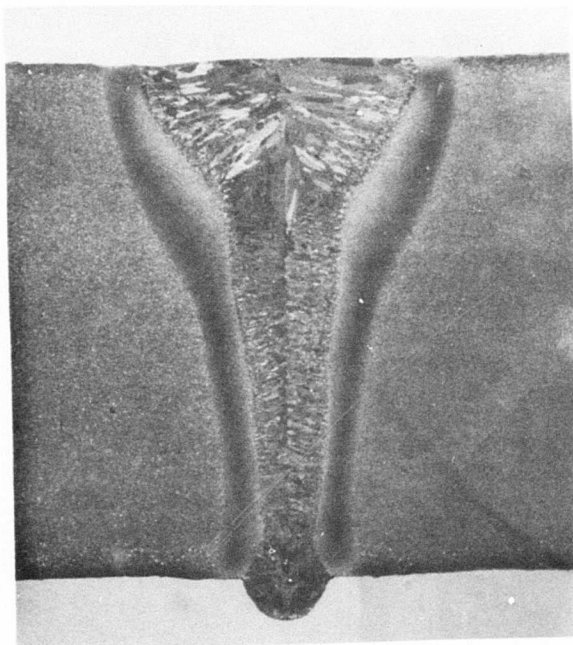
L-2470

JUNE 1975

MATERIAL: LA C/S 300 M 1/2"

POWER RECORD: 80G

TOP BEAD 3X



6X

POWER ON WORK	13.5 KW
TRAVEL SPEED	30 IPM
TELESCOPE	f/20
FOCUS	32-1/2"
EDGE PREPARATION	
	BLANCHARD GROUND-DEBURR-WIRE BRUSH-
	ACETONE RINSE-ACID FERRIC CHLORIDE-
	WATER RINSE-ALCOHOL DRY
WELD GAS (JET)	HELIUM 100 CFH
TRAIL GAS	ARGON 25 CFH
BACK-UP GAS	HELIUM 10 CFH
SHIELD	7-1
STAND-OFF	.03"
SET-BACK	1/4"
FIXTURE	#24
TOP BEAD COLOR	SILVER
UNDERCUT	NONE
SOUNDNESS	100% CLEAR
UNDERBEAD SHAPE	VERY IRREGULAR
	0.10" WIDE X .075"
REMARKS	GOOD WETTING

UNDER BEAD 3X

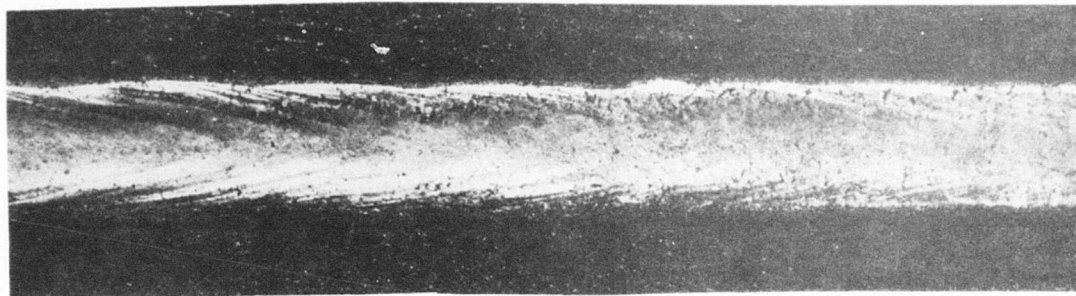
M-2645

L-2470

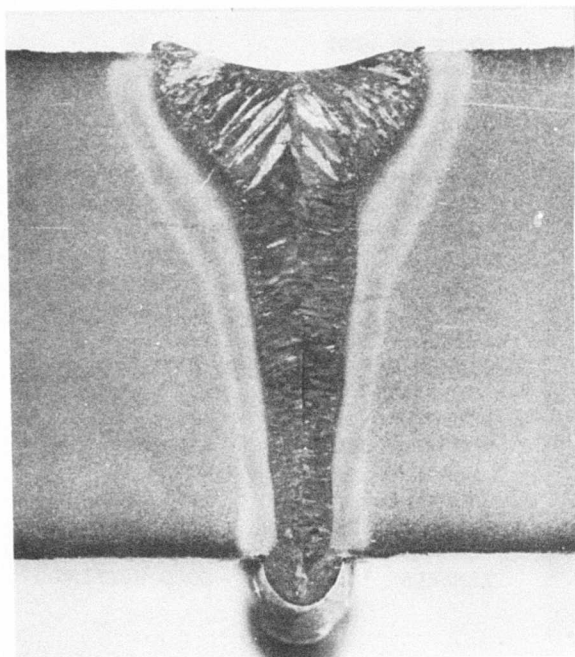
JUNE 1975

MATERIAL: LA C/S 300 M 1/2"

POWER RECORD: 80H

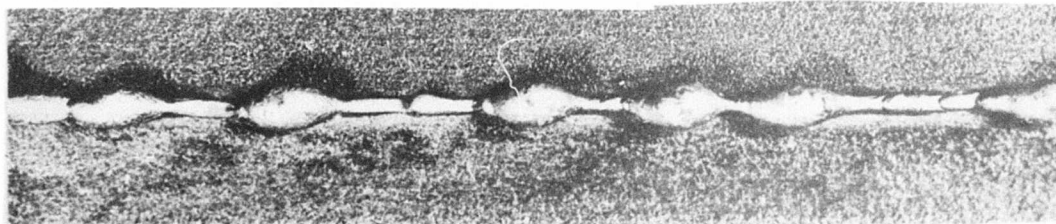


TOP BEAD 3X



6X

POWER ON WORK	12.6 KW
TRAVEL SPEED	32-1/2 IPM
TELESCOPE	f/20
FOCUS	32-1/2 "
EDGE PREPARATION	
BLANCHARD GROUND-DEBURR-WIRE BRUSH-	
ACETONE RINSE-ACID FERRIC CHLORIDE-	
WATER RINSE-ALCOHOL DRY	
WELD GAS (JET)	HELIUM 100 CFH
TRAIL GAS	ARGON 25 CFH
BACK-UP GAS	HELIUM 10 CFH
SHIELD	JET TRAILER 7-1
STAND-OFF	.03"
SET-BACK	1/4"
FIXTURE	24
TOP BEAD COLOR	SILVER
UNDERCUT	NONE
SOUNDNESS	SLIGHT POROSITY
UNDERBEAD SHAPE	IRREGULAR (COX COMB)



UNDER BEAD 3X

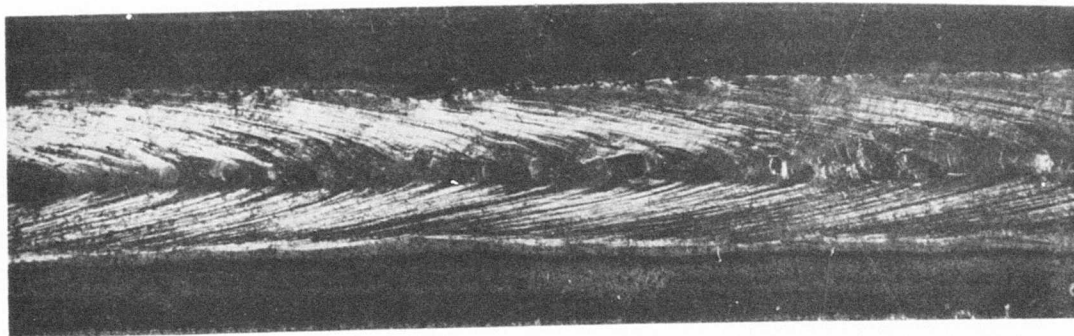
M-2644

L-2470

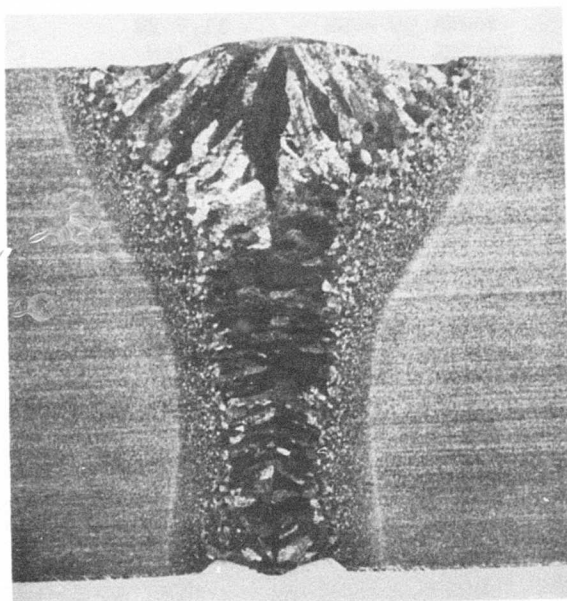
JUNE 1975

MATERIAL: TITANIUM 6-4 1/2"

POWER RECORD: 81A

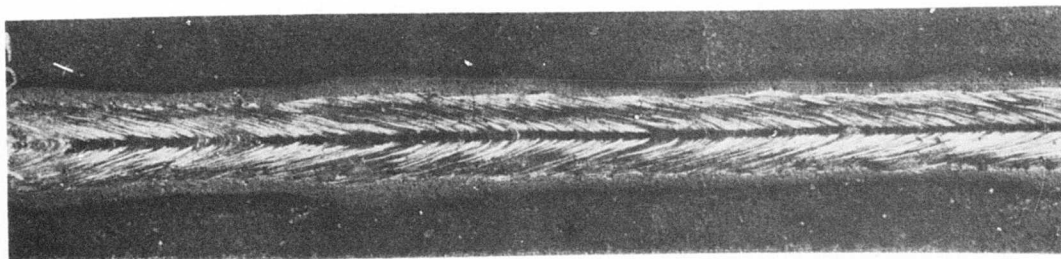


TOP BEAD 3X



6X

POWER ON WORK	13.5 KW
TRAVEL SPEED	30 IPM
TELESCOPE	f/20
FOCUS	32-1/2"
EDGE PREPARATION	
BLANCHARD GROUND-DEBURR-WIRE BRUSH-	
ACETONE RINSE	
WELD GAS (JET)	HELIUM 100 CFH
TRAIL GAS	ARGON 25 CFH
BACK-UP GAS	HELIUM 10 CFH
SHIELD	HOOD A
STAND-OFF	.03"
SET-BACK	3/8"
FIXTURE	#24
TOP BEAD COLOR	BRIGHT SILVER
UNDERCUT	.01" GAP
SOUNDNESS	100% CLEAR
UNDERBEAD SHAPE	.14" WIDE VARIABLE
	X FLAT TO SUCKBACK-
	UNIFORM



UNDER BEAD 3X

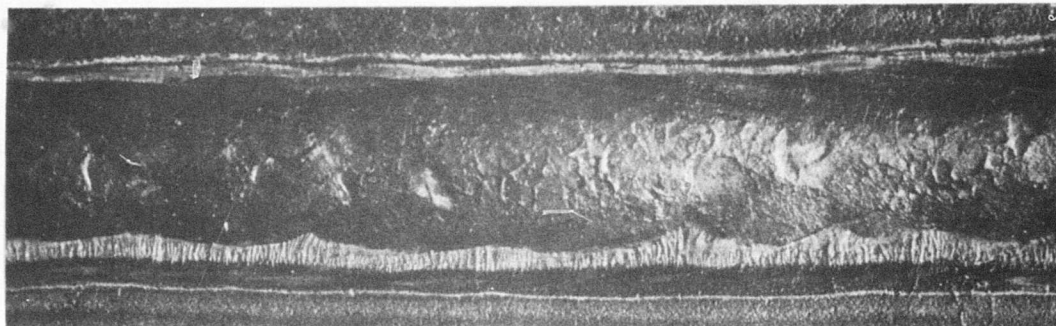
M-2642

L-2470

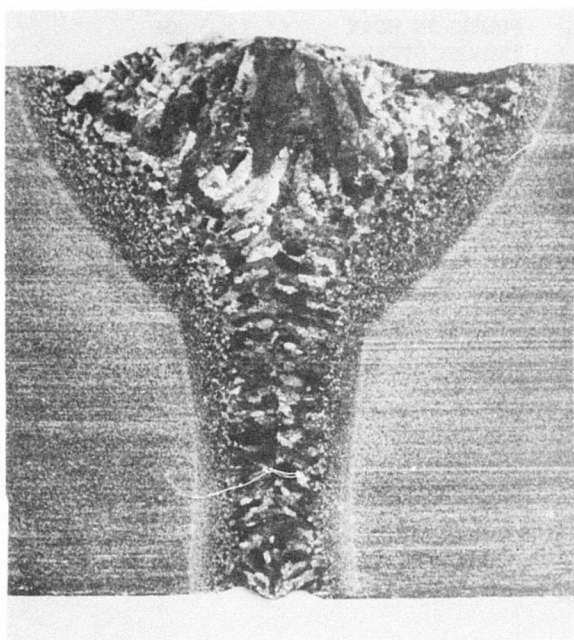
JUNE 1975

MATERIAL: TITANIUM 6-4 1/2"

POWER RECORD: 81B

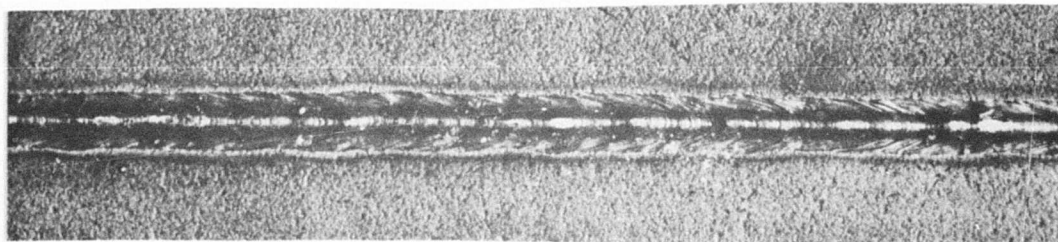


TOP BEAD 3X



6X

POWER ON WORK	11.7 KW
TRAVEL SPEED	30 IPM
TELESCOPE	f/20
FOCUS	32-1/2"
EDGE PREPARATION	
BLANCHARD GROUND-DEBURR-WIRE BRUSH-	
ACETONE RINSE	
WELD GAS (JET)	HELIUM 100 CFH
TRAIL GAS	ARGON 25 CFH
BACK-UP GAS	HELIUM 10 CFH
SHIELD	HOOD A
STAND-OFF	.06"
SET BACK	3/8"
FIXTURE	#24
TOP BEAD COLOR	BROWN
UNDERCUT	NONE
SOUNDNESS	100% CLEAR
UNDERBEAD SHAPE	LOW PROFILE-
	UNIFORM
	.095" WIDE X FLAT



UNDER BEAD 3X

M-2643

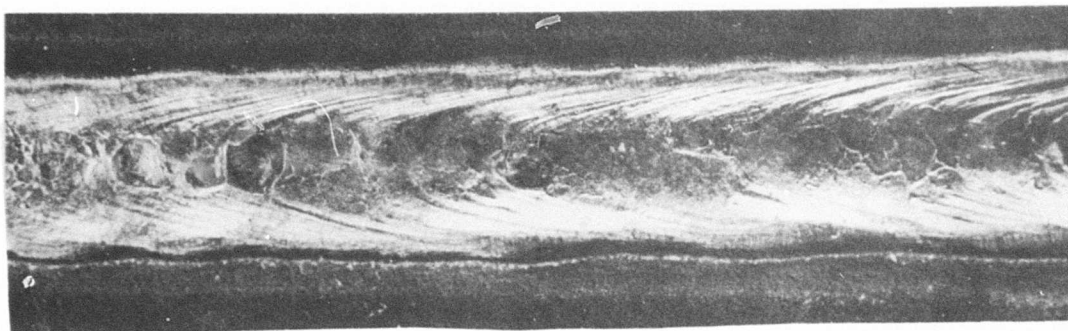
L-2470

JUNE 1975

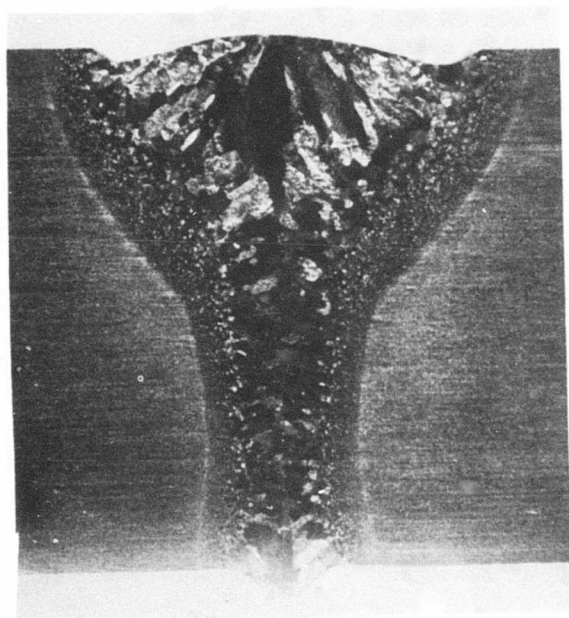
D-14

MATERIAL: TITANIUM 6-4 1/2"

POWER RECORD: 81C

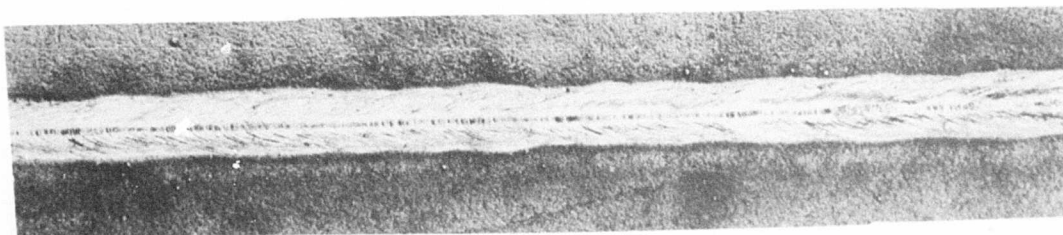


TOP BEAD 3X



6X

POWER ON WORK	10.8 KW
TRAVEL SPEED	30 IPM
TELESCOPE	f/20
FOCUS	32-1/2"
EDGE PREPARATION	
BLANCHARD GROUND-DEBURR-WIRE BRUSH-	
ACETONE RINSE	
WELD GAS (JET)	HELIUM 100 CFH
TRAIL GAS	ARGON 25 CFH
BACK-UP GAS	HELIUM 10 CFH
SHIELD	HOOD A
STAND-OFF	.06"
SET-BACK	3/8"
FIXTURE	#24
TOP BEAD COLOR	SILVER BROWN
UNDERCUT	NONE
SOUNDNESS	100% CLEAR
UNDERBEAD SHAPE	.125" WIDE X .022"
	VERY UNIFORM
REMARKS	MODERATE CROWN



UNDER BEAD 3X

M-2658

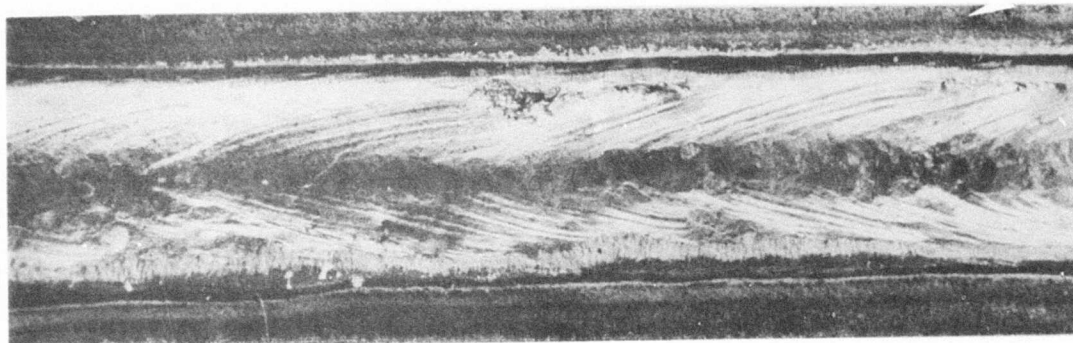
L-2470

JUNE 1975

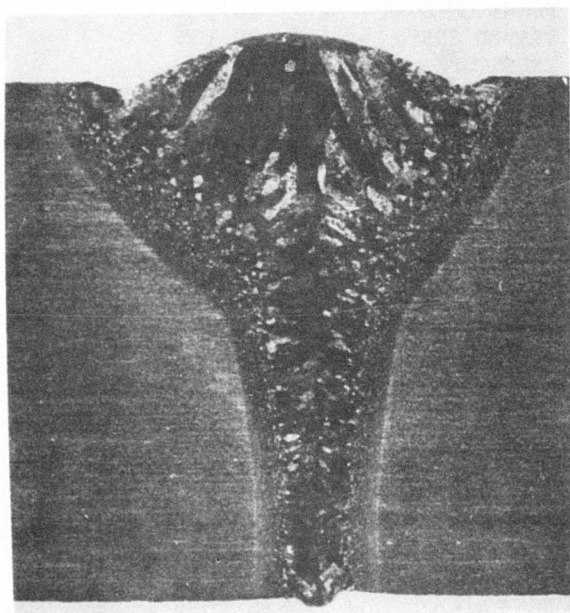
D-15

MATERIAL: TITANIUM 6-4 1/2"

POWER RECORD: 81D

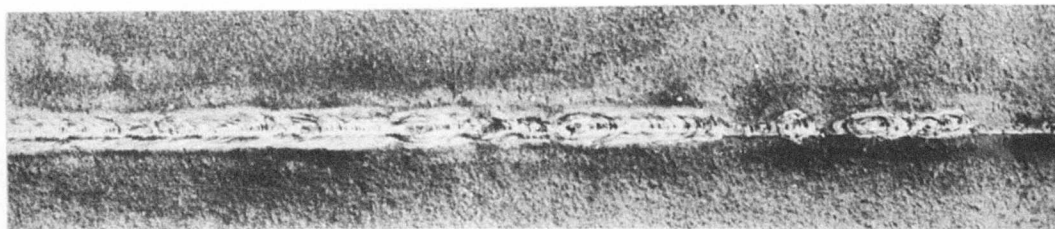


TOP BEAD 3X



6X

POWER ON WORK	9.9 KW
TRAVEL SPEED	30 IPM
TELESCOPE	f/20
FOCUS	32-1/2"
EDGE PREPARATION	
BLANCHARD GROUND-DEBURR-WIRE BRUSH-	
ACETONE RINSE	
WELD GAS (JET)	HELIUM 100 CFH
TRAIL GAS	ARGON 25 CFH
BACK-UP GAS	HELIUM 10 CFH
SHIELD	HOOD A
STAND-OFF	.03"
SET-BACK	3/8"
FIXTURE	#24
TOP BEAD COLOR	SILVER
UNDERCUT	NONE
SOUNDNESS	1 to 4 DEFECTS/INCH
UNDERBEAD SHAPE	INCOMPLETE. VERY LONG TIME TO PENE- TRATE



UNDER BEAD 3X

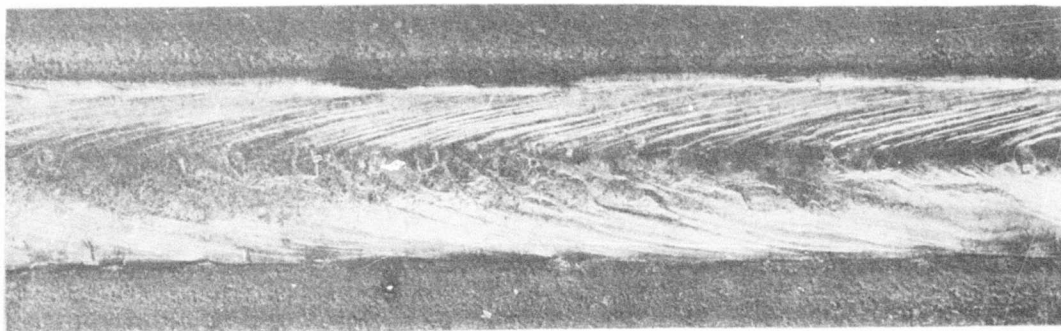
M-2659

L-2470

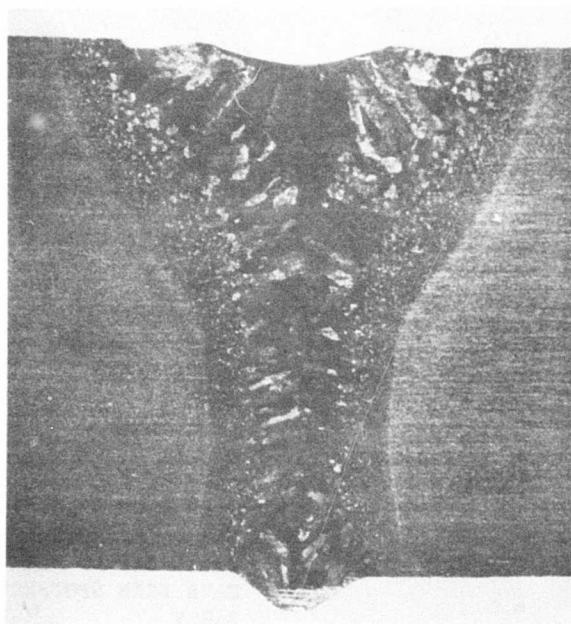
JUNE 1975

MATERIAL: TITANIUM 6-4 1/2"

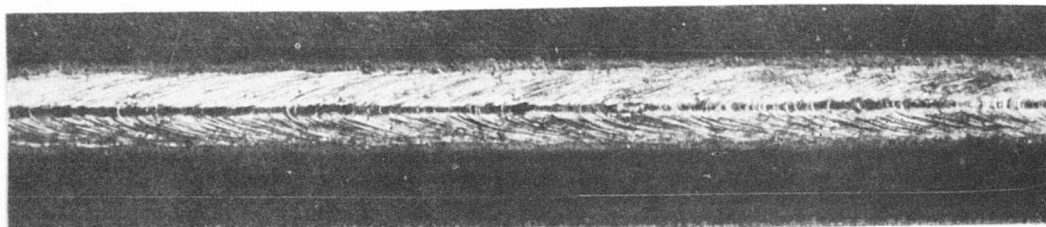
POWER RECORD: 81E



TOP BEAD 3X



6X



UNDER BEAD 3X

POWER ON WORK	10.8 KW
TRAVEL SPEED	30 IPM
TELESCOPE	f/20
FOCUS	32-1/2"
EDGE PREPARATION	
BLANCHARD GROUND-DEBURR-WIRE BRUSH-	
ACETONE RINSE-DETERGENT-ALCOHOL DRY	
WELD GAS (JET)	HELIUM 100 CFH
TRAIL GAS	ARGON 25 CFH
BACK-UP GAS	HELIUM 10 CFH
SHIELD	HOOD A
STAND-OFF	.03"
SET-BACK	3/8"
FIXTURE	#24
TOP BEAD COLOR	SILVER BROWN
UNDERCUT	NONE
SOUNDNESS	0 TO 1 DEFECT/INCH
UNDERBEAD COLOR	SILVER
SHAPE	VERY UNIFORM
	.10" WIDE X .04"
	MODERATE CROWN

M-2660

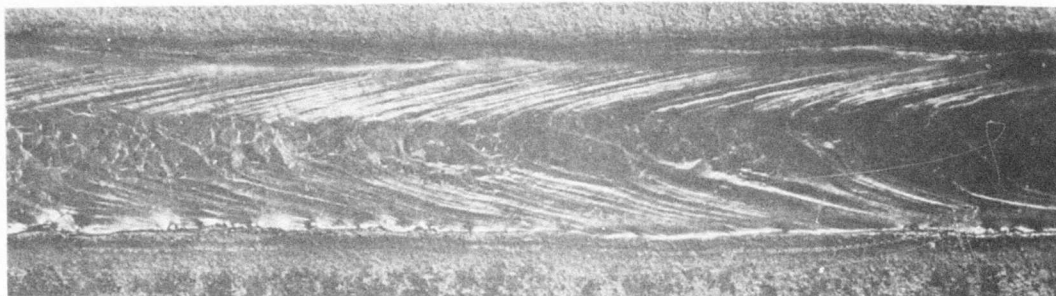
L-2470

JUNE 1975

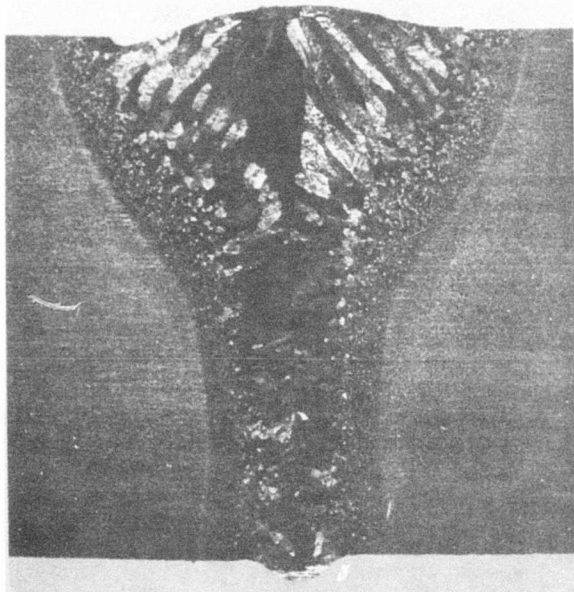
D-17

MATERIAL: TITANIUM 6-4 1/2"

POWER RECORD: 81F

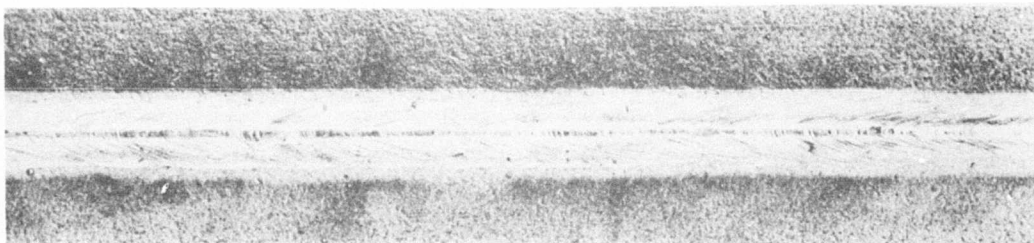


TOP BEAD 3X



6X

POWER ON WORK	10.8 KW
TRAVEL SPEED	30 IPM
TELESCOPE	f/20
FOCUS	32-1/2"
EDGE PREPARATION	
BLANCHARD GROUND-DEBURR-WIRE BRUSH-	
ACETONE RINSE-DETERGENT-ALCOHOL DRY	
WELD GAS (JET)	HELIUM 100 CFH
TRAIL GAS	ARGON 50 CFH
BACK-UP GAS	HELIUM 10 CFH
SHIELD	HOOD A
STAND-OFF	.03"
SET-BACK	3/8"
FIXTURE	#24
TOP BEAD COLOR	BROWN-BLUE*
UNDERCUT	NONE
SOUNDNESS	100% CLEAR
UNDERBEAD COLOR	SILVER
SHAPE	VERY UNIFORM
	.10" WIDE X .03"
	MODERATE CROWN
*REMARKS	TRAIL SHIELD MAY
	HAVE BEEN STOPPED
	EARLY



UNDER BEAD 3X

M-2661

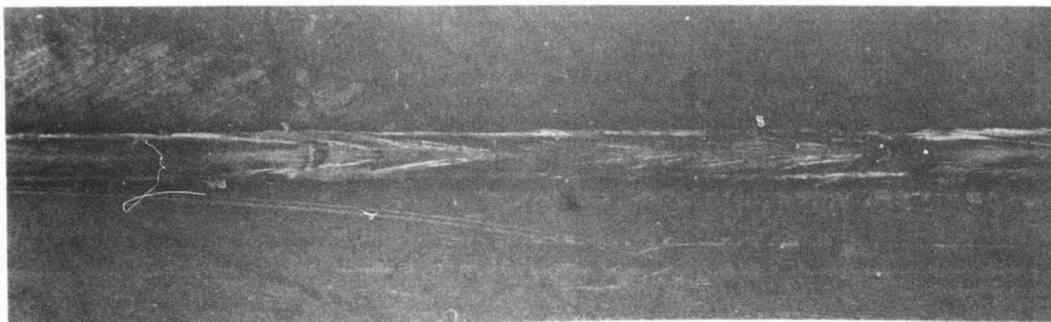
L-2470

JUNE 1975

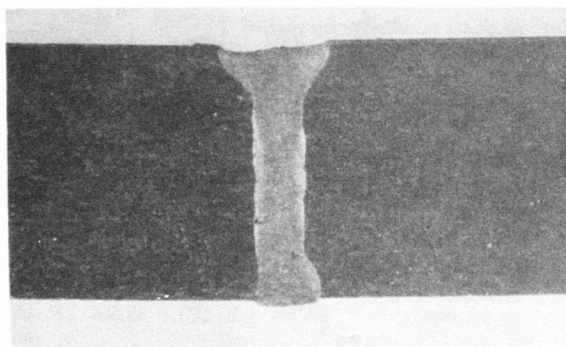
D-18

MATERIAL: INCO 718 1/4"

POWER RECORD: 76A

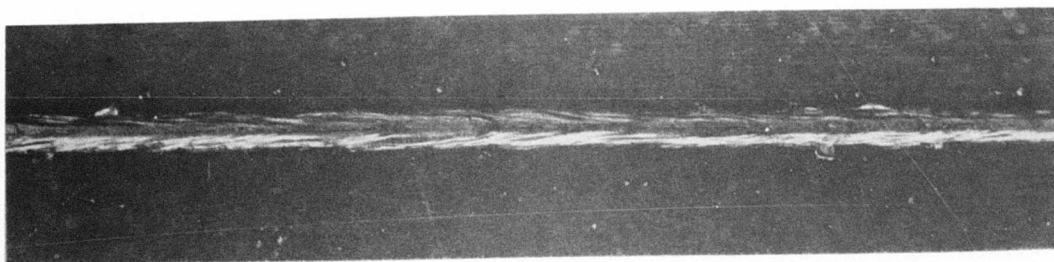


TOP BEAD 3X



6X

POWER ON WORK	8.4 KW
TRAVEL SPEED	100 IPM
TELESCOPE	f/7
FOCUS	28-1/8"
EDGE PREPARATION	
FLYCUT-DEBURR-ACETONE RINSE	
WELD GAS (JET)	HELIUM 100 CFH
TRAIL GAS	ARGON 25 CFH
BACK-UP GAS	HELIUM 10 CFH
SHIELD	SR-7
STAND-OFF	.04"
SET-BACK	7/16"
FIXTURE	FDS
CHILL BAR	#210
TOP BEAD COLOR	BLUE TO LIGHT BLUE
UNDERCUT	.005" TO .01"
SOUNDNESS	100% CLEAR
UNDERBEAD COLOR	WHITE
SHAPE	.075" WIDE X .005"



UNDERBEAD 3X

M-2652

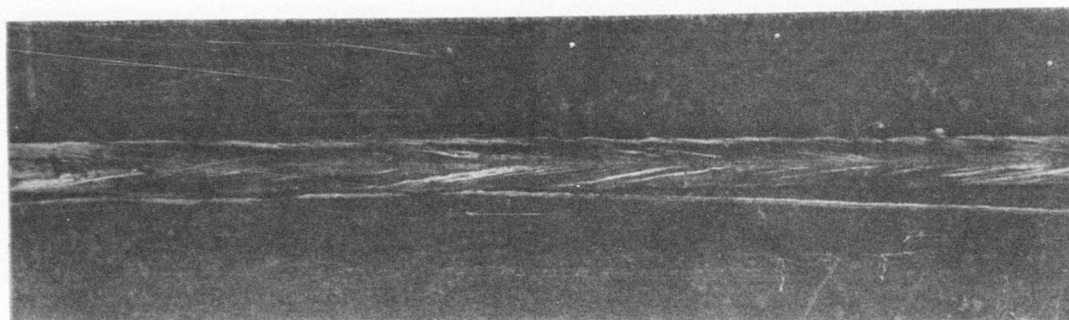
L-2470

JUNE 1975

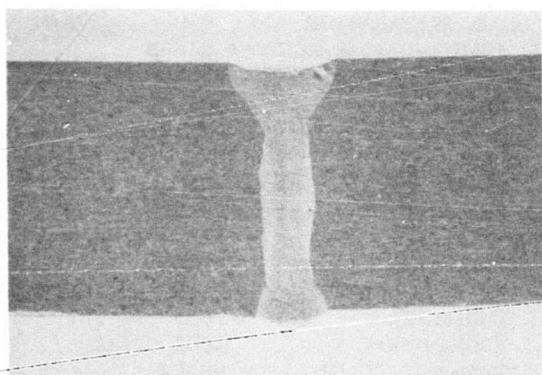
D-19

MATERIAL: INCO 718 1/4"

POWER RECORD: 76B

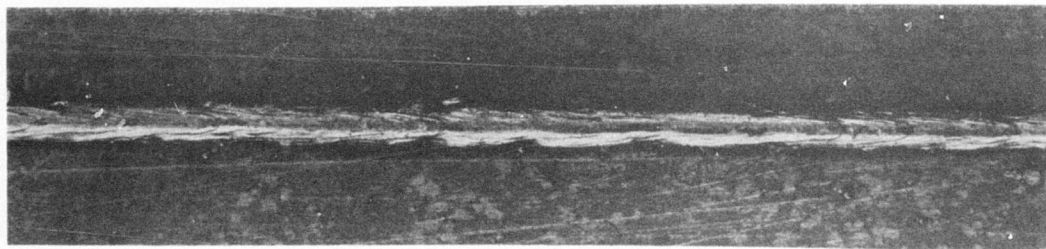


TOP BEAD 3X



6X

POWER ON WORK	7.7 KW
TRAVEL SPEED	100 IPM
TELESCOPE	f/7
FOCUS	28-1/2"
EDGE PREPARATION	
FLY CUT-DEBURR-ACETONE RINSE	
WELD GAS (JET)	HELIUM 100 CFH
TRAIL GAS	ARGON 25 CFH
BACK-UP GAS	HELIUM 10 CFH
SHIELD	SR-7
STAND-OFF	.040"
SET-BACK	7/16"
FIXTURE	FDS
CHILL BAR	#210
TOP BEAD COLOR	LIGHT BLUE
UNDERCUT	.005"
SOUNDNESS	SINGLE PORE IN 14"
UNDERBEAD COLOR	WHITE
SHAPE	.075" WIDE X .01"



UNDER BEAD 3X

M-2653

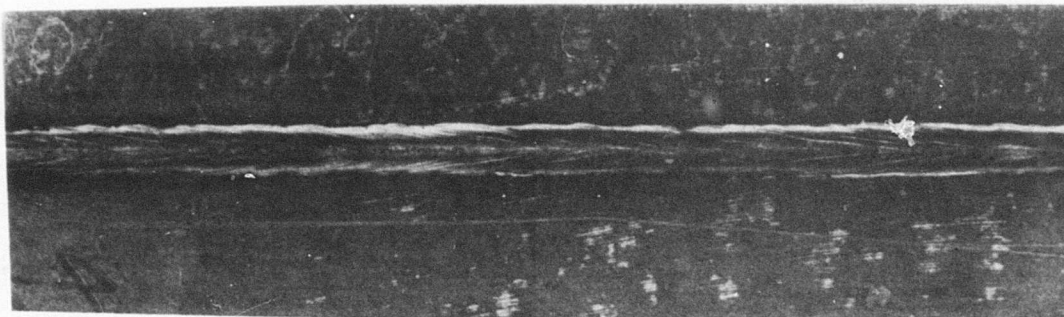
L-2470

JUNE 1975

D-20

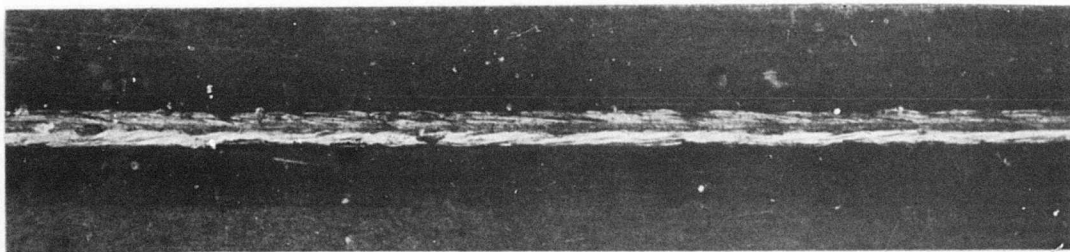
MATERIAL: INCO 718 1/4"

POWER RECORD: 76C



TOP BEAD 3X

POWER ON WORK	7.0 KW
TRAVEL SPEED	100 IPM
TELESCOPE	f/7
FOCUS	28-1/8"
EDGE PREPARATION	
FLYCUT-DEBURR-ACETONE RINSE	
WELD GAS (JET)	HELIUM 100 CFH
TRAIL GAS	ARGON 25 CFH
BACK-UP GAS	HELIUM 10 CFH
SHIELD	SR-7
STAND-OFF	.04"
SET-BACK	7/16"
FIXTURE	FDS
CHILL BAR	#210
TOP BEAD COLOR	BRUSH-LIGHT BLUE
UNDERCUT	.005" to .010"
SOUNDNESS	SINGLE PORE IN 14"
UNDERBEAD COLOR	WHITE
SHAPE	.070" WIDE X .010"



UNDER BEAD 3X

M-2654

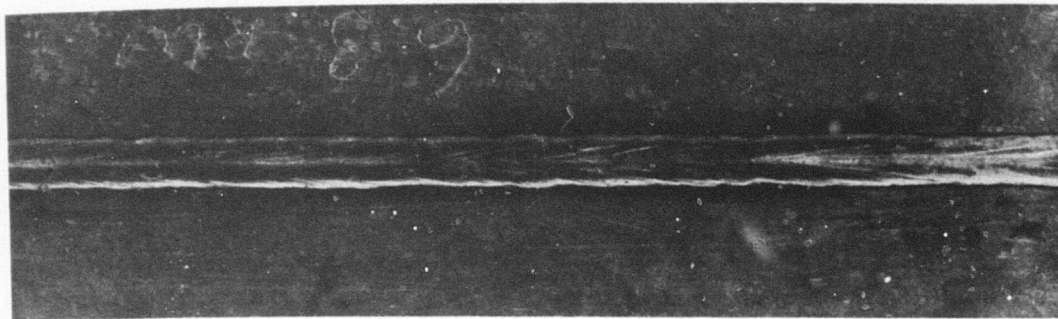
L-2470

JUNE 1975

D-21

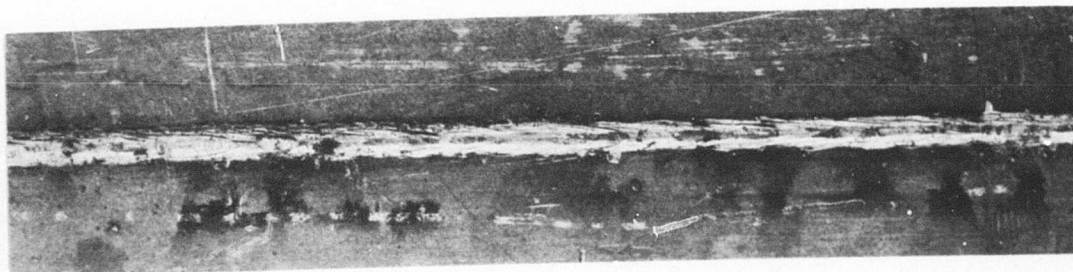
MATERIAL: INCO 718 1/4"

POWER RECORD: 76D



TOP BEAD 3X

POWER ON WORK	6.3 KW
TRAVEL SPEED	100 IPM
TELESCOPE	f/7
FOCUS	28-1/8"
EDGE PREPARATION	
FLYCUT-DEBURR-ACETONE RINSE	
WELD GAS (JET)	HELIUM 100 CFH
TRAIL GAS	ARGON 25 CFH
BACK-UP GAS	HELIUM 10 CFH
SHIELD	SR-7
STAND-OFF	.04"
SET-BACK	7/16"
FIXTURE	FDS
CHILL BAR	#210
TOP BEAD COLOR	BRUSH-LIGHT BLUE
UNDERCUT	.005"
SOUNDNESS	100% CLEAR
UNDERBEAD COLOR	WHITE
SHAPE	.070" WIDE X .012"



UNDERBEAD 3X

M-2655

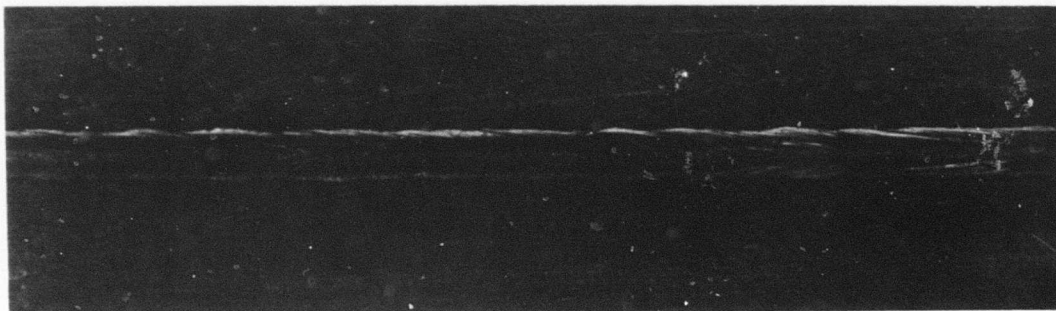
L-2470

JUNE 1975

D-22

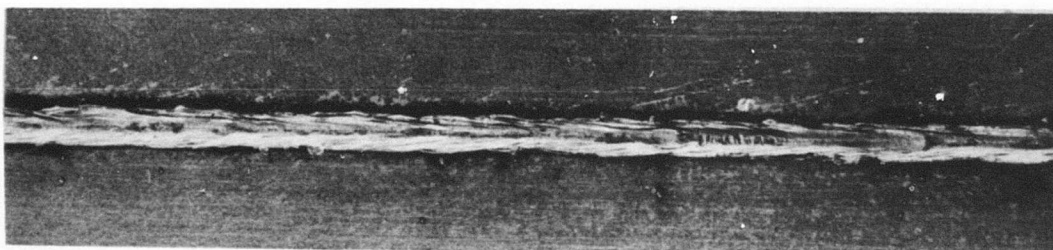
MATERIAL: INCO 718 1/4"

POWER RECORD: 76E



TOP BEAD 3X

POWER ON WORK	7.7 KW
TRAVEL SPEED	100 IPM
TELESCOPE	f/7
FOCUS	28-1/8"
EDGE PREPARATION	
FLYCUT-DEBURR-WIRE BRUSH-	
DETERGENT-WATER RINSE-	
ALCOHOL DRY	
WELD GAS (JET)	HELIUM 100 CFH
TRAIL GAS	ARGON 25 CFH
BACK-UP GAS	HELIUM 10 CFH
SHIELD	SR-7
STAND-OFF	.04"
SET-BACK	7/16"
FIXTURE	FDS
CHILL BAR	#210
TOP BEAD COLOR	LIGHT BLUE - WHITE
UNDERCUT	0 - .005"
SOUNDNESS	100% CLEAR
UNDERBEAD COLOR	WHITE
SHAPE	.075" WIDE X .01"



UNDER BEAD 3X

M-2656

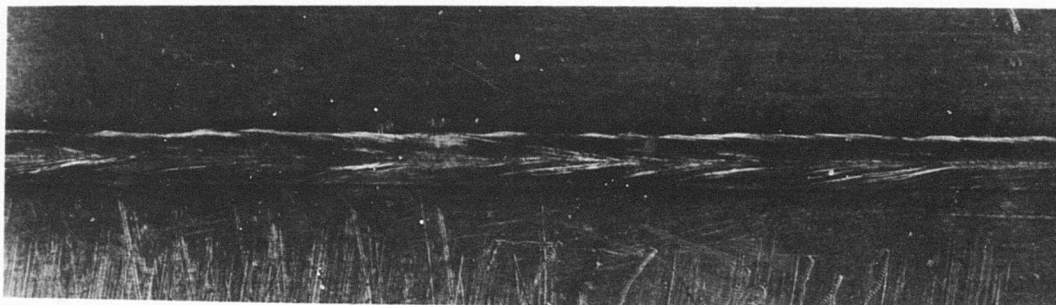
L-2470

JUNE 1975

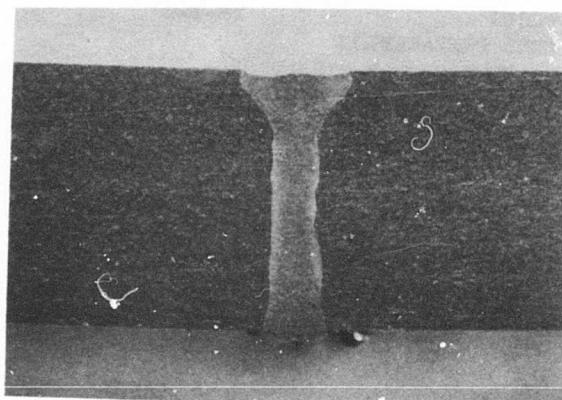
D-23

MATERIAL: INCO 718 1/4"

POWER RECORD: 76F

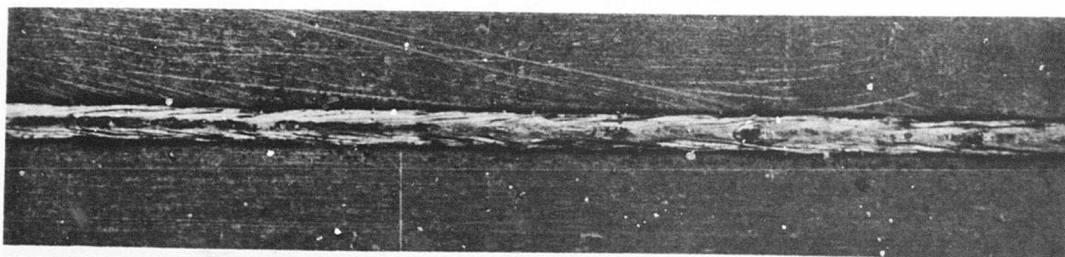


TOP BEAD 3X



6X

POWER ON WORK	6.3 KW
TRAVEL SPEED	100 IPM
TELESCOPE	f/7
FOCUS	28-1/8"
EDGE PREPARATION	
FLYCUT-DEBURR-WIRE BRUSH-DETERGENT-	
WATER RINSE-ALCOHOL DRY	
WELD GAS (JET)	HELIUM 100 CFH
TRAIL GAS	ARGON 25 CFH
BACK-UP GAS	HELIUM 10 CFH
SHIELD	SR-7
STAND-OFF	.04"
SET-BACK	7/16"
FIXTURE	FDS
CHILL BAR	#210
TOP BEAD COLOR	WHITE - LIGHT BLUE
UNDERCUT	0 - .005"
SOUNDNESS	ONE PORE IN 14"
UNDERBEAD COLOR	WHITE
SHAPE	.075" WIDE X .005"



UNDER BEAD 3X

M-2657

L-2470

JUNE 1975

D-24

APPENDIX E

DESIGN AND TEST SPECIMEN FABRICATION DRAWINGS

300M ALLOY STEEL

TEST DESCRIPTION AND SPECIMEN "BLANKS" REQUIRED

300M ALLOY STEEL												
SPECIMEN THICKNESS	BASE METAL TENSILE		WELDED TENSILE				FRACTURE TOUGHNESS		AXIAL FATIGUE		STRESS CORROSION	
	GRAIN DIRECTION		GRAIN DIRECTION				BASE METAL	WELDED	BASE METAL	WELDED	K _{ISCC}	SMOOTH
	TRANS.	LONG.	TRANSVERSE		LONG.							
			WELD	REPAIR	ALT-1	ALT-2						
1/4"	T7B-1 T7B-2	L7B-1 L7B-2	ATT-1 ATT-2 ATT-3	RTT-1 RTT-2 RTT-3	ALT-1 ALT-2 ALT-3				F7B-1 F7B-2 F7B-3	FTW-1 FTW-2 FTW-3		SCS-1 SCS-2 SCS-3
3/8"	T7B-3 T7B-4	L7B-3 L7B-4	ATT-4 ATT-5 ATT-6									
1/2"	T7B-5 T7B-6	L7B-5 L7B-6	ATT-7 ATT-8 ATT-9						F7B-4 F7B-5 F7B-6	FTW-7 FTW-8 FTW-9 FTW-10 FTW-11 FTW-12		
3/4"	T7B-7 T7B-8	L7B-7 L7B-8	ATT-10 ATT-11 ATT-12	RTT-4 RTT-5 RTT-6	ALT-4 ALT-5 ALT-6		F7B-1 F7B-2 F7B-3	F7B-1 F7B-2 F7B-3			SCX-1 SCX-2 SCX-3	

SPECIMEN IDENTIFICATION

TiB NICKEL ALLOY

T7B NICKEL ALLOY

TEST DESCRIPTION AND SPECIMEN "BLANKS" REQUIRED

TEST DESCRIPTION AND SPECIMEN "BLANKS" REQUIRED	SPECIMEN THICKNESS	BASE METAL TENSILE	WELDED TENSILE	FRACTURE TOUGHNESS	AXIAL FATIGUE	STRESS CORROSION				
GRAIN DIRECTION	LONG.	GRAIN DIRECTION	LONG.	BASE METAL	WELDED	BASE METAL	WELDED	K _{ISCC}	SMOOTH	
TRANS	LONG.	TRANSVERSE	LONG.	BASE METAL	WELDED	BASE METAL	WELDED	K _{ISCC}	SMOOTH	
		WELD	REPAIR	BASE METAL	WELDED	BASE METAL	WELDED	K _{ISCC}	SMOOTH	
								K _{ISCC}	SMOOTH	
								K _{ISCC}	SMOOTH	
								K _{ISCC}	SMOOTH	
								K _{ISCC}	SMOOTH	
								K _{ISCC}	SMOOTH	
								K _{ISCC}	SMOOTH	
								K _{ISCC}	SMOOTH	
								K _{ISCC}	SMOOTH	
								K _{ISCC}	SMOOTH	
								K _{ISCC}	SMOOTH	
								K _{ISCC}	SMOOTH	
								K _{ISCC}	SMOOTH	
								K _{ISCC}	SMOOTH	
								K _{ISCC}	SMOOTH	
								K _{ISCC}	SMOOTH	
								K _{ISCC}	SMOOTH	
								K _{ISCC}	SMOOTH	
								K _{ISCC}	SMOOTH	
								K _{ISCC}	SMOOTH	
								K _{ISCC}	SMOOTH	
								K _{ISCC}	SMOOTH	
								K _{ISCC}	SMOOTH	
								K _{ISCC}	SMOOTH	
								K _{ISCC}	SMOOTH	
								K _{ISCC}	SMOOTH	
								K _{ISCC}	SMOOTH	
								K _{ISCC}	SMOOTH	
								K _{ISCC}	SMOOTH	
								K _{ISCC}	SMOOTH	
								K _{ISCC}	SMOOTH	
								K _{ISCC}	SMOOTH	
								K _{ISCC}	SMOOTH	
								K _{ISCC}	SMOOTH	
								K _{ISCC}	SMOOTH	
								K _{ISCC}	SMOOTH	
								K _{ISCC}	SMOOTH	
								K _{ISCC}	SMOOTH	
								K _{ISCC}	SMOOTH	
								K _{ISCC}	SMOOTH	
								K _{ISCC}	SMOOTH	
								K _{ISCC}	SMOOTH	
								K _{ISCC}	SMOOTH	
								K _{ISCC}	SMOOTH	
								K _{ISCC}	SMOOTH	
								K _{ISCC}	SMOOTH	
								K _{ISCC}	SMOOTH	
								K _{ISCC}	SMOOTH	
								K _{ISCC}	SMOOTH	
								K _{ISCC}	SMOOTH	
								K _{ISCC}	SMOOTH	
								K _{ISCC}	SMOOTH	
								K _{ISCC}	SMOOTH	
								K _{ISCC}	SMOOTH	
								K _{ISCC}	SMOOTH	
								K _{ISCC}	SMOOTH	
								K _{ISCC}	SMOOTH	
								K _{ISCC}	SMOOTH	
								K _{ISCC}	SMOOTH	
								K _{ISCC}	SMOOTH	
								K _{ISCC}	SMOOTH	
								K _{ISCC}	SMOOTH	
								K _{ISCC}	SMOOTH	
								K _{ISCC}	SMOOTH	
								K _{ISCC}	SMOOTH	
								K _{ISCC}	SMOOTH	
								K _{ISCC}	SMOOTH	



SPECIMEN IDENTIFICATION

6AL-4V TITANIUM ALLOY

TEST DESCRIPTION AND SPECIMEN "BLANKS" REQUIRED												
SPECIMEN THICKNESS	BASE METAL TENSILE		WELDED TENSILE				FRACTURE TOUGHNESS		AXIAL FATIGUE		STRESS CORROSION	
	GRAIN DIRECTION		GRAIN DIRECTION		WELDED	BASE METAL	WELDED	BASE METAL	WELDED	K _{ISCC}	SMOOTH	
	TRANS.	LONG.	WELD	TRANSVERSE								LONG
1/4"	T7B-1 T7B-2	L7B-1 L7B-2	ATT-1 ATT-2 ATT-3	ETT-1 ETT-2 ETT-3	ALT-1 ALT-2 ALT-3			F7B-1 F7B-2 F7B-3	FTN-1 -2 -3 -4 -5 -6		SCS-1 SCS-2 SCS-3	
3/8"	T7B-3 T7B-4	L7B-3 L7B-4	ATT-4 ATT-5 ATT-6									
1/2"	T7B-5 T7B-6	L7B-5 L7B-6	ATT-7 ATT-8 ATT-9					F7B-4 F7B-5 F7B-6	FTN-7 -8 -9 -10 -11 -12			
3/4"	T7B-7 T7B-8	L7B-7 L7B-8	ATT-10 ATT-11 ATT-12	ETT-4 ETT-5 ETT-6	ALT-4 ALT-5 ALT-6	F8M-1 F8M-2 F8M-3	F8W-1 F8W-2 F8W-3			SCC-1 SCC-2 SCC-3		

SPECIMEN IDENTIFICATION

2219 ALUMINUM ALLOY

TEST DESCRIPTION AND SPECIMEN "BLANKS" REQUIRED												
SPECIMEN THICKNESS	BASE METAL TENSILE		WELDED TENSILE			FRACTURE TOUGHNESS		AXIAL FATIGUE		STRESS CORROSION		
	GRAIN DIRECTION		GRAIN DIRECTION			BASE METAL	WELDED	BASE METAL	WELDED	K _{ISCC}	SMOOTH	
	TRANS.	LONG.	WELD	TRANSVERSE								LONG.
				WELD	TRANSVERSE							
1/4"	T7B-1 T7B-2	L7B-1 L7B-2	ATT-1 ATT-2 ATT-3	RTT-1 RTT-2 RTT-3	ALT-1 ALT-2 ALT-3	FTB-1 FTB-2 FTB-3		FTB-1 FTB-2 FTB-3	FTW-1 -2 -3 -4 -5		SCS-1 SCS-2 SCS-3  2x12	
3/8"	T7B-3 T7B-4	L7B-3 L7B-4	ATT-4 ATT-5 ATT-6									
1/2"	T7B-5 T7B-6	L7B-5 L7B-6	ATT-7 ATT-8 ATT-9			FTB-4 FTB-5 FTB-6		FTB-4 FTB-5 FTB-6	FTW-7 -8 -9 -10 -11 -12			
3/4"	T7B-7 T7B-8	L7B-7 L7B-8	ATT-10 ATT-11 ATT-12	RTT-4 RTT-5 RTT-6	ALT-4 ALT-5 ALT-6	FBM-1 FBM-2 FBM-3	FAN-1 FAN-2 FAN-3			SCC-1 SCC-2 SCC-3	 2x6	

SPECIMEN IDENTIFICATION

1	2	3	4	5	6	7	8	9	10	11	12	13	14	15	16	17	18	19	20	21	22	23	24	25	26	27	28	29	30	31	32	33	34	35	36	37	38	39	40	41	42	43	44	45	46	47	48	49	50	51	52	53	54	55	56	57	58	59	60	61	62	63	64	65	66	67	68	69	70	71	72	73	74	75	76	77	78	79	80	81	82	83	84	85	86	87	88	89	90	91	92	93	94	95	96	97	98	99	100
---	---	---	---	---	---	---	---	---	----	----	----	----	----	----	----	----	----	----	----	----	----	----	----	----	----	----	----	----	----	----	----	----	----	----	----	----	----	----	----	----	----	----	----	----	----	----	----	----	----	----	----	----	----	----	----	----	----	----	----	----	----	----	----	----	----	----	----	----	----	----	----	----	----	----	----	----	----	----	----	----	----	----	----	----	----	----	----	----	----	----	----	----	----	----	----	----	----	----	-----

GENERAL NOTES
OWNER'S QUALITY ASSURANCE PROGRAM

1. ANNOINED SURFACES $\frac{1}{2}$, HOLES
- AND SPACES $\frac{1}{2}$, PER ANCH BELL
2. QUAM DIRECTION $\frac{1}{2}$
3. FLIT BATH $\frac{1}{2}$
4. MAXIMUM CM OF CUTS
5. PASTIFICATION STANDARDS PER DTS 4790
6. DMS TO BE MET AFTER PLATING
7. DENTARY BE MET 3.02
8. CRYSTALLINE SURFACES WHICH ARE
- SHOWN AS VERTICAL OR PARALLEL
- ARE TO BE REPRODUCTION IN BE SHOWS.

ON ALL FIELD SPECIMENS SURFACES MARKED THUS:

ARE PARALLEL TO NOTED DATUM WITHIN SPECIFIED TOLERANCE, AND MUST LIE IN THE SAME PLANE WITHIN .005.

ALL SURFACES MARKED THUS: 1 8 100 ARE PERPENDICULAR TO NOTED DATUM WITHIN SPECIFIED TOLERANCE. WELDING JOINTS
MIL WELDED ALUMINUM ALLOY (2219) SPECIMENS MUST BE CHECK AND STRAIGHTENED TO MEET REQUIREMENTS OF NOTE 9 PRIOR TO MACHINING.

2. WELDED JOINTS: ALL WELDED JOINTS MUST BE CHECKED AND STRAIGHTENED TO MEET REQUIREMENTS OF NOTE 9 AFTER NORMALIZING AND TEMPERING AND PRIOR TO MACHINING AND HEAT TREATING.

TO MACHINING AND HEAT TREATING.
3. USE "NO-CARB" COATING DECARBURIZATION CONTROL ON ALL 300M ALLOY SPECIMENS PRIOR TO NORMALIZING AND TEMPERING.
4. NORMALIZE AND TEMPER ALL 300M ALLOY SPECIMENS PER DPS 5.00 EXCEPT TEMPER AT A TEMPERATURE NOT TO EXCEED 1250°F (MAX.) TO ACHIEVE A BHN 311 (MAX.).

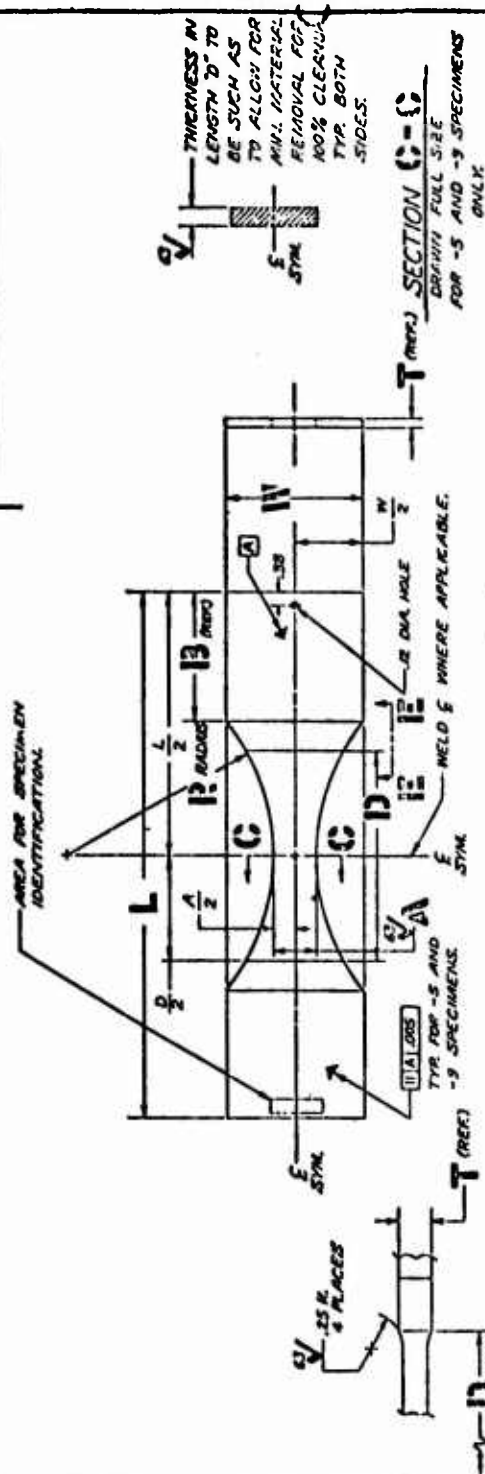
EXCEED 1250 F. (MAX.) TO ACHIEVE A 50% SAVING.
5. COPPER PLATE ALL 500M ALLOY SPECIMENS PER DRS 249
(TORRANCE) AFTER MACHINING.

WE TREAT ALL 300M ALLOY SPECIMENS 275-305,000 PSI PER DPS 3.00 (TOLERANCE) AFTER MACHINING.

IN A SALT BATH FURNACE (LONG BEACH), SPECIMENS MUST BE SUSPENDED VERTICALLY DURING HEAT-TREATMENT TEMPER STRAIGHTEN SPECIMENS

AS REQUIRED, (CHECK MARKS)
AFTER COPPER STRIP
AND BEFORE FIRST FULL
TEMPER),

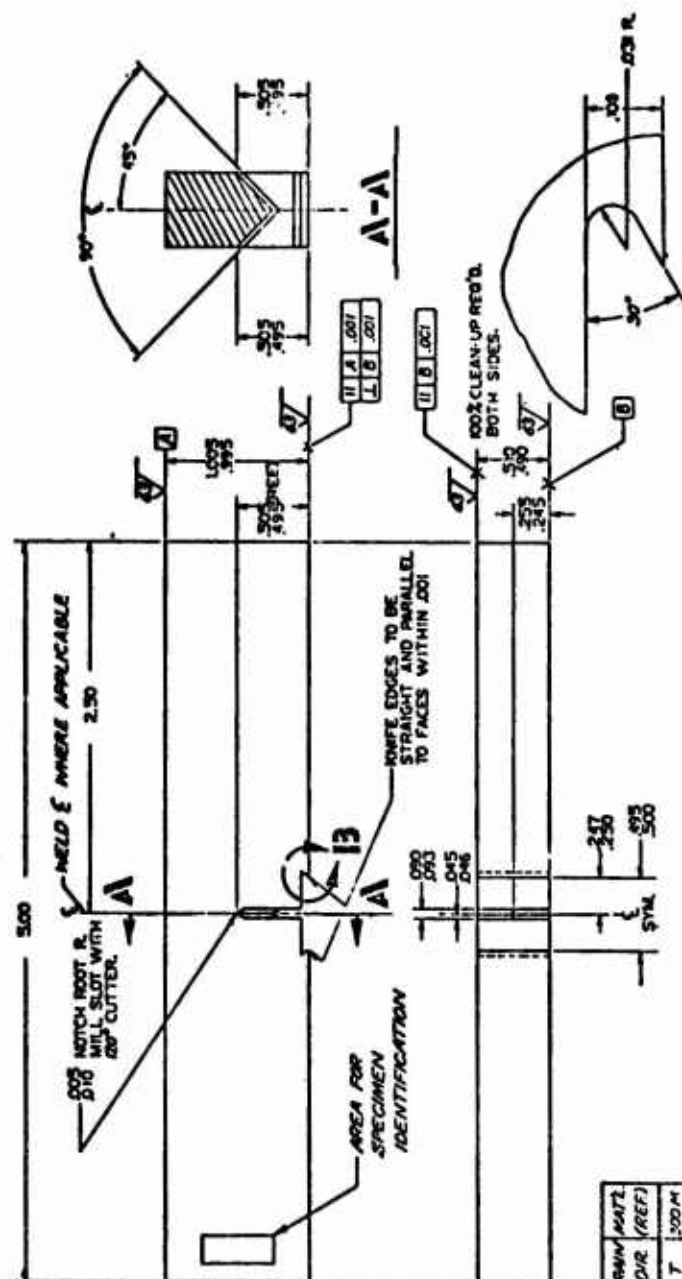
[illegible]



-3, -5, -7, -9 SPECIMEN (AFML)

VIEW E-E
DRAWN FOUR TIMES
FOR -5 AND -9 SPECIMENS ONLY

DASH SPECIMEN NO.	LENGTH-OR-BACK IDENTIFICATION	WELD OR BACK METAL	SPRINT MATT. DIR. (REF)	A	A/2	B	L	L/2	P _{ROD}	T	W	W/2	D	D/2
-3	178-15-12	BASE METAL	L	300M	500	375	15.00	7.50	6.00	.25	4.00	2.00	2.00	1.00
-5	178-15-17	WELDED	L	300M	1000	500	15.00	7.50	6.00	.25	4.00	2.00	4.00	2.00
-7	178-15-18	WELDED	L	250M	1250	625	27.00	13.50	6.00	.50	5.00	2.50	8.00	4.00
-9	178-15-19	WELDED	L	200M	1250	625	22.00	11.00	6.00	.50	5.00	2.50	6.00	3.00



DETAIL -27-29-31,33,35,37-39, SPECIMEN
-41,42,43

VIEW 13
TYPICAL 2 PLACES
SCALE 10/1

[illegible]

DOUGLAS

88277

EC008251

2-11-85

ENGINEER ORDER

NEW RELEASE
DAC 25-1229 (9-71)

DATE 25-1229 (9-71)

RC

VI

MW

AW

IS

TS

AW

IS

TS

AW

IS

TS

AW

IS

TS

AW

IS

TS

AW

IS

TS

AW

IS

TS

AW

IS

TS

AW

IS

TS

AW

IS

TS

AW

IS

TS

AW

IS

TS

AW

IS

TS

AW

IS

TS

AW

IS

TS

AW

IS

TS

AW

IS

TS

AW

IS

TS

AW

IS

TS

AW

IS

TS

TYPE OF DRAWING:

- A SECTION LIST
- B SPEC OR SOURCE CONTROL
- C DAC STANDARD DRAWING
- D REWORK
- E SERVICE CHANGE
- F MODIFICATION
- G UNDIMENSIONED
- H SPECIAL SPARE
- I OTHER

EG MADE BY

DESIGN APPROVAL

CHECK ED

CHECK DWG

STRESS

WEIGHTS

CHANGE CONTROL

MATERIAL

PRODUCT SUPPORT

RELEASE DATE

CUSTOMER

INCORP VIR NO.

INCORP SERIAL NO.

INCORP DATE

INCORP BY

INCORP DATE

INCORP BY

INCORP DATE

INCORP BY

INCORP DATE

INCORP BY

INCORP DATE

INCORP BY

INCORP DATE

INCORP BY

INCORP DATE

INCORP BY

INCORP DATE

INCORP BY

INCORP DATE

INCORP BY

INCORP DATE

INCORP BY

INCORP DATE

INCORP BY

INCORP DATE

INCORP BY

INCORP DATE

INCORP BY

INCORP DATE

INCORP BY

INCORP DATE

INCORP BY

INCORP DATE

INCORP BY

INCORP DATE

INCORP BY

INCORP DATE

INCORP BY

INCORP DATE

INCORP BY

INCORP DATE

INCORP BY

TITLE

DISOCA03
SPECIMENS - LASER
WELD

RELEASE

DEVELOPMENT
PRODUCTION
NON PROD

DESIGN SECTION

T2

MAJOR SUB-NO.

1

TOTAL NO. OF INPUT SHEETS

1

ADV DATE

1

SIZE

1

DRAWING NUMBER

ZC008251

PRINT DISTRIBUTION

DEVELOPMENT

PRINT NO.

1

PRINT DATE

1

PRINT BY

1

PRINT CHECKED

1

PRINT APPROVED

1

PRINT REVISION

1

PRINT DESCRIPTION

1

PRINT DATE

1

PRINT BY

1

PRINT CHECKED

1

PRINT APPROVED

1

PRINT REVISION

1

PRINT DESCRIPTION

1

PRINT DATE

1

PRINT BY

1

PRINT CHECKED

1

PRINT APPROVED

1

PRINT REVISION

1

PRINT DESCRIPTION

1

PRINT DATE

1

PRINT BY

1

PRINT CHECKED

1

PRINT APPROVED

1

PRINT REVISION

1

PRINT DESCRIPTION

1

PRINT DATE

1

PRINT BY

1

PRINT CHECKED

1

PRINT APPROVED

1

PRINT REVISION

1

PRINT DESCRIPTION

1

PRINT DATE

1

PRINT BY

1

PRINT CHECKED

1

PRINT APPROVED

1

PRINT REVISION

1

PRINT DESCRIPTION

1

PRINT DATE

1

PRINT BY

1

PRINT CHECKED

1

PRINT APPROVED

1

PRINT REVISION

1

PRINT DESCRIPTION

1

PRINT DATE

1

PRINT BY

1

PRINT CHECKED

1

PRINT APPROVED

1

PRINT REVISION

1

PRINT DESCRIPTION

1

PRINT DATE

1

PRINT BY

1

PRINT CHECKED

1

PRINT APPROVED

1

PRINT REVISION

1

PRINT DESCRIPTION

1

PRINT DATE

1

PRINT BY

1

PRINT CHECKED

1

PRINT APPROVED

1

PRINT REVISION

1

PRINT DESCRIPTION

1

PRINT DATE

1

PRINT BY

1

PRINT CHECKED

1

PRINT APPROVED

1

PRINT REVISION

1

PRINT DESCRIPTION

1

PRINT DATE

1

PRINT BY

1

PRINT CHECKED

1

PRINT APPROVED

1

PRINT REVISION

1

PRINT DESCRIPTION

1

PRINT DATE

1

PRINT BY

1

PRINT CHECKED

1

PRINT APPROVED

1

PRINT REVISION

1

PRINT DESCRIPTION

1

PRINT DATE

1

PRINT BY

1

PRINT CHECKED

1

PRINT APPROVED

700821	
--------	--

1780027

[illegible]

IN AUTM	INCORP VIB N
---------	--------------

REASON: TO CLARIFY THERMAL TREATING PROCEDURES

PRINT DISTRIBUTION	Yes	No
DEVELOPMENT		
Orig at _____		
Dup at _____		
WAS SUB MITT FILE WITH OAC PLANNING ACTION REQUIRED		

151800Z	ROUTING NUMBER
---------	----------------

GENERAL NOTES
UNLESS OTHERWISE NOTED

1. MACHINED SURFACES $\pm .01$, HOLES AND SPACES $\pm .01$ PER ANGLES
2. GRAIN DIRECTION $\pm .01$
3. FLAT FILLING $\pm .01$
4. MAXIMUM MATCH OF CUTS $\pm .01$
5. MAXIMUM MATCH OF CUTS $\pm .01$
6. MAXIMUM MATCH OF CUTS $\pm .01$
7. MAXIMUM MATCH OF CUTS $\pm .01$
8. MAXIMUM MATCH OF CUTS $\pm .01$

9. CENTERLINE AND/OR SURFACES WHICH ARE SHOWN AS PERPENDICULAR OR PARALLEL ARE TO BE WITHIN $\pm .01$ IN 10 INCHES.

10. ON ALL WELDED SPECIMENS STAINLESS STEEL THROAT: $\pm .01$ $\pm .01$ ARE PERPENDICULAR TO NOTED DATUM WITHIN SPECIFIED TOLERANCE. WELDED ALUMINUM ALLOY (2024) AND 70 INCHES SPECIMENS MUST BE CHECK AND STRAIGHTENED TO MEET REQUIREMENTS OF NOTE 9 PRIOR TO MACHINING.

11. WELDED 300M ALLOY SPECIMENS MUST BE CHECK AND STRAIGHTENED TO MEET REQUIREMENTS OF NOTE 9 AFTER NORMALIZING AND TEMPERING AND PRIOR TO MACHINING AND HEAT TREATING.

12. USE COPPER PLATE DECARBURIZATION CONTROL ON ALL 300M SPECIMENS (41, 501, 505, 507, 509, 515 AND 579) PRIOR TO NORMALIZING AND STRESS RELIEVING.

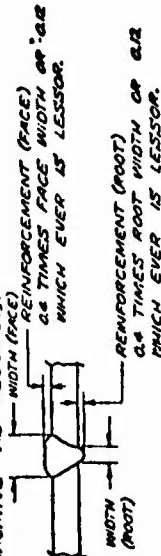
13. NORMALIZE ALL 300M SPECIMENS PER DPS 5.00 TEMPER AT 115 TO 1200°F PER DPS 5.00 PER DPS 5.00 AFTER MACHINING AND HEAT TREAT.

14. RECUPER PLATE ALL 300M SPECIMENS (41, 501, 505, 507, 509, 515 AND 579) PER DPS 5.00 AFTER MACHINING AND HEAT TREAT.

15. WELDED 6AL-4V TITANIUM ALLOY SPECIMENS MUST BE CHECK AND STRAIGHTENED TO MEET REQUIREMENTS OF NOTE 9 PRIOR TO MACHINING AND STRESS RELIEVING.

16. STRESS RELIEVE WELDED 6AL-4V TITANIUM ALLOY SPECIMENS AFTER MACHINING PER DPS 6.33.

18. WELD REINFORCEMENT IN GAGE LENGTH ON BOTH SIDES OF ALL SPECIMENS TO BE AS SHOWN BELOW (MACHINE AS REQUIRED).



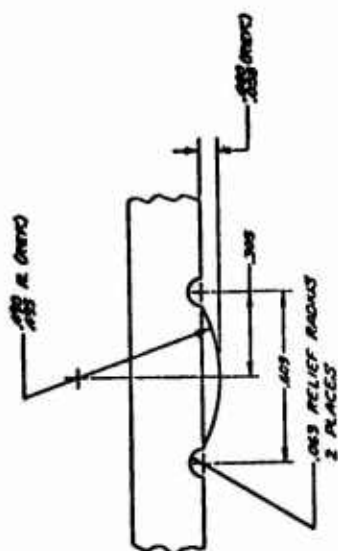
19. RETEMPER ALL 300M SPECIMENS (41, 501, 505, 507, 509) AT 1200°F TO ACHIEVE $R_c 32$ (MAX.) CHECK AND STRAIGHTEN AS REQUIRED.

20. AGE HARDEN ALL INCONEL 718 SPECIMENS (519, 521, 525 AND 535) TO ACHIEVE $R_c 36$ (MIN.) PER DPS 6.30 AFTER MACHINING.

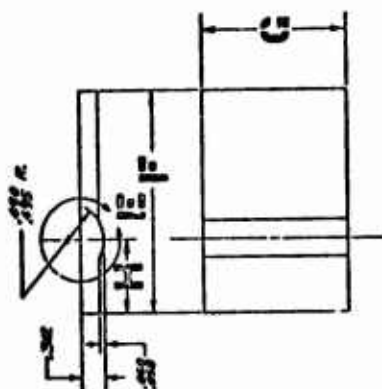
REV	DESCRIPTION	DATE	APPROVED
A	SEE E.O.	11/15/64	ELM
B	SEE E.O.	11/15/64	ELM
C	SEE E.O.	11/15/64	ELM
D	SEE E.O.	11/15/64	ELM
E	SEE E.O.	11/15/64	ELM

SEE SEPARATE PARTS LIST

BATCH NUMBERS OF THIS Dwg ODD BATCH NUMBERS SHOWN EVEN BATCH NUMBERS OPPOSITE		UNLESS OTHERWISE SPECIFIED DIMENSIONS ARE IN INCHES. TOLERANCES ANGLES $\pm .01$ - .30 2 PLACE DEC $\pm .01$ 3 PLACE DEC $\pm .001$		CONTRACT NO.	
FINISH				STRESS	
				CHECK	
TEST Assy	USED ON			DESIGN	
FIRST APPLICATION				PREP BY	ELM/11/15/64
FOR COMPLETE USAGE DATA SEE ENGINEERING RECORDS				DESIGN ACTIVITY APPROVAL	
ORIGINAL DATE 5/15/64	UNIG SECTION	RELEASE CODE	CUSTOMER APPROVAL	SPECIMEN- LASER WELD TENSILE PROPERTY	
FORM 100				88277	20008236
DOUGLAS AIRCRAFT COMPANY LONG BEACH, CALIFORNIA					



NO SCALE
VIEW



-3 AND -5 GRIP FACING
FOUR PARTS OF EACH DRAW NUMBER
ARE REQUIRED
MAKING FROM 4150 STZ GRIP PER ANK-5-0758
MENT TREAT 40-80,000 ASD PER DCS 502
NO SCALE

DATE	1 st	2 nd	3 rd
10			
-3	4.00	2.50	1.50
-5	7.00	3.50	2.00

DOUGLAS	SIZE	CODE	IDENT	NO
				88277
				ZC008236

DOCK NO.	SUBJECT	WELDED	GRAIN OR CASE DIR. (INCH)	L	$\frac{L}{2}$	$\frac{W_1}{2}$	$\frac{W_2}{2}$	$\frac{W_3}{2}$	$\frac{W_4}{2}$	$\frac{W_5}{2}$	T	C	$\frac{C}{2}$	D	$\frac{D}{2}$
-1	TTT-4-5	BASE	T 300M	12.00	6.00	2.00	1.00	1.00	1.00	1.00	.250	8.00	4.00	10.00	5.00
-1	TTT-4-5	METAL	L												
-501	TTT-4-5	WELDED	T												
-501	TTT-4-5		L												
-505	TTT-4-5		L	12.00	6.00	2.00	1.00	1.00	1.00	1.00	.250	8.00	4.00	10.00	5.00

CANCELLED -503

(E)

-525	TTT-4-5	WELDED	T 300M	12.00	6.00	2.00	1.00	1.00	1.00	1.00	.250	8.00	4.00	10.00	5.00
-505	TTT-4-5	WELDED	T 300M	12.00	6.00	2.00	1.00	1.00	1.00	1.00	.250	8.00	4.00	10.00	5.00
-507	TTT-4-5	BASE	T 300M	12.00	6.00	2.00	1.00	1.00	1.00	1.00	.250	8.00	4.00	10.00	5.00
-507	TTT-4-5	METAL	L												
-505	TTT-4-5	WELDED	T												
-505	TTT-4-5		L												
-509	TTT-4-5		L												
-509	TTT-4-5		L												

CANCELLED -511

CANCELLED -511

CANCELLED -513

CANCELLED -513

CANCELLED -517

-513	TTT-4-5	BASE	T 718	12.00	6.00	2.00	1.00	1.00	1.00	1.00	.250	8.00	4.00	10.00	5.00
-513	TTT-4-5	METAL	L												
-521	TTT-4-5	WELDED	T												
-521	TTT-4-5		L												
-525	TTT-4-5		L	12.00	6.00	2.00	1.00	1.00	1.00	1.00	.250	8.00	4.00	10.00	5.00

CANCELLED -523

(E)

-525	TTT-4-5	WELDED	T 718	12.00	6.00	2.00	1.00	1.00	1.00	1.00	.250	8.00	4.00	10.00	5.00
-525	TTT-4-5	WELDED	T 718	12.00	6.00	2.00	1.00	1.00	1.00	1.00	.250	8.00	4.00	10.00	5.00

FOR CONTINUATION OF TABULATION SEE SH. 7.



ILLUSTRATION OF SPECIMEN
GIVEN DIRECTION (INCH)

DOUGLAS C 88277 EC008236

11-11-6

CONTINUED FROM SL. 7.

E-21

DOUGLAS

83277

50100000

211

ENGINEER: ORDER

NEW RELEASE

DAC 25-1100 (R. 71)

RECEIVED AUTOMATICALLY
 10/10/71
 10/10/71
 10/10/71

OTHER MODEL USAGE

DESIGN SECTION

72

RELEASE

DEVELOPMENT

A

MAJOR SUB/DOC

ADV DATE

C

TOTAL NO. OF SHEETS

SHEET 1 OF 1

SIZE DRAWING NUMBER

ZC008236

TYPE OF DRAWING:

- A SECTION LIST
 B SPEC OR SOURCE CONTROL
 C DAC STANDARD DRAWING
 D REMARK
 E SERVICE CHANGE
 F MODIFICATION
 G UNDIMENSIONED
 H SPECIAL SHAPE
 I OTHER

ENGINE FIVE CHG (Series Order)

D50C403

TITLE

SPECIMEN - LASER WELD

TENSILE PROPERTY

TENSILE PROPERTY

TENSILE PROPERTY

TENSILE PROPERTY

TENSILE PROPERTY

TENSILE PROPERTY

TENSILE PROPERTY

TENSILE PROPERTY

TENSILE PROPERTY

TENSILE PROPERTY

TENSILE PROPERTY

TENSILE PROPERTY

TENSILE PROPERTY

TENSILE PROPERTY

TENSILE PROPERTY

TENSILE PROPERTY

TENSILE PROPERTY

TENSILE PROPERTY

TENSILE PROPERTY

TENSILE PROPERTY

TENSILE PROPERTY

TENSILE PROPERTY

TENSILE PROPERTY

TENSILE PROPERTY

TENSILE PROPERTY

TENSILE PROPERTY

TENSILE PROPERTY

TENSILE PROPERTY

TENSILE PROPERTY

TENSILE PROPERTY

DESIGN APPROVAL

CHECKED BY

F. Schmid

CHECKED BY

F. Schmid

CHECKED BY

F. Schmid

CHECKED BY

F. Schmid

CHECKED BY

F. Schmid

CHECKED BY

F. Schmid

CHECKED BY

F. Schmid

CHECKED BY

F. Schmid

CHECKED BY

F. Schmid

CHECKED BY

F. Schmid

CHECKED BY

F. Schmid

CHECKED BY

F. Schmid

CHECKED BY

F. Schmid

CHECKED BY

F. Schmid

CHECKED BY

F. Schmid

CHECKED BY

F. Schmid

CHECKED BY

F. Schmid

CHECKED BY

F. Schmid

CHECKED BY

F. Schmid

CHECKED BY

F. Schmid

CHECKED BY

F. Schmid

CHECKED BY

F. Schmid

CHECKED BY

F. Schmid

CHECKED BY

F. Schmid

CHECKED BY

F. Schmid

CHECKED BY

F. Schmid

CHECKED BY

F. Schmid

CHECKED BY

F. Schmid

ADDED: TO SPECIMEN IDENTIFICATION COLUMN IN TABULATION ON SH. 6.7 & 8:
 PREFIX "S" FOR 300M STEEL
 PREFIX "N" FOR 718 NICKEL
 PREFIX "T" FOR 6AL-4V TITANIUM
 PREFIX "A" FOR 2219 ALUMINUM

CHANGED: "T" DIMENSION FOR -583 SPECIMEN IS NOW .500
 WAS .250.

CHANGED: "W" DIMENSION FOR -547 AND -549 SPECIMEN
 IS NOW .760/.740 WAS 1.010/.990 ALSO "W" DIMENSION

IS NOW .380/.370 WAS .505/.495

REASON: TO CLARIFY DRAWING.

PRINT DISTRIBUTION	YES	NO
DEVELOPMENT		
Orig at		
Orig at		
MAIL SUB W/DC ELSE		
WITH DAC PLANNING		
ACTION PICKUP		

DRAWING NUMBER	MAIL CODE	DEPT	QTY
ZC008236	1-18	CI-253	2
	1-18	CI-253	2

EXTRA EDS	EXTRA DWGS	MAIL CODE	DEPT	QTY
E. HAYMADE	E. HAYMADE	1-18	CI-253	1
M. HAYMADE	M. HAYMADE	1-18	CI-253	1

ENGINEER ORDER

DAC 25-1708 (12-72)

RC	MI	MP	AW	IS	DESIGN SECTION	OTHER MODEL USAGE	RELEASE	MAJOR SUB/MDC	TOTAL NO. OF INPUT SHEETS
					T2		DEVELOPMENT		
					LOM		PRODUCTION		
							NON PROD.		
HANDLING INSTRUCTIONS (MI)					TITLE				
1. INTERCHANGEABILITY OF PARTS NOT AFFECTED. CHANGE OF MATERIAL OR UNDESIRABLE PARTS OF ORIGINAL.					SPECIMEN - LASER WELD				
2. EFFECTIVITY CONFORM AT NOTED.					TENSILE PROPERTY				
3. PARTS MUST CONFORM AT NOTED.					DJ50CA03				
4. SCRAP.									
5. NOTED.									
6. RETROFIT (DELIVERED ARTICLES).									
7. MADE BY					E. J. HAYMAN				
DESIGN APPROVAL					CHECK E.O.				
SPEC COMPLIANCE					CHECK DNG				

1,2 L7		MODEL	SECTION	RELEASE S.O.	HI NO.	1ST FUS AFF	EFFECTIVITY (S SERIAL NUMBERS PER LINE MAXIMUM)	DWG CONFIGURATIONS	PEO PER ARTICLE		NEXT ASSEMBLY DRAWING NO.	U CO
									NEW	FOR-TR		
1		CR02	-	DJSOC003	2	TEST ONLY						1
2												2
3												3
4												4
5												5

